GENE THERAPY FOR METHYLMALONIC ACIDURIA

EDWARD WONG SERN YUEN

B.Biotechnology (Hons)

Thesis submitted for the degree of

Doctor of Philosophy

in

Discipline of Paediatrics

School of Paediatrics and Reproductive Health

Faculty of Health Sciences

University of Adelaide

Genetics and Molecular Pathology

SA Pathology

Women's and Children's Hospital

South Australia

November 2012

TABLE OF CONTENTS

ABBREVIATIONS

AAV	Adenoviral-Associated Virus
AdoCbl	Adenosylcobalamin
Adv	Adenovirus
APC	Antigen Presenting Cells
Apo	Apolipoprotein
BIV	Bovine Immunodeficiency Virus
C3-Carnitine	Propionyl-carnitine
C4DC	Methylmalonylcarnitine
CAE	Caprine Arthritis-Encephalitis Virus
CAI	Codon Adaptation Index
CAM	Chloroamphenicol
CF	Cystic Fibrosis
CFD	Codon Frequency Distribution
CIP	Alkaline Phosphatase Calf Intestine
CNS	Central Nervous System
CTL	Cytotoxic T-lymphocytes
DCA	Dicarboxylic Acid
DCC	Dicarboxylic Acid Carrier
DMEM	Dulbecco's Modified Eagles Medium
DMG	3'3-dimethylglutaric Acid
DTT	Dithiothreitol
EDTA	Ethylenediamine Tetraacetic Acid
EF1-α	Elongation Factor 1- alpha
F. IX	Factor IX
FCS	Foetal Calf's Serum

FH	Familial Hypercholesterolemia
FIV	Feline Immunodeficiency Virus
GagPol	*p*HCMVGagpollstmlwhvpre
GC/MS	Gas Chromatography/Mass Spectrometry
GFP	Green Fluorescent Proteins
GFR	Glomerular Filtration Rate
GH	Growth Hormone
GP64-FIV	GP64 pseudotyped FIV vector
GPI	Glycosylphosphatidylinositol
GPT	Glutamic Pyruvic Transaminase
GSH	Glutathione
HCCL	Hydroxycobalamin-[L-lactin]
HeBS	Hepes Buffered Saline
HEK293T	Human Embyonic Kidney
HEPES	N-[2-Hydroxyethyl]piperazine-N'-[2-ethanesulfonic acid]
HIV-1	Human Immunodeficiency Virus Type 1
HIV-2	Human Immunodeficiency Virus Type 2
hNAC	Na^+-Coupled Carboxylate Transporters
HPLC	High-Performance Liquid Chromatography
HRP	Horse Radish Peroxide
HSV	Herpes Simplex Virus
IFN	Type 1 Interferons
IG	Immunoglobulin
IH	Intrahepatic
IL-I	Interleukin-1
IM	Inner Membrane

IMS	Inner Membrane Space
IP	Intraperitoneal
IV	Intravenous
IU	Infectious Unit
LDH	Lactate Dehydrogenase
LPC	Lysophosphatidylcholine
LV	Lentivirus
MCA	2-methylcitric Acid
MCM	Methylmalonyl Coenzyme A mutase
MeOH	Methanol
MHC	Major Histocompatibility Complex
MMA	Methylmalonic Acid
MMAuria	Methylmalonic Aciduria
MMLV	Moloney Murine Leukaemia Virus
MPP	Mitochondrial Process Peptidase
MPS IIIA	Mucopolysaccharidosis Type IIIA
Mut^0	Complete MCM Deficiency
Mut^-	Partial MCM Deficiency
Mw	Molecular Weigh
m/z	Mass/Charge
NEMPs	Nuclear Encoded Mitochondria Proteins
Neo	Neomycin Phosphotransferase
NIH3T3	Mouse Embryo Fibroblasts
OH-Cbl	Hydroxycobalamin
OM	Outer Membrane
OTC	Ornithines Transcarbamylase
OXPHOS	Oxidative Phosphorylation

PA	Propionic Acid
PAuria	Propionic Aciduria
PBS	Dulbecco's Phosphate Buffered Saline
PEP	Processing Enhancing Proteins
pHe	Extracellular pH
PKU	Phenylketonuria
PS	Penicilin-Streptomycin
Rev	*p*HCMVRevmlwhvpre
ROS	Reactive Oxygen Species
SDS	Sodium Dodecyl Sulphate
SDS-PAGE	Sodium Dodecyl Sulphate-Polyacrylamide Gel Electrophoresis
SIN	Self-Inactivating
SIV	Simian Immunodeficiency Virus
Tat	*p*cDNA3.1Tat101ml
TBG	Thyroid Hormone-Binding Globulin
TBS	Tris-buffered Saline
TCA	Citric Acid Cycle
TEMED	N,N,N'N'-tetramethylenediamine
TIM	Translocase of Inner Membrane
TOM	Translocase of Outer Membrane
TMB	3'3'5'5'-tetramethylbenzidine
TNF-α	Tumour Necrosis Factor-α
Tris base	Tris[hydroxymethyl]amino methane
TVS	Tubulovesicular Structures
VSV	Vesicular Stomatitis Virus

VSV-G	Vesicular Stomatitis Virus-G Envelope Glycoprotein
X1-SCID	X-linked Severe Combined Immunodeficiency

THESIS ABSTRACT

Methylmalonic aciduria (MMAuria) most commonly results from a deficiency of methylmalonyl coenzyme A mutase (MCM). Current treatments for MMAuria remain unsatisfactory and research on novel therapies remains a high priority. A lentiviral (LV) vector was developed to treat *in vitro* and *in vivo* models of MMAuria.

The overall aim of this project was to examine the therapeutic effect of a LV vector that expresses human MCM transgene in MCM knockout fibroblasts and a MMA affected, mut -/- muth2, murine model.

In the first study, a self-inactivating LV vector that expressed human MCM, HIV-1SDmEF1αhMCM, was constructed and transduced into MCM knockout fibroblasts. Normal cells and untransduced MCM knockout fibroblasts served as controls. Real-time PCR showed a high level of vector copy number, 8 ± 2 copies/cell in LV-treated MCM-knockout fibroblasts, resulting in correction of both the MCM enzyme activity and propionate metabolism in MCM-knockout fibroblasts.

The HIV-1SDmEF1αhMCM was then delivered intravenously into mut -/- muth2 mice (n=2). Untreated mut -/- muth2 mice (n=2) and normal mice (n=5) were used as controls. Vector was detected at a copy number of 0.19 ± 0.04 copies/cell in liver. Nevertheless, the MCM enzyme analysis showed only a modest restoration of enzyme activity in the treated mice, resulting in a mild reduction of plasma and urine MMA levels in the treated animals. These data suggest success in targeting the liver with the intravenous gene delivery approach. Nevertheless, it was required to improve the human MCM transgene expression in order to enhance the level of restoration of MCM enzyme activity to further reduce the MMA levels.

In the second study, a LV vector that expresses a codon-optimised human MCM transgene, HIV-1SDmEF1αmurSigHutMCM, was produced and transduced into MCM-knockout fibroblasts. High levels of vector, 20 ± 0.8 copies/cell, were detected in LV-treated MCM-knockout fibroblasts. Western blot analysis and MCM enzyme activity analysis by HPLC demonstrated a high level of MCM expression in the treated fibroblasts, resulting in the correction of MCM enzyme activity, with the formation of a significant level of succinyl coenzyme A (179 ± 19 nM/min/µg of total cell protein).

The HIV-1SDmEF1αmurSigHutMCM was then injected intravenously into mut -/- muth2 mice (n=5). Untreated mut -/- muth2 (n=6) and normal mice (n=6) were used as controls. The HIV-1SDmEF1αmurSigHutMCM-treated mice achieved near-normal weight for sex. The western blot analysis demonstrated significant MCM enzyme expression in the liver of treated mice, with the measurement of high level of enzyme activity (66 ± 21 nM/min/µg of total cell protein). Biochemical analyses demonstrated that the normalization of MCM enzyme activity in the treated group was associated with a reduction in plasma and urine MMA levels. Furthermore, that a significantly lower MMA concentration, 133± 20 µM/g tissue, was measured in the liver compared to the untreated mice, 1003 ± 124 µM/g tissue.

These results confirm that HIV-1SDmEF1αmurSigHutMCM provides significant, if incomplete, biochemical correction for the treatment of this disease, suggesting that gene therapy is a potential treatment for MMAuria.

DECLARATION

This work contains no material which has been accepted for the award of any other degree or diploma in any university or other tertiary institution and, to the best of my knowledge and belief, contains no material previously published or written by another person, except where due reference has been made in the text.

I give consent to this copy of my thesis, when deposited in the University Library, being made available for loan and photocopying, subject to the provisions of the Copyright Act 1986.

I also give permission for the digital version of my thesis to be made available on the web, *via* the University's digital research repository, the Library catalogue, the Australiasian Digital Theses Program (ADTP) and also through web search engines, unless permission has been granted by the University to restrict access for a period of time.

SIGNED: …..... DATE: ……

ACKNOWLEDGEMENTS

I especially want to thank my supervisors, Dr. Janice Fletcher and Associate Professor Donald S. Anson for their guidance, support and patience throughout my PhD.

I would also like to thank the following people for their contribution to the work described in this thesis:

1) Dr. Heidi L. Peters and Nicole Buck, from Murdoch Children's Research Institue, who have supported my work through providing the mouse model for my research;

2) Dr. David Johnson, Rosemarie Gerace and Minh-Uyen Trinh, from Women's and Children's Hospital, who have provided technical assistance for biochemical analyses in my research;

3) Dr. Peter Clements and Enzo Ranieri, from Women's and Children's Hospital, for their technical assistance with the High-Performance Liquid Chromatography experiments;

4) Lynn Scarman for her assistance and expertise with the mouse and animal care attendants at the Women's and Children's Hospital animal facility.

Thank you to the University of Adelaide for providing me with the opportunity to undertake my PhD and supporting me with scholarship. I would also like to thank the members of the Department of Genetic Medicine, Women's and Children's Hospital for providing me with a supportive place to conduct my research.

To all the other members of the gene therapy group: Dr. David Parsons, Dr. Julie Bielicki, Dr. Rachel Koldej, Dr. Karlea Kremer, Dr. Alice Stocker, Dr. Martin Donnelly, Dr. ChuanHe Liu, Chantelle McIntyre, Richard Bright, Patricia Cmielewski, Stanley Tan, SuePing Lim, SinLay Kang, and Nigel Farrow. Thank you for your support and critical analyses on my research.

My deepest gratitude goes to my family for their love and support throughout my PhD. I would not get this far without your encouragement.

Chapter 1 : Introduction and Review

1.1 Preface

An inherited deficiency of methylmalonyl coenzyme A mutase (MCM) activity results in the condition known as methylmalonic aciduria (MMAuria). MMAuria is a rare autosomal recessive disorder of organic acid metabolism that affects approximately 1 in 80,000 children. As MCM requires adenosylcobalamin (AdoCbl) as a coenzyme, deficiency in MCM activity can result from a deficiency of either the apoenzyme, or the cofactor. This thesis addresses the most common form of MMAuria, that is, patients with MMAuria resulting from a deficiency of the apoenzyme.

As with most inherited metabolic deficiencies there is a spectrum of disease severity. Severely affected individuals may present in the neonatal period with overwhelming illness, consisting of metabolic acidosis, ketonuria and lethargy. In addition, a number of long-term complications are now recognized, such as chronic renal failure and neurological dysfunction. Untreated there is often progression to coma and death. Therapeutic options for MMAuria are limited and essentially involve strict dietary protein restriction whilst maintaining a high caloric intake. Despite such treatment, morbidity and mortality remain high and chronic long-term complications persist. Therefore, the development of an effective therapy for MMAuria remains a high priority. Positive results from limited trials of liver and combined liver/kidney transplantation, while not being curative, strongly suggest that a metabolic sink therapy may be efficacious.

Gene therapy offers a more generally applicable approach to treatment of MMAuria than organ transplantation as organs for transplantation are difficult to obtain and transplantation

requires long term immunosuppression, with its associated complications. In addition, liver is easily targeted by gene therapy as it is highly exposed to the circulation.

With the aim of developing an effective gene therapy approach for MMAuria, a self-inactivating lentiviral (LV) vector that expresses human MCM under the transcriptional control of the elongation factor 1α gene (EF1-α) promoter was developed. The main aims of the work presented in this thesis were firstly, to evaluate the efficacy of gene therapy using human MCM *in vitro* and *in vivo* in a disease model, and secondly, to develop strategies to improve the expression of MCM *in vivo* and hence the efficacy of the therapy. Outcomes to be evaluated include MMA levels in plasma, urine and tissues, assessed by tandem mass spectrometry as well as stable isotope dilution gas chromatography/mass spectrometry, direct measurement of MCM activity in liver tissue, and the physical growth of the treated MMA mice compared to normal and untreated controls.

In this chapter an overview of the natural history of MMAuria disease, MCM biogenesis and its structure will be presented. This will be followed by a discussion of the incidence of MMAuria, its clinical description, long-term complications, diagnosis and various treatments that may be applied to this particular disease. Also, a review of gene therapies, viral vector systems and animal models of disease will be given. The specific aims of this thesis will be outlined at the conclusion of this chapter.

1.2 The Natural History of MMAuria

Propionate metabolism is the major catabolic pathway of amino acids such as valine, isoleucine, methionine, threonine, odd-chain fatty acids, the cholesterol side-chain, thymine and uracil. MCM is one enzyme in this pathway, catalyzing the conversion of L-

methylmalonyl coenzyme A into succinyl coenzyme A, before its entry into the citric acid cycle. This reaction also requires a cofactor, adenosylcobalamin (AdoCbl) [1] (Figure 1-1).

The occurrence of patients who died from life-threatening or metabolic ketoacidosis, in whom an elevation of ketoacids, glycine and several other amino acids were found, drew the attention of physicians and clinicians and provided an impetus to investigate the metabolism of propionate and methylmalonate.

During the 1960s, several papers illustrated the significance of vitamin-B12 coenzyme (now named AdoCbl) for the isomerisation activity of methylmalonyl coenzyme A to succinyl coenzyme A [2, 3] by demonstrating that, in some patients, metabolic ketoacidosis with increased of the MMA levels in urine resulted from a deficiency of AdoCbl. These reports also demonstrated that patients who received supplemental AdoCbl showed a large decrease in MMA levels. In 1967, Oberholzer *et al*., (1967) [4], and Stokke *et al*., (1967) [5] described the first cases of MMAuria, in patients who failed to respond to supplementation with AdoCbl. They described two ill infants with metabolic acidosis and ketosis, with a high level of methylmalonic acid (MMA) found in the blood and urine. The increase of MMA was shown to be due to a failure to convert L-methylmalonyl coenzyme A into succinyl coenzyme A due to a deficiency of MCM activity. Rosenberg and his colleagues also discovered a group of patients with similar symptoms in the following year. In this study, some of the patients responded to administration of pharmalogical doses of AdoCbl. These patients' condition was significantly improved after the treatment, with a large decrease in MMA excretion [6]. Their findings indicated that AdoCbl deficiency can also be a cause of MMAuria. Mudd *et al*., (1969) [7] identified a, vitamin B-12 unresponsive, 7-week-old patient whose clinical presentation showed not only a high level of MMA in the plasma and urine, but also of homocystine, and cystathionine and low levels of methionine.

These early studies showed that the MMAuria can result from many different biochemical defects: Two distinct defects of the mutase apoenzyme, one which produces complete mutase deficiency, (*mut*^{0}), and the other that results in a partial mutase deficiency, (*mut*$^{-}$); became evident. Other mutations associated with cblA, cblB and cblD that result in a defect of AdoCbl synthesis have also been described. The focus of this thesis is the most common form of MMAuria, the "mutase" form, that is, patients with MMA resulting from a deficiency of the apoenzyme.

Figure 1-1 Propionate catabolism.

This figure demonstrates the breakdown of several essential amino acids (isoleucine, valine, methionine, and threonine), and odd chain fatty acids and cholesterol, through the propionate catabolic pathway, to succinyl coenzyme A, prior to its entry of the citric acid cycle (TCA). The pathway shows that the lack of methylmalonyl coenzyme A mutase leads to the elevation of both MMA and propionic acid (PA) due to the reverse reaction. Accumulations of these toxic metabolites can cause the metabolic disease known as MMAuria. The figure is cited from Hofster *et al*., (2004) [1].

Propionate Catabolism

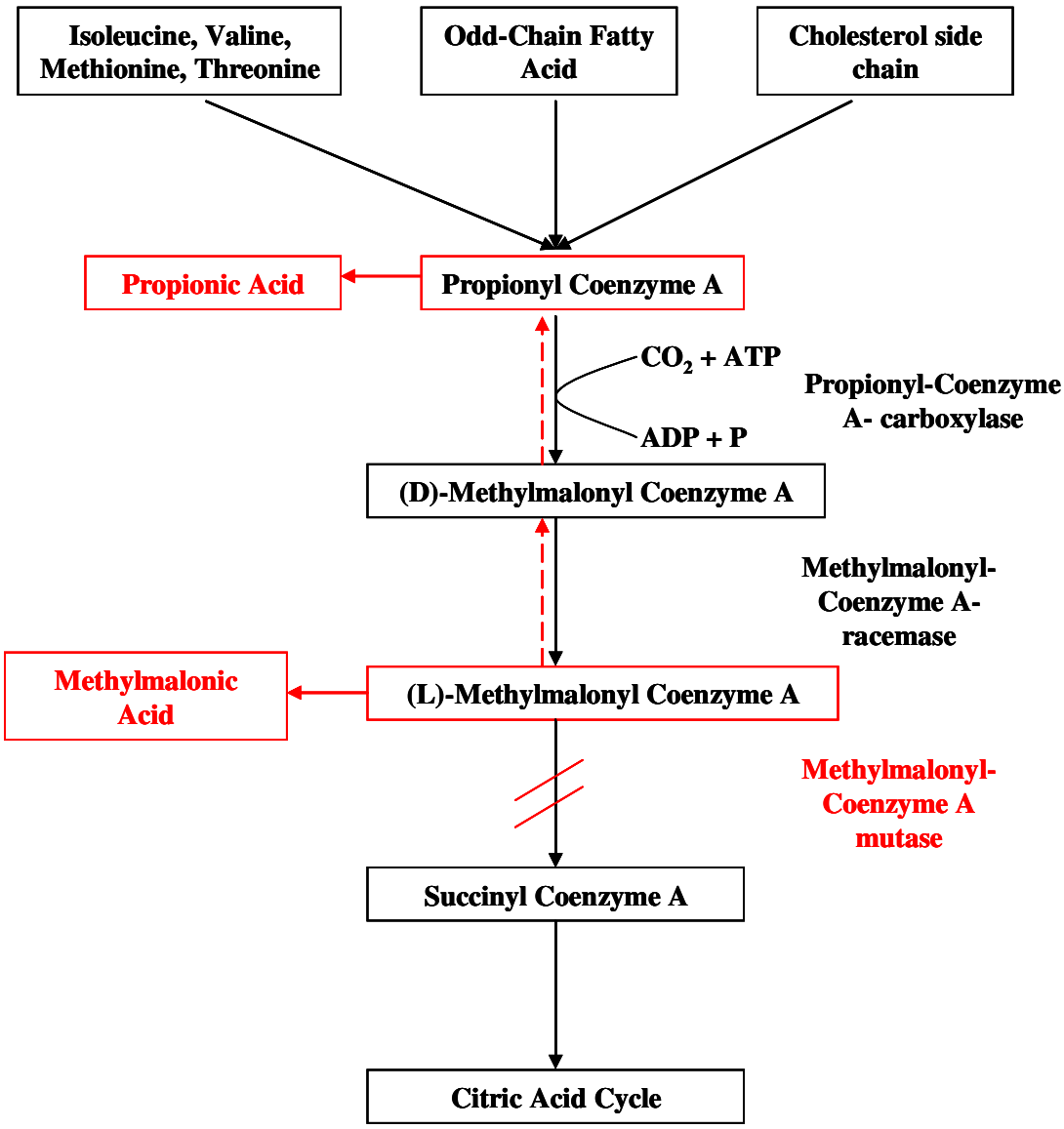

1.3 MCM Biogenesis

The majority of the mitochondrial proteins, including MCM, are nuclear-encoded matrix enzymes [8]. In 1984, Fenton and his colleagues [9] investigated the biosynthesis of MCM. In their observations, they showed that the mutase protein is firstly synthesized by the cytoplasmic polyribosomes as a large precursor (~ 82 kDa) that is approximately 3-4 kDa larger than the mature mutase subunit. The formation of the functional MCM enzyme appeared to take place in the mitochondria as most of the matured enzyme was found only in the mitochondria. Thereby, consistent with most of the mitochondrial proteins, the precursor MCM enzyme is translocated to mitochondria, where post-translation processing takes place, directed by 32-amino acid leader peptides [10].

The schematic illustrates the delivery of mitochondrial proteins from the cytosol (Figure 1-2). The precursor enzyme containing the leader peptide is directed to a receptor/pore complex in the mitochondrial membrane, known as the Translocase of Outer Membrane (TOM), by cytosolic chaperones. The precursor enzyme is then transported through to the inner membrane of the mitochondria and bound to a second receptor, known as the Translocase of Inner Membrane (TIM) and transported into the inside of the mitochondrion. The maturation of the enzyme involves the removal of the leader peptide by the action of the proteases, mitochondrial process peptidase (MPP) [11] within the mitochondrial matrix, followed by the assembly of the individual subunits into a functional multimeric mitochondrial enzyme.

The data published by Fenton *et al*., (1984) [9] showed that the translocation and synthesis processes are energy-dependent. This was demonstrated by the fact that the entire processing pathway was suppressed with the use of mitochondrial energy metabolism inhibitors. Their study had also demonstrated that the half-life of processing pre-MCM to matured enzyme occurs within the range of 6 to 9 minutes. In addition, for pre-MCM, unlike other mitochondrial enzymes such as pre-ornithine transcarbamylse and pre-carbamyl phosphate

synthetase, a long half-life with several hours was observed under conditions where the processing pathway was suppressed by mitochondrial energy metabolism inhibitors.

Figure 1-2 The mitochondrial protein import machinery.

The precursor proteins with N-terminal positively charged leader peptides are transported and recognised by the TOM. Following this, the precursor proteins are transported through to the inner membrane and bound to the TIM. Once across the mitochondrial membrane, the 32-amino acids leader peptide is cleaved off by the MPP (mitochondrial process peptidase). IM, inner membrane; OM outer membrane; IMS, inter membrane space. The figure is cited from Matouschek *et al*., (2000) [12].

1.4 The Structure of MCM

The mature human MCM is a homodimer that binds to 2 mol of AdoCbl per mol of dimer [13]. Each of the subunits is composed of two essential domains, the N-terminal domain and C-terminal domain The N-terminal domain is made up of an eight-stranded β/α barrel led by an extended segment wrapping around the other subunit. A long linker region encloses the N-terminal domain and connects it to C-terminal domain. The C-terminal domain is made up of five parallel β- sheet strands. These two domains pack on each other, sandwiching the corrin ring of the cobalamin and forming the active site cavity (Figures 1-3a and 1-3b).

The catalytic mechanism of the MCM involves a radical mechanism, in which the role of AdoCbl acts as a reversible free radical generator. The catalysis begins with the homolysis cleavage of the carbon – cobalt (III) bond of AdoCbl, induced by binding of the substrate, leading to the formation of a radical form of AdoCbl with a Co (II) oxidation state. The 5'-adenosyl radical abstracts a hydrogen atom from the substrate, producing a protein-bound 5'deoxyadenosine and a substrate radical, which is followed by a rearrangement that generates a product radical. The final product is produced by recovering the H-atom from the methyl-group of 5'-deoxyadenosine and regenerating the 5'deoxyadenosyl radical. The process is depicted in Figure 1-4.

Genetic analyses have identified a whole set of mutations at the *MUT* locus that constitute the two phenotypes. Mutations that contribute to the mut^0 phenotype include G623R [14], R93H [15], W105R, A377E [16], G630E and G703R [17]. On the other hand, mutations of G626C, G648D [18] and G717V [19] give rise to the mut^- phenotype.

The mutations G630E and G703R are at the AdoCbl binding site, and effectively prevent the binding of AdoCbl. The changes of G623R and G626C appear to affect the positioning of His-627, resulting in a defect in its function in providing the bottom ligand for the bound

AdoCbl. The G717V mutation results in an unstable protein due to the poor folding of the β/α strand to form the AdoCbl-binding domain. Other mutations, their affects and phenotype, are summarized in Table 1-1.

Figure 1-3a Topology diagram of the human MCM.

The diagram shows the human MCM in schematic form. Rectangles indicate helices, bold arrows indicate β strand and coils or turns are shown by a thin line. COB indicates adenosylcobalamin. The mutations discussed in the text are shown as filled circles. The figure is cited from Thomä *et al*., (1996) [13].

Figure 1-3b. The yellow and green colours indicate the two subunits. The darker coloring in each subunit indicate the $(\beta/\alpha)_8$ barrel. The B_{12} domain is indicated in lighter coloring. The coenzyme A threads through $(\beta/\alpha)_8$ barrel to reach the deeply buried active site. The corrin ring of B_{12} is sandwiched between the the $(\beta/\alpha)_8$ barrel and the B_{12} domain. The figure is cited from Thomä *et al*., (1996) [13].

MCM reaction mechanism

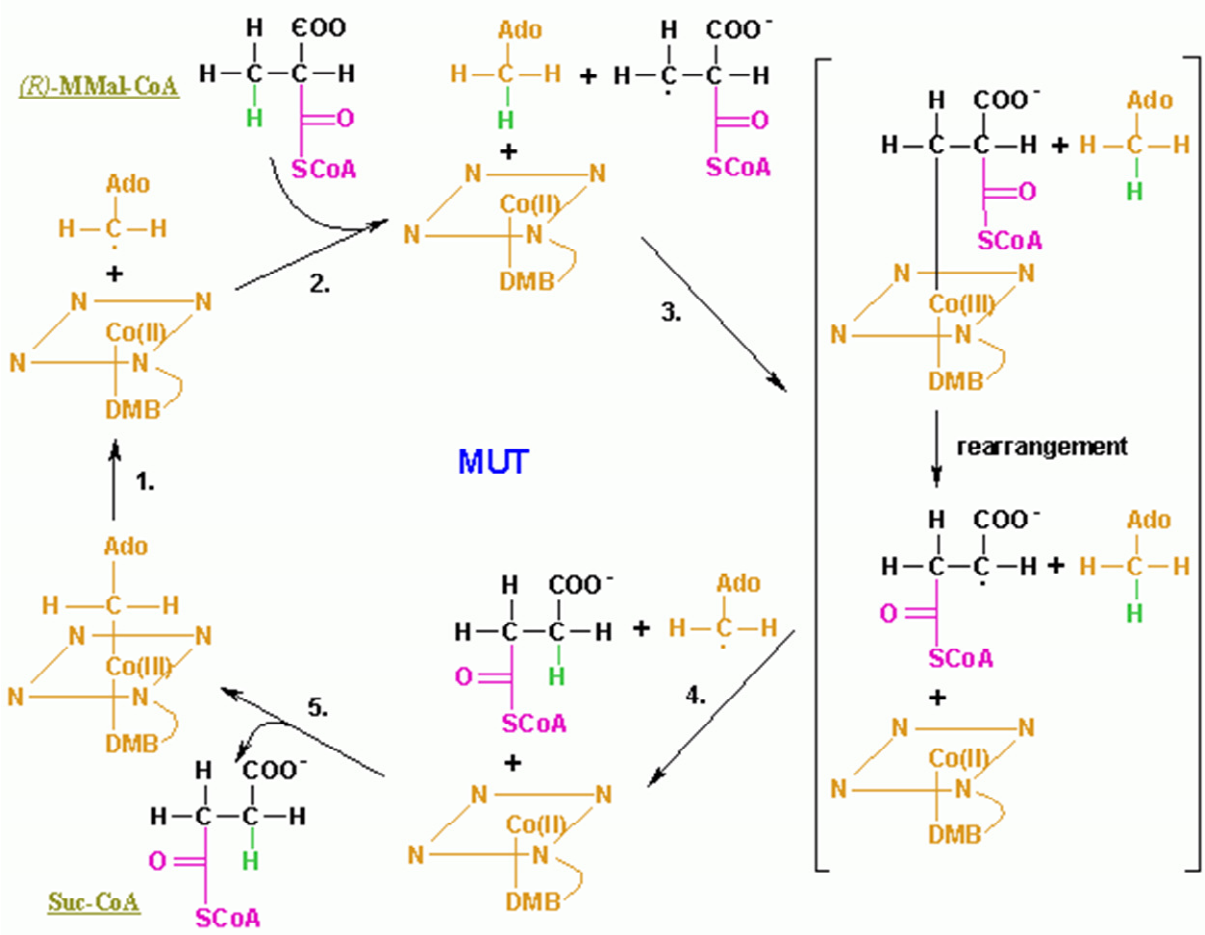

Figure 1-4. Summary of the reaction mechanism of MCM.

Table 1-1. Summary of mutations in the human MCM gene. Cited from Thomä *et al*., (1996) [13].

1.5 Incidence

Newborn screening by mass spectrometry has identified approximately 1:80,000 [20-23] children are affected by MMAuria (these numbers include the deficiency in AdoCbl and MCM), including 1:48,000 in Massachusetts [20], 1:83,131 in Quebec [21] and 1:51,100 in Japan [23]. However, a review by Deodato *et al*., (2006) [24] showed that the incidence of MMAuria in Italy and Germany is approximately 1:115,000 and 1:169,000, respectively. These analyses also failed to show any sex or ethnic predilection for MMAuria disease.

1.6 The Clinical and Laboratory Presentation of MCM Deficiency

MMAuria patients may present with a number of physical characteristics that include minor facial dysmorphisms, including high forehead and broad nasal bridge, congenital heart defects, hydronephrosis, epicanthic folds, long, smooth philtrum and triangular mouth. Patients can also be phenotypically normal.

The clinical presentations of this disease have also been well defined. A survey of equal numbers of males and females by Matsui *et al*., (1983) [25] characterised the common clinical signs and symptoms of MMAuria. The major manifestations are lethargy, failure to thrive, recurrent vomiting, dehydration, respiratory distress, muscular hypotonia, developmental delay, hepatomegaly and coma. In severe cases, if untreated, there is often progression to death or permanent brain damage, particularly affecting the basal ganglia. Upon presentation, the laboratory findings exhibit an increase in anion gap metabolic acidosis, ketosis, hyperammonaemia, hyperglycinemia and hypoglycaemia.

In patients with mut^0 deficiency, 80% of the clinical signs typically appear within in the first week of life, and 90% present by the end of the first month. Patients in the mut^- group may present later, and generally their conditions are milder than the previous group. Particularly

when diagnosed early and treated, these children may survive into adulthood, with less frequent episodes of metabolic decompensation than severe patients.

In addition, the late-onset forms show chronic symptoms of various degrees. These include intermittent ataxia, behavioural disturbances, poor feeding with selective refusal of protein-rich foods, anorexia, recurrent vomiting, failure to thrive and neurodevelopmental delay.

Metabolic acidosis is characterized by decreased serum pH and bicarbonate concentration. The pH value and serum bicarbonate concentration in healthy individuals range from 7.37 – 7.43 and 21-28 mmol/L, respectively. In contrast, pH values as low as 6.9 and serum bicarbonate concentration as low as 5 mmol/L are observed in MMAuria patients [25]. Also, an increase in the anion gap is often seen in patients. The anion gap is defined as $[Na^+] - [Cl^- + HCO_3^-]$ is normally in the range of 7 – 16 mmol/L in healthy individuals. However, a value of greater than 16 mmol/L is often observed in organic aciduria patients [26].

Hypoglycaemia is defined as a blood glucose level less than 2.6 mmol/L at all ages. Nevertheless, it is of note that hypoglycaemia can result from a variety of diseases. Hence, it is important to carry out adequate diagnostic tests in order to identify the cause.

Hyperammonaemia is defined as an increase in the concentration of NH_3, greater than 110, µmol/L in the blood. In newborns with severe metabolic disease, the concentration of NH_3 can be as high as 180 µmol/L. As with hypoglycaemia, several different diseases can result in the elevation of NH_3 concentration. These are urea cycle disorders, organic acidurias and long-chain fatty acid oxidation defects. With the ammonia concentration as the only marker, it is difficult to distinguish between these diseases. Further investigation of hyperammonaemia needs to include other indicators such as plasma amino acids, urine

organic acids and plasma acylcarnitine profile. Thereby, it is essential to carry out several tests in order to identify the underlying cause.

Ketosis is also frequently found in organic aciduria patients. It results from the elevation of ketone bodies in the blood. Normal serum reference ranges for ketones bodies are 0.05 – 0.29 mmol/L, whereby a higher concentration of ketone bodies, ranging from 0.2-1.8 mmol/L, is often observed in organic aciduria patients.

Some other less frequent conditions that are found in MMAuria patients are leukopenia, anemia and thrombocytopenia.

1.7 Long-term Complications in Specific Organs

Patients who survive into adulthood are often affected by recurrent episodes of metabolic decompensation. Metabolic stress, such as viral illness, or high protein intake, can cause metabolic decompensation, which can be life threatening or associated with metabolic stroke. Therefore, maintaining adequate growth and nutrition remains a constant problem in affected individuals. Recently, long-term complications associated with selective organ impairment have been recognized. The major complications are neurological deficits [27], chronic renal failure [28], cardiomyopathy [29] and pancreatitis [30].

1.7.1 Cerebral Effects of MMAuria

Brain tissue is prone to the harmful effects of reactive oxygen species (ROS), also known as free radicals. Investigation of the aetiology of cell damage induced by these free radicals suggests that the brain's susceptibility to oxidative damage is due to the imbalance of redox reactions resulting from the disruption of oxidative phosphorylation (OXPHOS) and the polyunsaturated fatty acid-rich cell membrane structure that is readily attacked by free

radicals. The formation of $O_2^{\cdot -}$ is largely due to the high demand for oxygen in the brain. Detailed descriptions of mechanisms for ROS production are best provided in the review by Wajner *et al*., (2004) [31].

The involvement of toxic organic acids in the accumulation of free radicals has been studied intensively *in vitro* and *in vivo*. These toxic organic acids were hypothesized to induce mitochondrial dysfunction by impairing the respiratory chain complexes.

The aetiology of the neuropathy in MMAuria has also been extensively studied. The clinical presentation of patients with neuropathy includes Leigh-like encephalomyopathy, muscle hypotonia, and dystonia. Several studies have demonstrated that neuropathy was induced by the accumulation of toxic metabolites. These toxic metabolites include MMA, 2-methylcitric acid, malonic acid, and propionyl coenzyme A [32]. In some cases, acute or progressive metabolic decompensation gives rise to abnormal structural changes in the basal ganglia. Studies have shown that cerebral lesions are mostly localised bilaterally in the globus pallidus [24].

The similarities in structure of MMA to the succinate dehydrogenase inhibitors, malonic acid and 3-nitropionic acid [33], suggest that MMA may be in itself a major neurotoxin. In fact, there are numerous studies that show the inhibitory effect of MMA on enzyme activity and on transporters in mitochondria [34-39] resulting in increased amounts of free radicals. In addition, studies have shown that mitochondria are open to MMA uptake into the mitochondria matrix [40], making them sensitive to the toxicity of MMA.

Another possible mechanism is the generation of other toxic metabolites such as 2-methylcitrate acid, the monocarboxylic metabolites such as propionyl coenzyme A and 3-hydroxypropionate, induced by the accumulation of MMA during metabolic decompensation.

It is suggested that these metabolites act synergistically with MMA to inhibit the TCA cycle and the mitochondrial respiratory chain, resulting in mitochondrial dysfunction and the impairment of energy metabolism, leading to cerebral energy deficiency and cell death [32, 41].

Morath *et al*., (2008) [39] hypothesized that the blood brain barrier may play a part in neurodegeneration. The blood brain barrier works as a functional barrier that protects the brain by restricting the entry of microscopic objects (e.g. bacteria) and large or hydrophilic molecules while allowing the diffusion of small hydrophobic molecules. The restriction of hydrophilic molecules transportation may entrap the dicarboxylic molecules (DCA) (e.g. glutarate, 3-hydroxyglutarate, L-2- and D-2-hydroxyglutarate), MMA and MCA in the central nervous system (CNS), leading to neurodegeneration [42].

The MMA-induced inhibition of the TCA cycle may also subdue the glutathione transport activity, the best known antioxidant agent, leading to the disruption of antioxidant defense mechanisms and cell death [43].

Another side-effect of MMA is its ability to suppress the creatinine kinase activity in mitochondria, resulting in the decrease of the cellular ATP/ADP ratio [36, 44]. The impairment of the ATP/ADP ratio can cause the depolarization of the mitochondrial membrane and accumulation of intracellular Ca^{2+}, subsequently resulting in necrotic and apoptotic cell death [35, 41, 45].

1.7.2 Renal Effects

Another commonly seen and severe long-term complication that impacts MMAuria patients is chronic renal failure. This is predominantly found in patients with the apomutase deficiency

and usually occurs in adolescence. The pathophysiology of chronic renal failure in MMAuria has been extensively studied, and it is often accompanied by progressive tubulointerstitial nephritis with interstitial fibrosis, tubular atrophy and mononuclear inflammatory infiltrates [46].

The pathophysiological mechanisms by which MMA causes renal failure are still poorly understood, mainly due to the lack of an appropriate model. However, the potential nephrotoxicity of MMA was shown by the study conducted by Kashtan *et al*., (1998) [47], in which proteinuria and renal tubular damage were observed after the administration of MMA to rats.

Several other hypotheses about the involvement of MMA in inducing renal failure have been suggested. One of these is that the structural similarity between MMA and another putative nephrotoxin, maleic acid, suggests that MMA may act in the same manner as maleic acid, impairing mitochondrial function and producing a Fanconi syndrome-like pathology [48], resulting in decrease of the glomerular filtration rate (GFR) and renin release [49]. However, although the clinical study by D'angio *et al*., (1991) [50] reported decreased activity of the rennin-angiotensin-aldosterone system in MMAuria patients, Fanconi-like tubulopathy was not observed [51].

Beyond this, whether MMA disrupts the normal uptake mechanisms in renal tubules, which involve the Na^+-coupled carboxylate transporters (hNAC), remains unknown. Several types of hNAC, as well as their site of expression, have been identified [52]. These transporters play a major role in the intracellular transport of the DCA and tricarboxylic TCA cycle intermediates. Furthermore, inhibitors of these transporters, such as maleic acid, fumarate, glutarate and α-ketoglutarate, have also been recognized. Therefore, it has been suggested

that the increase of MMA and MCA metabolites can lead to the inhibition of these transporters, and eventually deplete the energy substrates in proximal tubule cells.

Another possibility is the involvement of the dicarboxylic acid carrier (DCC). DCC is important, as it mediates the importation of glutathione (GSH) and DCAs into kidney mitochondria [53]. GSH is best known as an antioxidant. The large amount of MMA present in the proximal tubule cells may interfere with the transport of GSH into the mitochondria. As a consequence, cell death and chronic renal complication occurs.

Recently, a publication by de Keyzer *et al*., (2009) [54] demonstrated the observation of mitochondrial respiratory chain reaction deficiencies in renal tissues of MMAuria. The pathophysiologic mechanism for the deficit may be similar to what has been discussed in the brain injury induced by the accumulation of MMA. The disruption of the DCC may be the cause for the disturbance in OXPHOS metabolic pathway in mitochondria. Furthermore, a study has shown the importance of DCC in proximal tubular uptake of the di- and tricarboxylate molecules to replenish the metabolites in order to maintain the high level of energy required for normal kidney function [55].

A recent *in vitro* model, in which human proximal tubule cells were incubated with hydroxycobalamin-[L-lactin] (HCCL), has also been used to study the renal disease in MMAuria [56]. This study indicated that increased concentrations of MMA reduced the enzyme activity of complexes II and III in the respiratory chain. This phenomenon is most likely due to the disturbance by MMA to the synthesis of cytochromes *c* and *b*, which are the main components of complex II and III of respiratory chain. Moreover, the low concentration of GSH in this *in vitro* model supports the contention that the increase of ROS formation results in mitochondriopathy.

1.7.3 Cardiomyopathy

Another complication seen in MMAuria patients is cardiomyopathy. Clinical studies demonstrate fatal outcomes in propionic aciduria (PAuria) patients with cardiomyopathy [29]. Recently clinical observations of cardiac disease in MMAuria patients were reported [57], three MMAuria patients, one with *mut*$^{-}$ deficiency and another two of *mut*^{0} phenotype, were involved in the study. All three patients were found to have cardiomyopathy, presenting with symptoms such as tachycardia, respiratory distress and cardiac failure. Sudden death was reported in all these patients. Several causes that contributed to the observed mortality were also discussed.

It is known that cardiac dysrhythmia can be a life-threatening medical emergency that results in cardiac failure and sudden death. Ventricular tachycardia and ventricular fibrillation are two potential causes of arrhythmias. Several documented studies indicate that the accumulation of ROS and metabolic stress cause an imbalance of cardiac ions, leading to electrophysiological dysregulation and structural remodeling of the left ventricle in heart failure [58, 59].

ATP is the major source of energy for maintaining the balance of cardiac ions and for the contraction and relaxation mechanism. It has been shown that 30% of the volume of ventricular cardiocytes is composed of mitochondria. These muscle cells are seen to assemble around myofilaments, forming ATP production sites. Therefore, it is reasonable to assume that the disruption in mitochondria seen in MMAuria can cause the elevation of ROS, leading to heart failure or arrhythmias. The importance of mitochondrial oxidative phosphorylation to maintain the constant supply of ATP in mammalian cells has been described in detail [60, 61]. A disturbance of OXPHOS was observed in PAuria patients, associated with dilated cardiomyopathy [54]. During the occurrence of metabolic decompensation, the accumulation

of MMA may decrease the cellular ATP/ADP ratio due to the inhibitory effect of MMA on mitochondrial creatine kinase [44, 62].

Numerous studies have demonstrated that many cardiac diseases are associated with the existence of ROS. Outcomes from *in vivo* experiments show that ROS can cause reperfusion injury and cardiac diseases [63, 64]. In addition to this, the elevation of ROS has shown to enhance the rate of ROS production. These RO species include superoxide, hydrogen peroxide, hydroxylradicals and peroxynitrile, O_2^- . The heart is susceptible to these free radicals as the heart is a highly oxidative organ (i.e. consumes high level of oxygen). The pathophysiologic mechanism described in neuropathy, where ROS produced during metabolic decompensation result in mitochondriopathy, also seems to operate in heart. Moreover, MMA has been shown to compromise the GSH transport in mitochondria. GSH is a key antioxidant defence against ROS in cardiocytes. Therefore, it is assumed that the depletion of GSH may also contribute to the disease. In fact, numerous studies display the involvement of GSH deficiency associated with cardiac diseases, including ischemia [65-67], heart failure [68] and arrhythmia, which are all observed in organic acid-affected individuals.

In addition to GSH, NADH plays a key role against ROS as well as the recovery of ischemic myocardium. The TCA cycle is the main source of NADH generation for ATP production. A constant supply of TCA intermediates is required in order to maintain normal function. Therefore, the inhibition of succinyl coenzyme A formation resulting from the disturbance of propionate metabolism may shut down the entire cycle, leading to NADH depletion. Several *in vivo* studies indicate that normalization of cardiac contraction and relaxation functions can be restored with the replenishment of propionyl coenzyme A precursors [69, 70].

Another possible cause of arrhythmia in MMAuria might be the imbalance of Ca^{2+} ions. The elevation of Ca^{2+} ions in the mitochondrial matrix has been proved to influence mitochondrial

permeability, leading to the organelle dysfunction [45]. Clinical studies have indicated the development of cardiomyopathy and arrhythmia resulting from the disruption of intracellular ion homeostasis [71].

1.7.4 Pancreatitis

Observations of acute or chronic pancreatitis are found less commonly in patients with MMAuria and to date, only a small number of cases have been reported. However, as the symptoms of pancreatitis are less obvious, it is believed that there are many unreported cases associated with pancreatitis in MMAuria patients (Fletcher, personal communication, 2011). One factor may be because the symptoms of pancreatitis are vomiting, anorexia, abdominal pain and encephalopathy, all of which are commonly seen in MMAuria patients. In addition to this, diagnosis on the basis of the elevation of amylase and/or lipase concentrations in blood, which are the typical markers in pancreatitis patients, is not routinely performed.

Based on clinical reports, this type of complication is usually late onset and often accompanied with chronic renal failure [30, 72-74]. The pathophysiologic mechanism of this complication remains unknown. Apart from as the possible causes such as excess free radicals, carnitine deficiency and the lack of antioxidants during metabolic decompensation, the activation of the protease, zymogen, within the acinar cells is another potential cause of the disease. This idea is supported by *in vitro* and *in vivo* studies [75].

The study published by Bhoomagoud *et al*., (2009) [75] provided evidence that the change of the extracellular pH (pHe) may sensitize the acinar cell to secretagogue-induced pancreatitis. Their *in vitro* study showed that lactic acid would reduce the pHe, resulting in sensitization of the acinar cells and leading to the activation of the cerulem-dependent zymogen. Coincidently, the accumulation of lactic acid, resulting from a combination of excess

formation and decreased utilization of lactate, is commonly seen in MMAuria patients. However, it has been shown that the increase of lactic acid itself is not substantial enough to induce injury. In fact, their study indicates that the decrease of pHe can induce the release of the cytocolic protein, lactate dehydrogenase (LDH), which enhances the cerulem-induced injury.

In addition, their animal studies, in which rats were treated with acid load, provided evidence that pancreas injury can be caused by the infused acid, as their acid-treated rats presented the symptoms of pancreatitis. Nevertheless, clinical studies are required to validate this mechanism in patients.

1.7.5 Other Complications

Other complications such as growth failure are also found in MMAuria affected individuals. Elevated levels of PA are associated with anorexia. This interacts negatively with the dietary restriction on these patients. In addition, it is hypothesized that the faltering growth may be attributed to growth hormone (GH) deficiency [76]. Optic neuropathy has also been reported in isolated cases of MMAuria [77], as well as in PAuria.

In conclusion, the highly metabolically active brain, heart and kidneys are major sites of pathophysiology, and probably share many features of the pathophysiological mechanism in common, including oxidative damage, ion imbalances and GSH deficiency.

1.8 Diagnosis

Newborn screening for MMAuria by measurement of the acylcarnitine profile in dried filter paper whole blood spots by tandem mass spectrometry is now routine practice in Australia and many other industrialized countries. Acylcarnitines are in equilibrium with the respective

coenzyme A esters that accumulate in MMA, but are easier to detect. This non-specific biochemical test offers a rapid screening method to identify the MMAuria patients. In MMAuria the elevation of methylmalonylcarnitine (C4DC) and propionyl-carnitine (C3-carnitine) are the marker metabolites. A stable isotope internal standard allows absolute levels to be determined. Following derivatization to form butylesters these are analysed by tandem mass spectrometry. The normal level of C4DC is 0.02 – 0.23 μM in whole blood and levels above 1 μM are considered abnormal. However, it is shown that the C3-carnitine is also increased in other cases such as PAuria, AdoCbl defects, maternal vitamin B12 deficiency and can also be falsely elevated. The 2nd-tier testing for MMA, a more specific and sensitive marker, is available to minimize the possibility of false positive results [78] and has been used in some laboratories, including the South Australian Newborn Screening centre.

The diagnosis of MMAuria is confirmed by the quantitative analysis of urine and plasma organic acids using gas chromatography/mass spectrometry (GC/MS) to determine MMA levels. The same methods are used to monitor the metabolic status of MMAuria patients.

The use of an indirect enzyme assay for MCM enzyme activity, the [^{14}C]-propionate incorporation assay, can also be used. This assay requires the incubation of cells from affected individuals with the [^{14}C]-radiolabelled precursor, propionate, which is converted into the succinyl-coenzyme A, a precursor of the TCA cycle, leading to the production of radiolabelled proteins. A block in any step of this pathway can reduce the incorporation of ^{14}C into protein [79].

Patients with MMAuria disease should be assessed for their vitamin B12 responsiveness. The patients can be given hydroxycobalamin (OH-Cbl) intramuscularly or intravenously for a period of time followed by assessment of the levels of MMA and related metabolites in plasma and urine. B12 responsiveness is defined by the observation of a significant (greater

than 50%) reduction in metabolite production [80]. The review published by Manoli *et al.,* (1993) [81] has described in details the precise rules for follow-up of a positive newborn screen for MMAuria patient.

Other diagnosis methods such as direct gene sequence analysis should also be considered to confirm affected individuals. Approximately 200 mutations of the MUT gene have been identified [82]. Furthermore, sequence analysis is now readily available and enables the clinicians to identify the mutation more accurately, providing both confirmation and the possibility of prenatal diagnosis. Clinical reports have also shown that prenatal diagnosis of MMAuria can be performed through the measurement of MMA in amniotic fluid and maternal urine [79, 83], or by the determination of mutase enzyme activity and AdoCbl metabolism in cultured amniotic fluid cells.

1.9 Treatments and Outcomes

Several treatments have been introduced for MMAuria based on the biochemical understanding of the disease. However, the outcomes have been generally disappointing. As discussed above, amino acids such as valine, isoleucine, metheonine and threonine are the major precursors of propionate metabolism. Hence, in MMAuria patients, the catabolic pathway that is directly affected by MCM deficiency is challenged by increased protein intake.

1.9.1 Low-Protein/High-Caloric Diet

Conventional management of MMAuria involves strict dietary protein restriction while maintaining a high caloric intake. The reason for limiting protein intake is to prevent the presence of high levels of amino acids, particularly those listed above, within the body that leads to the accumulation of PA and MMA. However, this has to be monitored clinically and

biochemically to prevent protein malnutrition. Insufficient protein intake can lead to an increase in endogenous protein degradation, which in turn leads to metabolic decompensation and a chronic failure to thrive. In addition, prolonged fasting may cause the release of propiogenic odd-chain fatty acids derived from lipolysis. Thus, the level of protein intake must be kept at a level that can be tolerated, and which is enough to allow for growth and nitrogen losses. As a result, the protein-restricted diet may be supplemented with a special MMA-precursor-free amino acid mixture [81]. It is of note that this nutrional treatment regimen does not represent a curative treatment of this disease [84].

1.9.2 Glucose and Lipids Administration

The promotion of anabolism can be achieved by the introduction of glucose and lipids to the patients. In fact, 10% dextrose and intralipids are used clinically for management of unwell MMAuria patients. The 10% dextrose is a hypertonic solution of dextrose and provides a concentrated source of carbohydrate calories. Intralipid is a fat emulsion that is made up of 30% soybean oil, 1.2% egg yolk phospholipids, 1.7% glycerine and water. This provides a source of essential fatty acids. The administration of glucose can reduce catabolism of fat, which is used as an alternative fuel source, and hence avoid the production of ketone bodies. In addition to this, hypoglycaemia is a common pathophysiology observed in MMAuria patients [85], resulting from the inhibition of pyruvate carboxylase or glucogenesis through various mechanisms. The introduction of large amount of glucose enables the replenishment of the deficit.

The administration of intralipid provides extra calories to the affected individuals. Intralipid is composed of even-chain fatty acids, and hence, can avoid the activation of propionate catabolism.

1.9.3 Insulin

Insulin is also being considered as a potential management for MMAuria during acute illness. Although many laboratory studies have been done to evaluate its usefulness in treating the disease, its physiological effects promotes its use for treating the MMAuria patients clinically. These physiological effects include facilitating the uptake of amino acid precursors, promoting synthesis of fatty acids in liver [86], inhibiting the breakdown of fat in adipose tissue and increasing the uptake of glucose to the liver from several other tissues. One case report has been published on the utilization of insulin in combination with other regimens such as glucose administration, carnitine supplementation, low-protein/high-caloric diets, vitamin therapy (OH-Cbl and thiamine), and carglumic acid in MMA affected individuals with hyperammonaemia. The data showed a significant decrease of ammonia to normal within 3.5 days although the decrease in MMA levels was slower than that of ammonia [87]. Nevertheless, the real potential of insulin in treating MMAuria it is still unclear due to the involvement of other therapeutic managements. Therefore, more studies are required to investigate its use in the clinical treatment of MMAuria in the future.

1.9.4 Adenosylcobalamin Supplementation

Another regimen for this disease is AdoCbl supplements; however, the long-term outcomes in affected patients remain controversial. Clearly, none of the patients with mut^0 and mut^- would be expected to respond to AdoCbl supplementation [88]. However, the introduction of AdoCbl supplements has brought hope to patients with a deficiency of AdoCbl. Depending on the specific *Cbl*-mutation, patients respond to the supplementation to varying degrees. Regardless, it is essential to emphasise that although results show that the administration of AdoCbl produces a promising pharmacological effect on the patients, it can only reduce the MMA excretion rather than eliminate it. The possibility of using AdoCbl administration to improve the outcomes of pregnancy in women with MMAuria has also been studied [83, 89,

90]. Currently, 1mg per day to every other day of cobalamin B12 is clinically used for vitamin B12-responsive patients.

1.9.5 L-Carnitine Supplementation

Several case reports demonstrates the usefulness of L-carnitine supplementation in treating MMAuria [91]. Studies have shown that the accumulation of acyl-coenzyme A compounds in mitochondria associated with PAuria and MMAuria results in disruption of several metabolic pathways. Furthermore, in some cases, low levels of free carnitine are found in the organic acidurias due to the increased esterification with organic acid metabolites. Thereby, the purpose of L-carnitine administration is to remove the excess acyl-coenzyme A compounds by forming acylcarnitines and excretion of large amounts of acylcarnitine [91]. Moreover, studies have indicated that the administration of intravenous L-carnitine resulted in a better outcome than oral administration, with improvements in growth, less metabolic decompensation and a better tolerance of natural protein in the diet [92]. L-carnitine is currently being used orally at doses of 100 mg/kg/day.

1.9.6 Antibiotics

The importance of gut flora in the human body in the digestion of carbohydrates is well known. These bacteria provide the enzymes necessary for the breakdown of certain polysaccharides [93] into short chain fatty acids, a process known as fermentation. The products of fermentation are acetic acid, organic acids (e.g. >25% of PA comes from gut flora) [94] and butyric acid [95, 96]. Therefore, the elimination of these gut flora using either oral neomycin or metronidazole, at doses of 250 mg and 10-15 mg/kg/day respectively, improve the condition of MMAuria patients [97]. However, the risk of antibiotic-resistance gut flora with overuse may worsen the condition and pose a threat to the affected individuals.

For this reason, most protocols involve the intermittent use of antibiotics, for example for one week out of four.

1.9.7 Antioxidants

As mentioned earlier, increased MMA causes the depletion of GSH in the mitochondria, which leads to the build up of free radicals during oxidative stress. This phenomenon eventually results in cell death. Hence, another therapeutic option is to use oxygen-radical scavengers such as Coenzyme Q_{10}, GSH, MitoQ and idebenone. However, the beneficial effect of these drugs is not clear and needs to be further investigated [98, 99].

1.9.8 Other Treatments

In very few cases, N-Carbamylglutamate is used for the treatment of episodes of acute hyperammonaemia [81]. Hyperammonaemia is one complication that is observed in both PAuria and MMAuria patients and is due to the disturbance of the urea cycle in the liver. This is due to the inhibition of N-acetylglutamate synthase by the accumulation of propionyl coenzyme A in affected individuals, resulting in reduced production of carbymyl phosphate. Treatment of MMAuria using N-Carbamylglutamate, also known as carglumic acid, has been suggested as a means of reducing the ammonia level in affected individuals [100]. Although its impact in patients is less than laboratory studies would suggest, several cases have been reported regarding to the use of N-carbamylglutamate, which demonstrate the improvement of the clinical manifestation of MMAuria patients by reducing the ammonia levels in the blood [87].

1.9.9 Organ Transplantation

The study published by Chandler *et al.,* (2009), in which to investigate the pathophysiology of MMAuria and the examination of mitochondrial dysfunction that involved several tissues, such as liver, kidneys, pancreas and skeletal muscles, resulting in MMAuria, had revealed that the liver is a major target of mitochondrial pathology in MMAuria [101]. This is supported by the clinical studies, of which the liver and combined liver/kidney transplantations have been attempted with the aim of replacing the enzyme activity, thus preventing the need for dietary restriction and reducing long-term complications. To date, of all 27 reported cases of organ transplantations, liver transplantation (15 out of 27), kidney transplantation (6 out of 27) and combined liver-kidney transplantation (6 out of 27) have been reported [102]. Although this therapeutic option appears to protect the patients against acute metabolic decompensation and the quality of life is improved, the effectiveness of this treatment is still controversial [103, 104]. Clinical evaluation [102] showed that most of the patients who received organ transplantation suffered from common post-operative sequalae such as infection (7 out of 27), acute rejection (6 out of 27), immunosuppressive medication toxicity (3 out of 27) and continued neurologic deterioration (5 out of 27). Moreover, a clinical report published by Chakraprani *et al.,* (2002) [105] demonstrated the observation of progressive renal impairment after liver transplantation. This is also supported by Kaplan *et al.,* (2006) [103] and Kasahara *et al.,* (2006) [104], who both challenge the rationale of liver transplantation. However, a recent report of combined liver-kidney transplantation suggests stabilization is possible using this approach [106].

Despite the availability of these therapeutic options mentioned above, the outcomes reported are often disappointing, with morbidity and mortality remaining high, and with the chronic long-term complications remaining.

Beyond this, there have been no new advances in the treatment of this devastating chronic disease, and it is evident that the development of new therapy is a major priority.

1.10 Gene Therapy

Gene therapy is the treatment of disorders by introducing specific engineered genes into a patient's cells. It involves delivery of functional genes into the target cells to ameliorate, or cure the disease [107]. Proof-of-principle experiments in cell culture systems and success in animal models have demonstrated the general feasibility of gene therapy for many disease conditions. However, in terms of inherited diseases, and with the current available techniques, gene therapy is currently most applicable to monogenic diseases caused by recessive mutations [108], for example cystic fibrosis, in which a single functional copy of the gene associated with the disease is sufficient to rescue the mutant phenotype.

The theory behind somatic gene therapy is that genes are introduced into the cells within the body to promote the *in vivo* production of therapeutic proteins. Gene therapy can be categorized as either *ex vivo* therapy, in which the cells are treated with the genes outside the body before the transplantation of these corrected cells into the body, or *in vivo* therapy, in which the genes are introduced into the body directly. In addition, based on the vehicle used for gene delivery that is administered to the recipients, gene therapies can be classified into two groups. These are virus-based gene therapy, in which a genetically engineered, attenuated virus is used as a vector, and DNA-based gene therapy, in which pharmaceutical formulations of DNA are used.

Vectors are the means for introducing genes into cells. Depending on the vector, the methods used for introducing gene vectors may be varied. These methods include intraperitoneal, intramuscular and intravenous injection. Different delivery methods may also lead to gene

delivery to certain tissues and cell types. However, achieving therapeutic levels of gene transfer and expression still remains a significant challenge [109]. For example, in order for the gene to be expressed, it must be delivered into the nucleus of the cell. In addition, the DNA must be received by a large number of cells for the treatment to be effective. The challenge is even greater when the gene has to be expressed in a specific cell type, or when abnormal expression could be detrimental. All of these issues indicate an efficient gene delivery method is required for gene therapy to be successful.

1.10.1 Gene Therapy Applications

The applicability of gene therapy for any inherited disease depends on many factors. Firstly, the gene defect underlying the condition must be well studied. Secondly, the extent of gene expression, and when and how the gene functions in the body are all key factors that need to be investigated at the pre-clinical stage. In addition, the response of the body to the vector itself must be well understood. This is because not only must the efficacy of the approach be shown, but also the potential side effects of the gene therapy must be understood. For example, in 1999, an 18-year-old U.S. teenager, Jesse Gelsinger, died soon after receiving a gene therapy treatment for a rare inborn error of metabolism, the urea cycle defect ornithine transcarbamylase (OTC) deficiency. Additionally, several patients treated for severe combined immunodeficiency have succumbed to T-cell leukaemia that was caused by side effects of the treatment. Nevertheless, in some cases the promising results from animal studies have brought gene therapy for those particular diseases into human clinical trials [110]. A few examples are presented below.

1.10.2 Gene Therapy for Severe Combined Immunodeficiency

X-linked severe combined immunodeficiency (X1-SCID) is caused by the lack of differentiation of T- and natural killer lymphocytes. The disease results from defects in the

gene encoding the gamma cytokine receptor. Apart from gene therapy, the only treatment for this disorder is bone marrow transplantation. Therefore, gene replacement in the haematopoietic compartment has been seen as a potential cure for this disease. In 2004, Cavazzano-Calvo and her co-workers reported the success of gene therapy for this disease using a retroviral vector derived from Moloney murine leukaemia virus (MMLV) [111]. Fourteen patients have been treated and the data showed that the patients had been immunologically reconstructed by this new approach. Despite these promising results, a significant side effect of the treatment has become apparent. T-cell leukaemia has now been found in some of the recipients due to the characteristics of the vector used. Three patients developed T-cell leukaemia and one of these patients has now died. The genetic analysis showed that the morbidity was due to the activation of the proto-oncogenes LMO2, BMI1 and CCND2, and that this resulted from the vector integration. In addition, other genetic defects were also observed in these patients including chromosomal translocations, the activation of NOTCH1 *via* gain-of-function mutations, deletion of the tumor suppressor gene CKDN2A, 6q interstitial losses, and SIL-TAL1 rearrangement [112]. A number of technological approaches are currently being studied in an attempt to solve these issues. These include the utilization of self-inactivating vectors and the exploitation of non-oncogenic vectors. Recently, reports have also shown the possibility to cure the disease by using vectors derived from lentiviruses (LVs) or spumaviruses. However, further investigation is required before they can be used in clinical trials.

1.10.3 Gene Therapy for Cystic Fibrosis (CF)

CF, one of the most common lethal genetic disorders among Caucasians, has been targeted chiefly for somatic gene therapy. The disease results from the faulty gene that encodes the CF transmembrane conductance regulator which, through a complex aetiology, leads to progressive lung dysfunction. Several approaches have been developed in an attempt to cure

the disease but the results have been disappointing. In the early 90's gene therapy for CF was tested in a human clinical trial. Adenovirus was used as a vector due to its natural tropism for the airway [113, 114]. However, the results were unsatisfactory as the virus failed to infect the appropriate human airway target cells and was too immunogenic. In the late 90's a different vector system was used to overcome these difficulties. Based on the promising outcomes from primates, adenoviral-associated virus (AAV) was used as an alternative vector for the treatment [115]. However, the efficiency remains low as a result of the lungs defence systems. Non-biological vectors such as liposomes were also used as a vector but, again, failed to be effective. Attempts to use adenovirus (Adv) and LV as carriers are being studied in conjunction with the strategy to increase their efficiency by using lysophosphatidylcholine (LPC) to increase the efficiency of gene delivery [116-118]. The LV vector system has shown some potential to ameliorate the disease [119, 120].

1.10.4 Gene Therapy for Metabolic Diseases

The success of gene therapy for metabolic disease in animal models has been widely reported. Metabolic diseases such as familial hypercholesterolemia (FH), OTC deficiency, phenylketonuria (PKU), and MMAuria are all caused by single gene defects and in each case the pathology results from the accumulation of freely diffusible toxic metabolites. This suggests that these diseases may be treatable by the creation of a sink within the body that is capable of metabolizing these compounds. For instance, Chandler and Venditti have recently demonstrated rescue of a murine model of MMAuria, using an AAV-8 vector expressing mouse MCM. Their work showed not only that the mouse MCM can be expressed *in vivo* and functions properly, but also that the lifespan of the MMAuria mice, which usually die within 24 hours, was prolonged after treatment [121]. (This approach will be discussed more fully in the discussion section of Chapter 4 and 5). As we described previously, the patients who received organ transplantation as a treatment for MMAuria still suffered from side-

effects including infection, acute rejection and immunosuppressive medication toxicity. However, patients may be able to avoid these side-effects with gene therapy. Therefore, the successful development of gene therapy for MMAuria *in vivo* may provide an alternative treatment for patients in the future.

1.11 Viral Vector Systems

Gene therapy relies on the availability of an effective technology for gene delivery to the chosen tissue. However, in practice, this has been hindered by the inefficient delivery achieved with current approaches. Therefore, much effort has been put into the development of effective gene delivery methods. The development of viral vectors is based on the fact that viruses have evolved highly efficient mechanisms for introducing their genomes into host cells. Several viral vector systems are currently being investigated. These include Advs, AAVs, retroviruses, herpes simplex viruses (HSVs), LV and other viral vector systems. Adenoviruses, in particular, are now being used in human clinical trials for certain diseases, such as CF. Their strengths and weaknesses of each vector system are briefly described below.

1.11.1 Adenoviruses (Advs)

Advs are double-stranded linear DNA viruses, which are approximately 30-35kb in length. They usually cause respiratory, intestinal and eye infections in human. These viruses have evolved to become one of the promising vector systems in gene therapy due to their high efficiency in infecting dividing and non-dividing cells *in vitro* and *in vivo*. However, their major disadvantage is that their DNA is not incorporated into the host cells' DNA. This means that repeat dosing is required to sustain gene expression in the host cells. In addition, adenoviruses often stimulate inflammatory responses and this can limit the dosage used in the treatment [122]. Furthermore, the risk of attenuated virus forming infectious virus *via*

recombination in the patient is also a major concern [123]. However, Advs are currently being used for cancer treatment in clinical trials [124-126] where some of these identified drawbacks are potentially advantageous. Nevertheless, problems such as non-specificity of transgene expression that can induce toxicity in normal cells, the limitation of the therapeutic effect with the use of non-replicative viruses and poor transduction in human tumours due to the limited surface expression of the Adv receptor have limited its use. Much work has been done in these areas throughout the years to resolve the limitations of Advs. Currrently, the use of cancer-specific promoter systems, such as carcinoembryonic antigen (CEA), α-fetoprotein (AFP), mid-kine (MK), survivin, and telomerase, and the attempt to target not only cancer cells but also metastasized cancer cells by modifying the viral proteins, had been developed. Also, several modifications have been done to the Adv fiber in order to improve transduction efficiency for cancer treatment. Such newly modified cancer-specific Adv is ready to be tested *in vivo* and for clinical trials [127].

1.11.2 Adeno-Associated Viruses (AAVs)

AAV is a member of the parvovirus family and is a single-stranded DNA virus. Its replication cycle requires the presence of a helper virus such as adenovirus or herpes simplex virus. The ability of AAV to integrate stably into the host chromosome makes them a useful tool to treat these diseases for which long-term gene expression is required although in some tissues integration is slow and inefficient. They are also able to infect non-dividing cells such as neurons. Moreover, the wild type viruses are non-pathogenic. However, the use of AAV vectors in gene therapy is restricted by their small DNA capacity that typically does not exceed 4.5 kb.

1.11.3 Retroviruses

Retroviruses have also appeared to have a great potential for gene therapy. MMLV is the classic example of this family of viruses. Retroviruses have a single strand RNA genome. They infect the host cell through a specific receptor mediated process that results in the delivery of the RNA genome into the cytoplasm of the target cell. The RNA molecules are then reverse-transcribed into double-stranded DNA which integrates into the host genome, a reaction that is catalysed by a virus encoded enzyme, integrase.

The ability of these viruses to integrate their genes into the host genome enables long-term expression of the inserted gene. Therefore, repeat dosing is not required during treatment, thus minimizing the risk of an immunogenic response. However, a disadvantage of using retroviruses is that integration can also result in insertional mutagenesis, which can lead to the occurrence of cancer in the recipients. Also, retroviruses can potentially recombine with other viruses in the environment and give rise to infectious agents. These issues need to be addressed before this vector system can be fully utilized [128] in the clinic.

LV vectors have emerged as another useful choice for gene therapy. They appear ideal for long-term gene delivery/expression *in vivo*, in particular where the liver is the principle target tissue. Following is a brief description of this vector system.

1.11.4 Lentiviruses (LVs)

LV vectors, members of the family of retroviruses, can be divided into two groups. The first comprises primate-related viruses such as human immunodeficiency virus types 1 and 2 (HIV-1 and HIV-2), or simian immunodeficiency virus (SIV). The second consists of non-primate related viruses such as feline immunodeficiency virus (FIV), bovine immunodeficiency virus (BIV) and caprine arthritis-encephalitis virus (CAE). Unlike other

retroviruses, lentiviruses have the ability to transduce non-dividing cells, making *in vivo* gene delivery much more efficient.

In addition, like all retroviruses, LV vectors have the ability to integrate into the host genomes resulting in sustained expression and replication of the expression cassette into the daughter cells. Their vector proteins are not expressed in the host and they accommodate up to 8 kb or more of DNA insert.

1.12 Immune Response to Viral Vector

Although the potential application of gene therapy for treatment of genetic and acquired diseases have been extensively studied, the activation of innate responses against the viral vector and the acquired response that target the viral transduced cells, resulting in the poor transduction efficiency, has received great attention from many researchers as this may influence long-term stable expression of a therapeutic gene in patients. Immune responses can be triggered by contaminants in the production of viral vectors, as well as the cells used for virus production and inhibitors from the producing cell lines and by the vector particle itself. Although studies point to at least some causes of the immune response, comprehensive strategies to overcome this barrier are yet to be achieved.

1.12.1 The Activation of Immune Response by Viral Proteins

The immune response triggered by viral proteins can destroy the transduced cells and transgene product. Several *in vivo* studies have demonstrated an immune response against the transgene product in animals that received a viral vector [129, 130]. Briefly, a short-term and rapid innate response is activated due to the recognition of the virus by various cytokines such as interleukin-1 (IL-1), Tumour necrosis factor α (TNF-α) and Type 1 interferons (IFN). The accumulation of these cytokines, resulting from the inflammatory response, triggers antigen

presenting cells (APC), and subsequently, leads to the activation of the adaptive immune system.

The recognition of the foreign proteins or transgenic cells is due to the binding of T-cell receptors on T cells to antigens presented by the major histocompatibility complex (MHC) class I and II molecules. The adaptive immune system possesses the ability to recognise and kill transgenic cells, preventing the long-term expression of the desired gene. Moreover, memory cells are produced after the first exposure to each particular non-self antigen, potentially affecting the outcome of gene therapy and prohibiting the re-administration of viral vectors.

1.12.2 The Activation of Immune Response by Contaminants from Virus Production

Another potential trigger for the activation of the immune response is contaminants, such as host cell proteins, in the vector dose that originate from the production process. Baekelandt *et al*., (2003) [131] have demonstrated that impurities in LV vectors, such as membrane fragments derived from HEK293T cells *via* a budding mechanism, stimulate the immune response in the transduced host.

The last step of the LV life cycle is the production of viral envelope. The viral envelope largely consists of components derived from the host cell's membrane. This is because budding usually takes place either at the cell surface, through the plasma membrane or through membranes of the trans-Golgi or endosomal network. The plasma membranes are enriched in cholesterol, certain lipids, and glycosylphosphatidylinositol (GPI)-anchored proteins that function in various metabolic and signaling pathways [132, 133]. The cell surface also includes proteins that can induce an immune response.

Other impurities, such as inhibitory molecules from the cell line used for production, most often HEK293T cells, may also affect transduction efficiency. In fact, evidence from studies conducted by Le Doux *et al*., (1996) [134] suggested that poor gene transduction could be due to inhibitors released by the producer cells [134-136].

1.12.3 Strategies to Overcome Immune Response in LV vectors

Numerous strategies to optimise transduction efficiency by the production of high quality recombinant LV have been studied. Currently, the HEK293T cell line is commonly used in virus production due to its rapid growth and transfectability that facilitate large-scale virus production [137]. However, the use of the HEK293T cells can cause increased contamination of virus as HEK293T cells easily detach from the culture dish, resulting in inflammation and an immune response [131] if inadequate virus purification is performed.

Recently, a study conducted by Smith *et al*. (2009) [138] provided evidence to support the use of COS-1 cells in place of HEK293T cells for recombinant LV production. In their study, in which a three-plasmid LV packaging system was used, they presented the data that showed COS-1 cells work as effectively as HEK293T cells to produce infection-competent LV. In addition, they demonstrated that virus produced by COS-1 is better than the equivalent virus produced in HEK293T cells in terms of transduction ability by the measurement of GFP-expression in MCF-7 human breast cancer cells. They also measured the quality of LV produced by the COS-1. By analysing p24 levels they demonstrated that approximately 50-74 ng/mL of p24 equivalent of LV particles was produced from HEK294T cells compared to 18 ng/mL from COS-1 cells. Nevertheless, in terms of specific infectivity, LV produced from COS-1 cells demonstrated a ratio of infection-capable virus particles to total particles of approximately 0.31%, two to three-folds higher than HEK293T cells-produced LV, which had a ratio of 0.11-0.16%. Their results also demonstrated the disadvantage of using HEK293T

cells for virus production due to its characteristic of easily detaching from the plastic cell culture surface, which was shown to contaminate the LV with incompletely assembled p24 protein, reducing the viral particles performance index. In contrast, COS-1 cell culture supernatant contained only fully assembled p24 protein. The data suggested that the LV produced in COS-1 cells contains fewer impurities than the virus packaged in HEK293T cells. This advantage might help to reduce the risk of stimulating the immune response within the host although further experiment is required to validate this deduction.

Another possible strategy that can be employed to minimize the risk of stimulating the immune response is the use of a GP64 pseudotyped vector. Studies by Sinn *et al*., (2005, 2007 and 2008) [139-141] showed that persistent gene expression *in vivo* could be achieved using GP64 pseudotyped FIV vector (GP64-FIV). One of Sinn's studies [141], in which the efficacy of repeated administration of GP64-FIV to murine nasal epithelia was assessed, demonstrated that although a minimal level of adaptive immune response was detected against the GP64-FIV, this level was insufficient to affect gene transfer. Moreover, analysis at 4, 24 and 72 hours after delivery, indicated only a small increase in the response at 4 hours after delivery and a return to naive levels at 24 or 72 hours. Another study published by Pichlmair *et al*., (2007) [142] demonstrated a rapid and transient innate immune response in liver after administration of a VSV-G pseudotyped LV vector due to the production of contaminating tubulovesicular structures (TVS) during preparation of the vector. Their study showed an immediate induction of IFN α/β, produced by plasmacytoid dendritic cells (pDC), after the administration of VSV-G pseudotyped vectors, followed by the stimulation of cytotoxic T-lymphocytes (CTLs).

Another potential strategy to overcome the immune response is the employment of IFN α/β antibodies or IFN α/β receptor antagonists. However, further studies are required to evaluate their value to improve the effectiveness and persistency of gene expression in the target cells.

Macrophages play a key role in the body's defense system. They are derived from monocytes, which are part of the innate immune system, in found as cells resident in tissues. Their role is to engulf foreign molecules through phagocytosis and produce several kinds of proteins that are involved in the inflammatory process, such as complement proteins and IL-1. One of the limitations of gene transduction efficiency into hepatocytes is due to vector uptake by the Kupffer cells in the liver [143]. Kupffer cells being specialized macrophages located in the liver. The depletion of these cells has been shown to increase gene transduction efficiency [144-146]. A study by Snoeys *et al*., (2006) [147] demonstrated that this can also potentially be achieved with the use of intralipids, which act to block vector uptake into Kupffer cells.

1.13 Women's and Children's Hospital HIV-1 Vector System

The HIV-1 vector system used for this study utilises a number of different helper plasmids and a transfer vector [148-150]. These helper plasmids comprise expression plasmids for GagPol (*p*HCMVGagpollstmlwhvpre), Rev (*p*HCMVRevmlwhvpre), Tat (*p*cDNA3.1Tat101ml) and VSV-G (*p*HCMV-G). These plasmids encode the requisite viral proteins (Gag and Gagpol, Rev, Tat and VSV-G, respectively) for virus production. VSV-G is used in place of the HIV-1 envelope protein as it generates virus with a pantropic pseudotype that is able to infect most cell types with high efficiency. The transfer vector is a self-inactivating (SIN) vector, by virtue of a deletion in the 3' LTR U3 region. Virus is produced by transient transfection of these plasmids into 293T cells by $CaPO_4^-$ mediated co-precipitation. Two days after transfection the virus is harvested from the cell medium, purified and concentrated by ultrafiltration and ultracentrifugation, or, subsequently, by ion exchange chromatography.

1.14 Animal Model

The development of novel therapeutic approaches is highly dependent on accurate animal models to facilitate preclinical studies. This study will use an animal model of MMA that has been developed by Dr Heidi Peters from the Murdoch Children's Research Institute Cell and Gene Therapies Group (CID). The production of this animal model involved three stages as outlined below.

1.14.1 Knockout Mice

The coenzyme A binding domain in the MCM gene was disrupted to produce a null (knockout) phenotype in homozygous mice (Mut - / -) [151]. Heterozygous (Mut + / -) mice are biochemically and phenotypically normal. However, homozygous mice have a neonatal lethal phenotype. While they are indistinguishable from heterozygote littermates until ~ 18 hours, these mice then show a great reduction in activity and feed less. They then develop progressive deep sighing respirations indicative of acidosis and die within 24 hours. Biochemical assessment of homozygote mice demonstrates that an increase in urine MMA levels, to approximately 5 mM/mM of creatinine, after birth. Serial measurements on individual mice show a progressive increase of urine MMA level to 20 mM/mM of creatinine prior to death. The analysis of acylcarnitines demonstrated an increase in propionyl carnitine by 6-fold, compared to the normal prior to death. Also, an approximately 7-fold increase of the ratio of propionyl carnitine to free carnitine and to acetylcarnitine, prior to death, was found in these mice.

1.14.2 Transgenic Mice

A 170 kb genomic fragment containing the intact human mutase locus and flanking regulatory elements was used to produce a transgenic mouse line. Characterisation of these mice shows

that two copies of the human transgene are integrated at a single site in the transgenic line (muth2).

1.14.3 "Rescue" Transgenic Mice

A breeding program between the muth2 transgenic mice and heterozygous knockout mice is used to produce the knockout mice harbouring two copies of human transgene (Mut -/- muth2, or "Rescue" transgenic mice).

Biochemical assessments demonstrated that the hemizygous Mut -/- muth2 mice harbouring two copies of human transgene are biochemically and phenotypically consistent with an intermediate form of MMA. They are rescued from neonatal lethality and are marginally smaller than age and sex matched littermates. Biochemically, there is a significant increase in MMA level in the blood (500 mM at 8 weeks old) and urine (10-fold increase at 3 days of age). Their mutase enzyme activity, as measured by the propionate incorporation assay in cultured fibroblasts, is 20% of wild type control. Based on the study published by Peters *et al.,* (2012), their survival curve demonstrated that the mut -/- muth2 mouse model encountered a significant mortality rate in the first 6 months. The rate then reaches a plateau and follows the loss seen in control mice [152] and Appendix IV. Nevertheless, based on their data, this mouse model is able to live long enough (approximately 2 years) to allow therapeutic strategies to be successfully applied.

1.15 Research Questions and Hypotheses

Gene therapy may provide an option for treating the disease caused by MCM deficiency, either alone or to complement and improve conventional therapies. In most circumstances, except the blood brain barrier which has limited transport capacity for DCAs MMA and MCA [42], the toxic metabolites that accumulate in MMAuria are freely diffusible, suggesting that

the disease may be treatable by the creation of a sink that is capable of metabolizing these compounds. This means that gene therapy can be targeted to a particular organ, the obvious one being the liver, which is highly exposed to the circulation and is relatively easy to target for gene delivery. The partial success of liver transplantation in metabolic correction supports this proposal. On the other hand, it may be true that for effective treatment of the neurological and renal disease a targeted gene delivery approach (i.e., directly to the CNS and kidneys) will be required.

Therefore, there are a number of issues that remain to be investigated before the suitability of liver-mediated gene therapy can be assessed. These include:

1. the ability of gene therapy to deliver sufficient enzyme activity into the liver to normalize biochemistry; and
2. the optimal means for gene delivery to the liver in terms of efficiency and specificity of targeting.

1.15.1 Hypotheses

1. LV vectors will provide an efficient means for delivering the human MCM gene to the liver and that this will result in the efficient and long-term expression of MCM.

2. The expression of human MCM in the liver of hemizygous mut -/- muth2 mice will result in the restoration of MCM enzyme activity in the liver and, hence, create a metabolic sink, resulting in the reduction of MMA level in plasma and urine.

1.16 Aims of the Project

The overall objectives of this thesis were twofold. Firstly, this project will evaluate the vector that expresses human MCM under the transcriptional control of the elongation factor 1-alpha (EF1-α) promoter to determine if a LV vector is capable of delivering sufficient MCM activity to the MCM-deficiency fibroblasts. Secondly, to investigate the efficiency of the LV vector expressed in liver to correct the biochemical defect in all tissues, and the overt physical defects, in a mut -/- muth2 mouse model.

Hence, in order to achieve these objectives the specific aims were to:

1. to treat the MCM deficient fibroblasts with LV expressing human MCM

2. to investigate the viral transduction using real-time PCR

3. to measure the correction of metabolic pathway using [^{14}C]- radiolabelled propionate assay and high performance liquid chromatography

4. to treat the hemizygous mut -/- muth2 mouse model with LV expressing human MCM;

5. to assess the effect on disease biochemistry and pathology;

Chapter 2 : Materials and Methods

2.1 Materials

2.1.1 Tissue Culture

Disposable polystyrene tissue culture plates were from Corning Inc., NY, USA, tissue culture flasks were from Cellstar, Greiner bio-one, Monroe, North Carolina, USA and the pipettes were from Sarstedt Australia Pty, Ltd., SA, Australia. Other materials for tissue culture were obtained from the following suppliers.

Dulbecco's modified Eagle's medium (DMEM)	Sigma Chemical Co., St. Louis, MO, USA
Foetal Calf's Serum (FCS)	Gibco-BRL, Grand Island, NY, USA
Dulbecco's Phosphate Buffered Saline (PBS)	Sigma Chemical Co., St. Louis, MO, USA
Trypsine–Versene gamma irradiated	SAFC BioScience, Lenexa, Kansas, USA
Hexadimethrine bromide (Polybrene)	Sigma Chemical Co., St. Louis, MO, USA
Opti-Pro™ SFM	Gibco-BRL, Grand Island, NY, USA
Calcium Phosphate (pure phase)	Sigma Chemical Co., St. Louis, MO, USA
Calcium Chloride (USA testing specification)	Sigma Chemical Co., St. Louis, MO, USA
Bovine Serum Albumin (for electrophoresis)	Sigma Chemical Co., St. Louis, MO, USA
L-Glutamine solution (suitable for cell culture)	Sigma Chemical Co., St. Louis, MO, USA
Mouse serum albumin (essentially globulin free)	Sigma Chemical Co., St. Louis, MO, USA

2.1.2 Antibiotics

Gentamicin Sulfate	Astral Scientific Pty Ltd, NSW, Australia
Penicillin – Streptomycin (PS)	Sigma Chemical Co., St. Louis, MO, USA
Chloramphenicol	Sigma Chemical Co., St. Louis, MO, USA

2.1.3 Cell Lines

Human embryonic kidney (HEK293T)	ATCC CRL - 11268
Mouse embryo fibroblast (NIH3T3)	ATCC CRL - 1658
MCM knockout fibroblast	Murdoch Children's Research Institute, Melbourne, Vic, Australia

2.1.4 Antibodies

Mouse polyclonal to methylmalonyl coenzyme A Mutase(ab67869)	Abcam plc, Cambridge Science Park, Cambridge, UK
Mouse monoclonal to beta actin-horse radish peroxide (HRP) conjugate(ab8226)	Abcam plc, Cambridge Science Park, Cambridge, UK
Sheep anti-Mouse IG-HRP conjugated (AP326P)	Chemicon, Merck Millipore, Biillerica, MA, USA

2.1.5 Biochemical Assay Reagents

2.1.5.1 Urine Organic Acids

Ethyl Acetate (AR grade)	Chem-Supply, Gillman, SA, Australia
Diethyl ether ((for HPLC, and GC)	Merck Pty Ltd., Kilsyth, Vic, Australia
Iso-octane (for HPLC, and GC)	Allied Signal Inc., Muskegon, MI, USA

Pyridine (UNIVAR, AR grade)	Ajax Chemical, Sydney, Australia
Dichloromethane (UNICHROM, for HPLC)	Ajax Finechem, NSW, Australia
3,3-dimethylglutaric acid (DMG)	Sigma Chemical Co., St. Louis, MO, USA
Concentrated hydrocholoric acid (AR grade)	Fisher Scientific Inc., Vic, Australia
BSTFA/1% TCMS	Selectra-Sil, UCT Inc., Bristol, PA, USA

2.1.5.2 Determination of Plasma MMA

(2-($^2H_3$)-methyl)-malonic acid)	Sigma Chemical Co., St. Louis, MO, USA
BSTFA/1% TCMS	Alltech, Grace Davison Discovery Sciences, Vic, Australia
Methylmalonic acid level 2 serum toxicology control	Utak Laboratories Inc., Valencia, CA, USA
Methylmalonic acid	Sigma Chemical Co., St. Louis, MO, USA

2.1.5.3 Determination of MMA on Dried Blood Spots

(2-($^2H_3$)-methyl)-malonic acid)	Cambridge Isotope Laboratories, Inc., Andover, MA, USA
Acetonitrile (HPLC grade)	Scharlau, Sentmenat, Spain
Formic acid	Sigma Chemical Co., St. Louis, MO, USA

2.1.6 Electrophoresis Reagents

Acrylamide	Bio-rad Laboratories, Inc., NSW, Australia
N-N'-Methylene-bis-acrylamide	Gradipore, Pyrmont, NSW, Australia

Ammonium persulphate	Bio-rad Laboratories, Inc., NSW, Australia
N,N,N'N'-tetramethylenediamine (TEMED)	Bio-rad Laboratories, Inc., NSW, Australia
Coomassie brilliant blue R250	Sigma Chemical Co., St. Louis, MO, USA
Sodium dodecyl Sulphate (SDS)	Sigma Chemical Co., St. Louis, MO, USA

2.1.7 Ligation Assay

Ligation buffer (10x concentrated)	Roche Diagnostic GmbH, Mannheim, Germany
T4 DNA ligase	Roche Diagnostic GmbH, Mannheim, Germany
DNA polymerase (Klenow)	New England BioLabs Inc., Ipswich, MA, USA
Alkaline Phosphatase Calf Intestinal (CIP)	New England BioLabs Inc., Ipswich, MA, USA

2.1.8 Markers

Spp-1 *Eco*RI size markers	Geneworks, Adelaide, SA, Australia
Prestained protein ladder (Cat No:10748-010)	Life Technologies Corporation, Invitrogen, Vic, Australia

2.1.9 Primers

HIV-1 gag primers (forward and reverse), mouse transferrin primers (forward and reverse) and the Taqman probes (FAM-labelled) for both sets of primers were obtained from Life Technologies Corporation, Vic, Australia.

*p*BlueT7	Life Technologies Corporation, Invitrogen, Vic, Australia
*p*BlueRev	Life Technologies Corporation, Invitrogen, Vic, Australia
RREf	Gibco-Brl, Grand Island, NY, USA

2.1.10 Radiochemical

[1-^{14}C]-propionate (1.0 mCi/mL)	ICN radio-chemicals, Irvine, CA, USA

2.1.11 Restriction Enzymes

*Apa*I	NEB, Genesearch Pty. Ltd. Arundel, Queensland, Australia
*Bam*HI	NEB, Genesearch Pty. Ltd. Arundel, Queensland, Australia
*Bcl*I	NEB, Genesearch Pty. Ltd. Arundel, Queensland, Australia
*Bss*HII	NEB, Genesearch Pty. Ltd. Arundel, Queensland, Australia
*Eco*RI	NEB, Genesearch Pty. Ltd. Arundel, Queensland, Australia
*Nde*I	NEB, Genesearch Pty. Ltd. Arundel, Queensland, Australia

2.1.12 Substrates for Enzyme Reactions

Coenzyme B_{12}	Fluka Chemie GmbH, Buchs, Switzerland

Methylmalonyl coenzyme A tetralithium salt hydrate	Sigma Chemical Co., St. Louis, MO, USA
Succinyl coenzyme A sodium salt	Sigma Chemical Co., St. Louis, MO, USA

2.1.13 Buffers and Solution

2 x HEBS	50 mM HEPES, pH 7.05, 280 mM NaCl, 1.5 mM Na_2PO_4
2 x TY	16% (w/v) tryptone, 10% (w/v) yeast, 5% (w/v) NaCl
Lysis buffer	50 mM Tris-HCl 8, 2 mM NaCl, 1mM EDTA, 0.5% Tween-20
10 x TBE buffer	890 mM Tris base, 890 mM boric acid, 20 mM EDTA

SDS-PAGE Gel Stock Solution:

Solution A	30% Acrylamide, 0.8% N-N'-Methylene-bis-acrylamide (stored at 4 °C)
Solution B	10% SDS (stored at room temperature)
Solution C	3 M Tris-HCL, pH 8.65 (stored at room temperature)
Solution D	10% ammonium persulfate in distilled H_2O (made fresh)
Solution E	0.5 M Tris-HCL, pH 6.8, 0.4% SDS (stored at room temperature)

10% SDS-PAGE separating gel	10 mL solution A, 0.3 mL solution B, 3.75 mL solution C, 0.25 mL solution D and 15.7 mL distilled water, 18 µL TEMED
4.5% stacking gel	3 mL solution A, 5 mL solution E, 12 mL distilled H_2O 100 µL solution D, 20 µL TEMED
5x SDS electrophoresis buffer	125 mM Tris base, 0.96 M glycine, 17 mM SDS
SDS-PAGE transfer buffer	0.192 M Glycine, 25 mM Tris base and 20% (v/v) MeOH
Coomassie Brilliant Blue R250 stain	10% (v/v) acetic acid, 0.25% (w/v) Coomassie Brilliant Blue R250 and 45% (v/v) methanol
De-stain solution	45% (v/v) methanol and 10% (v/v) acetic acid
2x Tris buffered saline (TBS)	40 mM Tris-HCL, pH7.4, 0.5 M NaCl
SDS-PAGE blocking solution	1% (w/v) diploma skim milk powder in 1x TBS and 0.1% (v/v) Tween-20
2x Fairbanks buffer	10% (w/v) sucrose, 0.2% (w/v) SDS, 1.88 mM EDTA, 0.001% (w/v) bromophenol blue, 2 mM Tris-HCl, pH 6.8
10x Agarose gel loading buffer	50% (v/v) glycerol, 1 mM EDTA pH 8.0, 0.25% (w/v) bromophenol blue

2.1.14 Chemicals

Acetic acid glacial (UNIVAR AR grade)	Ajax Finechem, NSW, Australia

Agarose, low EEO	AppliChem, Darmstadt, Germany
Bacto™ Agar	Beckon, Dickinson and Company, Sparks MD,USA
Bacto™ Typtone	Beckon, Dickinson and Company, Sparks MD, USA
Bacto™ yeast extract	Beckon, Dickinson and Company, Sparks MD, USA
Big dye terminator v3.1 premix reagent	Life Technologies Corporation, Applied Biosystems, Vic, Australia
Big dye sequencing buffer	Life Technologies Corporation, Applied Biosystems, Vic, Australia
Bio-rad dye reagent concentrate	Bio-Rad Laboratories, Inc., NSW, Australia
10% Dextrose (IV infusion BP, 1000 mL)	Baxter Healthcare Pty. Ltd., NSW, Australia
Dextrose (to USP testing specification)	Sigma Chemical Co., St. Louis, MO, USA
Diploma Skim milk powder	Bonlac Foods, Melbourne, Vic, Australia
Dithiothreitol (DTT)	Bio-Rad Laboratories, Inc., NSW, Australia
Ethanol, 100% (AR grade)	Chem-supply, Gillman, SA, Australia
Ethidium bromide	Ameresco, Ohio, USA
Ethylenediaminetetraacetic acid (EDTA) (Electrophoresis grade)	ICN Biomedicals, Inc., Ohio, USA
Formic acid	Ajax Chemicals, Auburn, Australia
Glycerol	Merck Pty Ltd., Kilsyth, Vic, Australia
Glycine	Merck Pty Ltd., Kilsyth, Vic, Australia

Isofluorane	Abbott Australasia Pty. Lte., Botany, NSW, Australia
Isopropanol (UNIVAR AR grade)	Ajax Finechem, NSW, Australia
Methanol (HPLC grade)	Fisher Scientific Inc., Vic, Australia
N-[2-Hydroxyethyl]piperazine-N'-[2-ethanesulfonic acid] (HEPES)	Sigma Chemical Co., St. Louis, Mo, USA
OptiPhase 'HiSafe' 3 scintillant	Fischer Chemicals, Leicester, England
Potassium dihydrogen orthophosphate (UNIVAR AR grade)	Asia Pacific Specialty Chemicals Limited, NSW, Australia
Potassium Chloride (ACS reagent)	Sigma Chemical Co., St. Louis, Mo, USA
Sodium Acetate	Merck Pty Ltd., Kilsyth, Vic, Australia
Sodium Chloride	Ajax Finechem, NSW, Australia
Sodium Hydroxide (UNIVAR AR grade)	Ajax Finechem, NSW, Australia
Sodium phosphate	Ajax Finechem, Auburn, Australia
Sucrose (UNIVAR AR grade)	Ajax Finechem, NSW, Australia
50x TE buffer pH 7.5 (Ultrapure MB grade)	USB corporation, Cleveland, OH, USA
3,3,5,5-Tetrabomophenolsulfonphthalein (Bromophenol Blue)	BDH Chemicals Ltd., Poole, England, UK
3'3'5'5'-tetramethylbenzidine (TMB) (Liquid substrate system for membranes)	Sigma Chemical Co., St. Louis, Mo, USA
Trichloroacetic acid (ACS reagent)	Sigma Chemical Co., St. Louis, Mo, USA
Tris[hydroxymethyl]amino methane (Tris base)	Sigma Chemical Co., St. Louis, Mo, USA
Tween-20	BDH Chemicals Ltd., Poole, England, UK

2.1.15 Miscellaneous Materials

Capillary tubes (D941G-240-85-85 µL)	Radiometer, Copenhagen, Denmark
Screw cap vials (5182-0715)	Agilent Technologies Pty Ltd., Mulgrave, Vic, Australia
250 µL glass flat bottom vial insert (5181-3377)	Agilent Technologies Pty Ltd., Mulgrave, Vic, Australia
Red screw caps (5182-0722)	Agilent Technologies Pty Ltd., Mulgrave, Vic, Australia
1.5 mL clear glass snap ring vials	Grace Davison Discovery Sciences, Vic, Australia
250 µL glass flat bottom inserts	Grace Davison Discovery Sciences, Vic, Australia
11 mm snap top cap clear with PTFE/silicone	Grace Davison Discovery Sciences, Vic, Australia
Water for injection BP 100 mL	Pfizer (Perth) Pty. Ltd., Bentley, WA, Australia
Syringe filter Millex HV 0.45 µM filter	Millipore Corp., Carigtwohill, Co. Cork, Ireland
Syringe filter sterile EO (0.8 µM , non-pyrogenic, hydrophilic)	Sartorius Stedim Biotech GmbH, Goettingen, Germany
Syringe filter (0.2 µM)	Whatman Inc., Clifton, NJ, USA
Disposable screw cap culture tubes	Corning Inc., NY, USA
Deep skirted GPI 38-430 threaded phenolic screw cap with rubber liner	Corning Inc., NY, USA
MicroAmp Optical 8-cap strip	Applied Biosystems, Foster city, CA, USA
MicroAmp Optical 8-tubes strip	Applied Biosystems, Foster city, CA, USA

MicroAmp Optical 96-well reaction plate with barcode	Applied Biosystems, Foster city, CA, USA
MicroAmp Optical adhesive film (PCR compatible, DNA/RNA/RNAse free)	Applied Biosystems, Foster city, CA, USA

2.2 Methods

2.2.1 Cell Culture Techniques

2.2.1.1 Cell Lines

HEK293T cells, NIH3T3 cells and MCM knockout fibroblasts were routinely grown in Dulbecco's Modified Eagle Medium (DMEM) with 10% (w/v) fetal calf serum (FCS) in T75 flasks. It is of note that HEK293T cell line is used in our virus production method due to its rapid growth and transfection ability, facilitating large-scale virus production as described in section 1.12.3. Moreover, it is most widely used cell line in virus production. On the other hand, while COS-1 cells have been proposed as an alternative virus production cell line, there is little literature evidence that they are widely used, suggesting that their advantages may be overstated.

2.2.1.2 Cell Maintenance and Subculturing

Media was aspirated and 4 mL (per T75 flask) of PBS was used to rinse the cell monolayer. The PBS was then aspirated and 4 mL of trypsin-versene solution diluted 10-fold in PBS added and the flask incubated at RT until the cell monolayer detached from the substratum. DMEM/10% (w/v) FCS media was added and the cells were spritzed into a single cell suspension. Depending on the cells confluency, cells were then subcultured into a new flask containing the appropriate amount of growth media at a ratio ranging from 1:2 to 1:6.

2.2.1.3 Cell Harvesting

(A) From T75 flasks

The cell harvesting procedure is similar to the subculturing process with some minor modifications. Media was initially aspirated and 4 mL of PBS was used to rinse the cell

monolayer. The PBS was then aspirated and 4 mL of trypsin-versene solution diluted 10-fold in PBS added and the flask incubated at RT until the cell monolayer detached from the substratum. The cells were then collected into a 10 mL sterile tube containing 4 mL of 0.1% (w/v) FCS in PBS. The cells were then pelleted using a Megafuge 1.0R (Heraeus) at 1,500 g at room temperature for 5 minutes. The supernatant was aspirated and the cells resuspended in 1 mL of PBS by gentle pipetting. The cells were pelleted again and the supernatant aspirated. The cells were finally resuspended in 30 µL of PBS and stored it at -80 °C.

(B) Cell harvested from 6 - well plates

The procedures were taken similar to those as described above except 1 mL/well of 1 x PBS, 1 mL/well of trypsin-versene and 1 mL/microfuge tube of 0.1% (w/v) FCS in PBS were used when harvesting.

(C) Cell harvested from 12 - well plates

The procedures were taken similar to those as described above except 1 mL/well of 1 x PBS, 0.5 mL/well of trypsin-versene solution and 0.5 mL/microfuge tube of 0.1% (w/v) FCS in PBS were used when harvesting.

2.2.1.4 Large-Scale Virus Production

HEK293T cells were subcultured 1:4 into 5 x T75 flasks and incubated for 2 days until confluent. The 5 flasks were then subcultured 1:2 into 10 x T75 flasks. On the following day, the 10 flasks were expanded into 10 x 150 mm dishes. After overnight incubation, the cells were subcultured into 25 x 150 mm dishes. Cells were then harvested on the following day with 7 mL of trypsin / versene diluted 10-fold in PBS and 7 mL of complete media to spritz. The harvested cells were pooled into 2 x 1 L bottles containing 200 mL of complete media in each bottle. Cell numbers were determined using a haemocytometer and adjusted to

3.75 x 10^5 cells per mL in DMEM/10% (w/v) FCS/pen strep. The cell suspension was then dispensed into twenty one 245 x 245 mm plates at 107 mL/plate.

The cells were transfected the next day with the following plasmids:

Plasmid	DNA per plate (μg)
Vector (*p*HIV-SDmEF1αhMCM)	158
Tat	3.16
Rev	3.16
GagPol	7.9
VSV-G	7.9

$CaPO_4$ co-precipitation was performed by adding the plasmid DNA mix to 320 μL of 0.25 M $CaCl_2$ with H_2O added to give a total volume of 3.2 mL and then mixing the DNA/$CaCl_2$ solution with an equal volume of 2 x HEBS over 25 seconds while vortexing. The mixture was then further incubated for 90 seconds [150] before being gently dispensed onto the plates and incubated for 8 hours. The media was then changed by aspirating the media from the plate and replacing it with 170 mL/plate of pre-warmed Opti-Pro SFM supplemented with 20 mL and 10 mL of 200 mM glutamine and 100x PS antibiotic solutions, respectively. The plates were then incubated for 2 days before harvesting the supernatant.

2.2.1.5 Virus Purification Using QuixStand System

Virus purification consists of three major steps: filtration, ultrafiltration and ultracentrifugation.

A) Filtration

The virus-containing cell culture supernatant (total volume of 4.5 L) was collected from the plates and pooled into a weighed container. The virus suspension was then withdrawn from

the container and slowly pumped through an Amersham 0.45 µM hollow fibre cartridge (CFP-4-E-4MA, GE Healthcare Australia Pty. Ltd., Rydalmere, NSW, Australia) to remove cell debris and collected in a new 5 L of pre-weighed container. When the majority of the virus solution had been filtered, the original container was rinsed with 100 mL of 0.1% (w/v) BSA in PBS and filtration continued until all the solution had been filtered and collected.

B) Ultrafiltration and Diafiltration

Ultrafiltration was then performed in order to concentrate the virus into a predetermined volume so that it could be more easily concentrated further by ultracentrifugation. A 750 kDa ultrafiltration cartridge (UFP-750-E-4x2MA, GE Healthcare Australia Pty. Ltd., Rydalmere, NSW, Australia) was set up as in the schematic diagram 2.2.1-1. The filtered virus was circulated through the ultrafiltration system until all the filtered virus had been drawn into the reservoir (the total volume at this point should be approximately 1 litre). Following this, diafiltration was performed by feeding 3 L of PBS with 0.1% (w/v) BSA into the ultrafiltration setup and then continuing ultrafiltration until the virus solution was concentrated to approximately 360 mL.

C) Ultracentrifugation

The concentrated virus solution was refiltered through a serial assembly of three different filters, consisting of 0.8 µM, 0.45 µM, and 0.2 µM, prior to decanting into 6 x SW32 tubes (30 mL per tube). The virus was then pelleted by ultracentrifugation at 20,000 rpm for 90 minutes at 4 °C in a Beckman Coulter Optima L-100k ultracentrifuge. The supernatant was discarded and the virus pellets were resuspended in an appropriate volume (i.e. 1 to 1.5 mL) of 0.9% (w/v) NaCl and stored at -80 °C until use.

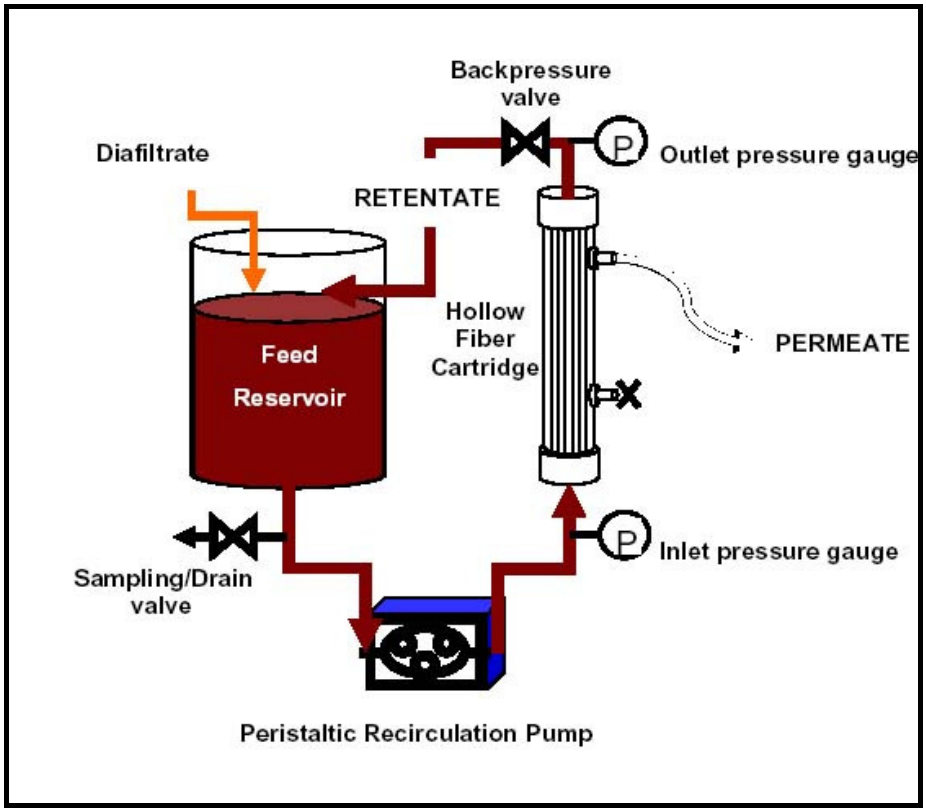

Figure 2.2.1-1 Schematic diagram of QuixStand system

2.2.1.6 Medium-Scale Virus Production

Medium scale production was performed as the large scale lentivirus production method but with some modifications. Ion exchange chromatography replaced ultra/diafiltration in the purification procedure. The schedule of subculture process was the same as described in method 2.2.1.4 with less plates used. The minor changes were that the cells were harvested and pooled in a single sterile 1 L bottle. Cell count was performed with haemocytometer and adjusted to 0.372 x 10^6 cells/mL. The cell suspension was plated onto six 245 x 245 mm plates and incubated overnight at 37 °C. Transfection was carried out *via* $CaPO_4$ co-precipitation and 293T cells were transfected with the same plasmid system and amount of DNA as described in section 2.2.1.4.

2.2.1.7 Ion Exchange Chromatography

The cell culture supernatant was pumped through an assembly of a Polydisc™ AS, 0.45 µM disposable polypropylene filter device and 2 x Mustang Q X75 ion exchange devices in series using a Watson Marlow Bredel 323 Dz pump (Figure 2.2.1-2). After all the virus had been loaded, the 0.45 µM filter was removed and the Mustang Q filter assembly washed with 3 x 10 mL of PBS. The virus was then eluted with 4 mL of 1.5 M NaCl into a sterile 10 mL tube. Four mL of 2% (v/v) mouse serum albumin was immediately added and mixed by gentle pipetting. The virus was then decanted into 2 x Beckman SW60 tubes and pellet by ultracentrifugation at 20,000 rpm, 4 °C for 90 minus in a SW60 rotor. The supernatant was discarded and the viral pellet resuspended in 300 µL of 0.9% (w/v) NaCl with the addition of 1% (w/v) mouse serum albumin to a final concentration of 0.1% (w/v) mouse serum albumin. The virus was then aliquoted into sterile tubes and stored at -80 °C until use (Figure 2.2.1-2).

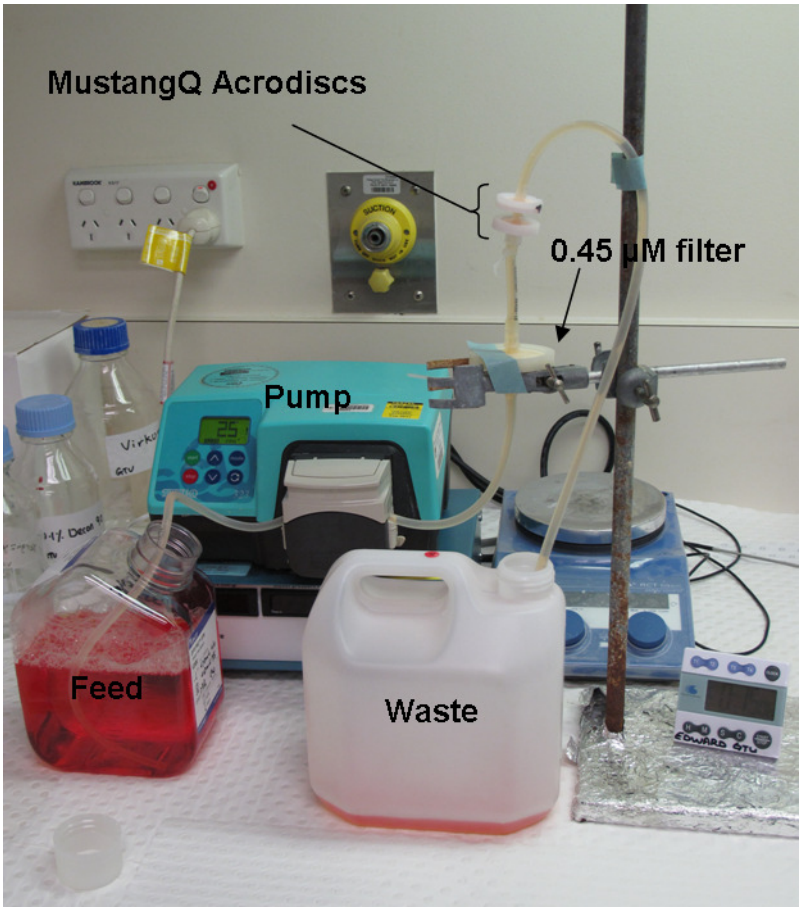

Figure 2.2.1-2 Photograph of medium-scale virus production setup

2.2.1.8 Small-Scale Virus Production

The HEK293T cells subculture procedures were same as described in section 2.2.1.2 except that they were expanded in DMEM/5% (w/v) FCS. The cells were subcultured 1:2 into 2 x T75 flasks and incubated for 2 days until confluent. The 2 flasks were then subcultured 1:2 into 4 x T75 flasks and further incubated until confluent on the next day. Cells were harvested with 4 mL of trypsin / versene solution diluted 20-fold in PBS and 4 mL of media to spritz and pooled into a 100 mL flask. Cell numbers were determined using a haemocytometer and adjusted to 3.75 x 10^5 cells per mL in DMEM / 5% (w/v) FCS / pen strep to make up a total volume of 11.5 mL. The cell suspension was then dispensed into a 100 mm dish and further incubated at 37 °C for 24 hours.

For virus production, transfection was carried out followed the procedures as stated in 2.2.1.4 with the plasmids mixture given below:

Plasmids	DNA per dish (1x)
Desired vector	18 µg
Tat	360 ng
Rev	360 ng
GagPol	1.8 µg
VSV-G	900 ng

$CaPO_4$ co-precipitation was performed by adding the plasmid DNA mix to 36 µL of 0.25 M $CaCl_2$ with H_2O added to give a total volume of 360 µL and then mixing the DNA/$CaCl_2$ solution with an equal volume of 2 x HEBS over 25 seconds while vortexing. The mixture was then further incubated for 90 seconds before being gently dispensed onto plates and incubated for 8 hours. Media was changed 8 hours after transfection with pre-warmed DMEM/5% (w/v) FCS and further incubated for 2 days. Media containing virus was harvested and filtered through a 0.2 µM filter. 1 mL of media was put aside for virus titre

measurement. The remaining media was adjusted to 20 mL with pre-warmed media supplemented with polybrene (to a final concentration of 4 μg/μL) and the addition of FCS to a final concentration of 10% (w/v) prior to adding to the target cells.

2.2.1.9 Elisa for the p24 Viral Coated Protein

HIV-1 p24 Elisa was performed using XpressBio p24 Elisa kits as per the manufacturer's instructions Standards were determined by diluting the p24 positive control in PBS/1% (w/v) FCS to concentrations of 200, 100, 50, 25, 12.5 pg/mL and with PBS/1% FCS only as a negative control. All virus samples were diluted in PBS/1% (w/v) FCS. Unconcentrated (i.e. cell culture supernatants) virus samples were diluted 1:6,000 whereas concentrated virus samples (i.e. final virus preparations) were diluted between 1:2,500,000 and 1:5,000,000. The OD at 490 nm was determined by Perkin Elmer 1420 multilabel counter with Wallac 1420 manager version 3 revision 4 software. A standard curve, of OD490 versus p24 concentration, was then plotted. The fit in the standard curve should yield an $R^2 > 0.9$. The slope *m* and the intercept *b* were determined. The virus concentration was then calculated based on the equation generated using these two parameters (Table 2.2.1-1). In addition, the concentration of lentiviral vector from each virus production (large- and medium-scale) is reported in Table 2.2.1-3.

Edward LV-MMA p24 ELISA Result: 06/11/2009

Std (pg/mL)	450 nm
0	0.410
12.5	0.513
25	0.657
50	0.916
100	1.344
200	2.202

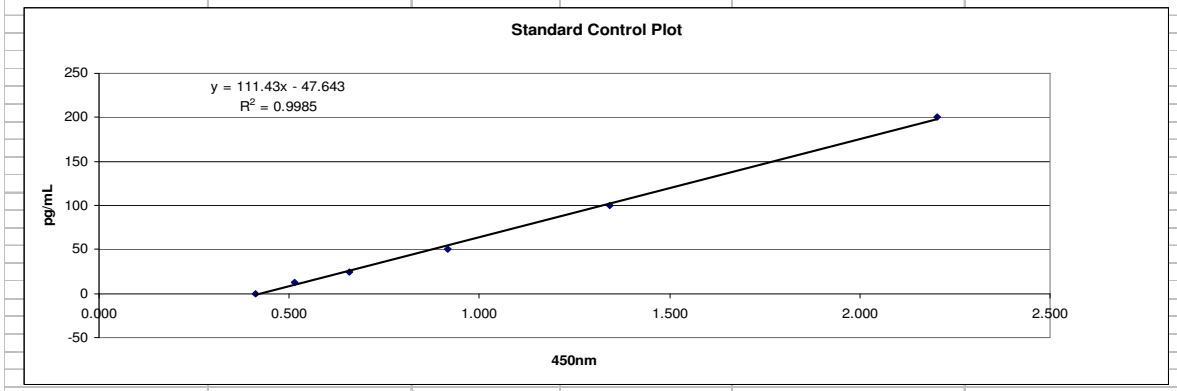

y=111.43x-47.643

Samples	Volume started (mL)	Virus x-fold concentrated
Pre-filter	1015	
Post-filter	1112	
Post-ultrafiltration	60.32	20
Final virus	0.3	3333

Samples	p24 dilution factor (1/x)	Abs(450nm)	Virus protein (pg/mL)	Virus production dilution factor	Virus protein (pg/mL)	Total Reservoir Volume (mL)	Total Mass	Each sample p24 recovery (%)
Pre-filter	2000	2.745	516552.0939		516552.0939	1020	526883.1357	100
Post-filter	2000	1.900	328074.543		328074.543	1120	367443.4881	69.73908694
Post-ultrafiltration	2000	3.072	589320.8577	20	11786417.15	586.9	6917448.228	1312.899913
Post-ultrafiltration waste	2000	0.521	20768.54317		20768.54317			
Post-ultracentrifugation waste	2000	0.917	109159.9815		109159.9815			
Final virus	**2000**	**3.146**	**605790.3525**	3333	2019099245	**0.3**	605729.7735	114.9647298
Pre-filter	10000	1.052	695397.1684		695397.1684	1020	709305.1118	100
Post-filter	10000	0.731	337830.8407		337830.8407	1120	378370.5416	53.34383403
Post-ultrafiltration	10000	2.833	2680232.678	20	53604653.56	586.9	31460571.18	4435.407366
Post-ultrafiltration waste	10000	0.383	-49467.1327		-49467.1327			
Post-ultracentrifugation waste	10000	0.565	153271.3047		153271.3047			
Final virus	**10000**	**3.134**	**3015273.572**	3333	10049906816	**0.3**	**3014972.045**	425.0599629

Table 2.2.1-1 Example of Determination of Total p24

2.2.1.10 Determination of Virus Titre by Real Time PCR

(A) 20 x gag and mouse transferrin PCR mix

The 20 x gag and mouse transferrin PCR mixes both consist of forward and reverse primers, each at a final concentration of 18 μM, and 5 μM of a TaqMan probe oligo. The primer stocks were kept at 100 μM in 0.5 x TE buffer, and the probe was supplied at 100 μM. The 20x PCR mix was prepared (total volume of 500 μL) by mixing 90 μL each of the forward and reverse primers with 25 μL of probe and 295 μL of 0.5 x TE buffer. The 20x mixes were aliquoted, (50 μL per aliquot), and stored at -20 °C until use.

Gag sequence:

Forward primer sequence: AGCTAGAACGATTCGCAGTTGAT

Reverse primer sequence: CCAGTATTTGTCTACAGCCTTCTGA

Probe sequence: 6FAM- CCTGGCCTGTTAGAAAC-NFQ

Mouse transferrin sequence:

Forward primer sequence: AAGCAGCCAAATTAGCATGTTGAC

Reverse primer sequence: GGTCTGATTCTCTGTTTAGCTGACA

Probe sequence: 6FAM- CTGGCCTGAGCTCCT-NFQ

(B) Titre assay and Sample preparation

NIH3T3 cells were plated in a 24-well plate at 0.25 x 10^6 cells/ well in a volume of 0.5 mL. Enough wells were set up to assay each sample in triplicate and including 3 wells as a negative control. After incubation at 37 °C, 5% CO_2 for 3 hours to allow the cells to attach the media was exchanged for DMEM/10% (w/v) FCS containing polybrene and gentamicin, at final concentrations of 4 μg/μL and 50 μg/μL, respectively, followed by an appropriate amount of virus. For viral supernatant samples from different purification stage, 1 μL or 0.1

μL of sample was added; And for concentrated virus, 2 μL and 10 μL of a 1:40000 dilutions virus were added. Incubation was continued for another 24 hours. Each well was then subcultured 1:4 into a new 24 well plate every 2 days for 2 weeks. Cells were harvested using 0.5 mL/well of Trypsin-versene solution diluted 10-fold in PBS. The cell suspension was transferred to 10 mL tube containing 2.5 mL of 1% (w/v) FCS in PBS and the cells pelleted at 1,500 g for 5 minutes using Heraeus Megafuge 1.0R. The supernatant was aspirated and the cells resuspended in 3 mL of PBS. The cells were again pelleted and the supernatant aspirated. Genomic DNA was then isolated using a Wizard SV genomic DNA isolation kit (Promega, NSW, Australia).

Gag and mTransferin assays were setup with the following reaction mix:

20 x assay mix	1 μL
2 x Taqman Universal PCR Master mix	10 μL
MilliQ H_2O	4 μL
gDNA sample	5 μL

The standard for the assay is genomic DNA isolated from NIH3T3 cells containing 1 copy of the virus genome per cell. The reading was determined by Applied Biosystems 7300 Real Time PCR system using 7300 System SDS software. The cycle threshold (Ct) values for each sample were determined. Virus titre was calculated by the following formulae: (Table 2.2.1-2). In addition, the virus titre from each virus production (large- and medium- scale) used in the study is reported in Table 2.2.1-3.

Virue titre Calculation Formulae

δCt = Ct of gag – Ct of mTransferin for a sample

$\delta\delta$Ct = δCt – the average δCt of the standard

$2^{\delta\delta Ct}$ = 2 raised to the prior of $\delta\delta$Ct

$1/2^{\delta\delta Ct}$ = 1 divided by $2^{\delta\delta Ct}$ = the copy number of gag within a cell

Titre = 250,000 x copy number x 1000/volume of virus added in µL
= infectious units/mL

Instrument Type: Applied Biosystems 7300 Real-Time PCR System															
Comments	**2 weeks real-time PCR**														
SDS v1.3															
Well	Sample Name	Detector	Task	Ct	ΔCt	Average Dct	ΔΔCt	$2^{-\Delta\Delta Ct}$	$1/2^{\Delta\Delta Ct}$	Virus Added (ul)	Titre (IFU/mL)	Ave Titre (IU/ml)	Total Volume (mL)	Total IU	Recovery (%)
A1	Pre-filter 1	gag	Unknown	34.62	6.99		7.285	155.9565	0.006412044	1	1.60E+06				
B1	Pre-filter 2	gag	Unknown	32.87	5.7		5.995	63.77858	0.015679246	1	3.92E+06				
C1	Pre-filter 3	gag	Unknown	32.28	5.38		5.675	51.0911	0.019572882	1	4.89E+06	3.47E+06	1015	3.52E+09	100
D1	Post-filter 1	gag	Unknown	32.57	5.35		5.645	50.03966	0.01998415	1	5.00E+06				
E1	Post-filter 2	gag	Unknown	33.06	6.1		6.395	84.15634	0.011882647	1	2.97E+06				
F1	Post-filter 3	gag	Unknown	32.72	5.31		5.605	48.67132	0.020545981	1	5.14E+06	4.37E+06	1112	4.86E+09	137.8202907
G1	Post-ultrafiltration 1	gag	Unknown	33.49	6.36		6.655	100.7754	0.009923055	0.1	2.48E+07				
H1	Post-ultrafiltration 2	gag	Unknown	31.79	5.3		5.595	48.33512	0.020688889	0.1	5.17E+07				
A2	Post-ultrafiltration 3	gag	Unknown	34.02	7.34		7.635	198.776	0.005030788	0.1	1.26E+07	2.97E+07	60.32	1.79E+09	50.83976279
B2	Post-ultracentrifugation 1	gag	Unknown												
C2	Post-ultracentrifugation 2	gag	Unknown												
D2	Post-ultracentrifugation 3	gag	Unknown												
E2	Post-ultrafiltration waste 1	gag	Unknown												
F2	Post-ultrafiltration waste 2	gag	Unknown												
G2	Post-ultracentrifugation waste 1	gag	Unknown	34.34	7.52		7.815	225.1902	0.004440691	0.1	1.11E+07				
H2	Post-ultracentrifugation waste 2	gag	Unknown	35.06	7.86		8.155	285.0359	0.00350833	0.1	8.77E+06				
A3	FV 0.01 1	gag	Unknown	29.5	1.77		2.065	4.18434	0.238986329	0.01	5.97E+09				
B3	FV 0.01 2	gag	Unknown	28.8	1.7		1.995	3.986161	0.250867937	0.01	6.27E+09	6.12E+09	0.3	1.84E+09	52.1255456
C3	FV 0.05 1	gag	Unknown	27.85	-0.22		0.075	1.053361	0.949342121	0.05	4.75E+09				
D3	FV 0.05 2	gag	Unknown	27.46	-0.7		-0.405	0.755236	1.32408891	0.05	6.62E+09	5.68E+09	0.3	1.71E+09	48.38330132
E3	Control 1	gag	Unknown												
F3	Control 2	gag	Unknown												
G3	Control 3	gag	Unknown	37.44	10.11		10.405	1355.867	0.000737535						
H3	Standard	gag	std	33.97	-0.34		-0.045	0.96929	1.031683179						
A4	standard	gag	Std	34.45	-0.25	-0.295	0.045	1.031683	0.969289817						
B4	negative	gag	negative												
C4	negative	gag	negative												
A5	Pre-filter 1	mTRANSFERIN	Unknown	27.63											
B5	Pre-filter 2	mTRANSFERIN	Unknown	27.17											
C5	Pre-filter 3	mTRANSFERIN	Unknown	26.9											
D5	Post-filter 1	mTRANSFERIN	Unknown	27.22											
E5	Post-filter 2	mTRANSFERIN	Unknown	26.96											
F5	Post-filter 3	mTRANSFERIN	Unknown	27.41											
G5	Post-ultrafiltration 1	mTRANSFERIN	Unknown	27.13											
H5	Post-ultrafiltration 2	mTRANSFERIN	Unknown	26.49											
A6	Post-ultrafiltration 3	mTRANSFERIN	Unknown	26.68											
B6	Post-ultracentrifugation 1	mTRANSFERIN	Unknown	27.16											
C6	Post-ultracentrifugation 2	mTRANSFERIN	Unknown	27.49											
D6	Post-ultracentrifugation 3	mTRANSFERIN	Unknown	27.45											
E6	Post-ultrafiltration waste 1	mTRANSFERIN	Unknown	27.08											
F6	Post-ultrafiltration waste 2	mTRANSFERIN	Unknown	27.02											
G6	Post-ultracentrifugation waste 1	mTRANSFERIN	Unknown	26.82											
H6	Post-ultracentrifugation waste 2	mTRANSFERIN	Unknown	27.2											
A7	FV 0.01	mTRANSFERIN	Unknown	27.73											
B7	FV 0.01 2	mTRANSFERIN	Unknown	27.1											
C7	FV 0.05 1	mTRANSFERIN	Unknown	28.07											
D7	FV 0.05 2	mTRANSFERIN	Unknown	28.16											
E7	Control 1	mTRANSFERIN	Unknown	27.76											
F7	Control 2	mTRANSFERIN	Unknown	27.68											
G7	Control 3	mTRANSFERIN	Unknown	27.33											
H7	Standard	mTRANSFERIN	std	34.31											
A8	standard	mTRANSFERIN	std	34.7											
B8	negative	mTRANSFERIN	negative												
C8	negative	mTRANSFERIN	negative												

Table 2.2.1-2 Example of Titre Determination for HIV-1SDmEF1αhMCM

LV Vector Concentration and Titre

Stock	Amount of LV vector used (μg of p24 equivalent)	Total Infectious Unit (IU)
1 (From Large-Scale Virus Production)	912	7.5×10^8
2 (From Medium-Scale Virus Production)	140.7	1.8×10^9
3 (From Medium-Scale Virus Production)	141.5	1.33×10^9
4 (From Medium-Scale Virus Production)	100	1.1×10^9
5 (From Medium-Scale Virus Production)	133	1.4×10^9
6 (From Medium-Scale Virus Production)	130.6	1×10^9
7 (From Medium-Scale Virus Production)	148	1.2×10^9

Table 2.2.1-3 LV vector concentration and viral titre of each virus production.

2.2.2 *In Vivo* Methods

2.2.2.1 Animal Ethics

Ethics approval for studies in hemizygous mut -/- muth2 murine and normal mice was granted by the Animal Ethics Committee of the Women's and Children's Hospital and the Adelaide University. All procedures carried out on these animals were in accordance with the guidelines set at by these committees and in accordance with NHMRC recommendations.

2.2.2.2 Orbital Bleed

Mice were anaesthetized with isofluorane/oxygen mixture in an induction box. Mice were then transferred to a mask connected to an anaesthetic machine with scavenger in place. Mice were monitored until they reached a surgical depth of anaesthesia as verified by the absence of the foot pinching reflex. A capillary tube was then inserted *via* the lateral canthus, at an angle of about 45°, into the venous plexus behind the eye with a twisting motion and the blood allowed to flow through the tube. A maximum of 100 µL of blood was collected per mouse. The mask was removed from the mice after collection and pressure applied with a sterile swab until haemostasis was achieved. Mice were observed until fully conscious.

2.2.2.3 Intraperitoneal (IP) Injection

The mouse was restrained by hand. The injection was made by inserting the needle through the skin at the lower quadrant of the abdomen and advanced through the abdominal muscles.

2.2.2.4 Intravenous (IV) Injection

The injection was made through the dorsal tail vein. The mouse was restrained by using a mouse holder with its tail exposed outside the holder. The tail was held firmly and gently warmed with the use of a heating lamp for 5 to 10 minutes to induce vasodilation, allowing

the blood vessel to be easily seen by the naked eye. An insulin needle with its bevel facing up was used for injection through the skin and into the lumen of the vein. The needle was advanced to about half a centimetre to prevent the needle sliding out from the lumen. Virus was then delivered by gently pushing the syringe plunger. No resistance was felt once the needle was successfully inserted into the lumen.

2.2.2.5 Urine Analysis

Urine was collected from each mouse in individual metabolic cages (Hatteras Instruments, Inc) overnight, with food and water available *ad lib*. A 100 µL- 1 mL sample was analysed for creatinine and a volume equivalent to 250 µg creatinine was used for analysis of MMA as follows. Ten µL of DMG was added to each sample as an internal standard. One mL of water was then added and the sample acidified to pH < 2, as measured by Universal pH – indicator strips (Merck), with 6 M hydrochloric acid. Subsequently, the mixture was saturated with 1.5 g of sodium hydroxide. The sample was then extracted using the method published by Tanaka *et al.,* (1980) [153]. The extract was derivatised with 50 µL of BSTFA/1% TCMS at 60 °C for 30 minutes. Ten µL of the derivatised sample was diluted with 100 µL of a pyridine and iso-octane mixture (1 mL:99 mL) prior to injection into a Hewlett Packard (HP 6890 series) GC/MSD. A standard curve of MMA was used to quantify the organic acid level in the urine sample.

2.2.2.6 Blood Analysis

Blood samples were collected using orbital bleed (method 2.2.2.2) at 0, 1 week, and 1, 3, 5, 7, 9, and 12 months into a heparin-coated capillary tube. The blood samples were microcentrifuged at 18,300 *g* for 10 minutes, the plasma decanted and stored at 4 °C until analysis. For measurement of MMA in plasma, 10 µL of 15 µM stable isotope-labelled internal standard, (2-($^2H_3$-methyl)-malonic acid) was added to each 10 µL plasma sample

(PS), which was then extracted using the method published by Marcell *et al*., (1985) [154]. The extract was derivatised with 1% BSTFA by heating at 60 °C for 30 minutes and the TMS ester quantified using a Perkin Elmer Turbomass GC/MS. A 100 µL of positive control, MMA level 2 serum toxicology control, was processed in a same way in each batch. Simultaneously, a response ratio sample (RRS) was prepared by evaporating a mixture of 10 µL of 15 µM MMA working solution and 10 µL of 15 µM stable isotope-labelled internal standard, (2-($^2H_3$-methyl)-malonic acid), derivatised with 1% BSTFA as described above. Selected ion monitoring at 247 m/z (for MMA) and 250 m/z (for 2-($^2H_3$-methyl)-malonic acid) was performed. The ratio of ions m/z 247/250 for RRS (typically 1.0), PS and the control sample were calculated. The PS ratio divided by the RRS ratio and multiplied by 1.50 followed by a dilution factor of 10 gives the concentration of MMA acid in µmol/L. Valid results were determined if the concentration of the control sample was 1.3 ± 10% µmol/L.

2.2.2.7 Dried Blood Spot MMA Testing

For measurement of MMA in whole blood, blood samples were spotted onto a filter paper (Guthrie card) and allowed to dry. A 3 mm diameter sample (representing 3.2 µL of whole blood) was then punched from the card , placed in a 5 mL glass tube and 5 µL of 15 µM of 2-($^2H_3$-methyl)-malonic acid added as a stable isotope-labelled internal standard. The sample was then extracted with 200 µL of solution that consisted of 99.5% (v/v) acetonitrile/H_2O (at a ratio of 1:1) and 0.5% (v/v) formic acid at room temperature for 15 minutes with shaking. The sample was then transferred into a 96 well plate and the MMA level was quantified using MS mass spectrometry according to the method published by La Marca *et al*., (2007) [78].

2.2.2.8 Clinical Observations

Animals were monitored (observation/weighing) once daily for the first week after vector administration. Subsequently, they were monitored weekly (observation/weighing). As the

mut -/- muth2 mice were physically smaller than normals, and the disease could result in metabolic decompensation, these mice were given additional nutrition in the form of sunflower seeds to supplement basic mouse feed.

2.2.2.9 Animal Care Requirements Before and After Treatments

By analogy to the human condition, it was assumed that the mut -/- muth2 transgenic mice were metabolically brittle. Hence, care was taken during procedures to ensure the animals were metabolically supported during experimental procedures (especially during administration of treatment). This was achieved by giving dextrose (1 mL, 10% (w/v)) *via* IP administration 2 hours prior to treatment followed by fat emulsion (intralipid), at 40 µL/g, 1 hour before treatment. After treatment, mice were kept in an incubator (Model C-86, Air-Shields Inc. Hatboro, Pennyslvania, USA) at 29 °C in a darkened room. In addition, sunflower seeds were provided on the bottom of the cage and moistened food pellets in a petri dish supplied daily.

2.2.3 Molecular Techniques

2.2.3.1 Electroporation of *E.coli*

Electroporation of *E.coli* Sure cells was achieved by mixing 1 µL of plasmid DNA with 5 µL of just-thawed electrocompetent cells. The bacteria-plasmid mixture was transferred to a BTX disposable electroporation cuvette on ice. The cuvette was then placed in an Electro Cell Manipulator (BTX electronic genetics) and closed with the safety interlock lid. The mixture was then electroporated at 1.5 kV and quickly transferred to a 10 mL tube containing 1 mL of 2x TY media and incubated for 1 hour at 37 °C in a shaker. Three hundred µL of the mixture was spread onto agar plates containing the relevant selective antibiotic and allowed to dry. The plates were incubated at 37 °C overnight to allow colonies to grow.

2.2.3.2 Rapid Plasmid Mini Prep

A single colony was grown in 1 mL of 2 x TY containing the appropriate antibiotic at 37 °C overnight in a shaking incubator. Five hundred µL of the culture was then removed and the cells pelleted at 18,300 *g* for 1 minute in a microcentrifuge. The supernatant was aspirated and pellet resuspended in 100 µL of lysis buffer (Section 2.1.13). One hundred µL of phenol chloroform was added and mixed by vortexing for 30 seconds. The samples were then centrifuged at 18,300 g for 5 minutes. Approximately 90 µL of the aqueous phase (top layer) was transferred to a fresh eppendorf tube and 60 µL of isopropanol added. The mixture was vortexed and then incubated at room temperature for 1-2 minutes. The samples were then centrifuged at 18,300 *g* for 10 minutes. The supernatant was aspirated and 50 µL of 70% (v/v) ethanol was added. The samples were then microcentrifuged again at 18,300 *g* for 10 minutes. Subsequently, the supernatant was aspirated and the DNA pellet resuspended in 20 µL of 0.5x TE buffer.

2.2.3.3 Restriction Enzyme Digestion of DNA

Digestion was carried out by incubating the DNA with the selected restriction enzyme under the conditions recommended by the manufacturer for 1-2 hours.

2.2.3.4 Ligation Protocol

The DNA to be ligated (inserts and vectors) were quantified by gel electrophoresis. The ligation was then set up with approximately 0.3 µg of vectors and a 3-fold molar excess of insert in 10 µL of 1 x ligation buffer and 1 µL of T4 DNA ligase in a total volume of 20 µL and incubated at 16 °C overnight.

2.2.3.5 Phenol Chloroform Extraction

An equal volume of phenol chloroform was added to the sample followed by vigorous vortexing for 2 minutes. The samples were then microcentrifuged at 18,300 *g* for 5 minutes. The aqueous phase (top layer) was then removed to a new eppendorf tube.

2.2.3.6 Ethanol Precipitation

One tenth volume of 3M Sodium Acetate, pH 5.2, was added to the samples and mixed by vortexing. Two point five to three volumes of absolute ethanol was then added to the samples and mixed by inversion. The samples were then incubated at room temperature for 1 hour followed by microcentrifuged at 18,300 *g* for 1 hour. The supernatant was discarded and the DNA pellet was resuspended in a suitable volume of 0.5x TE buffer.

2.2.3.7 Propionate Labelling

Cells were plated in 6-well plates and grown in DMEM/10% (w/v) FCS for 48 hours. The growth medium was then removed and the cell monolayer rinsed twice with PBS before addition of 1 mL/well of DMEM/1% (w/v) FCS/200 μM propionic acid/10 mM HEPES, pH7.5/1 μCi per mL [^{14}C]-propionate for 20 hours. The cells were then harvested, washed twice with PBS by resuspension and finally resuspended in 100 μL of 20 mM Tris-HCl pH 7.0, 0.5 M NaCl. The cells were lysed by 6 cycles of freeze/thaw and clarified by microcentrifugation at 18,300 *g* for 5 minutes at room temperature. Total protein of the supernatant was determined using the Biorad Protein Assay Kit (BIO-RAD Laboratories, Inc, NSW, Australia). The [^{14}C]-propionate incorporation into TCA precipitable material was subsequently determined by liquid scintillation counting (WALLAC 1409).

2.2.3.8 Trichloroacetic Acid Precipitation

Thirty eight µL of 24% (w/v) trichloroacetic acid was added to the samples, mixed, and incubated on ice for 30 minutes. The samples were then microfuged at 18,300 *g* and 4 °C for 15 minutes after which the supernatant was aspirated and 300 µL of cold acetone added to the pellet. The samples were then centrifuged at 4 °C for 5 minutes, the supernatant aspirated, and the pellet air dried at 37 °C. The pellet was then resuspended in 200 µL of 0.5 M Sodium Hydroxide. Counts were determined by addition of 2 mL of OptiPhase 'HiSafe' 3 liquid scintillation cocktail (Perkin Elmer) prior to analysis using a Tri-Carb 2910 TR Liquid Scintillation Analyzer (Perkin Elmer).

2.2.3.9 MCM Enzyme Assay

Fibroblasts were harvested as described in section 2.2.1.3 and lysed by sonication at 25 W for 20 minutes at 0 ^{o}C. The cell lysates were then microcentrifuged at 4,200 *g* for 10 minutes at 4 °C and the supernatant decanted and assayed for MCM enzyme activity by a modification of the method of Kikuchi *et al*., (1989) [155]. The reaction mixture (in a final volume of 90 µL) contained 0.2 M Tris-sulphate buffer, pH 7.5, 0.8 mM methylmalonyl coenzyme A, cell lysate (~100 µg total protein) and 130 µM AdoCbl. The reaction mixture without the methylmalonyl coenzyme A was pre-incubated for 10 minutes at 37 °C before initiating the reaction by addition of the methylmalonyl coenzyme A. A 45 µL aliquot was then immediately removed from the mixture and the reaction terminated by the addition of 7.3 µL of 24% (w/v) trichloroacetic acid (zero time point sample). The remainder of the reaction was incubated for 15 minutes at 37 °C and then terminated as stated above. The samples were centrifuged at 16,900 *g* by microcentrifugation for 10 minutes, the supernatant decanted to a fresh tube and neutralised with 7.5 µL of 1 M Tris-base. Twenty µL of the final supernatant was then used for High-Performance Liquid Chromatography (HPLC) analysis.

The HPLC system consisted of a G1379A degasser, a G1312A Bin Pump and a G1328 manual injector (Agilent). An Alltech Alltima™ C18-LL HPLC column (5 µM, 150 x 2.1 mm) was equilibrated with 100% solvent A (50 mM KH_2PO_4, pH 3.5) for 20 minutes prior to injecting the sample. Once injected, solvent A was gradually mixed with increasing proportions of solvent B (100% (v/v) MeOH) over 5 minutes to the desired ratio of 80:20 for subsequent analysis. A flow rate of 0.5 mL/min was used for assaying samples. The coenzyme A derivatives were detected at 254 nm using a G315B DAD UV detector. Methylmalonyl coenzyme A and succinyl coenzyme A peaks were detected at approximately 11 min and 13 min, respectively.

2.2.3.10 Isolation of Genomic DNA

DNA was isolated from cultured cells and tissue samples using the Wizard SV genomic DNA isolation kit according to the manufacturer's instructions.

2.2.3.11 Real-Time PCR Analysis for Gene Vector Copy Number

Vector copy number was determined by real time PCR analysis of HIV-1 *gag* gene sequences present in the vector as described in section 2.2.1.10 with results normalized to transferrin gene sequence copy number.

2.2.3.12 Agarose Gel Electrophoresis

Separation of DNA fragments was performed on 1.5% (w/v) agarose gels in 1x TBE buffer, containing 0.5 µg/mL Ethidium bromide. The gel was prepared on the Kodak Biomax QS710 gel apparatus. All DNA samples, including the marker, were made to 1x loading buffer. Gels were run at 90 mV until the dye marker had migrated an appropriate distance. Gels were photographed under UV light using UVIPhoto MW version 11.01 for Windows.

2.2.3.13 Large-Scale Plasmid Purification

Large scale plasmid purification was performed using the Endofree Plasmid Gigaprep (Qiagen GmbH, Hilden, Germany) kit as specified by the manufacturer.

2.2.3.14 Agarose Gel Extraction of DNA Fragments

The Adbiotech Gel Extraction Kit (Cat # GEK-1) was used to extract DNA fragments from agarose gel.

2.2.3.15 Bio-Rad Protein Assay

The protein assay was conducted by following the instruction given by the manufacturer (Bio-Rad). The standard curve was generated by using 1, 3, 5, 10, 15, 20 µg of BSA protein. Generally1 µL of cell lysate was assayed.

2.2.3.16 DNA Sequencing

DNA sequencing used 0.5 µg of the desired DNA, 1 µL of primer, 2 µL of Big Dye Terminator v3.1 reagent, 1 µL of 5x Big Dye sequencing buffer and water to make up a total volume of 10 µL. Sequencing reactions were run under following conditions in a thermal cycler (Bio-rad).

1x	94 °C	1:30 mins	
	95 °C	20 seconds	→ 25x
	50 °C	20 seconds	
	60 °C	4 minutes	
1x	60 °C	5 minutes	
1x	4 °C	hold	

Sequencing products were precipitated with the addition of 40 µL of 75% (v/v) isopropanol and incubated at room temperature for 15-20 minutes. Products were microcentrifuged for 15-20 minutes. The supernatant was aspirated and washed with 250 µL of 75% (v/v) isopropanol. Samples were then microcentrifuged for 5 minutes. Again the supernatant was aspirated and the pellet dried at 65 °C. Sequencing reactions were analysed at the SA pathology sequencing facility at the following link: (http://www.imvs.sa.gov.au/wps/wcm/connect/sa+pathology+internet+content/imvs/diagnostic+services/genetics+and+molecular+pathology/gene+sequencing). DNA sequences were analysed using software Vector NTI advance v11.0 (Invitrogen Corporation).

Primer sequences:

The target sites of the T7, Rev and RREf primers are shown in Figures 2.2.3-1 and 2.2.3-2.

*p*Blue T7 – GACGTTGTAAAACGACGGCCAG

*p*Blue Rev – CACAGGAAACAGCTATGACCATG

RREf – CTAAGGGATCAACAGCTCCT

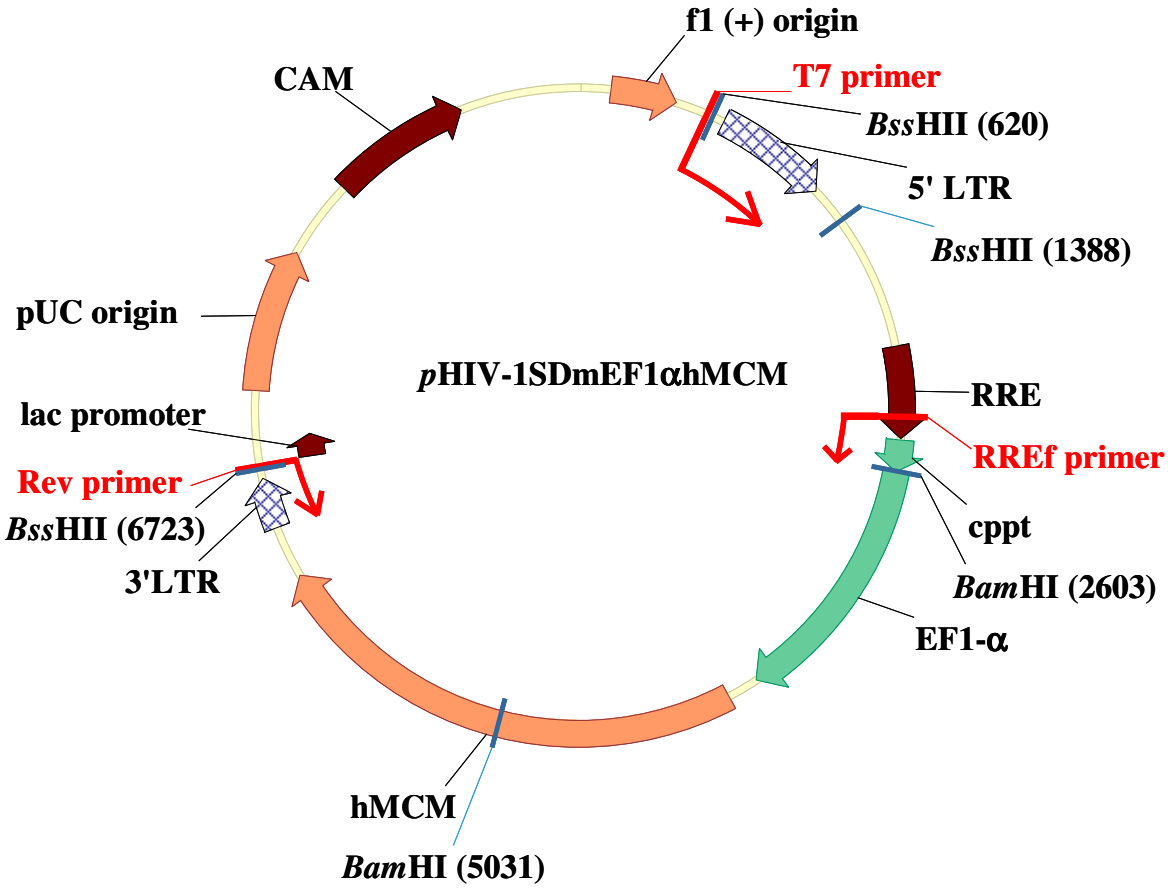

Figure 2.2.3-1. Target sites for the T7, Rev and RREf primers in the *p*HIV-1SDmEF1αhMCM vector.

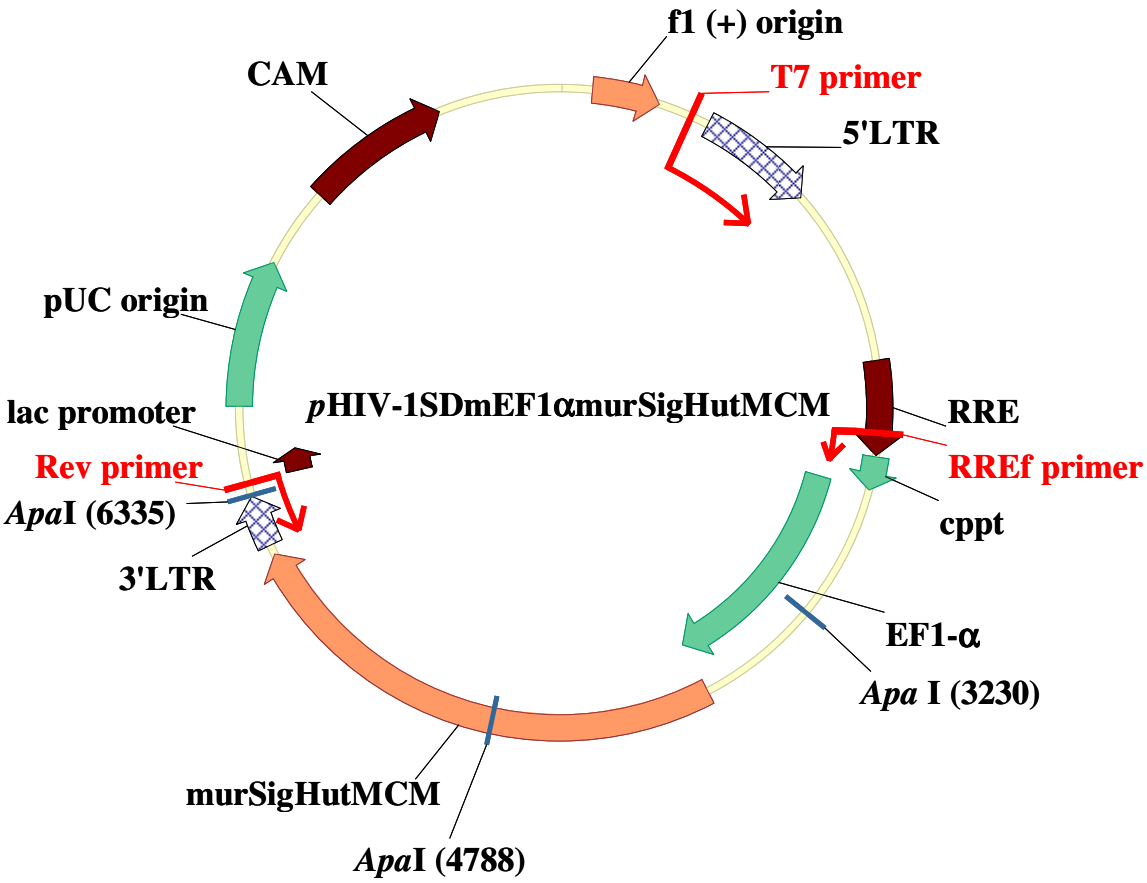

Figure 2.2.3-2. Target sites for the T7, Rev and RREf primers in the *p*HIV-1SDmEF1αmurSigHutMCM vector.

2.2.3.17 Western Blots

Western blotting is the transfer of electrophoresed proteins from a polyacrylamide gel onto a nitrocellulose or PVDF membrane. The membrane is then probed with antibodies allowing detection of specific proteins.

The crude cell lysate samples were clarified by microcentrifugation at 18,300g, 4°C for 10 minutes. The cleared lysate was then decanted into a new eppendorf tube. The protein concentration was then determined using the Bio-rad protein assay. A 10 µL sample containing 25 µg of lysate protein was prepared, mixed with an equal volume of 2x Fairbanks buffer with 2% (w/v) DTT, and incubated at 100 °C on a heating block prior to loading onto a 10% (w/v) polyacrylamide minigel. Simultaneously, a benchmark™ pre-stained protein standard, at 10 µL/ well, was loaded. The gel was electrophoresed at 40 mA using a 2103 Power Supply (LKB BIOCHROM) until the blue dye front was at the bottom of the gel (approximately 60 minutes).

Following this, the transfer procedure was carried out by blotting onto a nitrocellulose or PVDF membrane. The required materials (case, sponge, Whatman chromatography paper, membrane, gel) are pre-wet in transfer buffer and stacked in the following order:

- Cassette (clear side)
- Sponge
- Whatman chromatography paper
- Membrane
- Gel
- Whatman chromatography paper

- Gel
- Sponge
- Cassette (Black side)

After this, the case was placed in the transfer apparatus with a small magnetic bar at the bottom. Transfer was done at 250 mA using Electrophoresis Power Supply EPS 500/400 (Pharmacia) for 60 minutes in a cooled chamber with stirring.

The polyacrylamide gel was stained with 0.25% (w/v) Coomassie Brilliant Blue / 45% (v/v) methanol and 10% (v/v) acetic acid for 45 minutes followed by de-staining with 45% (v/v) methanol and 10% (v/v) acetic acid to determine whether the proteins had been transferred from the gel.

The membrane was removed from the cassette and blocked for 2 hours in 50 mL of 20 mM Tris buffer, pH 7.4, 5% (w/v) skim milk, 0.25 M NaCl, 0.1% (v/v) Tween 20 with gentle agitation on a platform rocker (Bioline). Following this, the membrane was washed three times in 20 mM Tris buffer, pH 7.4, 0.25 M NaCl, for 5 minutes per wash. The membrane was then incubated with the anti- human methylmalonyl coenzyme A antibody and the mouse anti-beta actin monoclonal, diluted 1 in 750 and 1 in 500, respectively, in 3 mLs of 20 mM Tris buffer, pH 7.4, 0.25 M NaCl, 5% (w/v) skim milk overnight in a sealed bag at room temperature with gentle agitation. The membrane was then removed from the sealed bag and washed three times in 20 mM Tris buffer, pH 7.4, 0.25 M NaCl as described above. The membrane was then incubated with secondary antibody, HRP-conjugated sheep anti-mouse serum, diluted 1 in 1500 in 3 mLs of 20 mM Tris buffer, pH 7.4, 0.25 M NaCl, 5% (w/v) skim milk in a sealed bag at room temperature for 1 hour with gentle agitation. The membrane was

then removed from the sealed bag and washed 3 x 5 minutes each in 20 mM Tris buffer, pH 7.4, 0.25 M NaCl as above.

Subsequently, the membrane was probed with TMB until the bands were visualised prior to washing the membrane with water to stop the reaction. The membrane was air-dried and sealed in a plastic bag for photography.

A freeware analysis program, ImageJ v1.45, (http://imagej.nih.gov/ij/download.html) was used to analyse the band intensity to allow quantification.

2.2.3.18 Statistical Analysis

P values were considered significant in all cases if the values were less then 0.05. The statistic analysis of bodyweight was done by comparing the linear regression (R^2) between the treatment groups using SAS software (SAS Institute Inc.). In all cases, unless specified, all other statistical analyses were conducted using one-way ANOVA with a post-hoc Tukey's test to determine the significance differences in plasma and urine MMA level, MCM enzyme activity and MCM protein expression between treatment groups.

2.3 Optimization of the HPLC Method for Measurement of MCM Enzyme Activity

2.3.1 Introduction

The most widely used protocol to determine MCM enzyme activity is the measurement of [^{14}C] – propionate incorporation in cultured cells. However, the clinical value of this method has been questioned as it provides only an indirect measure of MCM activity. Several other methods have also been developed to directly measure MCM activity. These methods include radioactive assays, in which [^{14}C]-methylmalonyl coenzyme A (substrate) and [^{14}C] - succinyl coenzyme A (product) are separated by paper chromatography [156, 157], thin layer chromatography [158, 159], electrophoresis [160], potassium permanganate oxidation [161], or gas chromatography [162]. However, the technicalities associated with these methods have limited their use.

A simple and rapid nonradioactive assay for MCM activity using reverse –phase HPLC was reported by Kikuchi. *et al*., (1989) [155]. In addition, Corkey and colleagues [163] established an analytical method to separate a group of short-chain acyl-coenzyme A compounds. The establishment of the HPLC conditions to measure the methylmalonyl coenzyme A and succinyl coenzyme A in our study, which were discussed in section 2.2.3.9, was based on these studies. This section will discuss optimization of chromatographic conditions for the quantitative determination of methylmalonyl coenzyme A and succinyl coenzyme A.

2.3.2 Methods

2.3.2.1 Calibration Curve

A set of succinyl coenzyme A working standard solutions, at concentrations ranging from 0.1 mM to 1 mM, was prepared by diluting aliquots of a 4 mM stock solution in water. A calibration graph was constructed by plotting the peak areas versus concentration of succinyl coenzyme A.

2.3.2.2 Determination of Optimum Incubation Time and Methylmalonyl Coenzyme A Concentration

The reaction mixture, in a total volume of 200 µL, was prepared as described in section 2.2.3.9 with methylmalonyl coenzyme A at concentrations of 0.15 mM, 0.8 mM and 1.5 mM and 100 µg of HEK293T lysate protein. Incubation was at 37 °C for 30 minutes. Aliquots (25 µL) of each reaction were taken at 0, 1, 3, 5, 10, 15, 20 and 30 minutes. The reaction was stopped by adding 4 µL of 24% trichloroacetic acid to the sample. The trichloroacetic acid precipitated proteins were removed by centrifugation at 16,900 *g* for 10 minutes and the supernatant decanted to a fresh tube and neutralized with 4.5 µL of 1 M Tris-base. Twenty µL of the neutralised supernatant was then used for HPLC analysis.

2.3.2.3 Determination of the Optimum Quantity of Cell Lysate

The reaction mixture, in a total volume of 150 µL, was prepared as described in section 2.2.3.9 with either 0, 50, 100 or 250 µg total protein HEK293T cell lysate. Aliquots (25 µL) of each reaction were taken at 0, 1, 3, 5, 10 and 15 minutes and analysed as described in the previous section.

2.3.2.4 Determination of the Limit of Detection of HPLC

The reaction mixture was prepared using 100 µg of a mixture of normal and MCM deficient (mut -/- muth2 mouse) liver lysate in the following ratios (100:0, 90:10, 75::25 , 50:50, 25:75, 10:90, 7.5:92.5, 5:95, 2:98, 0:100). Each of these lysate mixtures was incubated with 0.8 mM of methylmalonyl coenzyme A in the presence of 120 µM of AdoCbl at 37 °C for 15 minutes. Aliquots (25 µL) of each sample were taken at 0 and 15 minutes. The reaction was stopped and samples prepared for HPLC analysis as described in the previous section.

2.3.3 Results

2.3.3.1 Chromatography

The chromatography trace of the methylmalonyl coenzyme A and succinyl coenzyme A standards are shown in Figure 2.3-1. The chromatography conditions were modified based on the conditions adapted from Kikuchi *et al*., (1989) [155] and Corkey *et al*., (1981) [163]. These modifications include, (A) Change of pH for the 50 mM KH_2PO_4 from 5.3 to 3.5, (B) The two mobile phases, 50 mM KH_2PO_4 (buffer A) and 100% methanol (buffer B), were mixed to the desired ratio of 80:20, starting from a ratio of 100% of buffer A in gradient conditions over 5 minutes and then run isocratically for the next 25 minutes, (C) The flow rate was reduced from 1.0 ml/min to 0.5 ml/min, and (D) A different C_{18} HPLC reversed phase column (Alltech Alltima™ C18-LL reversed phase column, 5 µM, 150 x 2.1 mm) than that specified in Corkey's study (Nova-pak™ C18 reversed phase column, 15 cm x 4 mm, Waters Association Inc.) was used. These modified conditions were used to ensure high sensitivity, rapid conversion and optimal peak shape. Under these conditions, the retention times for methylmalonyl coenzyme A and succinyl coenzyme A were approximately 11 and 13 minutes, respectively.

2.3.3.2 Calibration Curve

Calibration curves were linear, R^2 = 0.997, and demonstrated that peak areas were directly proportional to the amount of succinyl coenzyme A in the range of 0.1 mM to 1 mM. The amount of succinyl coenzyme A formed in the reaction was calculated based on this calibration standard curve as (y) = 35615x, where y is peak area and x is concentration (Figure 2.3-2).

2.3.3.3 MCM Assay

The conversion of methylmalonyl coenzyme A to succinyl coenzyme A was linear with time up to 15 minutes. Linearity was also achieved with each of the different amounts of cell lysate (Figure 2.3-3, Figure 2.3-4 and Figure 2.3-5).

2.3.3.4 Limit of Detection

The MCM enzyme activity from different ratios of active (normal) and deficient (mut -/- muth2 mouse) liver lysate samples was measured (Figure 2.3-6). The formation of succinyl coenzyme A, at 192.7 ng/min/μg of lysate protein, was detected in the sample in which 100% normal liver lysate was used in the reaction. This was then used as a reference for 100% MCM enzyme activity. The results using the other ratio mixtures demonstrated decreases in MCM enzyme activity with the reduction of the percentage of normal liver lysate. It shows the detection of MCM enzyme activity with the 10% of normal liver lysate mix. Nevertheless, the total MCM enzyme activity was higher than expected. Peters *et al*., (2012) [152], using the (indirect) [^{14}C] – propionate incorporation assay, determined a level of 20% of normal MCM activity in cultured fibroblasts extracted from the mut -/- muth2 mouse. Therefore, the 10% normal/90% mut -/- muth2 mouse liver lysate mixture should theoretically contain 28% (10% normal liver lysates + 20% x 90% mut -/- muth 2) of total MCM enzyme activity while the 5:95 mix should theoretically contain 24% of total MCM enzyme activity.

As the HPLC results showed that enzyme activity was not detected in the samples in which greater than 90% of the mut -/- muth2 liver lysates sample were used, this suggests the threshold for detection with the HPLC assay is about 25% of normal. However, this analysis is complicated by the fact that the [^{14}C] – propionate incorporation assay detects 7% activity in the MCM homozygous knockout mice, suggesting that this method may overstate MCM activity, especially at low levels. If the 7% figure is taken as background then the real level of MCM activity in the mut -/- muth2 mice is approximately 13% of normal. Based on this assumption, the MCM levels in the 10:90 and 5:95 normal: mut -/- muth2 mixes becomes 21% and 17%, respectively.

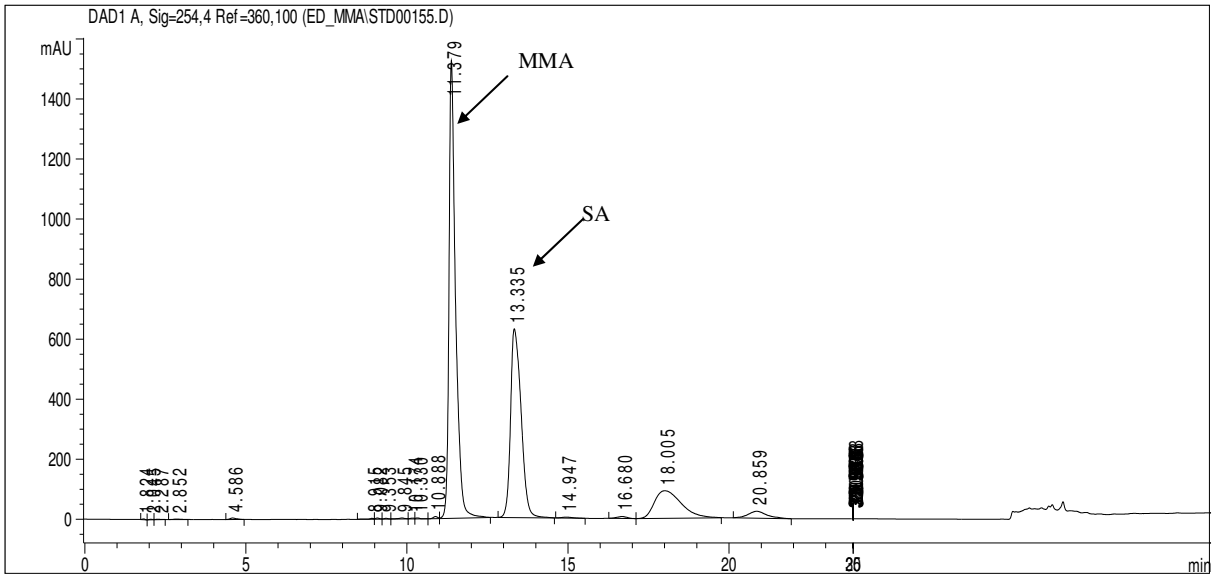

Figure 2.3-1. HPLC chromatogram of standard mixture of 1 mM methylmalonyl coenzyme A (11 min) and 0.5 mM succinyl coenzyme A (13 min).

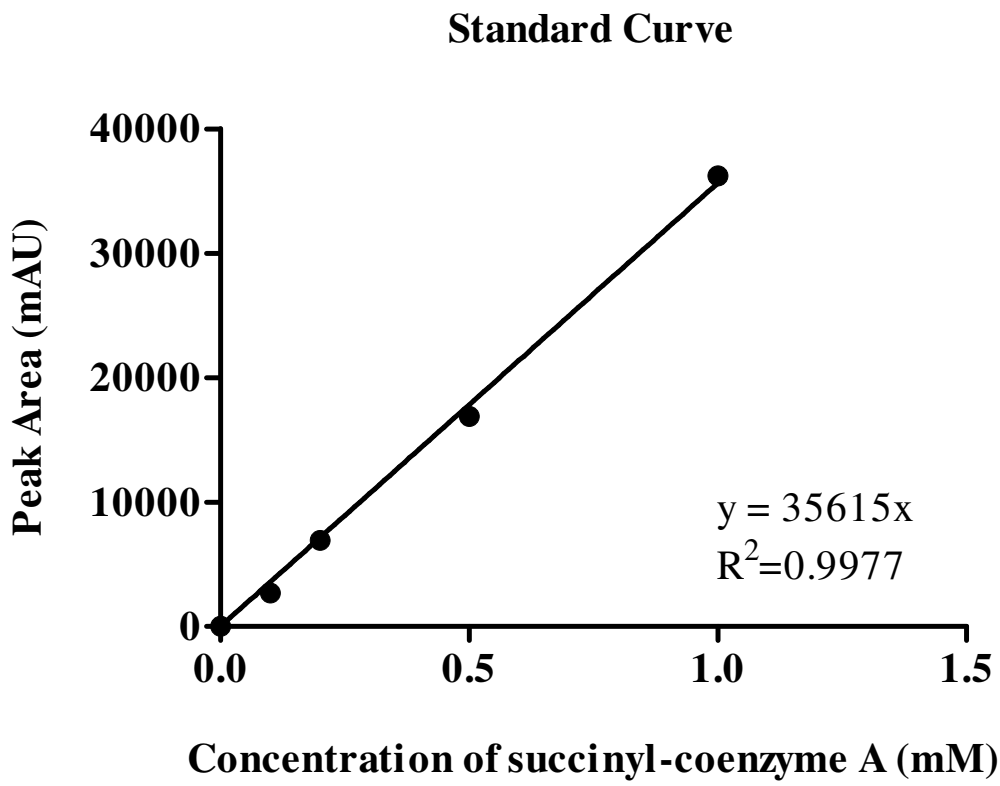

Figure 2.3-2. Graph of the standard curve of peak area (mAU) versus concentration of succinyl coenzyme A (mM). The solid line indicates the linear regression for the entire set of data set (y=35615x, r^2=0.9977). Each data point was measured in triplicate.

Figure 2.3-3. Determination of optimal methylmalonyl coenzyme A concentration.

High performance liquid chromatography assay of HEK293T cell lysate MCM activity showing the amount of succinyl-coenzyme A formed when (A) 0.15 mM, (B) 0.8 mM and (C) 1.5 mM of methylmalonyl coenzyme A was in a reaction mix containing 100 μg of HEK293T lysate protein and incubated for 30 minutes at 37 °C.

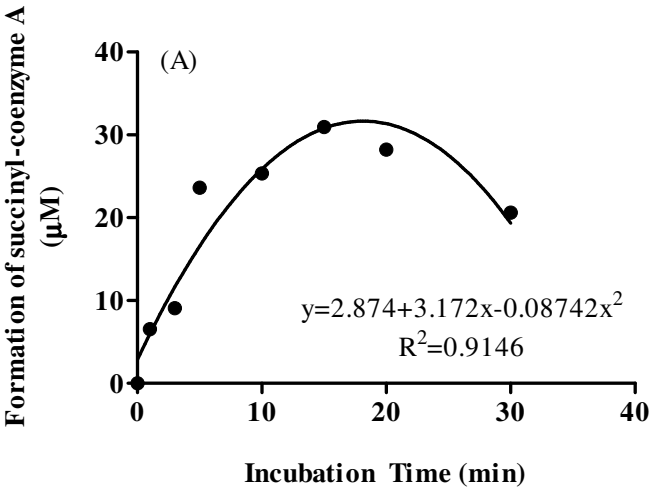
(A)
Formation of succinyl-coenzyme A (µM)
40
30
20
10
0
0
10
20
30
40
y=2.874+3.172x-0.08742x2
R2=0.9146
Incubation Time (min)

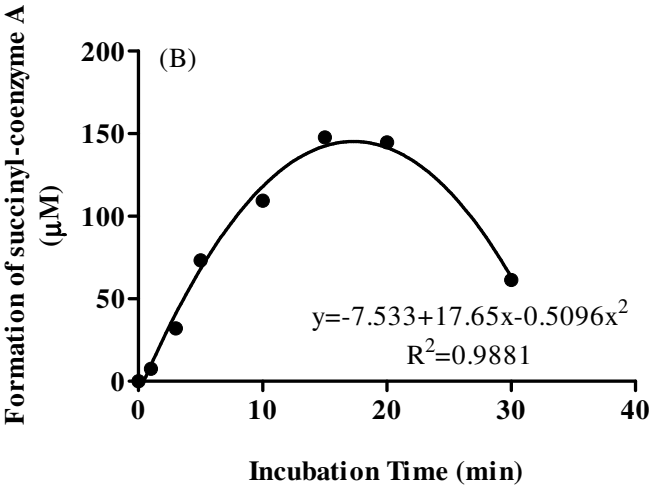
(B)
Formation of succinyl-coenzyme A (µM)
200
150
100
50
0
0
10
20
30
40
y=-7.533+17.65x-0.5096x2
R2=0.9881
Incubation Time (min)

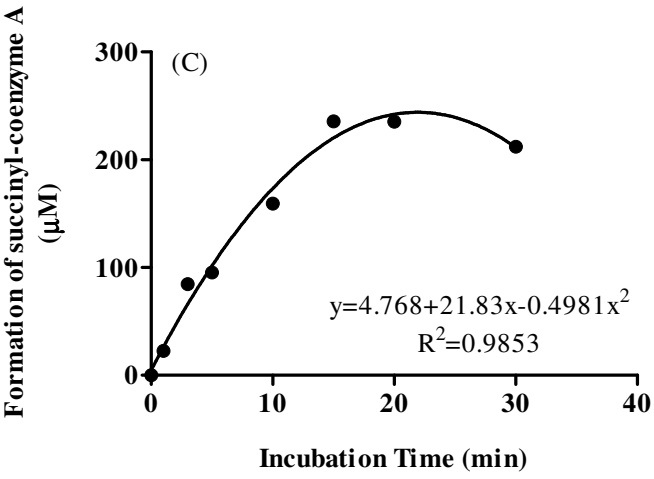
(C)
Formation of succinyl-coenzyme A (µM)
300
200
100
0
0
10
20
30
40
y=4.768+21.83x-0.4981x2
R2=0.9853
Incubation Time (min)

Figure 2.3-4. Corresponding to Figure 2.3-3, these graphs show the amount of succinyl coenzyme A formed within 15 minutes incubation time in which (A) 0.15 mM, (B) 0.8 mM and (C) 1.5 mM methylmalonyl coenzyme A were used in the reaction mix.

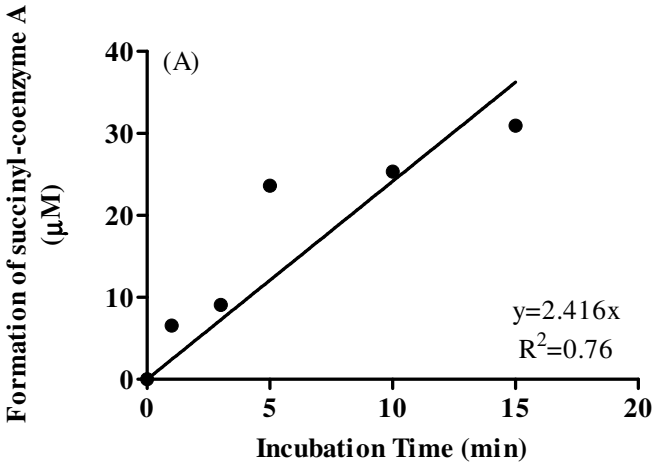
(A)
Formation of succinyl-coenzyme A (μM)
40
30
20
10
0
0
5
10
15
20
Incubation Time (min)
y=2.416x
R2=0.76

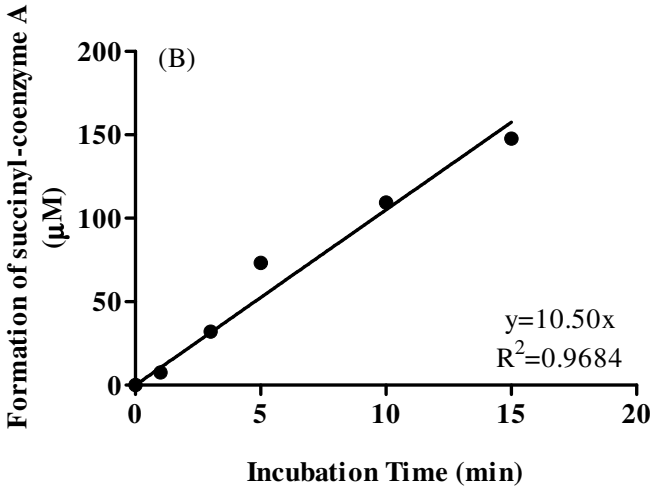
(B)
Formation of succinyl-coenzyme A (μM)
200
150
100
50
0
0
5
10
15
20
Incubation Time (min)
y=10.50x
R2=0.9684

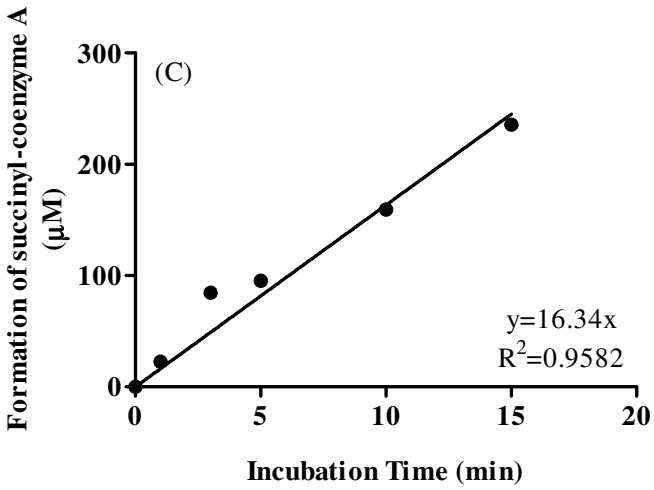
(C)
Formation of succinyl-coenzyme A (μM)
300
200
100
0
0
5
10
15
20
Incubation Time (min)
y=16.34x
R2=0.9582

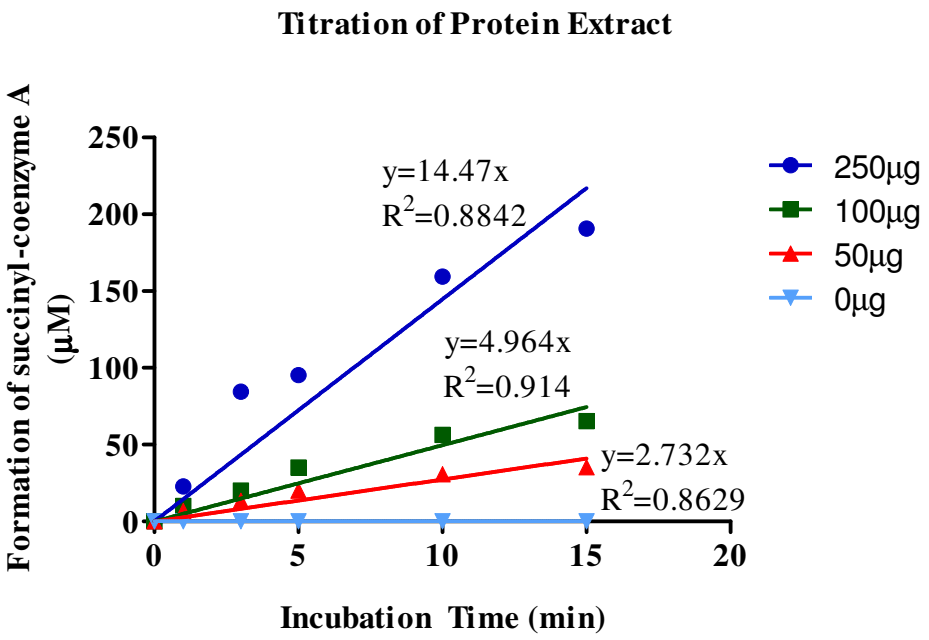

Figure 2.3-5. The graph shows the amount of succinyl coenzyme A formed with the incubation of different amounts of HEK293T lysate ranging from 0 µg to 250 µg total protein with 0.8 mM methylmalonyl-coenzyme A for 15 minutes at 37 °C. Solid lines indicate the linear regression for each set of data points.

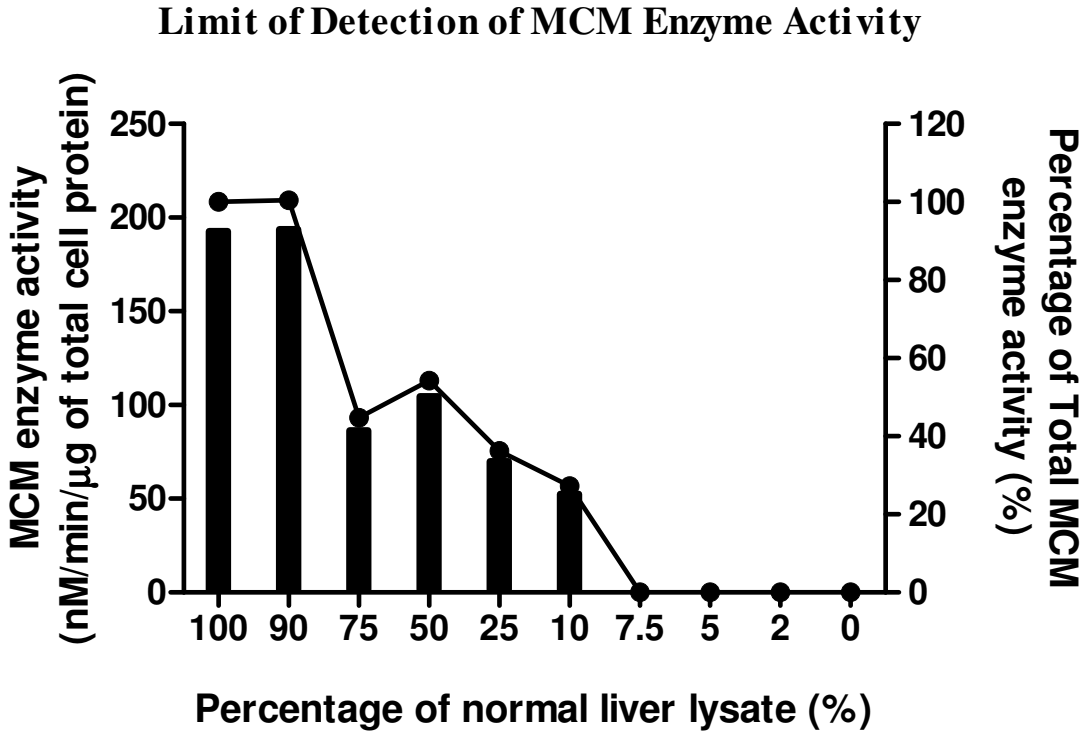

Figure 2.3-6. Mixtures of normal and MCM deficient liver lysates were used in a reaction mix containing 0.8 mM methymalonyl coenzyme A for 15 minutes. The bar chart represents the formation of succinyl coenzyme A (nM/min/µg of total cell protein) from the lysates mixtures. The line chart represents demonstrated the percentage of total MCM enzyme activity from the lysates mixtures.

2.3.4 Discussion

The [^{14}C] – radiolabelled propionate enzyme assay is mainly used in laboratories to determine MCM enzyme activity in cultured cells. Nevertheless, this method has been criticized for its lack of sensitivity and its indirect nature. Kikuchi *et al*., (1989) [155] developed an HPLC method to directly measure the enzyme activity. However, we were unable to separate the methylmalonyl coenzyme A and succinyl coenzyme A with the published method. This may have resulted from the use of a different HPLC system (Waters Association Inc.) than that described in the original paper. Therefore, several attempts were made to optimise the HPLC conditions in order to improve the performance of the separation system in our study.

The reverse-phase HPLC system was used in our study to separate the analytes of interest, methylmalonyl coenzyme A and succinyl coenzyme A, from the sample. The reverse-phase HPLC system used consists of two different phases: a silica non-polar stationary phase (column) and the aqueous polar mobile phase. Of these two phases, the selectivity of the mobile phase has always been the primary variable when developing a new reverse-phase HPLC method, rather than the selection of an appropriate column. However, the work published by Snyder *et al*., (2004) [164] demonstrated that the importance of column selection based on five selection parameters, hydrophobicity, resistance, hydrogen-bond acidity, hydrogen-bond basicity and cation exchange capacity. These parameters play a key role in influencing the retention of the analytes. The properties of 300 different columns were examined and summarized in Snyder's study. As mentioned previously, a Nova-pak™ C18 column was used in Kukichi's study [155] whereby an Alltech Alltima™ C18-LL column was used in our study, simply due to its ready availability. As discussed by Snyder, there is a clear difference, in terms of the properties mentioned above, between the two columns. These differences lead to the necessity of changing the mobile phase conditions to achieve the separation of the analytes of interest.

In addition, different types of mobile phase composition may also influence the separation of the molecules. There are two types of mobile phase composition: isocratic and gradient elution. The isocratic process uses a constant mobile phase composition throughout the process. On the other hand, the mobile phase composition in gradient elution mode is changed during the separation process. Both elution modes possess their advantages and disadvantages. Nevertheless, isocratic is more desirable than the gradient mode for several reasons. In general, there are more variables that influence the selectivity that need to be considered with the gradient elution method and, therefore, it is often more complicated to optimize. In addition, a lack of reproducibility of gradient elution methods between different instruments and laboratories has hindered its usefulness. The separation speed of gradient elution methods is also generally slower than the isocratic method due to the need for an equilibration stage between runs, which requires washing the column with at least 10 column volumes of the initial buffer.

Any appearance of baseline noise or disturbance in the background can also result in the inaccurate analysis of the peaks. And, lastly, the instrument setup for the gradient elution method is more complicated and requires regular maintenance [165]. Despite the fact that isocratic elution is generally preferred, the retention time of the components associated with gradient elution method is shorter, producing a narrower and sharper peak shape. This results in an improvement in peak height which is important for trace analysis. In contrast, the comparatively longer retention time of analytes using isocratic elution methods may cause an increase in peak width and result in the production of broader late-eluting peaks that interfere with the analysis. In addition, mobile phase pH also plays an important role in separation by changing the polarity of the analytes. Therefore, a buffer agent is used for the purpose of controlling pH.

In order to separate methylmalonyl coenzyme A and succinyl coenzyme A, the HPLC conditions developed by Corkey *et al*., (1981) [163], with the use of 50 mM KH_2PO_4, pH 5.3 running in isocratic conditions was assessed. However, the result was unsatisfactory with the overlapping of the peaks for methylmalonyl coenzyme A and succinyl-coenzyme A associated with the production of a broad and flat peak shape. Thereby, several modifications to the HPLC conditions were made. The first modification was the addition of methanol into the buffer. This was done by running both the mobile phase, 50 mM KH_2PO_4, pH 5.3, and methanol, in a gradient procedure. In addition, several different concentrations of methanol, ranging from 10% to 30%, were assessed. The results demonstrated that the use of 20% methanol significantly improved the shape of the peak, although the two peaks were still not completely separated. The next attempt involved the study of the effect of different pH values, ranging from 3.5 to 5.3, on analyte separation. The outcome showed that a buffer of pH 3.5, mixed with 20% methanol in a gradient method, resulted in the complete separation of methylmalonyl coenzyme A and succinyl coenzyme A.

One other minor modification to maximize the detection limit was the inclusion of a cleanup procedure with 100% methanol after each run. This cleanup process was important in order to remove residual materials that block the column, leading to the reduction of sensitivity. With these modifications it was possible to reproducibly separate methylmalonyl coenzyme A and succinyl coenzyme A.

The linearity of the enzyme activity for up to 15 minutes incubation in our hands (Figure. 2.3-4) is consistent to the result observed in the study conducted by Gaire *et al*., (1999) [166].

As expected, when extracts of MCM deficient fibroblasts were used no enzyme activity was detected. In addition, no enzyme activity was detected when liver cell lysates from the mut -/-muth2 mouse model were used despite the fact that these are estimated to contain between 13

and 20% of normal activity using the [^{14}C] – propionate incorporation assay (see 2.3.3.4 Limit of detection). This assay is based on measurement of the incorporation of [^{14}C] – propionate into macromolecules *via* the propionate metabolic pathway. Theoretically, no detectable radioactive macromolecules should be detected if there is a metabolic block in this pathway. However, the involvement of propionate in a second major pathway [167, 168] may undermine this assumption and this is supported by the measurement of 7% of normal incorporation of [^{14}C] – propionate in MCM knockout cells, supporting the idea that a direct assay for MCM activity is to be preferred. However, while the results presented above suggest that the HPLC method is specific for MCM enzyme activity, it is limited in its sensitivity to about 25% of normal MCM levels. Efforts to improve sensitivity by blocking turnover of product, succinyl coenzyme A, to succinate using streptozocin, a succinate thiokinase inhibitor [169], were unsuccessful.

The data obtained in this study was insufficient to determine the turnover number of the enzyme. Although a number of enzyme assays were performed, more, using a series of enzyme assays at varying substrate concentrations would be required to determine the parameters of interest. It may be of interest to study the enzyme kinetics of MCM using our HPLC method to compare with published data in future.

In a conclusion, this method provided rapid, reliable and reproducible results and is sufficiently sensitive to measure relatively low MCM activity.

Chapter 3 :Correction of MMAuria using HIV-1SDmEF1αhMCM

3.1 Construction of LV vector

3.1.1 Introduction

The toxic metabolites that accumulate in MMA are freely diffusible suggesting that the disease may be treatable by the modification of a single organ so that it becomes capable of metabolising these compounds. This means that gene therapy can be targeted to any organ, the obvious one being the liver, which is highly exposed to the circulation and is relatively easy to target for gene delivery.

Many different vector systems have been developed for gene therapy of metabolic disease. However, currently only two show real promise. These are AAV and LV derived vectors. Of all the AAVs vectors, AAV-2 has been studied most extensively. AAV vectors have proven useful for gene delivery to many tissues, especially liver, and can stably transduce both cycling and non-cycling cells. Numerous cases have also indicated their low immunogenicity, resulting in long-term transgene expression. As with AAV vectors systems, LV vectors, a subclass of retroviruses, have a proven ability to transduce both cycling and non-cycling cells and their obligatory integrative nature means they are genetically stable.

This study evaluates the ability of LV vectors that express human MCM under the transcriptional control of a heterologous promoter to correct the metabolic defect in a MMAuria affected model. Furthermore, the study will determine if the LV vector can deliver sufficient MCM enzyme activity to the liver of mut -/- muth2 mice to correct the biochemical defect in all tissues, as well as the overt physical defects seen in these mice.

This chapter is divided into three sections. The first section will describe the construction of the LV that carries the human MCM gene, as well as the results of analysis by restriction enzyme digestion and DNA sequencing. The second section will discuss the assessment of LV in MMA knockout fibroblasts. The last section will cover the evaluation of the efficacy of the LV vector in the mut -/- muth2 mouse model.

3.1.2 Vector Construction

The human MCM coding sequence was released from IMAGE clone 3908548 (Genbank accession number BC016282, Appendix I) [170] by digestion with 5' *Sal*I/3' *Bcl*I, and blunt-ended using Klenow, resulting in a fragment of 2581 base pairs (Figure 3.1-1). This was purified away from the cloning vector by agarose gel electrophoresis and isolated using the Adbiotech gel extraction kit as described in section 2.2.3.14.

The LV vector *p*HIV-1SDmEF1αLuciferase was used as the basis for the construction of a lentiviral vector expressing human MCM under the transcriptional control of the elongation factor 1α (EF1-α) gene promoter. To clone the human MCM into *p*HIV-1 vector, the luciferase coding sequence was removed from the vector by digestion with *Cla*I and *Nde*I. The vector was then made blunt-ended using Klenow. The purified MCM fragment was then ligated into the *p*HIV-1SDmEF1α vector to produce *p*HIV-SDmEF1αhMCM (Figure 3.1-2).

Figure 3.1-1: Isolation of the hMCM Coding Sequence

The fragment of human MCM at 2581 base pairs was visualised by electrophoresis on a 1.5% agarose gel. Lane 1: *Spp*I / *Eco*RI molecular weigh (Mw) marker, Lane 2: Fragment of human MCM at 2581 base pairs.

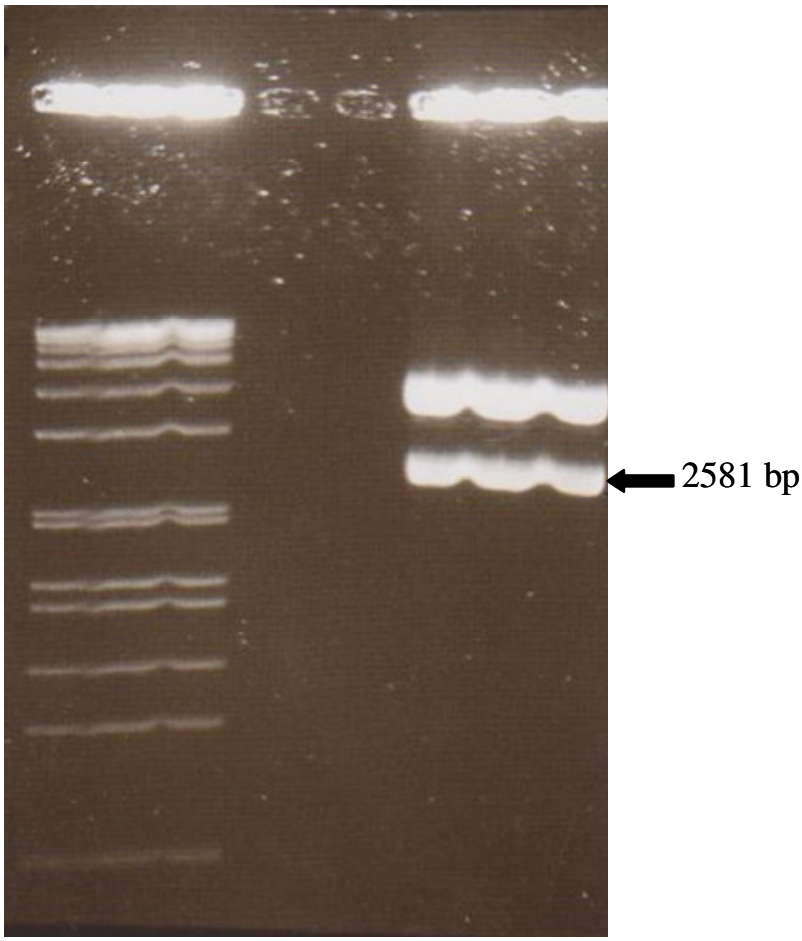
2581 bp

Figure 3.1-2 Construction of *p*HIV-1SDmEF1αhMCM

The hMCM gene was removed by digestion with 5'*Sal*I/ 3' *Bcl*I. This was then cloned into *p*HIV-1SDmEF1αLuciferase digested with 5' *Cla*I / 3' *Nde*I after both fragments were blunt ended with Klenow.

Preparation of *p*HIV-1SDmEF1αhMCM

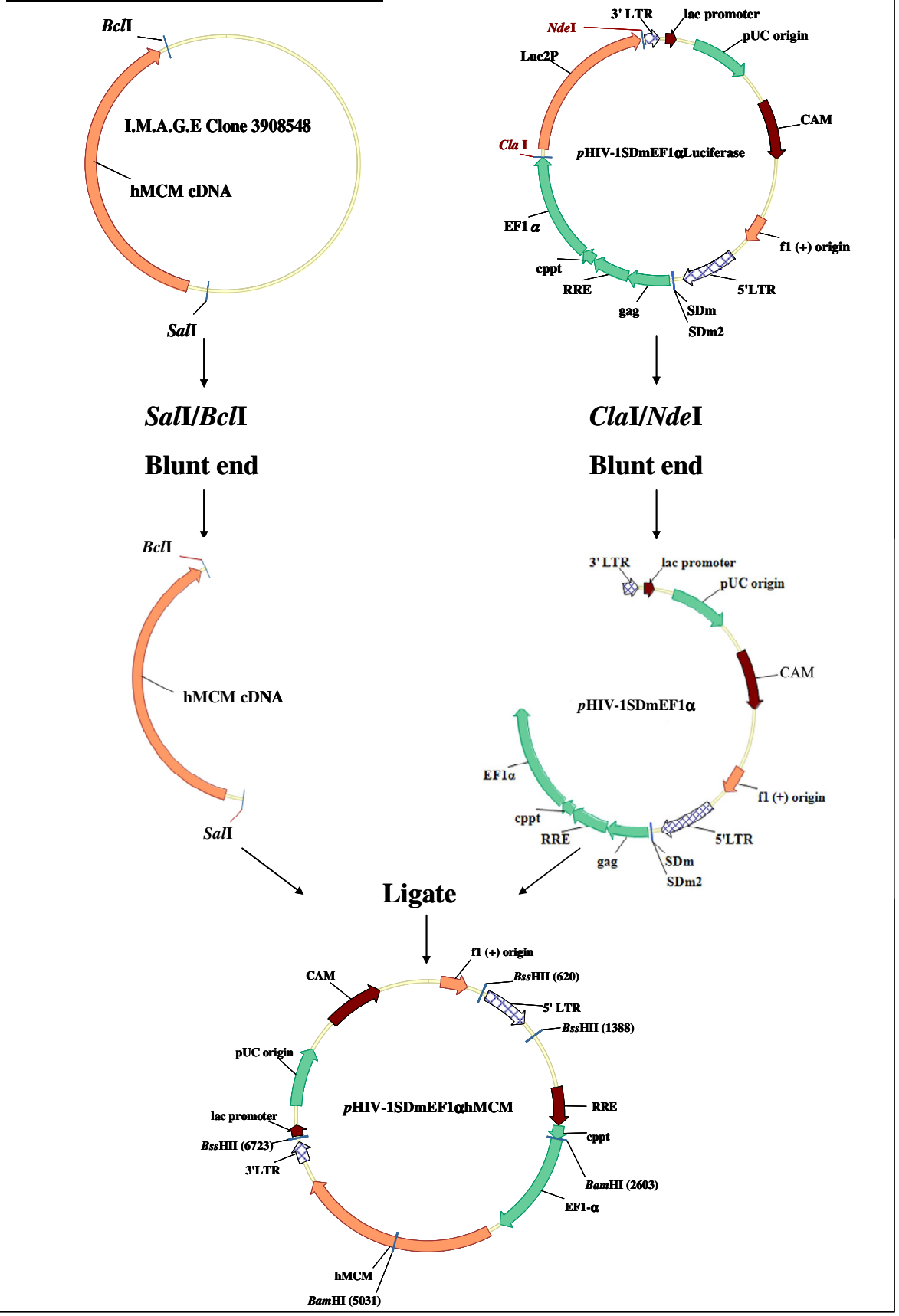

3.1.3 Analysis of Putative Clones

The ligation was electroporated into Sure *E. coli* electrocompetent cells and transformed cells selected on chloramphenicol (CAM) plates.

Individual clones were isolated and grown as 1 mL cultures and DNA extracted using the mini-prep DNA extraction method as described in section 2.2.3.2. The plasmid DNA was then analysed by digestion with *Bss*HII and *Bam*HI and the results of digestion were shown (Figure 3.1-4). Correct clones will result in 5 bands, these being 3227, 2428, 1654, 1215 and 727 bp.

Of the 24 clones analysed, C7, C11, C22 and C23 demonstrated the expected restriction pattern. Of these four colonies, C22 was selected for further analysis by DNA sequencing. The DNA was sequenced using *p*BlueT7, *p*Blue Rev and RREf primers with the method as described in section 2.2.3.16. These three primers sequenced across 3 different regions of the *p*HIV-1SDmEF1αhMCM (Figure 3.1-5). The *p*BlueT7 primer was used to examine across the cloning site into the 5' end of the *p*HIV-1SDmEF1αhMCM vector .The RREf primer was used to determine the RRE and the regions including the cppt and the EF1α promoter; and the REV primer was used to determine the regions including the 3'LTR and hMCM. As expected, the DNA sequencing results demonstrated that clone C22 was of the correct structure. Therefore, C22 was used for all future studies (Data not shown).

Figure 3.1-4: Restriction enzyme analysis of clones

Putative *p*HIV-1SDmEF1αhMCM clones were analysed by *Bss*HII / *Bam*HI digest. Clones of the correct structure should give fragments 3227, 2428, 1654, 1215 and 727 bp. Lane 1/16 : *Spp*I / *Eco*RI Mw marker, Lanes 2-16 : clones C1-C15, Lane 17-25 : clones C16-C24, Lane 26 : *Spp*I / *Eco*RI Mw marker.

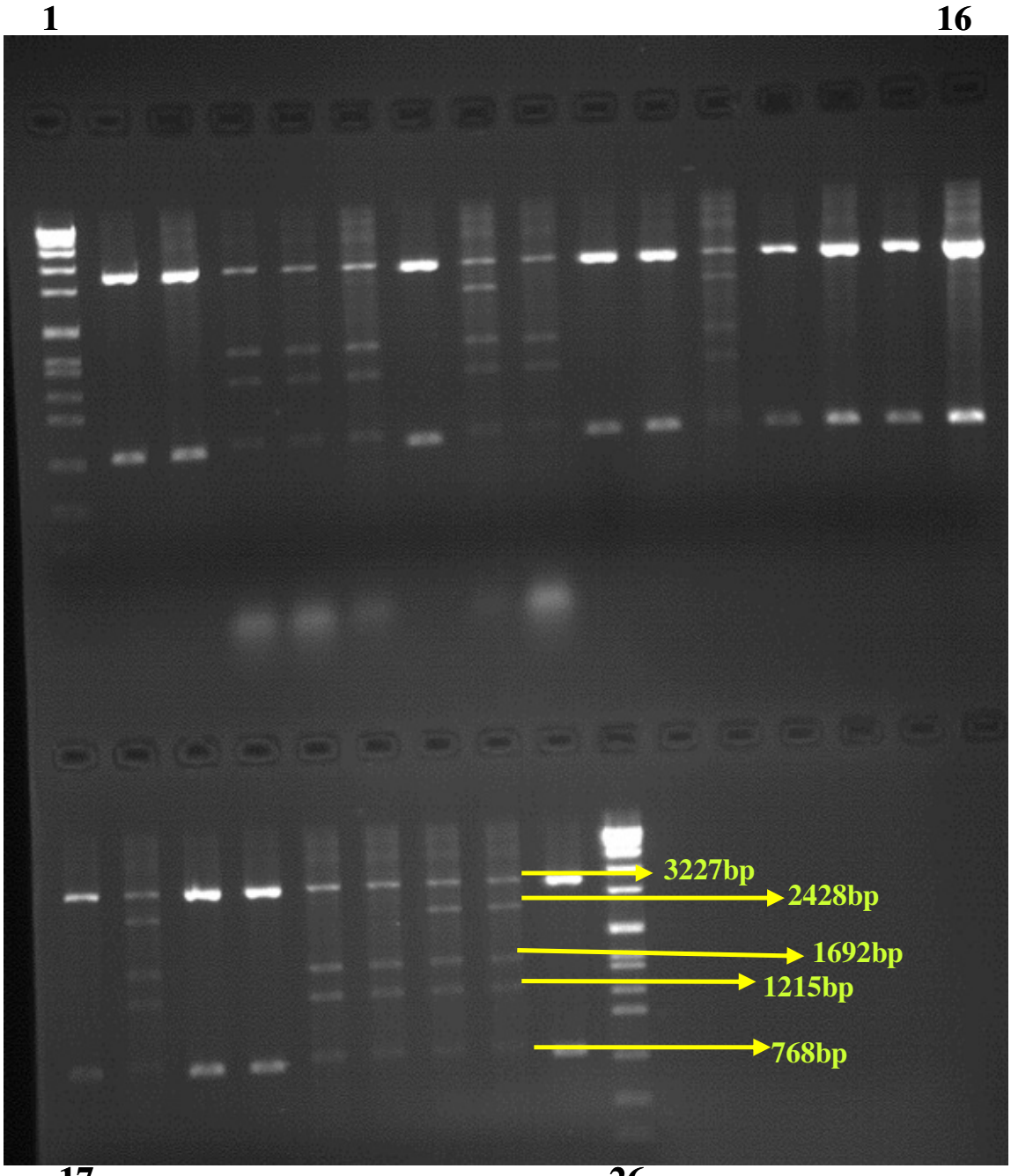
1
16
3227bp
2428bp
1692bp
1215bp
768bp
17
26

Figure 3.1-5 Schematic Diagram of *p*HIV-1SDmEF1αhMCM

SD = major splice donor; RRE = Rev response element; cppt = central polypurine tract; EF1-α = Elongation Factor 1α promoter; hMCM = human MCM gene coding sequence. The restriction sites used for cloning and for analysis are shown. The primer target sites for the *p*BlueT7, *p*BlueRev and RREf primers are also shown in this figure.

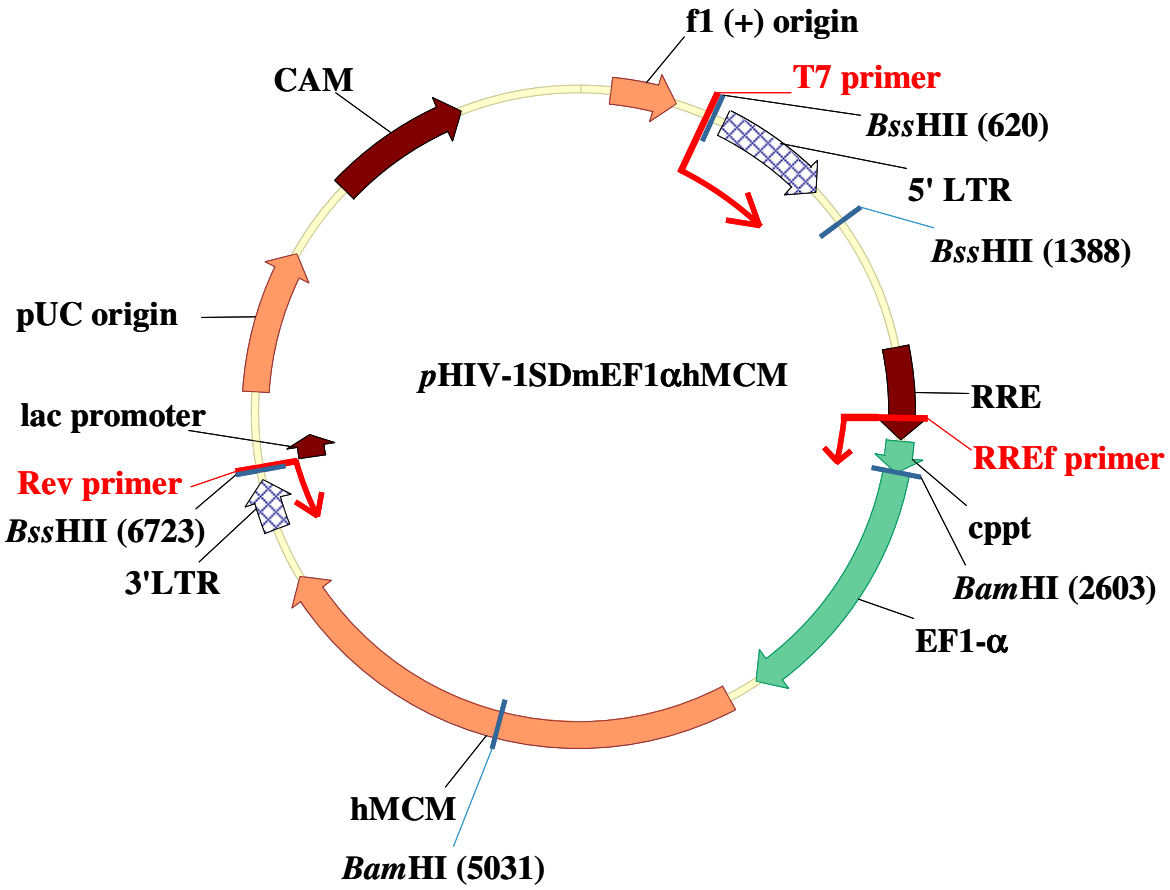
f1 (+) origin
T7 primer
BssHII (620)
5' LTR
BssHII (1388)
RRE
RREf primer
cppt
BamHI (2603)
EF1-α
hMCM
BamHI (5031)
3'LTR
BssHII (6723)
Rev primer
lac promoter
pUC origin
CAM
pHIV-1SDmEF1αhMCM

3.2 Lentiviral-Mediated Gene Transfer *in vitro*

3.2.1 Aim

The aim of these experiments was to evaluate the functionality of HIV-1SDmEF1αhMCM by assessing transduction efficiency, MCM enzyme production and phenotypic correction in MMA knockout fibroblasts.

HIV-1SDmEF1αhMCM was produced as outlined in section 2.2.1.8 and filtered through a 0.2 µM filter. DMEM/PS and FCS were added to the virus supernatant to make up a total volume of 20 mL and a final concentration of 10% FCS. Polybrene was then added to a final concentration of 4 µg/µL. Subsequently, the virus was transferred onto the MCM knockout fibroblasts and incubated for 24 hours. The virus containing medium was then exchanged for fresh DMEM/10% FCS. The virus transduced MCM knockout fibroblasts were subcultured for two weeks prior to harvest of some of the cells for the measurement of vector copy number by real-time PCR and MCM enzyme activity by high performance liquid chromatography (HPLC). Simultaneously, the rest of each culture was grown as described in section 2.2.1.2 and used for the [^{14}C]-radiolabelled propionate incorporation assay (see section 2.2.3.8).

3.2.2 Methods and Results

3.2.2.1 Assessment of HIV-1SDmEF1αhMCM Transduction

DNA was initially isolated from the fibroblasts as described in section 2.2.3.10. The quantification of HIV-1SDmEF1αhMCM viral transduction in the MCM knockout fibroblasts was achieved by the detection of HIV-1 provirus *gag* gene DNA in fibroblast genomic DNA. The results were normalized to the mouse transferrin gene, which served as a single copy gene sequence.

The results of this analysis showed that, as expected, vector sequences were not detected in the negative controls, untransduced MCM knockout fibroblasts. In contrast, the copy number in the cells transduced with the HIV-1SDmEF1αhMCM vector was 8 ± 2 copies /cell (p<0.05) (Figure 3.2-1).

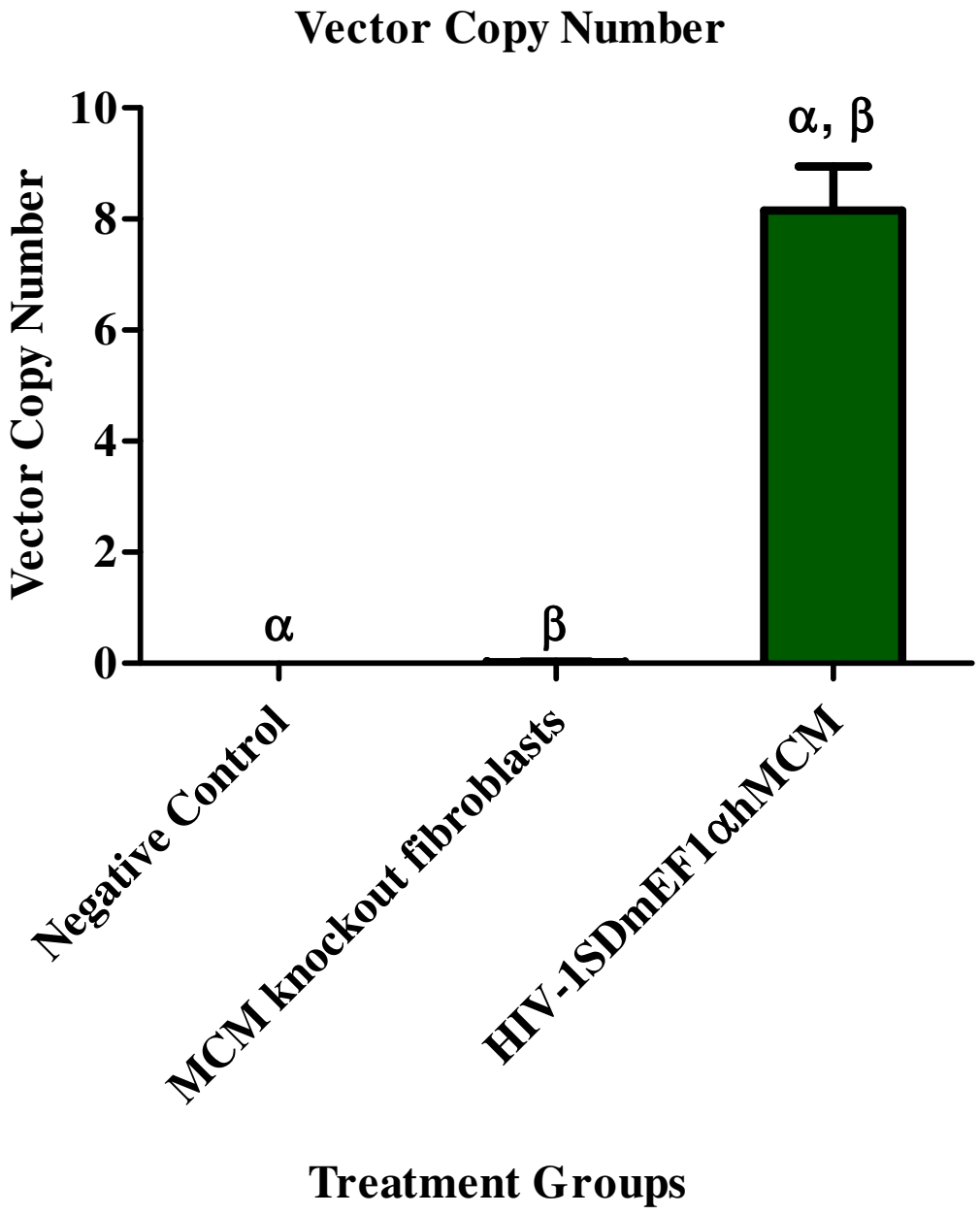

Figure 3.2-1 MCM knockout cells were transduced with HIV-1SDmEF1αhMCM and the resulting cultures assayed for vector copy number by real-time PCR. (n=6 for normal, HIV-1SDmEF1αhMCM untransduced *mut* knockout fibroblast and HIV-1SDmEF1αhMCM transduced *mut* knockout cultures). The standard bars represent the ± one standard error. α and β represent significant difference between the groups ($p<0.05$). The p value between the two groups was calculated by one-way ANOVA with Tukey's post hoc test.

3.2.2.2 Direct Measurement of MCM Enzyme Activity

To assess the restoration of MCM enzyme activity in HIV-1SDmEF1αhMCM treated MCM knockout fibroblasts, enzyme activity in cell extracts was measured directly by measuring the rate of conversion of methylmalonyl coenzyme A to succinyl coenzyme A in cell extracts as described in section 2.2.3.9.

The results demonstrated a high level of enzyme activity in the normal control group, with a mean ± SE of 26 ± 4 nmol/min/µg of total cell protein (Figure 3.2-2). Compared to the normal control, all the MCM knockout fibroblasts samples (n=5), except for one, showed no detection of enzyme activity. In order to avoid the possibility of peak interference from the background resulting in the inaccurate reading of the succinyl coenzyme A, a negative control assay was run, in which the running sample was setup under the conditions as described in section 2.2.3.9 but without the addition of cell extract. The negative control assay demonstrated no evidence of background peaks that would affect the readings. Therefore, it is believed that the production of succinyl coenzyme A detected in this particular sample, at 19 nM/min/µg of total cell protein, may be due to contamination during preparation of the sample. Nonetheless, the result presented a mean ± SE of 3 ± 3 nmol/min/µg of total cell protein in LV untreated MCM knockout fibroblasts, which was significantly different to normal control group ($p<0.05$, Newman-Keuls post-hoc test).

In contrast, the enzyme activity detected in HIV-1SDmEF1αhMCM transduced MCM fibroblasts was significantly higher than in untransduced MCM knockout fibroblasts (47 ± 10 nmol/min/µg of total cell protein, $p<0.05$, Newman-Keuls post-hoc test). Furthermore, this level was approximately 2-fold that found in wild type fibroblasts ($p<0.05$).

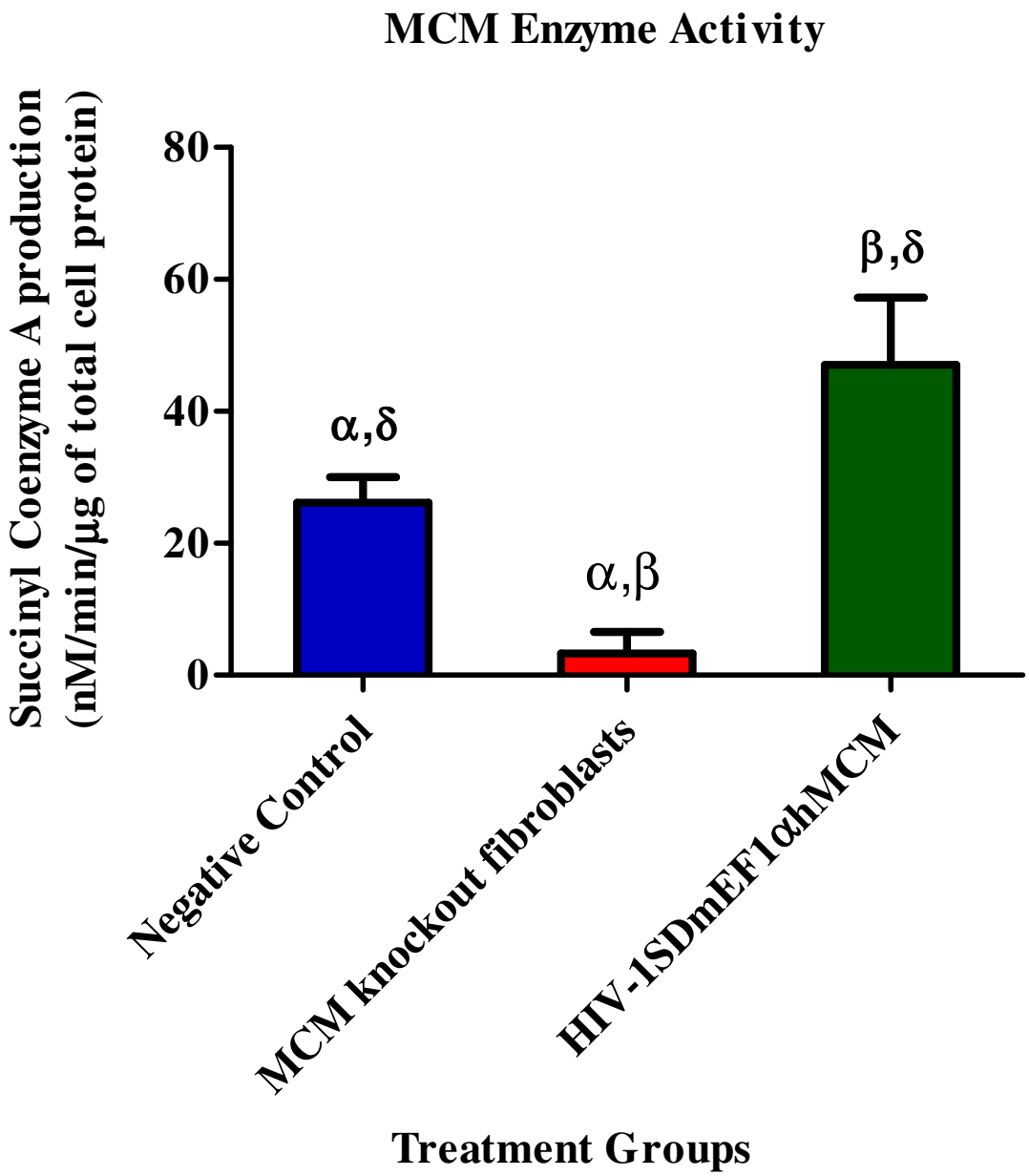

Figure 3.2-2 MCM knockout cells were transduced with 20 mL of the HIV-1SDmEF1αhMCM vector and the resulting mutase enzyme activity evaluated by HPLC. (n=6 for normal, untransduced MCM knockout fibroblast and HIV-1SDmEF1αhMCM transduced MCM knockout fibroblast). The standard bars represent ± one standard error. α, β and δ indicate significant difference between the treatment groups (p<0.05). The p value between the two groups was calculated by one-way ANOVA with Newman-Keuls post-hoc test.

3.2.2.3 Measurement of [^{14}C]-radiolabelled Propionate Incorporation

The propionate metabolism pathway has been described in detail in the introduction. The defect in any steps of this pathway will disrupt the ability of cultured cells to metabolize carbon into trichloroacetic acid-precipitable material from propionate through the propionate pathway and Krebs cycle. The normalisation of propionate metabolism in MCM deficient fibroblasts was therefore assessed using the [^{14}C]-radiolabelled propionate incorporation assay. This method was established by Hill and Goodman (1974) [168]. In their study, they demonstrated the incorporation of radioactivity from Na-propionate-1-^{14}C into trichloroacetic acid-insoluble cell material in human fibroblasts, cultured on glass microscope slides, autoradiographically. In 1976, Willard and his colleagues [171] proposed a similar method with modification based on this autoradiographic technique. In their study, the human fibroblasts or amniotic cells were cultured in a plastic flask and incubated in the cell cultured media containing Na-propionate-1-^{14}C. These cells were then harvested when confluent and incubated in 5% trichloroacetic acid. The trichloroacetic acid-precipitable material was collected and solubilized prior to the detection of the incorporation of the radioactivity by counting aliquots of the solubilized samples. These modifications allowed them to study the enzyme activity with small numbers of cells and allowed levels of enzyme activity to be quantitatively estimated by counting the solubilised samples using a scintillation counter. This modified procedure, unlike the autoradiography method developed by Hill and Goodman (1974) [168] does not need a long exposure time. Therefore, this more rapid method is also used as a diagnostic test for inborn errors of metabolism.

The results demonstrated a high level of [^{14}C]-propionate incorporation, with a mean ± SE of 38,710 ± 1,265 dpm/mg of protein, in normal cells (Figure 3.2-3). In contrast, the MCM knockout fibroblast showed a significantly lower level of incorporation, 506 ± 110 dpm/mg of protein, compared to the normal (p<0.05, Tukey's post hoc test). In addition, in accordance with the MCM enzyme activity result, the analysis of individual samples in the LV-untreated

group showed that the suspect sample (see 3.2.2.2 Direct Measurement of MCM enzyme activity) presented a slightly higher value for [^{14}C]-propionate incorporation, at 962 dpm/mg of protein, compared to the others, which ranged from 112 to 517 dpm/mg of protein, supporting the assumption that the suspect sample might have been contaminated. The gene corrected MCM deficient fibroblasts demonstrated a dramatic recovery in propionate incorporation into trichloroacetic acid- precipitable material with the mean level of [^{14}C]-radiolabelled propionate incorporation increasing to 17,347 ± 814 dpm/mg protein (p<0.05 compared to the MCM deficient fibroblasts). This, however, is still significantly less than (p<0.05) the level of enzyme activity observed in the normal fibroblasts.

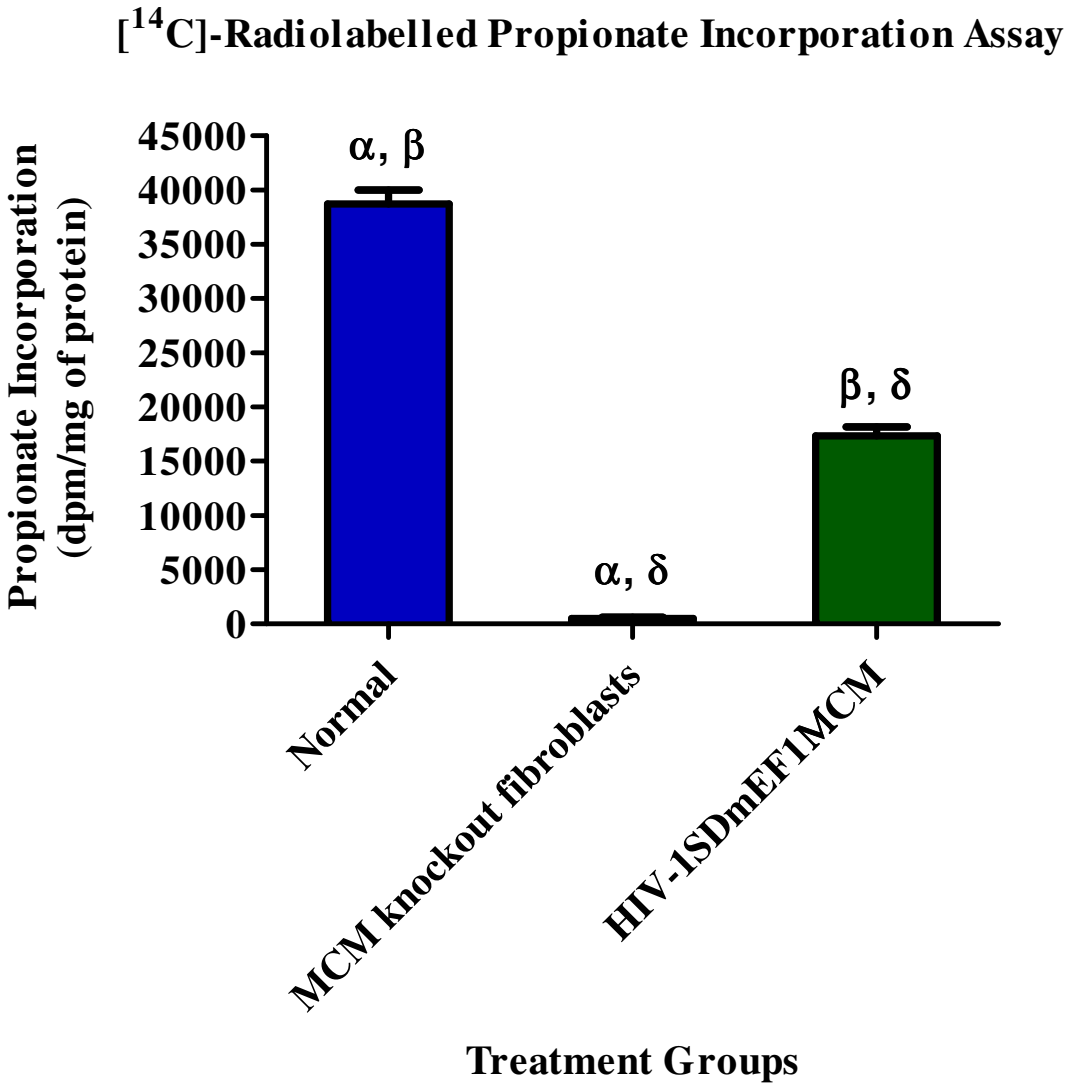

Figure 3.2-3 MCM knockout fibroblasts were transduced with 20 mL of the HIV-1SDmEF1αhMCM and the resulting cultures assayed for incorporation of [^{14}C]-propionic acid into trichloroacetic acid-precipitable material. (n=6 for normal, MCM knockout and HIV-1SDmEF1αhMCM transduced MCM knockout fibroblasts). The standard bars represent ± one standard error. α, β and δ represent a significant difference compared to the MCM knockout group (p<0.05). The p value between the two groups was calculated by one-way ANOVA with Tukey's post hoc test.

3.2.3 Discussion

These results of the analyses described above demonstrate the effectiveness of the LV vector, HIV-1SDmEF1αhMCM, in correcting both the enzymatic defect and propionate metabolism in MCM knockout cells. However, while efficient transduction and enzyme expression were achieved, resulting in a copy number of 8, and mutase activity approximately twice normal, propionate incorporation was less than half that seen in normal cells. In addition, comparison of copy number (2 versus 8) and enzyme activity (26 versus *versus* 47 nmol/min/µg of total cell protein) in normal and transduced cells suggests that expression from the vector is about ½ as efficient as that from the endogenous gene.

The discrepancy between the MCM enzyme activity and the vector copy number may be at least partly due to the transgene not being correctly localized. In fact, numerous studies have shown the crucial importance of the insertion site in transgene expression. The importance of transgene location has been studied extensively in Drosophila [172] and Yeast [173] and these studies show that inactivation of the transgene can occur due to integration near silent chromatin. This type of chromatin is found within eukaryotic genomes and plays a role in separating different transcriptionaly active regions [174]. This is known as position-effect variegation. While HIV-derived LV vectors have shown their ability to integrate into host genome, resulting in stable expression of the transgene, they are also subject to position-effect variegation due to their non-specific integration, and this can result in transgene silencing [175].

Robertson *et al*., (1995) [176] reported poor expression of globin transgenes in transgenic mice. This phenomenon was improved when these transgenes were integrated within the β-globin locus control region, producing a similar expression level as the endogenous mouse globin gene. In addition, several studies have identified a tissue-specific, positive regulatory element located upstream of the α-globin locus that plays a major role in producing a high

level of human alpha mRNA expression regardless of the integration sites in transgenic mice [177] and in cell culture [178]. Wilkemeyer *et al*., (1993) [179] reported the identification of regulatory elements in the MUT locus control region. Their results suggested that the MCM activity might be regulated at the transcriptional level, although the significance of any genetic regulation remains unknown.

Another possible explanation for the relatively low expression of MCM enzyme activity from the transgene may be the divergence of the human and mouse MCM mitochondrial transport signal. The study conducted by Wilkemeyer *et al*., (1990) [180], which investigated the primary structure and activity of mouse MCM, demonstrated a 94% identity between the human and mouse MCM sequences but a large variation in the mitochondrial targeting signals (with only 69% identity). The amino acid differences in the mitochondrial targeting sequence may result in the poor translocation of human MCM in mouse fibroblasts. This degree of divergence in the mitochondrial targeting signal is also found between human and mouse OTC. It is reported in Wilkemeyer's study that human and mouse OTC possess 92% identity in their amino acid sequence but only 69% identity in their mitochondrial targeting signal. Another study, conducted by Ye *et al*., (2001) [181], failed to effectively express functional human OTC, delivered by an Adv vector, in mice, suggesting that the pre-matured OTC enzyme was not properly transported to the mitochondrial due to differences in the mitochondrial targeting sequence. Therefore, it is hypothesized that this might also be the case in MCM enzyme. Nevertheless, further experimentation is required to validate this hypothesis.

3.3 Lentiviral-Mediated Gene Delivery *In Vivo*

3.3.1 Introduction

In the previous section, the cloning of human MCM into the LV vector and the efficacy of HIV-1SDmEF1αhMCM in correcting the MMAuria disease in MCM knockout fibroblasts were demonstrated. The preliminary data showed proof-of-principle for the restoration of the MCM enzyme activity using an LV vector. The aim of the experiment described in this section was to evaluate the efficacy and efficiency of HIV-1SDmEF1αhMCM in improving MMAuria disease using our MMAuria affected mouse model (mut -/- muth2), allowing a direct comparison of the results from the *in vitro* studies.

As described in the introduction, the pathology of MMAuria is due to the accumulation of diffusible toxic metabolites. It was then hypothesized that the clearance of these metabolites could be achieved by the creation of a metabolic sink. The numerous clinical reports on the relative success of liver transplantation, which improves, although not completely resolves, the condition of MMAuria patients [182-184] supports this contention. In addition, the large protein synthesis capacity of the liver, as well as it being a major organ involved in a number of metabolic diseases that result from enzyme defects, and being highly exposed to the circulation, have made it an obvious target for gene therapy of MMAuria and other metabolic diseases.

Possible routes of administration to achieve efficient liver-specific delivery have been extensively studied. IV injection is probably the simplest of these and has shown to be a safe, efficient and easy delivery method. Numerous studies indicated that a high level of gene transduction of hepatocytes can be achieved through intravenous injection, resulting in stable and high level gene expression in the liver [185, 186]. Therefore, this delivery method was chosen for this study.

3.3.2 Methods and Results

A preliminary study was done to determine the effectiveness of HIV-1SDmEF1αMCM in the mut -/- muth2 model. Two mut -/- muth2 mice, QUE 7.47 and QUE 6.94 at 8 weeks of age, were treated with HIV-1SDmEF1αhMCM using the protocol described in section 2.2.2.4. Mice were examined regularly for their physical and clinical signs after treatment. Blood and urine samples were collected regularly for measurement of plasma and urine MMA levels by GC/MS and mass spectrometry using the protocols described in section 2.2.2.6 and section 2.2.2.5 respectively. At autopsy, one year post-treatment, tissues including liver, spleen and kidneys were removed and used for measurement of MMA levels, vector copy number (real-time PCR method) and enzyme activity (HPLC method). Equivalent data was collected from normal (n=5) and untreated mut -/- muth2 (n=2) mice.

3.3.2.1 Physical Examination

Virus delivery was well tolerated by the treated mice although mild signs suggestive of discomfort, including partly closed eyelids and hunched back, were observed 2 hours after delivery. To minimize protein intake that could possibly worsen the metabolic stress, resulting from virus delivery, sunflower seeds, a high fat energy source, were given as a supplementary food. In addition, a small drop in body temperature (by 2 degrees), measured using a rectal thermometer, was observed in both treated mice after virus delivery. Therefore, these mice were transferred to a 29 °C humidicrib and monitored closely until fully recovered. The bodyweight of each mouse was measured weekly and plotted versus time. The fit of curves (R^2) of each treatment group was plotted and compared using the statistical software tool SAS 9.3 (SAS Institute Inc). From the model curves, there is no significant difference in the growth of mice between the treated and untreated mut -/- muth2 mice. The mice in the normal group weigh significantly more, on average, over the growth period (Figure 3.3-1).

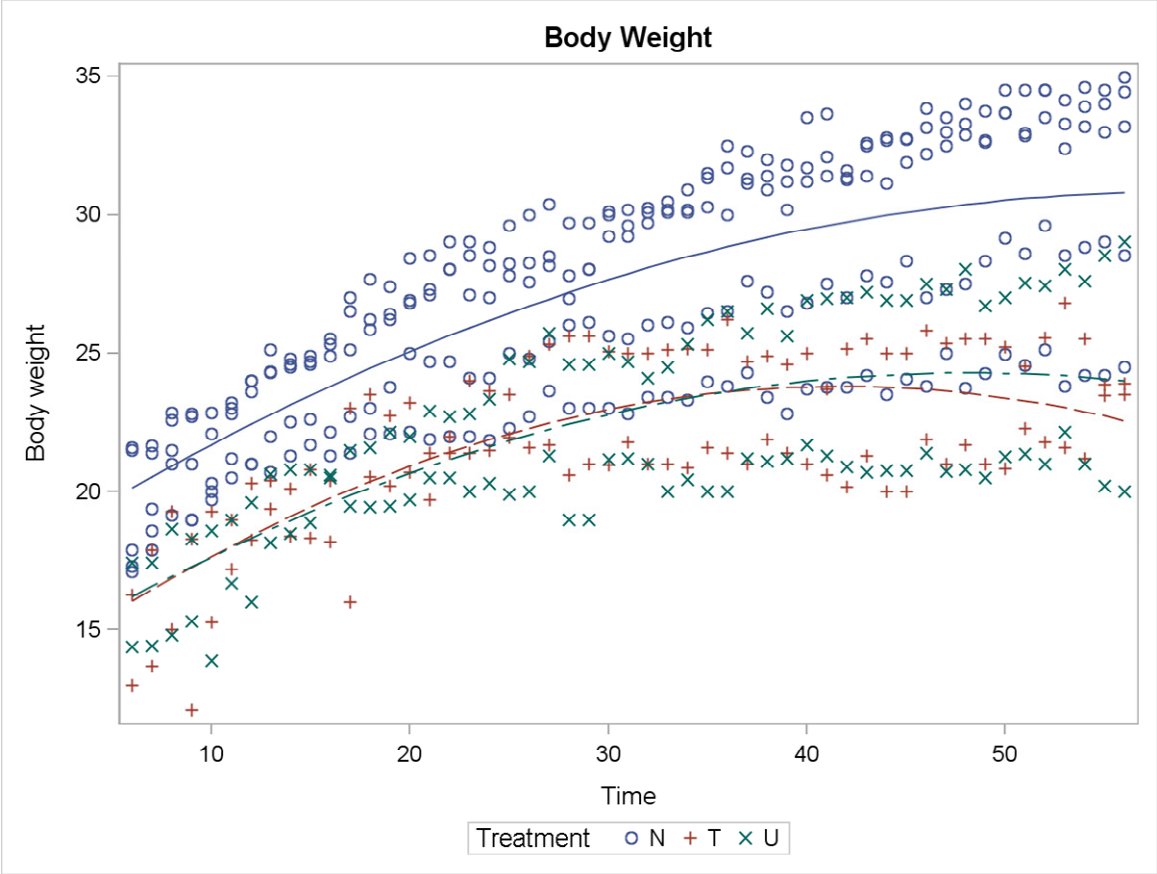

Figure 3.3-1 Body weight of individual mice from normal, untreated and the HIV-1SDmEF1αhMCM treated group. The curved line represents the fit of curves (R^2) of each treatment group, the blue solid line indicates the wild type group, the red and green dash line indicate HIV-1SDmEF1αhMCM treated and untreated groups, respectively. Statistical analysis on the fit- of-curves show that there is no significant difference between the treated and untreated groups.

3.3.3.2 Real-Time PCR

At autopsy, tissues including liver, spleen and kidneys were used for vector copy number determination. No copies of the vector were detected in normal or untreated mut -/- muth2 mice in all the tissues tested. In HIV-1SDmEF1αhMCM treated mut -/- muth2 mice, a significant increase in vector copy number (0.19 ± 0.04 copies per cell) was observed in the liver, and spleen (0.18 ± 0.01 copies per cell). On the other hand, no vector was detected in kidney. Due to the small number of animals in this pilot study, no statistical analysis was performed. However, this result is a good indication of the localization of the HIV-1SDmEF1αhMCM vector in the mouse after treatment (Table 3.3-1).

Vector Copy Number

Treatment Groups	Liver	Spleen	Kidneys
Normal (n=5)	N.D	N.D	N.D
Untreated (n=2)	N.D	N.D	N.D
HIV-1SDmEF1αhMCM treated (n=2)	0.19 ± 0.04	0.18 ± 0.01	N.D

Table 3.3-1 Vector copy number per cell in tissues from Normal (n=5), Untreated mut -/- muth2 control (n=2) and HIV-1SDmEF1αhMCM treated group (n=2). Results are presented as the mean ± SE. N.D. indicates not detected.

3.3.3.3 Determination of MCM Enzyme Activity in Liver

As described in the introduction to this section, the primary target for gene delivery was the liver, accordingly it was the organ chosen to compare the level of MCM enzyme activity in the mut -/- muth2 mice treated with HIV-1SDmEF1αhMCM to untreated mice and normal controls. Liver homogenate was prepared and assayed for MCM activity as described in section 2.2.3.9.

The results of this analysis showed a high level of enzyme activity in the normal group, with a mean ± SE of 18 ± 0.4 nM/min/µg total cell protein. In contrast, the untreated mut -/- muth2 group demonstrated only a low level of enzyme activity, 2 ± 1 nM/min/µg of total cell protein (11% of normal enzyme activity). Given the limited sensitivity of the HPLC method, as described in section 2.3.3.4, and based on Peters' studies [152], the low level readings detected within the mut -/- muth2 mice may not be an accurate value. However, enzyme activity analysis using this method still provides a valuable tool to investigate the level of restoration of enzyme activity in our *in vivo* studies, especially if enzyme activity values are relatively high. Of the two untreated mut -/- muth2 controls, QUE 7.38 gave a value of 3 nM/min/µg of total cell protein, while the second animal, QUE 7.41, gave a value of 0.9 nM/min/µg of total cell protein. Despite the acknowledged limitations of the enzyme assay, this is of relevance given the biochemical analyses that suggest that the MMAuria in this mouse was relatively mild (see below, sections 3.3.3.4 and 3.3.3.5), suggesting that QUE 7.38 may have been misidentified as being of the mut -/- muth2 genotype. On the other hand, the mean level of MCM enzyme activity showed a modest, although not significant, increase in the treated group compared to the untreated group, with a mean ± SE of 5 ± 0.3 nM/min/µg of total cell protein (with 4 and 5 nM/min/µg total cell protein detected in the individual HIV-1SDmEF1αhMCM treated mice). However, this is only approximately 28% of normal MCM enzyme activity.

The MCM enzyme activity in the mut -/- muth2 mice treated with HIV-1SDmEF1αhMCM and in the untreated mut -/- muth2 mice were both significantly (p<0.05) lower than in the normal group (Figure 3.3-2).

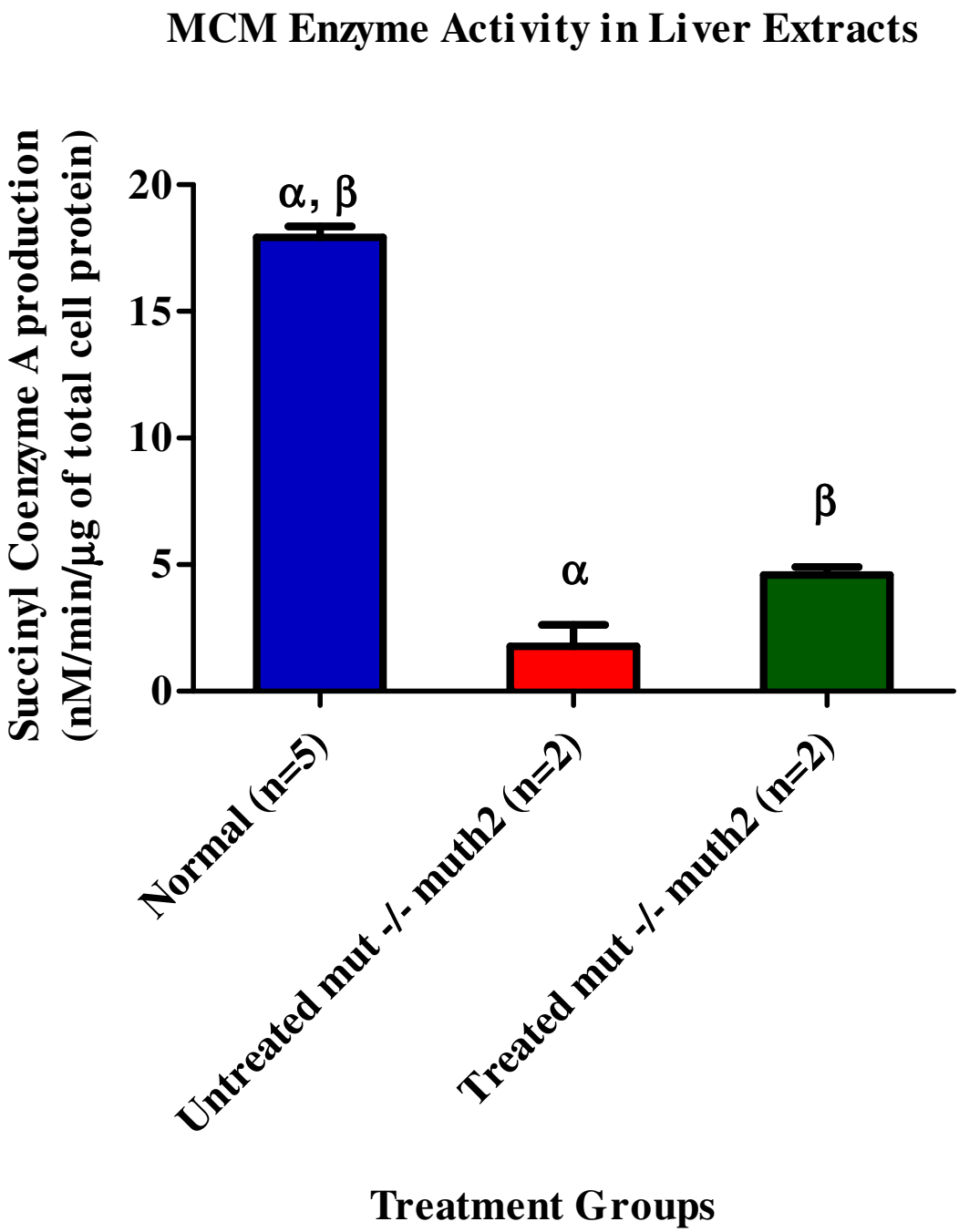

Figure 3.3-2 The mean level of hepatic enzyme activity from normal mice (n=5), mut -/- muth2 untreated mice (n=2) and HIV-1SDmEF1αhMCM treated mice (n=2). The HIV-1SDmEF1αhMCM treated mice had a mean ± SE of 5 ± 0.3 nM /min /µg of total cell protein and is modestly, but not significantly, increased compared to the mut -/- muth2 untreated group (2 ± 1 nM/min/µg of total cell protein). The standard bars represent ± one standard error. α and β are significant difference between groups (p<0.05). The p value was calculated by using one-way ANOVA with Tukey's post hoc test.

3.3.3.4 Plasma Analysis

Plasma was sampled from each mouse at pre-treatment, and 1 week, and 1, 3, 5, 7, 9, 11 and 12 months after treatment and MMA levels determined as described in section 2.2.2.6. All the data points from this analysis are shown in Figure 3.3-3. The blue line indicates the mean value of plasma MMA concentrations from wild type mice (n=5), the two red lines indicated the plasma MMA concentrations of the untreated mut -/- muth2 mice, QUE 7.38 and QUE 7.41, and the green lines the HIV-1SDmEF1αhMCM treated mice, QUE 7.47 and QUE 6.94. No decrease in the plasma MMA concentrations were observed in the two treated mice.

However, one of the HIV-1SDmEF1αhMCM untreated mice, QUE 7.38, presented a low level of plasma MMA, with an AUC value at 12 , compared to QUE 7.41, which presented a high level of plasma MMA, with an AUC value at 62, over 12 months of growth (Figure 3.3-4). The biochemical analysis results conducted by Peters *et al*., (2012) [152], who supplied the mut -/- muth2 mouse model for our study, demonstrated a consistently higher concentration of plasma MMA in hemizygous 2-copy rescue mouse model (mut -/- muth2) compared to the homozygous 2-copy rescue mouse model (mut -/- muth2/h2). Therefore, in accordance with the enzyme activity result, the low level of plasma MMA observed in QUE 7.38 suggests that it might be of a mut -/- muth2/h2 genotype, instead of the mut -/- muth2 genotype. Further analyses would be required to validate the hypothesis. Unfortunately, the live cell samples that would be required for the fluorescent *in situ* hybridisation assay used for genotyping were not available by the time this possible anomaly was discovered.

The data points of each individual mouse from the HIV-1SDmEF1αhMCM treated group, were integrated by calculating the area under the curve starting from 1 week until 12 months post-treatment using the trapezoidal rule, whereas the pre-treatment values were included in the integration method for both the normal and untreated groups (Figure 3.3-5). The result shows the resulting averaged total AUC for each group. The normal group demonstrated a

mean ± SE of 0.03 ± 0.01. In contrast, the untreated group had a mean ± SE of 37 ± 25, much higher than the normal group. Nevertheless, the statistical analysis was unable to differentiate between these 2 groups due to the large variance in plasma MMA and the small number of mice in the untreated group. In addition, the plasma MMA analysis demonstrated no evidence of reduction in the treated group compared to the untreated group, with the former having a mean ± SE of 41 ± 18. However, this outcome is inconclusive due to the fact that one of the HIV-1SDmEF1αhMCM untreated control mice, QUE 7.38, might be misidentified. If QUE 7.38 is excluded, there are some indications of a modest, non-significant, reduction of plasma MMA in the treated mice compared to QUE 7.41, which presented a high plasma MMA level (with an AUC value at 62).

Figure 3.3-3 Mut -/- muth2 untreated mice are labelled in red and HIV-1SDmEF1αhMCM treated mice in green. A mean plasma concentration for wild-type mice (normal control) is shown in blue.

Plasma MMA Concentration of Individual Mice Over Time

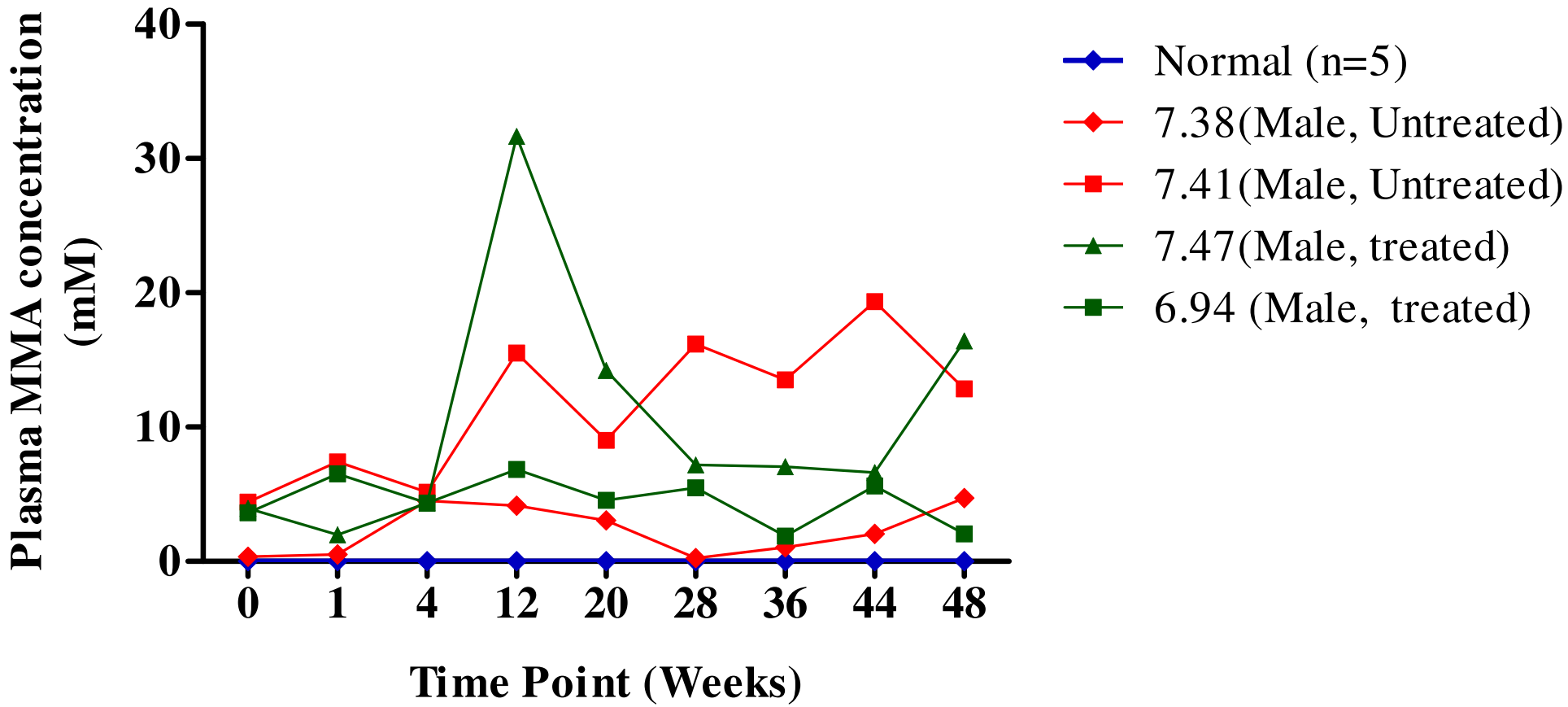

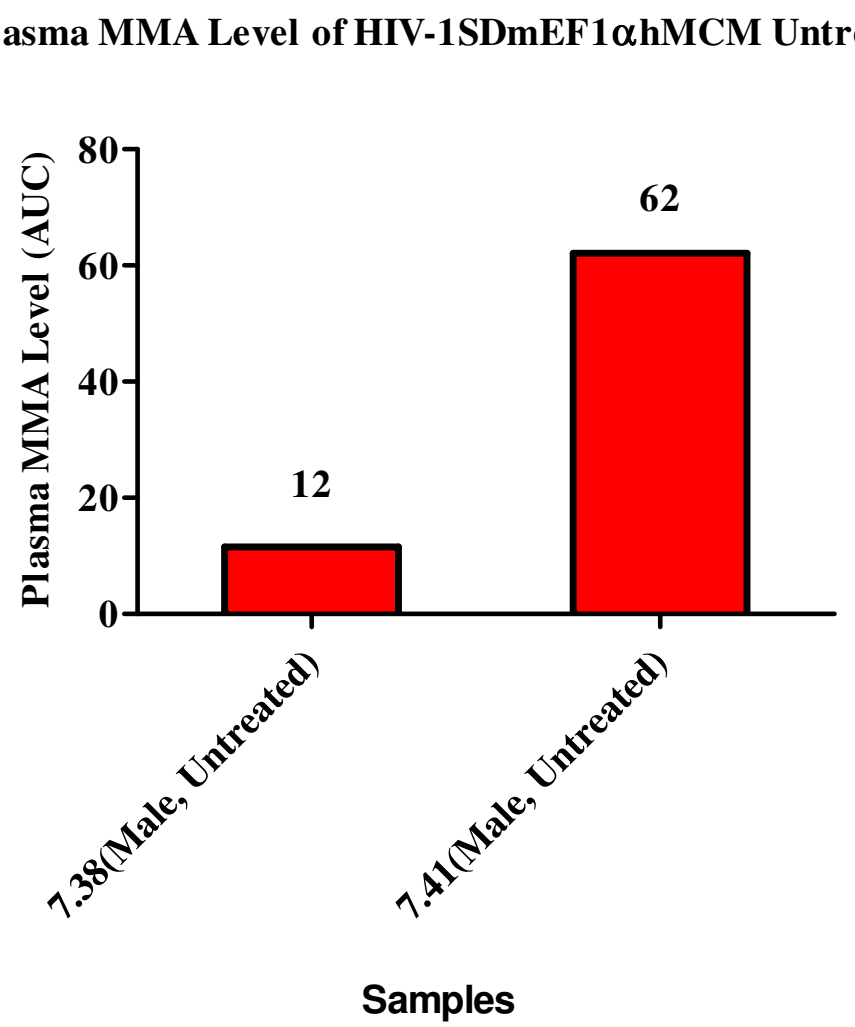

Figure 3.3-4 This graph demonstrated the plasma MMA level of QUE 7.38 and QUE 7.41 HIV-1SDmEF1αhMCM untreated control mice, with the AUC values at 12 and 62, respectively.

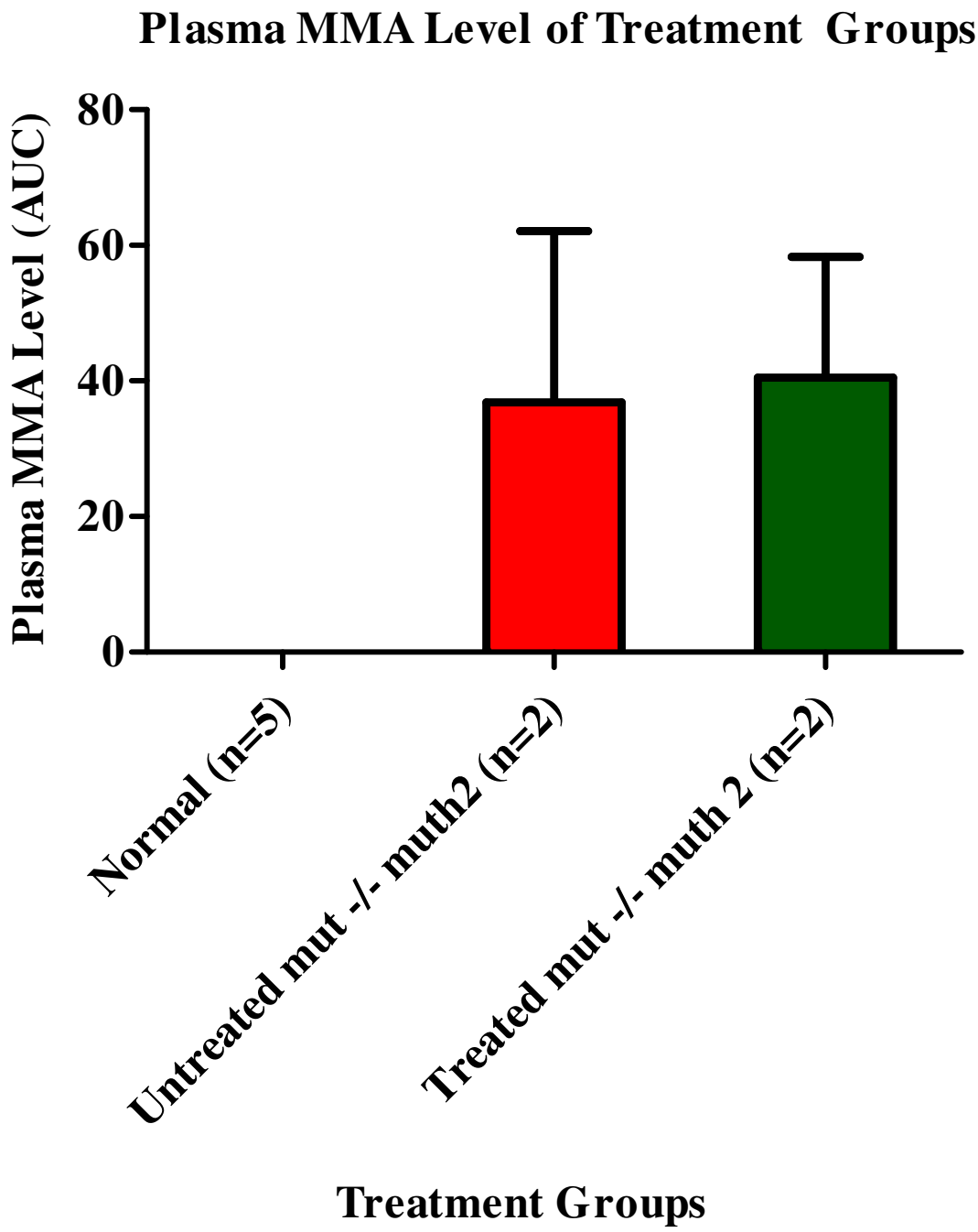

Figure 3.3-5 The data points of each individual mouse were integrated by calculating the area under the curve using the trapezoidal rule as stated and the averaged of total AUC for treatment groups were calculated. Data for normal mice (n=5), mut -/- muth2 untreated mice (n=2) and HIV-1SDmEF1αhMCM treated mice (n=2) are shown. The mut -/- muth2 untreated mice had a mean ± SE of 37± 25. No significance reduction was observed in the lentivirus treated mice, which had a mean ± SE of 41 ± 18. The standard bars represent ± one standard error.

3.3.3.5 Urine Analysis

Urine from each mouse was collected weekly after treatment. Analysis was performed on weekly samples from the HIV-1SDmEF1αhMCM treated and untreated control groups up to 2 months post-treatment. Following this, and to the end of the experiment, only monthly samples were analysed. For the normal controls (n=5) weekly samples were analysed for 2 months and thereafter only the sample representing the last time point of the experiment was analysed.

The mean concentration of urinary MMA from normal controls is indicated by the blue line. The red lines represents the urinary MMA concentration of the untreated mut -/- muth2 mice, QUE 7.38 and QUE 7.41, and the two HIV-1SDmEF1αhMCM treated mice, QUE 7.47 and QUE 6.94, are shown by green lines (Figure 3.3-6). In concordance with the plasma results, the low level of urine MMA observed in QUE 7.38 again indicates that this mouse may be misidentified. If the data from QUE 7.38 is excluded, the urine MMA level of both HIV-1SDmEF1αhMCM treated mice is lower than the other untreated control (QUE 7.41) over the 12 months of the experiment.

All the data points were integrated as described for plasma MMA. An elevation of the urinary MMA level, with a mean ± SE of 4 ± 3.5, was observed in the untreated group compared to the normal group, which had an averaged value that was too low to be detected. The analysis showed a modest decline in the treated group, with a mean ± SE of 3 ± 0.1 compared to the untreated group; however, this was not significant (Figure 3.3-7). However, as with the plasma MMA result, more data is needed to validate this analysis due to the fact that QUE 7.38 might not be of the correct genotype.

The urinary MMA levels of the untreated mut -/- muth2 control mice are shown in Figure 3.3-8. It showed a mild increase in urinary MMA level, with an AUC value of 0.7, in QUE 7.38

compared to QUE 7.41, which demonstrated a great increase in urinary MMA level, with an AUC value of 8. Statistical analysis to compare the untreated and treated groups was not possible due to the small number of mice used in the experiment.

Figure 3.3-6 Mut -/- muth2 untreated mice are shown in red and HIV-1SDmEF1αhMCM treated mice in green. Both the mut -/- muth2 mice were treated with HIV-1SDmEF1αhMCM at 8 weeks of age on the graph. The urinary MMA concentration of normal mice was not detectable.

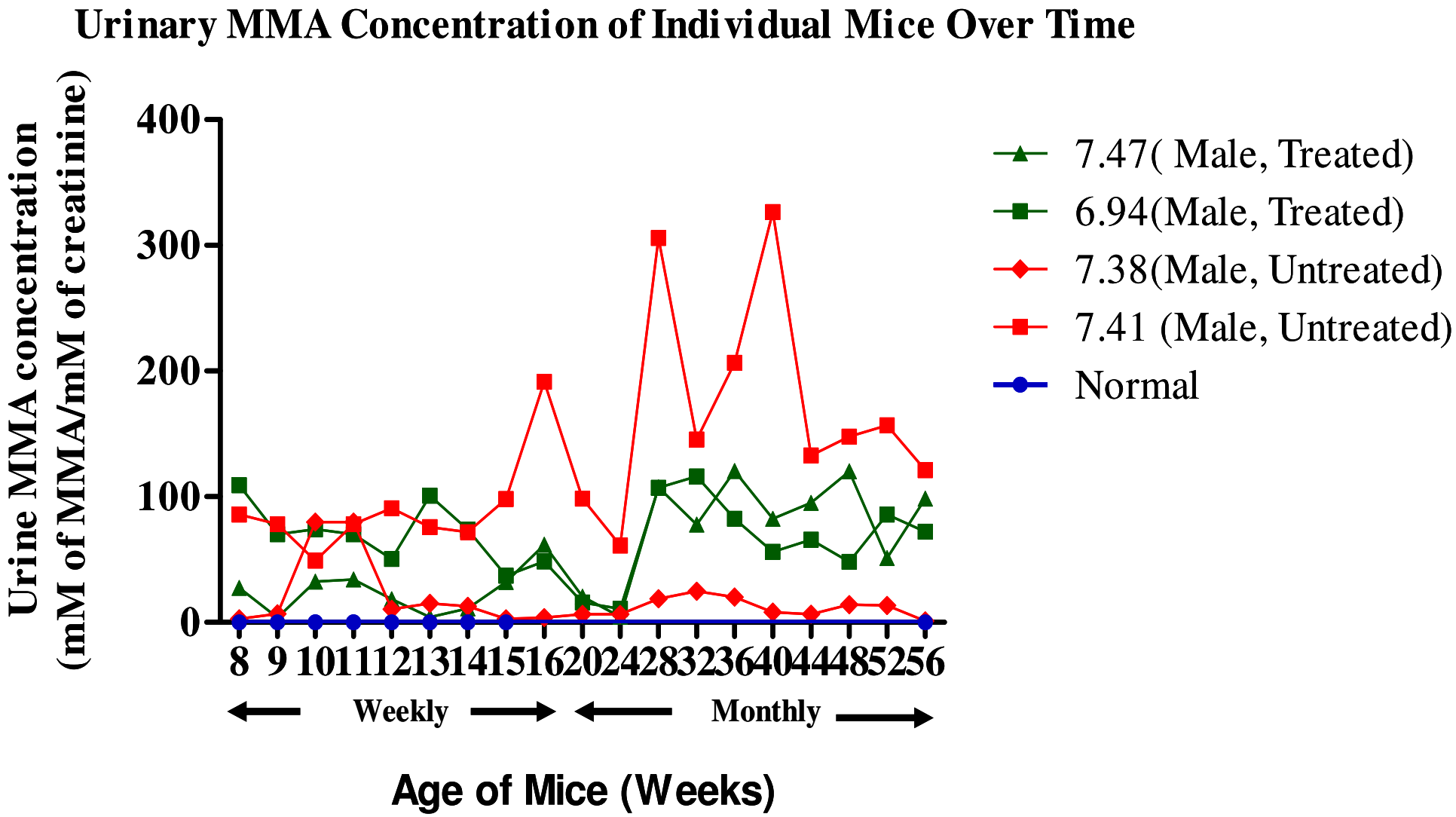
Urinary MMA Concentration of Individual Mice Over Time
Urine MMA concentration
(mM of MMA/mM of creatinine)
400
300
200
100
0
8 9 10 11 12 13 14 15 16 20 24 28 32 36 40 44 48 52 56
Weekly
Monthly
Age of Mice (Weeks)
7.47(Male, Treated)
6.94(Male, Treated)
7.38(Male, Untreated)
7.41 (Male, Untreated)
Normal

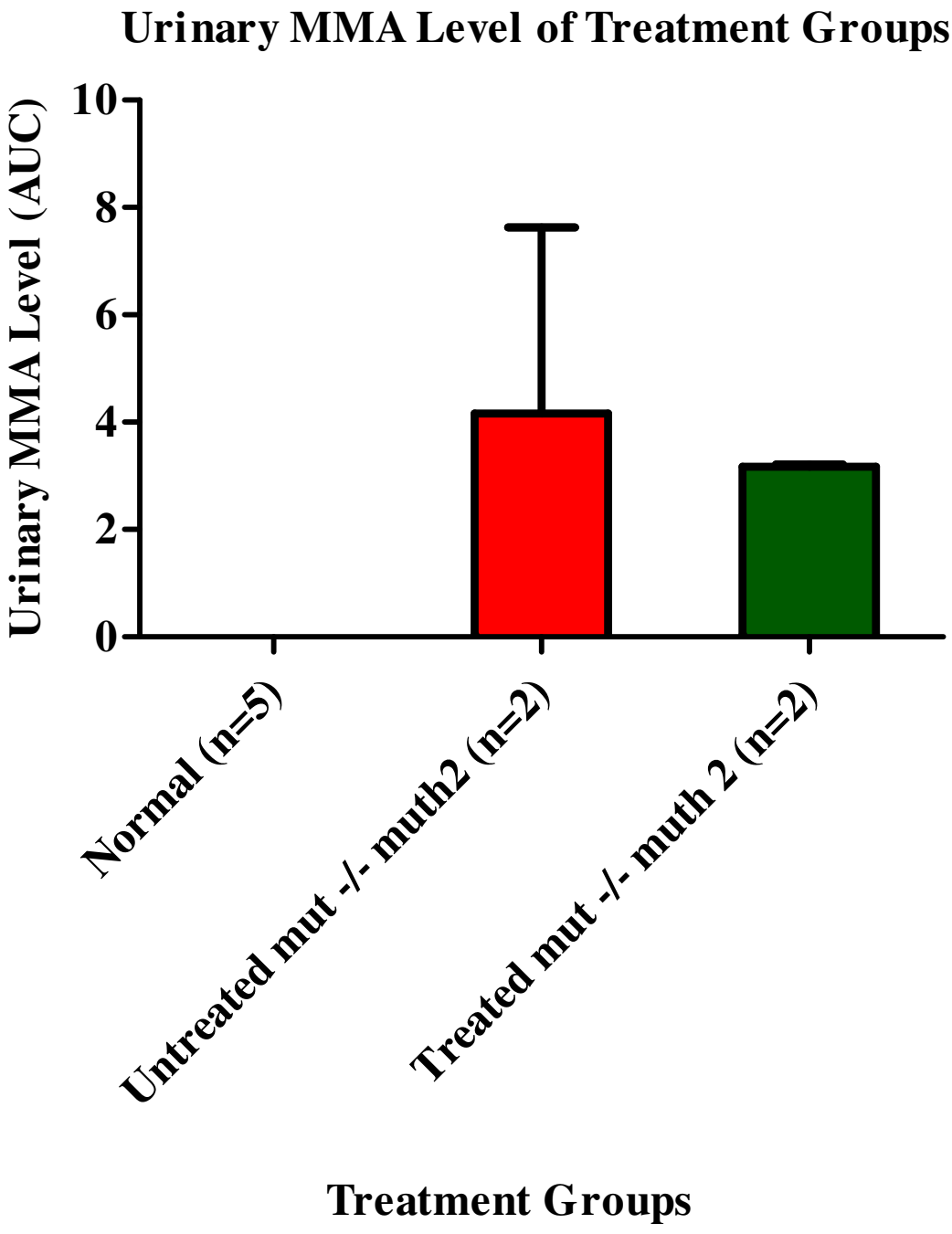

Figure 3.3-7 The data for each individual mouse from Figure 3.3-6 was quantified by integrating the area under the curve as described and the averaged total AUC values were calculated. The averaged of total AUC from normal mice (n=5, blue), mut -/- muth2 untreated mice (n=2, red) and HIV-1SDmEF1αhMCM treated mice (n=2, green) are shown. The mut -/- muth2 untreated mice had a mean ± SE of 4 ± 3. No significance reduction was observed in the lentivirus treated mice, which had a mean ± SE of 3 ± 0.1, compared to the untreated mut -/- muth2 controls. The standard bars represent ± one standard error.

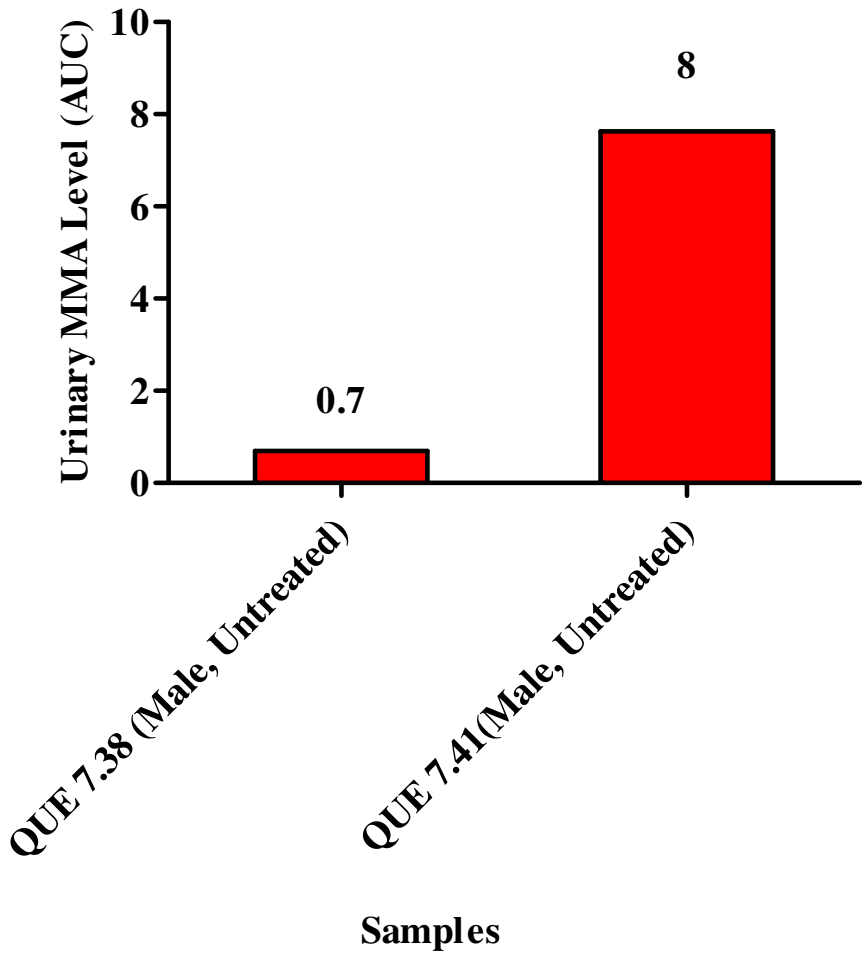

Figure 3.3-8 This graph demonstrated the urinary MMA level of QUE 7.38 and QUE 7.41 HIV-1SDmEF1αhMCM untreated control mice, with AUC values at 0.7 and 8, respectively.

3.3.3 Discussion

Following the successful correction of MCM enzyme activity in MCM knockout fibroblasts using HIV-1SDmEF1αhMCM, it was considered worthwhile to study the efficacy of the vector in an *in vivo* model of MMAuria (mut -/- muth2). This mouse strain provides an ideal model system for the development of new therapies for MMAuria as their MCM enzyme activity is only 20% of normal, and phenotypically they are similar to the human *mut*$^{-}$ form of the disease. In addition this mouse model lives long enough, benefiting from the low level of residual MCM activity, to allow for more flexibility in the timing of gene delivery while still allowing measurement of efficacy.

In our study, the non-tissue specific EF1-α gene promoter was used in an attempt to ensure strong and sustained expression of hMCM. Studies conducted by Kim *et al*., (1990) [187] and Uetsuki *et al*., (1989) [188] have characterised the molecular properties of the promoter region of the EF1-α gene. The studies from yeast [189] and mammalian cells [188] showed that the EF1-α gene is expressed abundantly in almost all tissues. In addition, it can be regarded as "housekeeping" gene, as it encodes an integral part of the translational machinery. Analysis using *in vitro* transcription assays, published by Uetsuki *et al*., (1989) [188] provided evidence that the promoter of the human EF1-α gene could direct transcription approximately 2-fold more effectively than the Adv major late promoters, suggesting that the EF1-α promoter is a strong one. A number of studies have also demonstrated that a high level of transgene expression can be achieved using this promoter in various viral vector systems [190-192].

The human MCM cDNA was used in preference to the mouse sequence as the mouse model used is null for murine MCM, raising the possibility of an immune response to the murine enzyme, but transgenic for the human MCM transgene [152] meaning it will be immune

tolerant for the human enzyme. Potential complications due to an immune response to the vector transgene were therefore avoided.

The *in vitro* data demonstrated the ability of the HIV-1SDmEF1αhMCM vector to correct the metabolic defect in MCM fibroblasts. However, analysis of vector copy number and enzyme activity showed that expression from the vector was about ½ as efficient as from the endogenous gene in fibroblasts. Despite this, pilot studies of the potential of the HIV-1SDmEF1αhMCM vector to correct the disease in the mut -/- muth2 MMA murine model were clearly warranted.

Due to a limitation on the number of animals available, only two mice, QUE 7.47 and QUE 6.94, were treated. Each of the mice received a 50 µg p24 equivalent IV dose of HIV-1SDmEF1αhMCM vector at 8 weeks of age. However, as shown in the results, these 2 mice showed no gain in their bodyweight compared to the untreated affected controls and their weight remained far from the normal range of age matched normal mice.

Vector copy number analysis indicated that, as expected, the transduction was detected primarily to the liver, with approximately 0.25 copies per cell. It should be of note that other than the liver, spleen and kidneys, the biodistribution of LV vector was measured in other tissues, including gut, brain and skeletal muscles in the study (data not shown). No vector copy number was detected in tissues other than the liver, spleen and kidneys. This observation is in accordance with previous findings that liver appears to be the main target after IV gene delivery [143, 193-195]. Additionally, the detection of vector 12 months post-treatment indicated the integration of the vector into the host DNA. This is consistent with the study published by Follenzi *et al*., (2002) [143] that showed the efficient gene transduction and expression in hepatocytes using an LV vector. A LV vector that expressed eGFP marker gene (LV-eGFP) was used to investigate the gene transduction of liver cells *in*

vivo. The LV-eGFP was administered into the SCID mouse mouse model *via* the tail-vein. The results indicated the detection of eGFP fluorescence in the mouse liver for up to 6 months, demonstrating successful gene transduction and stable expression of the transgene. Following this, they evaluated the therapeutic potential of LV vector in SCID disease by intravenously administering an LV vector that expressed the human clotting IX (hF.IX) cDNA into SCID mice. Long-term expression of the hF.IX transgene (up to one year) was seen in the treated mice, indicating stably transgene integration and sustained expression.

The success of intravenous gene delivery has resulted in the production of MCM in the liver of the mut -/- muth2 model. The enzyme activity showed only a modest increase of MCM enzyme activity in the HIV-1SDmEF1αhMCM treated group compared to the untreated (28% versus 11% of normal group). This level of MCM activity was not sufficient to significantly lower the MMA level in the plasma or in the urine, when compared to untreated affected mice, even if the data of the probably misidentified mouse, QUE 7.38, was excluded. This suggests a higher level of transduction and/or a more efficient vector will be needed in order to produce sufficient MCM enzyme activity to significantly ameliorate the disease pathology. In the study conducted by Kaleko *et al*., (1991) [196], which investigated the long-term expression of neomycin phosphotransferase (neo) in mouse heptocytes using the LN-retrovirus, it was demonstrated that there was a close correlation between the number of retrovirus infected cells and the dose of infectious vector particles. This finding suggests the possibility of producing a higher level of gene transduction by using a higher dose of infectious virus particles. In fact, this hypothesis is supported by other studies using lentiviral vectors [197-200]. A similar relationship has been observed with the vector system used in the study conducted by McIntyre *et al*., (2010) [193], which examined the effectiveness of a LV vector in correcting mucopolysaccharidosis type IIIA (MPS IIIA). This vector was essentially the same as that used in our study but with different transgene. In the MPS study, two groups of MPS IIIA mice were administered with either 50 µg of p24 equivalent or 75 µg

of p24 equivalent LV vector, respectively, again *via* the tail vein. Similar results were found, the liver was the main site of transduction followed by spleen. Furthermore, the study showed that the amount of integrated vector was increased by a third with the higher dose of vector. Therefore, a higher dose of the vector is clearly one way of increasing the efficiency of gene delivery.

Apart from increasing the dose of lentiviral vector, the gene transduction efficiency could possibly be optimized by manipulation of the specific infectivity of the lentivirus used. Koldej *et al*., (2005) demonstrated that the specific infectivity of the virus (i.e. infectious particles/ng p24) could be increased approximately 3-fold by decreasing the amount of gagpol plasmid used during vector production [150]. However, the disadvantage of this approach is that the total amount of virus is reduced.

In addition, Ye *et al*., (2001) [181] has discussed the use of a species-specific mitochondria import signal. This study, which investigated the efficacy of an adenoviral vector in treating OTC deficiency in rodent models, demonstrated the importance of using a species-specific amino-terminal leader peptide to enhance the translocation efficiency of the human OTC into the mitochondrion. Therefore, the efficiency of translocation of the human MCM into the murine mitochondria could potentially be improved with the use of a murine signal, again resulting in improved MCM expression.

Another strategy that is likely to help overcome the low levels of MCM expression is to codon-optimize the human MCM for expression in murine cells. Numerous studies have shown the advantages of using this strategy to enhance gene expression [201-203]. The study conducted by Mcintyre *et al*., (2010) [193], which investigated the therapeutic effect of a codon-optimised sulphamidase transgene in MPS IIIA mouse model, again delivered with the same LV vector, showed an increase of sulphamidase enzyme activity of 30% through the use

of a codon-optimised sulphamidase. These results suggest that the use of a codon-optimised hMCM may enhance MCM transgene expression in our study.

The study published by McIntyre *et al*., (2010) [193] also showed a widespread vector biodistribution after IV injection, although most vector was detected in the liver. This raises the possibility of choosing an alternative route of administration to increase the vector copy number in the liver. In fact, a number of studies have shown that the route of administration plays a major role in determining the transduction efficiency. A study published by Gonin *et al*., (2004) [204] demonstrated the biodistribution of different vectors with different routes of administration in the animal tissues. In concordance with the results published by McIntyre, they showed that liver appears to be the main target of gene transfer after intravenous injection. However, Gonin's study also indicated that the intrahepatic (IH) injection may be another option to deliver the vector into the liver. In addition, a number of other studies have shown that very efficient liver-specific gene transduction is achieved with this delivery method [121, 205-207]. However, the need for surgical procedures, such as laparotomy, may be contraindicated given the fragility of the MMAuria affected mouse model. Further studies are required to investigate its feasibility.

In conclusion, our results show some evidence that the correction of MMAuria disease *in vivo* can be achieved using LV. The results have shown success in targeting the liver with the intravenous delivery approach. However, it is clear that improvements in gene delivery to enhance the transduction efficiency are required. In addition, we have detected some restoration of MCM enzyme activity in the liver albeit at relatively low levels. This led to modest reductions of the MMA level in plasma and urine. These results suggested that a significant improvement in hMCM transgene expression is required in order to enhance MCM enzyme activity and so to further reduce the MMA level in the blood and urine. Nevertheless, through this preliminary study, a number of approaches have been raised to explore the

possibility of increasing gene transduction and MCM expression levels in the mitochondrion, such as specific infectivity, codon-optimization, a murine signal peptide and the use of a different route of administration.

Chapter 4 : Correction of MMAuria Using Codon-Optimised LV Vector with Murine Mitochondrial Transportation Signal

4.1 Constructions of Codon-Optimised LV Vector

4.1.1 Introduction

As discussed in Chapter 3, the low level of MCM enzyme activity observed in the studies presented in that chapter may be the result of the poor expression from the vector encoded human MCM cDNA in the murine model. Several strategies that could be used to improve the human MCM gene expression *in vivo* were also put forward. These strategies include the codon-optimization of the human MCM cDNA, increasing the dosage of vector and increasing the specific infectivity of the vector by reducing the amount of gagpol plasmid DNA used for virus production. Each of these strategies is discussed in the respective section of this chapter.

In addition, another possible reason for the poor expression of MCM activity may the use of the human mitochondrial importation signal in the mouse system. The mouse and human MCM amino acid sequences have a 94% homology [180]. Despite the similarity in the apoenzyme sequence, there are only 69% (20/32) residues identical in the mitochondrial targeting sequence (Figure 4.1-1A and B). This dissimilarity may have affected the translocation efficiency of the (human) enzyme into the (murine) mitochondria. A similar sequence divergence in the mitochondrial targeting sequence is also found between the mouse and chicken aspartate aminotransferases, and between the respective OTCs. In the latter case the study by Ye *et al*., (2001) [181] demonstrated that these differences affect the translocation efficiency of human OTC into the murine mitochondria. This is also likely to be the case for human MCM expressed in a mouse cell. Therefore, before the GenScript codon-optimization process, the human MCM sequence was modified by replacing the human

targeting sequence with the murine one in order to ensure efficient translocation of the enzyme in the mouse model.

Following this, the murine signalled human MCM (murSigHutMCM) was codon-optimised for expression in murine cells by GenScript. The mutase gene was initially analysed using Rare Codon Analysis Tools, a free software package provided by GenScript (http://www.genscript.com/cgi-bin/tools/rare_codon_analysis), in order to determine the need to optimize the mutase cDNA. The human MCM cDNA sequence was analysed in four different ways, these being the codon adaptation index (CAI), GC content, codon frequency distribution (CFD) and analysis of negative *cis*-elements and repeat sequences.

CAI indicates the distribution of codon usage frequency along the length of cDNA to be expressed in the target host organism. High protein expression levels can be achieved when the CAI value is 1 and it is considered to be ideal if CAI is greater than 0.8. The analysis tools also examine the GC content of the cDNA to be expressed in the target host organism. Different expression host organisms require different ranges of GC content. For example, based on the analysis, the ideal GC content for mouse is between 30% and 70%. GC contents that falls outside this range affect transcriptional and translation efficiency. The analysis tool also allows analysis of CFD, which is used to check the highest usage frequency of a codon for a given amino acid in the target host organism. Codons with values lower than 30 are likely to hamper expression efficiency. The analysis of negative *cis*-elements refer to sequence motifs that regulate gene expression at the transcriptional or translational level while negative repeat elements refer to direct or inverted repeats that may affect gene transcription or expression.

Mitochondrial Targeting Signal

(A)

Human - ATGTTAAGAGCTAAGAATCAGCTTTTTTTACTTTCACCTCATTACCTGAGGCAGGTAAAAGAATCATCAGGCT

Mouse - ATGTTGAGAGCTAAGAATCAACTTTTTTTGCTATCGCCCCATTACCTGAAGCAGAACATTCCATCATCAGCTT

Human - CCAGGCTCATACAGCAACGACTT

Mouse - CCAGATGGAAACGCCTTCTACAC

(B)

Human – Met-Leu-Arg-Ala-Lys-Asn-Gln-Leu-Phe-Leu-Leu-Ser-Pro-His-Tyr-Leu-Arg-Gln-Val-Lys-Glu-Ser-Ser-Gly-Ser-Arg-Leu

Mouse - Met-Leu-Arg-Ala-Lys-Asn-Gln-Leu-Phe-Leu-Leu-Ser-Pro-His-Try-Leu-Lys-Gln-Leu-Asn-Ile -Pro-Ser-Ala-Ser-Arg-Trp

Human – Ile-Gln-Gln-Arg-Leu

Mouse - Lys-Arg-Leu-Leu-His

Figure 4.1-1 (A) The figure shows the alignment of the mitochondrial transportation signal gene sequence from the human and mouse MCM genes. (B) Corresponding to Figure 4.1-1A, this figure shows the amino acid alignment of the mitochondrial transportation signal from the human and mouse MCM genes. The red highlighted indicates non-matching residues.

The analysis of the human MCM cDNA indicated that the CAI value of the cDNA is 0.74, which was slightly below the ideal value of 0.8. The analysis also demonstrated an average GC content of 42.03% and that the sequence was prone to the use of tandem rare codons that can reduce the efficiency of translation. In addition, the high number of negative *cis*-elements and repeat elements, 8 and 23 respectively, suggested that these may also affect gene transcription and expression (Appendix II).

After codon-optimization by GeneScript, the CAI showed a significant increase to a value of 0.81, which is within the ideal range for expression in mouse. The average GC content was also improved to 53.27%, as was the use of common codons found in the mouse. In addition, to maximize translation and improve mRNA stability, GenScript had also removed the negative *cis*-regulatory elements in the human MCM gene sequence. This is a region of DNA or RNA that downregulates the expression of genes. Also, the codon-optimised sequence showed a reduction in negative repeat elements from 23 to 12 (See Appendix III).

The aim of the experiments described in this chapter was to evaluate, *in vitro* and *in vivo*, the efficacy of a LV vector that utilises the codon-optimised cDNA that expresses a chimeric construct of human MCM transgene with murine signal (HIV-1SDmEF1αmurSigHutMCM) using a protocol identical to that used in previous chapter, thus allowing a direct comparison of the results of both experiments.

4.1.2 Vector Construction

The codon-optimised human MCM coding sequence (murSigHutMCM), optimised by GenScript, was isolated by digestion with 5'-*Cla*I/ 3'-*Nde*I, resulting in a sticky-end fragment of 2268 base pairs. This was purified away from the cloning vector by agarose gel electrophoresis and isolated as described in section 2.2.3.14.

In order to allow a direct comparison to the LV vector described in the previous chapter, the murSigHutMCM sequence was cloned into the same vector backbone as before. The luciferase coding sequence was removed from *p*HIV-1SDmEF1αLuciferase digestion with 5'-*Cla*I/3'-*Nde*I and a sticky-end ligation was performed to re-ligate the purified murSigHutMCM fragment into the vector as described in section 2.2.3.4. After electroporation into Sure *E. Coli* electrocompetent cells several clones were isolated and analysed (Figure 4.1-2).

4.1.3 Analysis of Putative Clones

DNA was extracted from colonies and processed using the mini-prep DNA extraction method described in section 2.2.3.2 and analysed by digestion with *Apa*I (Figure 4.1-3). The correct vector construct should contain fragments of 5876, 1558 and 1547 base pairs (Figure 4.1-4).

Lane 1 and 17 represent *Spp*I / *Eco*RI Mw markers. Each of the digested samples, designed as C1 to C24, was run in order. Most of the clones are shown to carry the correct sequence (i.e. lane 3-10, lane 22-25).

To further confirm the correct sequence, the plasmid DNA of the one clone, C8, selected for further use in our study, was processed as described in section 2.2.3.16 for DNA sequencing.

Figure 4.1-2 Construction of *p*HIV-1SDmEF1αmurSigHutMCM

The murSigHutMCM sequence was removed by digestion with *Cla*I/*Nde*I. This was then cloned into a *p*HIV-1SDmEF1αLuciferase digested with the same enzymes.

Preparation of *p*HIV-1SDmEF1αmurSigHutMCM

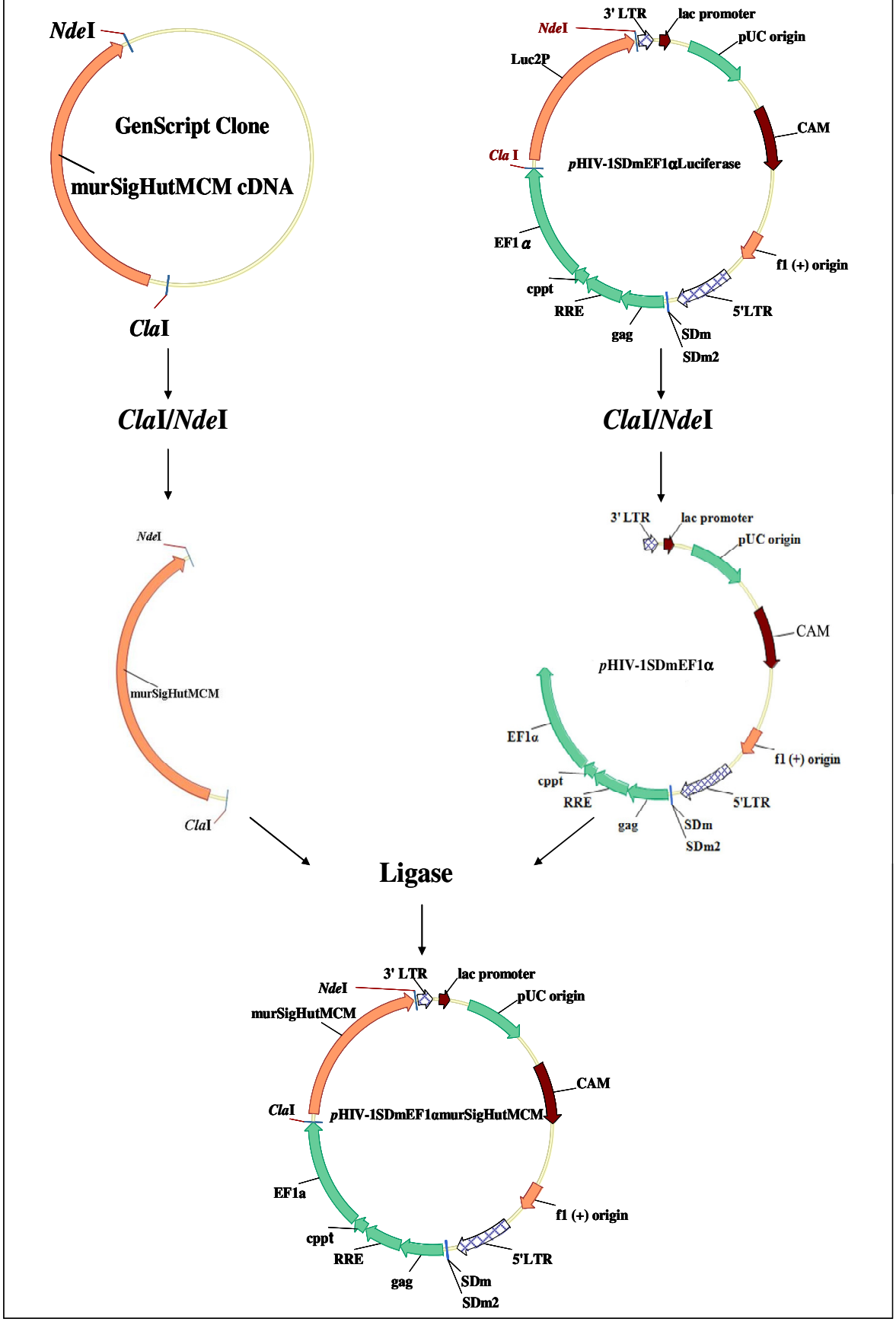

Figure 4.1-3 Restriction Enzyme Analysis of Clones

Clones were analysed by *Apa*I digest. Clones of the correct structure should give fragments of 5876 bp 1558 bp and 1547 bp. Lane 1/16 : *Spp*I / *EcoR*I Mw marker, Lanes 2-16 : clones C1- C15, Lane 17 : *Spp*I / *Eco*I Mw marker, Lane 18 – 27 : clones C16-C24.

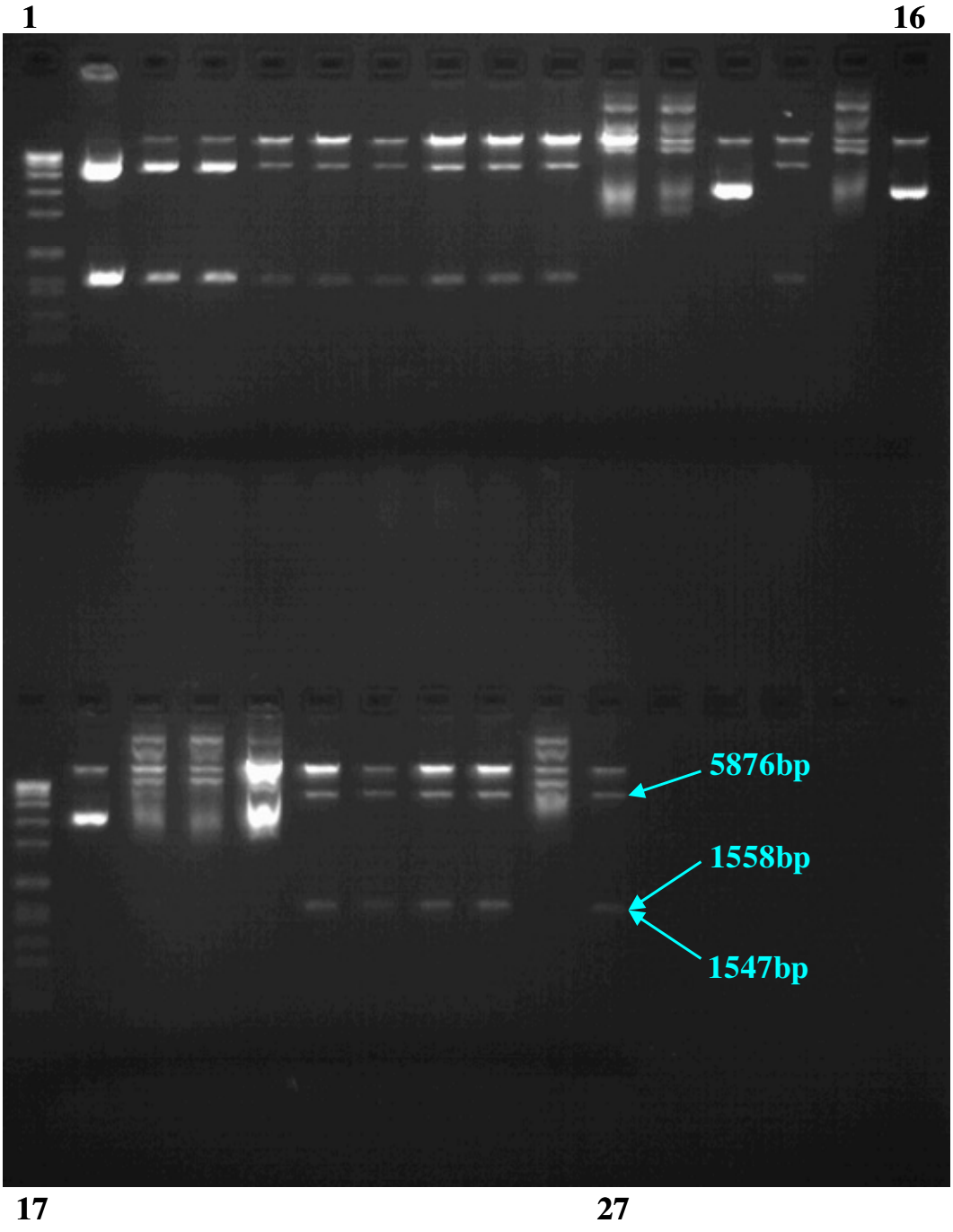
1
16
5876bp
1558bp
1547bp
17
27

Figure 4.1-4 Schematic Diagram of *p*HIV-1SDmEF1αmurSigHutMCM

SD = major splice donor; RRE = Rev response element; cppt = central polypurine tract; EF1α = Elongation Factor 1α promoter; murSigHutMCM = murine signalled human MCM gene coding sequence. The restriction sites used for cloning and for analysis are shown. The primer target sites for the *p*BlueT7, *p*Blue Rev and RREf primers are also shown in this figure.

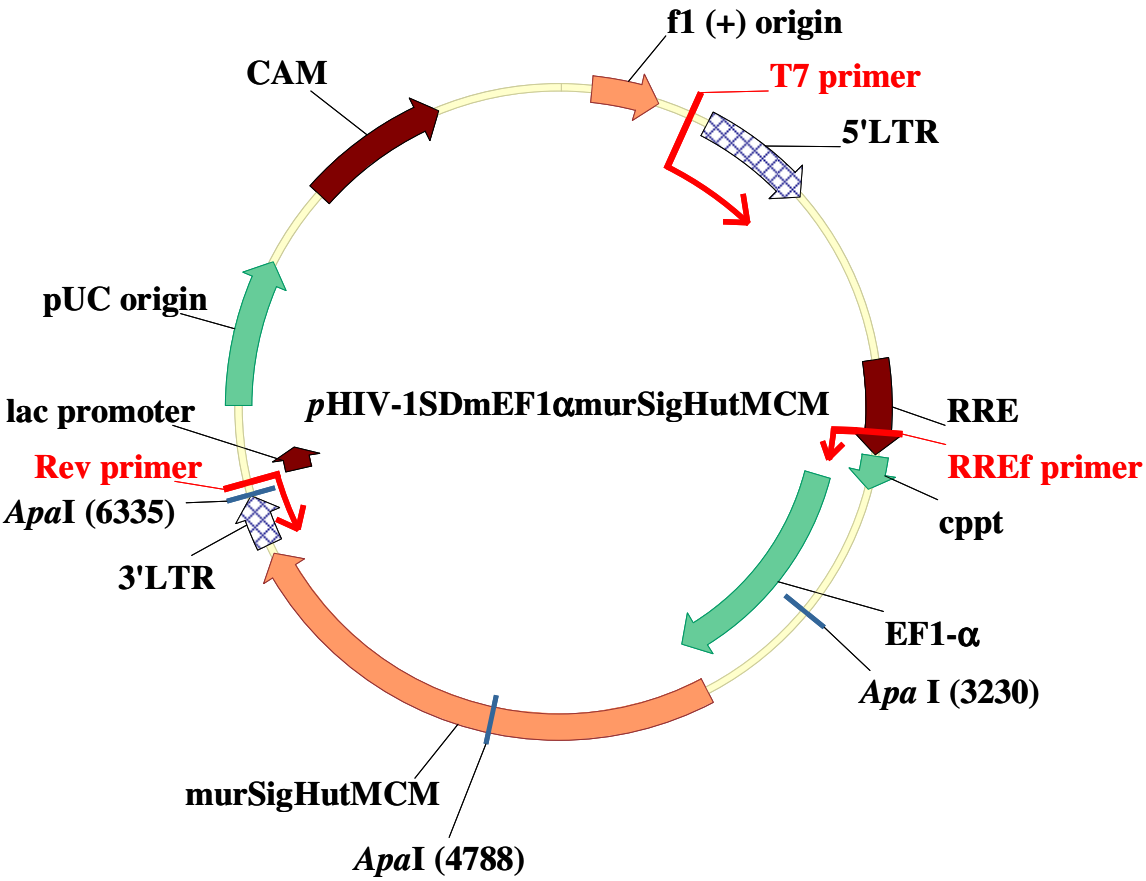
f1 (+) origin
CAM
T7 primer
5'LTR
pUC origin
lac promoter
pHIV-1SDmEF1αmurSigHutMCM
RRE
Rev primer
RREf primer
ApaI (6335)
cppt
3'LTR
EF1-α
Apa I (3230)
murSigHutMCM
ApaI (4788)

4.2 LV-Mediated Gene Transfer *In Vitro*

4.2.1 Aim

The aim of this experiment was to evaluate the gene expression capability of the codon-optimised human MCM with the murine signal peptide, HIV-1SDmEF1αmurSigHutMCM, in comparison to the previous vector construct, HIV-1SDmEF1αhMCM, *in vitro*. MCM knockout fibroblasts were separately transduced with each vector. Untransduced and HIV-1SDmSV40eYFP transduced MCM knockout fibroblasts were used as negative controls.

HIV-1SDmEF1αhMCM, HIV-1SDmEF1αmurSigHutMCM and HIV-1SDmSV40eYFP were produced as per the small-scale method described in Section 2.2.1.8, in a total volume of 20 mL. One hundred µL of the virus solution was retained for the measurement of total virus particles (p24 assay). The MCM knockout fibroblasts, in 3 x 100 mm cultured dishes, were transduced with the three different virus preps, as described in 4.2.1. The virus transduced fibroblasts were then subcultured to provide material for measurement of MCM enzyme activity, analysis of vector copy number and MCM protein expression (western blot analysis) as per the methods described in section 2.2.3.9, 2.2.3.11 and 2.2.3.17, respectively.

4.2.2 Methods and Results

4.2.2.1 Measurement of Total Virus Particles Produced by p24 Elisa

Total virus particles were measured by p24 Elisa assay, conducted as per the method described in section 2.2.1.9. The amount of p24 in the HIV-1SDmEF1αhMCM, HIV-1SDmEF1αmurSigHutMCM and HIV-1SDmSV40eYFP samples was 1.33 µg/mL, 1.16 µg/mL and 1.35 µg/mL, respectively.

4.2.2.2 Measurement of Vector Copy Number

MCM knockout fibroblast transduced with HIV-1SDmEF1αhMCM, HIV-1SDmEF1αmurSigHutMCM and HIV-1SDmSV40eYFP were maintained and subcultured 1:3 for 2 weeks prior to harvest for vector copy number measurement.

For determination of copy number the LV vector treated MCM knockout fibroblasts were harvested from the cultured dishes as described in section 2.2.1.3 and their DNA was isolated as described in section 2.2.3.10.

Vector copy number was quantified using the Taqman real-time PCR assay described in section 2.2.1.10. The assay detected the beginning of the *gag* sequence in the vector. At the same time, a control assay was performed. This assay detected the mouse transferrin gene which is a single copy gene in the haploid genome (i.e. 2 copies per cell). This control assay was used to correct for variation in cell equivalents of genomic DNA added to each reaction.

To determine the vector copy number in each sample they were analysed in triplicate and their cycle threshold (Ct) values obtained. These were then used to calculate the gene copy number. The result showed that no vector sequences were detected in the untreated MCM knockout fibroblasts. A significant vector copy number was detected in all the lentiviral transduced samples, with 16 ± 0.8, 20 ± 0.8 and 22 ± 2.1 copies in the HIV-1SDmSV40eYFP, HIV-1SDmEF1αmurSigHutMCM and HIV-1SDmEF1αhMCM samples, respectively (Figure 4.2-1).

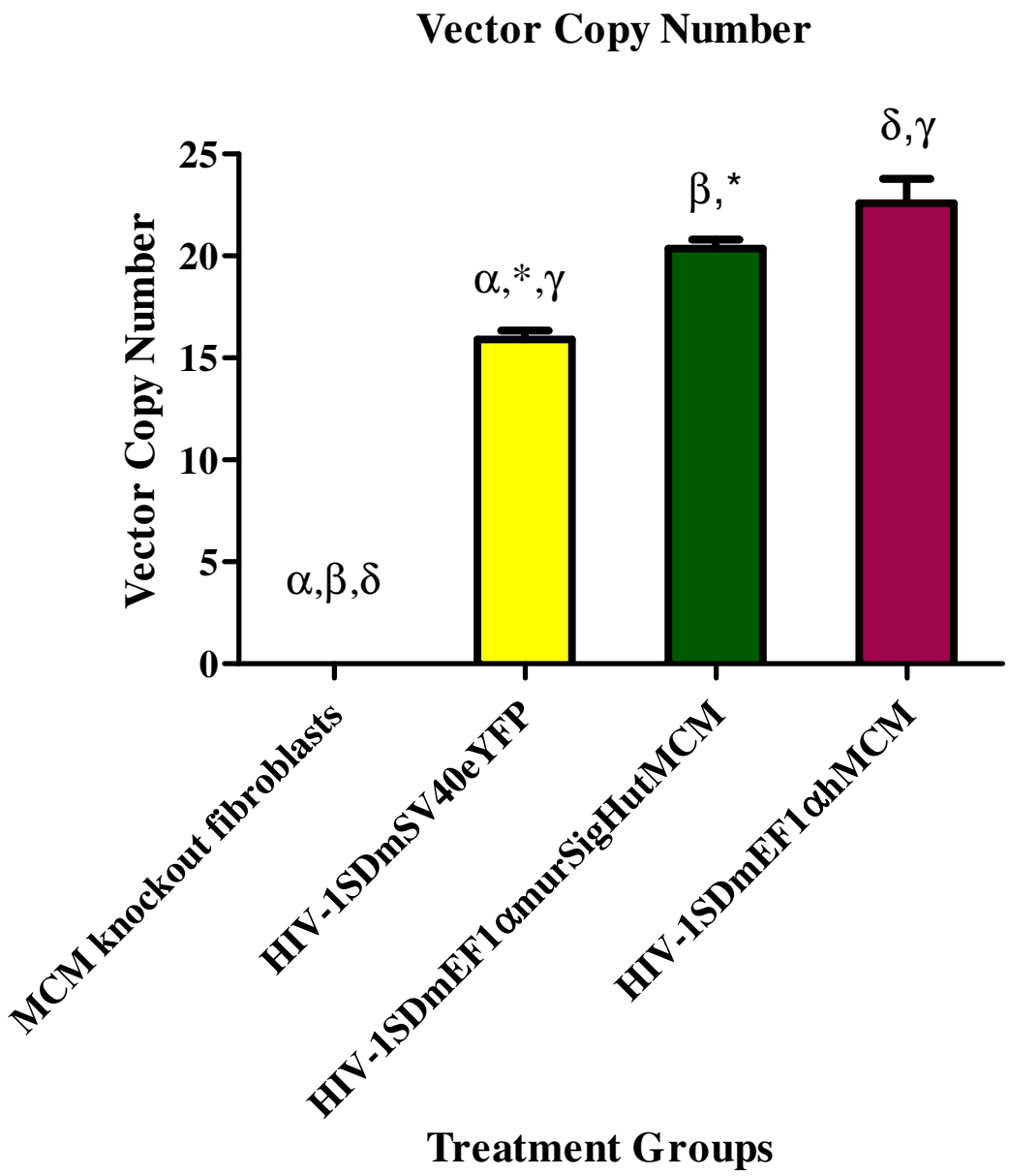

Figure 4.2-1 Comparison of the vector copy number between the MCM knockout fibroblasts transduced with HIV-1SDmSV40eYFP, HIV-1SDmEF1αmurSigHutMCM and HIV-1SDmEF1αhMCM. The resulting cultures were assayed for vector copy number by real-time PCR. (n=3 for MCM knockout fibroblast control, HIV-1SDmSV40eYFP, HIV-1SDmEF1αmurSigHutMCM and HIV-1SDmEF1αhMCM treated MCM knockout fibroblasts. The standard bars represent ± one standard error. α, β, δ represent a significant difference compared to the MCM knockout fibroblasts (p <0.05). * and γ represent a significant difference compared to the HIV-1SDmSV40eYFP (p<0.05). The p value amongst the groups was calculated by one-way ANOVA with Tukey's post-hoc test.

4.2.2.3 Western Blot Analysis

Western blot analysis was used to analyse expression of human MCM in transduced MCM knockout fibroblasts. Transduced MCM knockout fibroblasts were harvested as described in section 2.2.1.3 and processed for western blot analysis as described in section 2.2.3.17 using the anti-human MCM mouse polyclonal antibody. β-actin was also analysed using the anti-β-actin mouse monoclonal antibody to provide a loading control.

The analysis demonstrated that the expression at the protein level was completely restored in the corrected MCM knockout fibroblasts (Figure 4.2-2). Lanes 3 and 4 showed no detectable protein band, lane 3 being untransduced MCM knockout fibroblasts, which served as negative control, and Lane 4 being MCM knockout fibroblasts transduced with HIV-1SDmSV40eYFP. The positive control (HEK293T cells, Lane 2), showed a single band at 83kDa, slightly larger than the size expected for mature human MCM (78 kDa). Lane 5 shows cells transduced with HIV-1SDmEF1αhMCA and Lane 6 cells transduced with HIV-1SDmEF1αmurSigHutMCM, both exhibit the 83 kDa band corresponding to human MCM. In addition, several smaller reactive bands were also seen in these samples between 66 and 80 kDa.

ImageJ software was used to quantify the protein level by measuring the intensity of the bands. The result of this analysis demonstrated an increase in protein expression, by 3-fold, was observed in the HIV-1SDmEF1αmurSigHutMCM transduced sample compared to the HIV-1SDmEF1αhMCM treated MCM knockout fibroblast, with a value of 0.6 and 0.2 respectively after normalized to the loading control, as calculated using ImageJ. Nevertheless, statistical analysis could not be used to compare these two groups due to the small number of samples involved in these groups.

The detection of human MCM at 83kDa, rather than the expected 78 kDa, probably represents the expression of a pre-matured human MCM. As described in Chapter 1, pre-matured human

MCM, as found in the cytoplasm, is 3-4kDa larger than the matured and functional MCM (~78kDa) found after translocation into mitochondria.

The smaller bands seen in the HIV-1SDmEF1αmurSigHutMCM and HIV-1SDmEF1αhMCM samples may represent partially digested MCM as the cell lysates corresponding to these samples were kept at -20 °C for 1 year, possibly allowing the human MCM protein to have been digested by protease in the sample. The HEK293T sample provides some evidence in support of this in that it represents a fresh extract and it contains no smaller bands that react with the MCM antibody.

Figure 4.2-2 Western analysis of cell protein lysates from HEK293T cells, MCM knockout fibroblasts (transduced and untransduced) with the MCM antibody (reactive band at 83 kDa, labelled MCM) and beta-actin loading control (42 kDa). Twenty five µg of total protein samples was loaded per lane. Lane 1: Protein Ladder Marker; Lane 2: HEK293T cells; Lane 3: MCM knockout fibroblasts; Lane 4: HIV-1SDmSV40eYFP treated MCM knockout fibroblasts; Lane 5: HIV-1SDmEF1αhMCM treated MCM knockout fibroblasts; Lane 6: codon-optimised HIV-1SDmEF1αmurSigHutMCM treated MCM knockout fibroblasts. The intensity of the MCM expression from each protein lysate was determined using ImageJ and is corrected for loading using the β-actin band intensity.

Western Blot Analysis

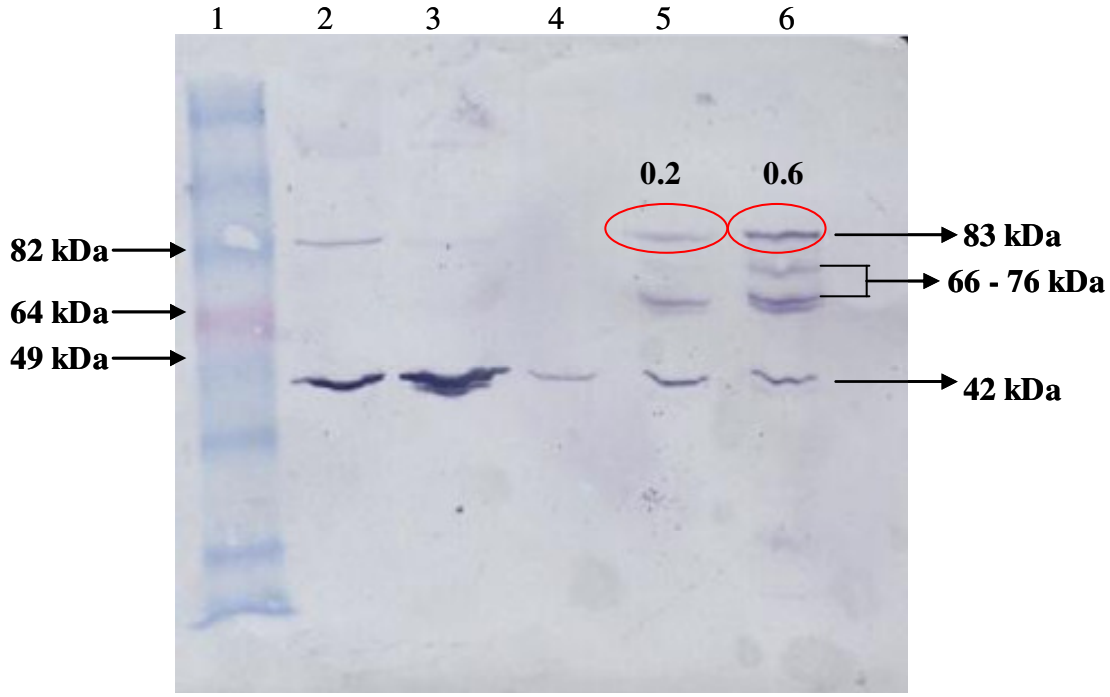

4.2.2.4 Direct Measurement of MCM Enzyme Activity by HPLC

MCM enzyme activity was measured according to the method described in section 2.2.3.9. This method directly measures the production of succinyl coenzyme A in cell lysates after the addition of AdoCbl. The result shows a significant increase of MCM enzyme activity in MCM knockout fibroblasts transduced with HIV-1SDmEF1αmurSigHutMCM compared to the untreated MCM knockout fibroblasts, with a mean ± SE of 179 ± 19 nM succinyl coenzyme A / min / μg of total cell protein been produced (p<0.05), approximately twice the activity in the HIV-1SDmEF1αhMMA treated MCM knockout fibroblasts (85 ± 13 nM / min / μg). Importantly, this level was significantly higher, by 5-fold, compared to the level found in the HEK293T cells (24 ± 1 nM / min / μg) (Figure 4.2-3).

In addition, our data showed that the restoration of MCM enzyme activity per vector copy number in LV transduced MCM knockout fibroblasts is significantly higher (p<0.05, paired t-test) in HIV-1SDmEF1αmurSigHutMCM transduced MCM knockout fibroblasts, with a mean ± SE of 9 ± 1 nM / min / μg total cell protein/ copy number, compared with the HIV-1SDmEF1αhMCM transduced samples (4 ± 1 nM / min / μg total cell protein/ copy number) (Figure 4.2-4).

Figure 4.2-3 MCM knockout cells (transduced and untransduced) and HEK293T cells were assayed for MCM enzyme activity as described in material and methods section 2.2.3.9. Samples were analysed in triplicate. The standard bars represent ± one standard error. α, β indicate significant difference compared to the HEK293T cells ($p< 0.05$, Tukey's post-hoc test). δ, * indicate significant difference compared to the MCM knockout fibroblasts ($p<0.05$, Tukey's post-hoc test). The expression of human MCM in both the HIV-1SDmEF1αhMCM and HIV-1SDmEF1αmurSigHutMCM transduced cells resulted in the correction of MCM enzyme activity, with the formation of succinyl coenzyme A at 85 ± 13 nM / min / μg of total cell protein and 179 ± 19 nM / min / μg of total cell protein, respectively. These results are also significantly different compared to the HIV-1SV40eYFP transduced MCM knockout fibroblast, which contain no detectable MCM enzyme activity.

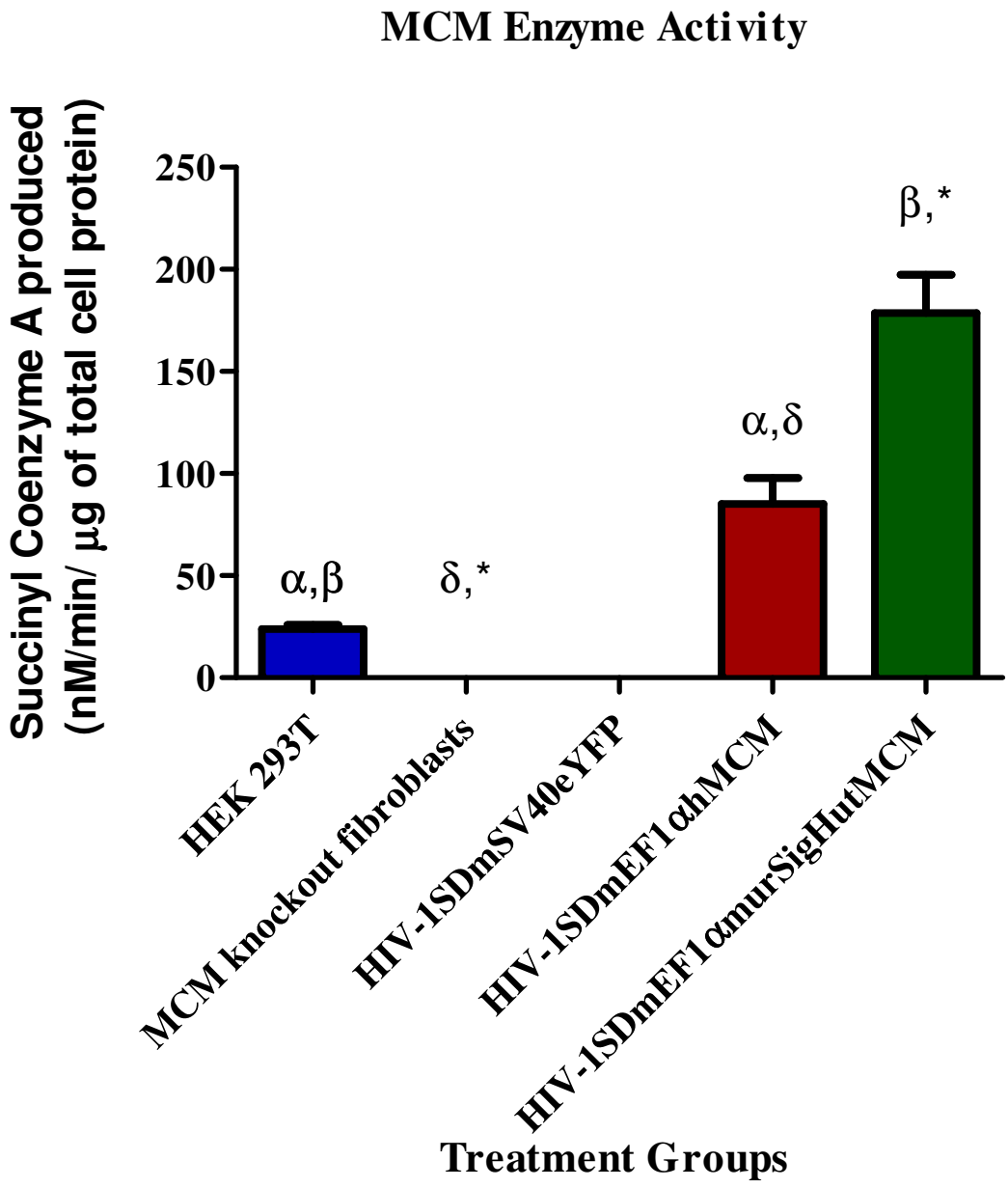
MCM Enzyme Activity
Succinyl Coenzyme A produced (nM/min/ µg of total cell protein)
250
200
150
100
50
0
α,β
δ,*
α,δ
β,*
HEK 293T
MCM knockout fibroblasts
HIV-1SDmSV40eYFP
HIV-1SDmEF1αhMCM
HIV-1SDmEF1αmurSigHutMCM
Treatment Groups

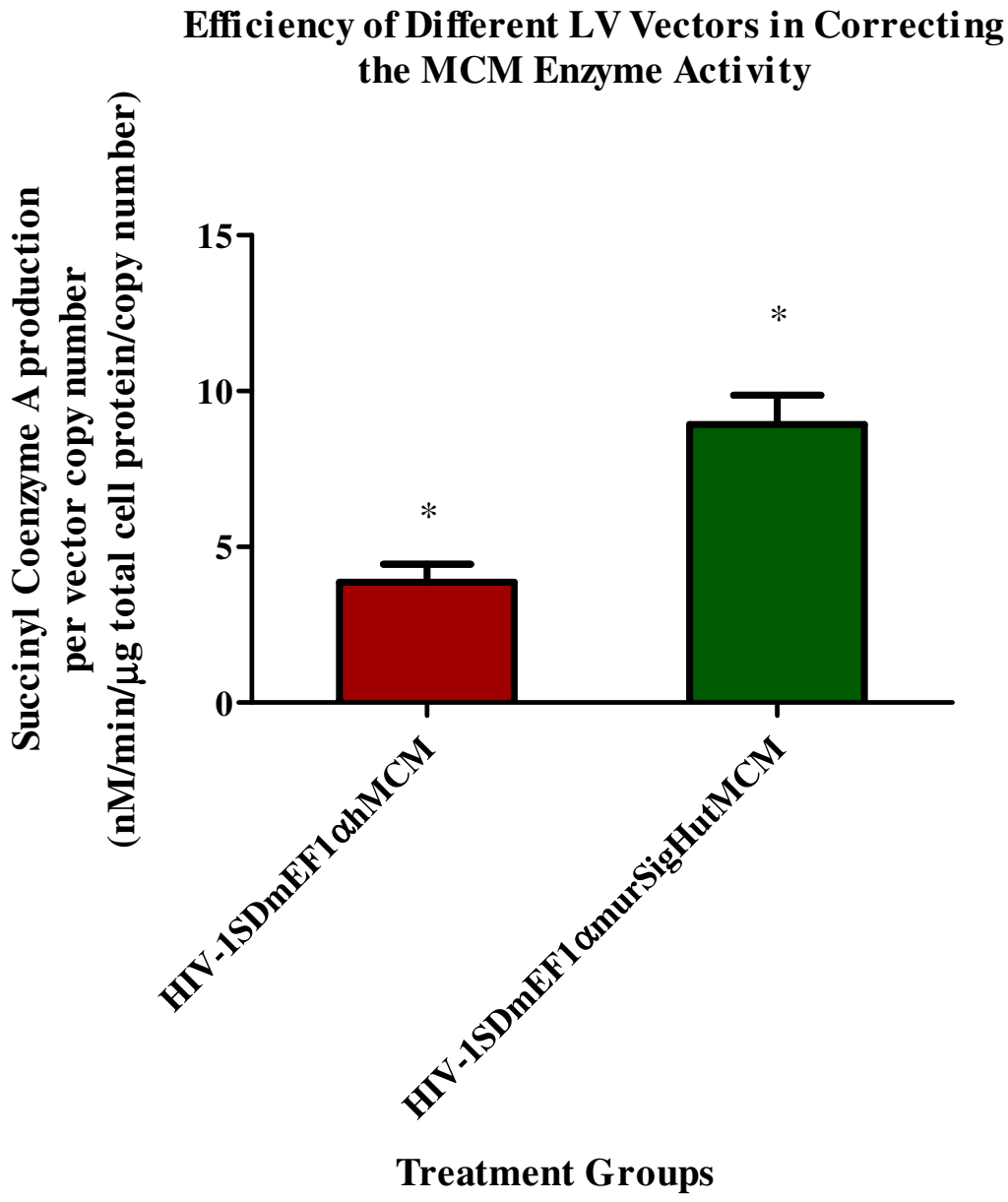

Figure 4.2-4 This figure demonstrated the level of MCM enzyme activity restored in MCM knockout cells transduced with two different LV vectors. Samples were analysed in triplicate and normalized to the vector copy number. The standard bars represent ± one standard error. * indicates significant difference between two groups (p<0.05, paired t-test).

4.2.3 Discussion

In chapter 3, it was shown that the poor expression of human MCM cDNA in MCM knockout mouse liver resulted in only a mild decrease in plasma and urine MMA levels. A few factors were raised to explain the findings. One of the likeliest explanations is that the low level of enzyme activity is due to a low level of protein expression in the murine cellular environment. This may be caused by the factors such transcriptional efficiency, mRNA processing and turnover, translation strength and protein stability [208].

Holm *et al*., (1986) [209] showed that the efficiency of protein expression could be enhanced by codon-optimization. Comparative studies showed that the pattern of codon usage differs between organisms [210, 211]. Many studies have shown that codon biases, in both unicellular and multicellular organisms, play a major role in translation efficiency. However, the function of codon bias in mammals, such as human and mouse, is still uncertain due to the contradictory results of many studies [212-217]. Nevertheless, a number of studies have demonstrated that the frequency of GC-ending codons (GC_3) may play a part in the level of gene expression. Ren *et al*., (2007) [218] had investigated the correlation between the codon usage and the level of gene expression using stem cells and progenitor cells. The potential of their differentiation ability provided an ideal model to understand the influence of codon usage in the pattern of gene expression at two different developmental stages based on the investigation of two parameters, the "level of gene expression", which was defined as the intensity of gene transcription in a particular cell type, and "fold change of gene expression", which was defined as the ratio of the expression levels of the same genes in two cell types. If the change of this ratio is higher than 2 or less than 0.5, this gene is defined as developmental-pivotal gene in their study. On the other hand, the genes were defined as developmental-specific genes if they were only expressed specifically at either early or later developmental stages. Their study demonstrated that the observation of a positive correlation between the two parameters in many of the mouse tissues. In particularly, compared to the

developmental-pivotal genes, the developmental-specific genes generally used more GC_3 codons. The study by Kim *et al*., (1997) [219] indicated that most of the frequently used codons found in mammals end with G or C and that these codons are translated more efficiently.

In addition, the study conducted by Konu *et al*., (2002) [220] demonstrated a positive correlation of mRNA expression levels and GC_3 in two rodent models. Also, their observation showed that a higher GC_3 value was found in 82% of highly expressed genes in the chosen tissues of the two rodent models. They proposed that this observation may be extended to other tissues of mammals. Wilkemeyer *et al*., (1993) [179] show that the level of MCM activity is regulated in a tissue-specific manner. In their study of MCM mRNA levels, they showed that the MCM gene was highly expressed in kidney and liver followed by brain, heart and muscle. Overall, it appears that it may be beneficial to prefer the use of GC_3 in an attempt to maximize translational efficiency.

In this regard, the codon-optimisation process for the human MCM sequence would seem to provide at least theoretical benefits in that the G+C content has been increased from 42.03% to 53.27% and the number of GC_3 codons has been increased from 365 to 452.

In the current study, we evaluated the expression efficiency of the codon-optimised murSigHutMCM in MCM knockout fibroblasts. Our quantitative real-time PCR result shows that all the treatment groups appeared to have broadly equivalent vector copy number.

The western blot analysis demonstrates that the human MCM enzyme was expressed in all the MCM vector transduced cells. It shows that the codon-optimization process has significantly enhanced the expression by 3-fold compared with the HIV-1SDmEF1αhMCM treated MCM knockout fibroblasts after normalization for loading.

Restoration of MCM enzyme activity was also demonstrated in these cells. The increase in enzyme activity was roughly proportional to the increase in MCM protein levels. Our results demonstrated that the restoration of MCM enzyme activity was improved, by 2.5-fold, after normalized to vector copy number, in the MCM knockout fibroblasts transduced with HIV-1SDmEF1αmurSigHutMCM compared with HIV-1SDmEF1αhMCM.

In conclusion, the codon-optimisation process at least doubles expression of MCM enzyme activity *via* an increase in MCM protein levels. In addition, the MCM is active in mitochondria, confirming the importance of correct translocation of MCM into mitochondria. Therefore, it is believed that increasing the mitochondrial transportation efficiency by using a murine mitochondrial targeting signal may play a significant role in this result.

4.3 LV-Mediated Gene Delivery *In Vivo*

4.3.1 Introduction

In the previous section, it was demonstrated that the HIV-1SDmEF1αmurSigHutMCM vector successfully corrected the MCM enzyme deficiency in MCM knockout fibroblasts and expressed MCM at approximately double the level of the first generation vector, suggesting it had potential for improved efficacy *in vivo*. Therefore, the HIV-1 SDmEF1αmurSigHutMCM vector was delivered to the mut -/- muth2 murine model and its efficacy and efficiency were evaluated following the experimental design described in Chapter 3, allowing a direct comparison of the results of both trials.

Some modifications were made to the virus delivery method. Intralipid was used in combination with the 10% dextrose as premedication before virus delivery, as although mice were previously pre-treated with 10% dextrose 2 hours before injection, signs indicative of discomfort still occurred in the LV treated mice. One possible cause of this might be acute metabolic decompensation resulting from the reaction to the injection exarcerbating the condition. This is consistent with symptoms observed in severe MMAuria patients, with a significant increase of MMA level found in plasma and urine during catabolic stress resulting from perinatal stress and acute illness such as infection and injury. It is shown that these events may lead to the increase in the amino acids (isoleucine, valine, methionine and threonine) that subsequently cause the accumulation of MMA in the patients (http://newenglandconsortium.org/for-professionals/acute-illness-protocols/organic-acid-disorders/methylmalonic-acidemia/). Intralipid is used clinically as one of the treatments for acute metabolic decompensation in MMAuria patients [1]. Therefore, this change in the regimen, with 10% dextrose followed by intralipid at 40 µL/g *via* intraperitoneal injection 2 hours prior to virus delivery, as described in section 2.2.2.9, was made.

In addition, several modifications in vector preparation were used in order to improve the quality of the virus and its specific infectivity. One of these modifications was the use of Mustang Q filters for virus purification. MustangQ is a strong ion exchange matrix. Rowley *et al*., (2004) [221] showed the advantages of using Mustang Q columns in virus purification compared to standard purification protocols, including reduced processing time, undetectable levels of the highly immunogenic proteins from the virus production cell line in the purified virus, and the removal of the need for specialized equipment for purification. Unpublished data from our group shows that virus produced by MustangQ triggered less immune response than virus produced from our standard virus production protocols, supporting these observations.

Koldej *et al*., (2005) [150] have shown that the specific infectivity of the LV from the virus production system used in this study is dependent on the amount of gagpol produced during virus production, with lesser amounts of gagpol increasing the specific infectivity of the virus. Therefore, in order to optimize the specific infectivity of the LV, the ratio of gagpol plasmids used in the production of virus was decreased. However, the reduction in the amount of gagpol in virus production will also result in a decrease in the virus yield. For example, her work demonstrated a 2-fold increase in the specific infectivity was observed when reducing the amount of gagpol by 4-fold. Simultaneously, a 1.3-fold reduction of virus titre was seen. Nevertheless, after the improvement of the purification method with the use of MustangQ filters, data from our group showed that a better quality of virus could be produced, with an enhancement in viral titre and specific infectivity, by 2-fold and 5-fold, respectively, achieved after purification. The amount of gagpol used (4-fold reduction) was chosen as it gave a significant increase in the specific infectivity while minimizing loss of yield. Despite these changes, the specific infectivity of the virus used in this study was lower than the first study, with the value of 1 x 10^7 IU/µg of p24 equivalent (1.3 x 10^9 IU/130 µg of p24 equivalent) produced with new protocol and 1.5 x1 0^7 IU/µg of p24 equivalent (7.5 x 10^8 IU/50 µg of p24

equivalent) from first study. However, it should be noted that this comparison of the two virus preparation protocols may be inappropriate as they were done a long time apart, meaning the two variables (titre and p24) were not directly compared in the same experiment, and both assays can be somewhat variable (titre because of variations in cell culture that cannot be controlled, and p24 because of the large dilutions involved). Therefore, the improved transduction seen, which was at least 10-fold higher compared to the first study (See Table 4.3-4), might be due to other factors such as the virus purity after the modification in virus production, the use of intralipid and higher total dose as much as it is due to the different plasmid mix used for transfection.

4.3.2 Methods and Results

Six severe MMA affected mice (mut -/- muth2), 3 males and 3 females, were treated with the codon-optimised HIV-1SDmEF1αmurSigHutMCM at the age of 8 weeks, with the additional requirement of a minimum body weight of 11g at time of treatment. Previous observations suggested that mice of this body weight were more resilient to the treatment regimen. The virus was delivered through intravenous injection of an approximately 130 μg p24 equivalent (Table 4.3-1) of total virus particles in a total volume of 300 μL using a 29 gauge insulin syringe as described in Section 2.2.2.4. Pre-treatment blood and urine samples were collected 1 week before treatment. The physical and clinical signs were examined regularly after treatment for 6 months. Blood samples were collected at 1 week, and 1, 3, 5 and 6 months after treatment and urine samples were collected on a weekly basis. Plasma and urine MMA level measurements were performed by GC/MS using the protocols described in Section 2.2.2.6 and 2.2.2.5, respectively. The brain, liver, kidneys and spleen tissues were removed at post-mortem examination. These samples were used for metabolic studies, vector copy number measurement, western blot analysis and enzyme activity assays. Results of these studies were used to compare with wild-type control, untreated mut -/- muth2 mice and with

the data from the initial study in which the animals were treated with the HIV-1SDmEF1αhMCM vector.

Virus Dosage

Mouse ID	Amount of LV vector used (μg of p24 equivalent)	Total Infectious Unit (IU)
8.403	140.7	1.8×10^9
8.418	141.5	1.33×10^9
10.16	100	1.1×10^9
10.27	133	1.4×10^9
10.25	130.6	1×10^9
10.27	148	1.2×10^9
Average	**132.3**	**1.3×10^9**

Table 4.3-1 The table shows the virus dose usage for each individual mouse

4.3.2.1 Physical Examination

Most mice received the injection with no obvious side effects. However, one of the treated mice, designated QUE 10.25, showed sign of discomfort after injection of virus. It was noted that the mouse was reluctant to move and was breathing heavily 2 hours post-injection, indicative of a possible metabolic crisis induced by the physiological stress associated with the treatment. The condition worsened over 2 hours with additional abnormal behaviours also indicative of stress, such as hunched back and crouching in one corner with partly closed eyelids, becoming apparent. In order to prevent dehydration and acute metabolic decompensation 300 μL of pre-warmed 10% glucose was administered intraperitoneally every 6 hours and the mouse was kept in a humidicrib at 29 °C with close supervision every hour. Sunflower seeds were given in place of normal chow after 6 hours. Despite this treatment, it failed to improve and demonstrated a weight loss of 2 grams on Day 1. Rough looking hair indicating a lack of grooming activity, and trembling, were observed at Day 2 post-treatment and the treatment regimen was changed to a combination of 10% glucose and intralipid (300

μL) given every 6 hours in order to provide better metabolic support. This appeared to improve the animal's condition as it started to feed itself by Day 5, its body weight increased by 1 gram from its minimum bodyweight at 9.8 gram on Day 2, and activity normalised. Based on these observations, treatment with 10% glucose and intralipid was stopped given on Day 6, although the animal was kept in the humidicrib at 29 °C with water and normal mouse chow with daily monitoring of weight and condition. However, the mouse was found dead on Day 13. No physical abnormalities or decrease in body weight (from the day when treatment with 10% dextrose and intralipid was stopped), were observed. Unfortunately, liver, kidneys, spleen, intestines and heart tissues had started to decompose by autopsy. A small piece of each tissue preserved in 10% formalin was sent for pathology examination at the Institute of Medical and Veterinary Science (IMVS) Pathology, South Australia. It was reported that these tissues were in a stage of autolysis, particularly the intestine. Diffuse macrovesicular and microvesicular steatosis of hepatocytes in liver, indicators of hepatocytes necrosis, were observed but no inflammation was found (Figure 4.3-1). The Animal Ethics Committee was informed of this death.

In contrast to QUE 10.25, virus delivery was well-tolerated by the other 5 (mut -/- muth2) mice and none of them showed any adverse responses. Regardless, each of the treated mice was maintained in the humidicrib at 29 °C for a minimum of 2 days with a supply of sunflower seeds and moistened food until they were all recovered with no observation of adverse responses. These mice started to consume normal food pellets at approximately 1 week after treatment. Following the therapy, they progressively gained body weight. Generally, the body weight of these treated mice began to increase 1 week after treatment and by the age of approximately 120 days, 2 months after treatment, their body weight was within the normal range (Figure 4.3-2). At the end of therapy, the average weight of the treated group was significantly heavier than the untreated group and was approximately 90% of normal mice. Moreover, the mice from the treated group were more active than untreated

mice. Importantly, they were otherwise difficult to distinguish physically from age-matched normal controls (Figure 4.3-3).

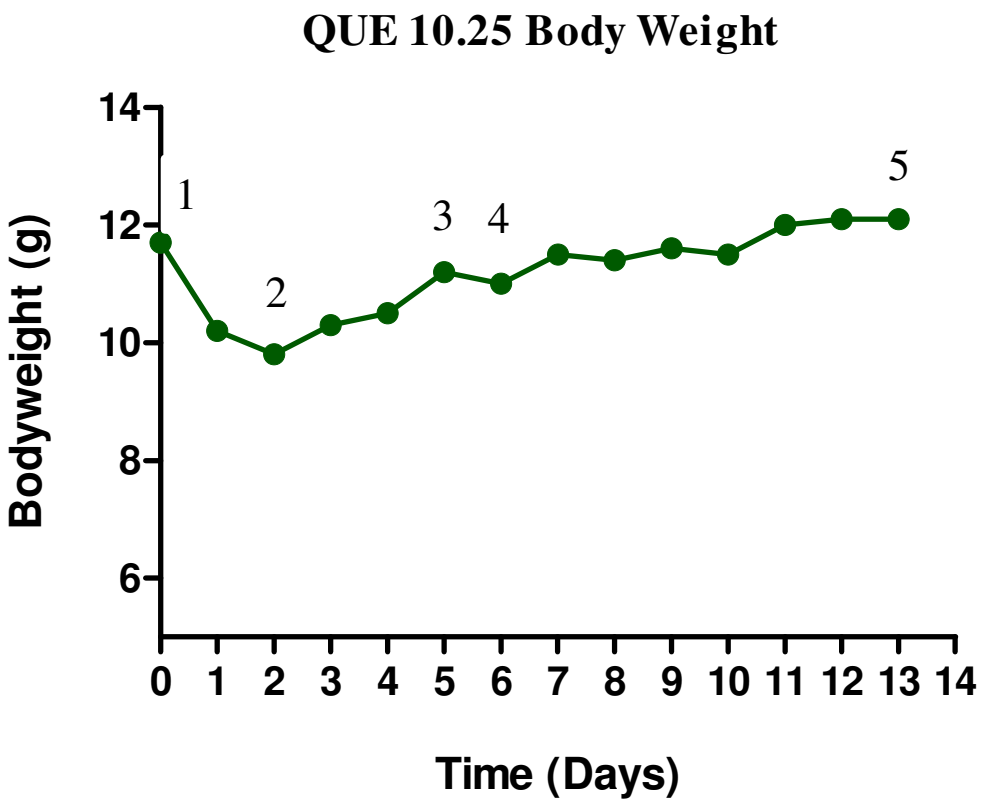

Figure 4.3-1. This figure shows the body weight of QUE 10.25 post-treatment. The treatments given in order are shown by number as below:

1) Treatment: 300 µL of HIV-1SDmEF1αmurSigHutMCM (130.6 µg of p24 equivalent). QUE10.25 was kept in a humidicrib at 29°C, provided with sunflower seeds, and 300 µL of pre-warmed 10% dextrose was given intraperitoneally once every 6 hours to prevent dehydration and provide metabolic support.
2) QUE10.25 was kept at humidcrib at 29°C and provided with sunflower seeds. A combination of pre-warmed 10% dextrose and intralipid (150 µL each) were given intraperitoneally once every 6 hours to prevent dehydration and provide better metabolic support
3) Mouse started to feed itself
4) Stopped administration of 10% dextrose
5) Death

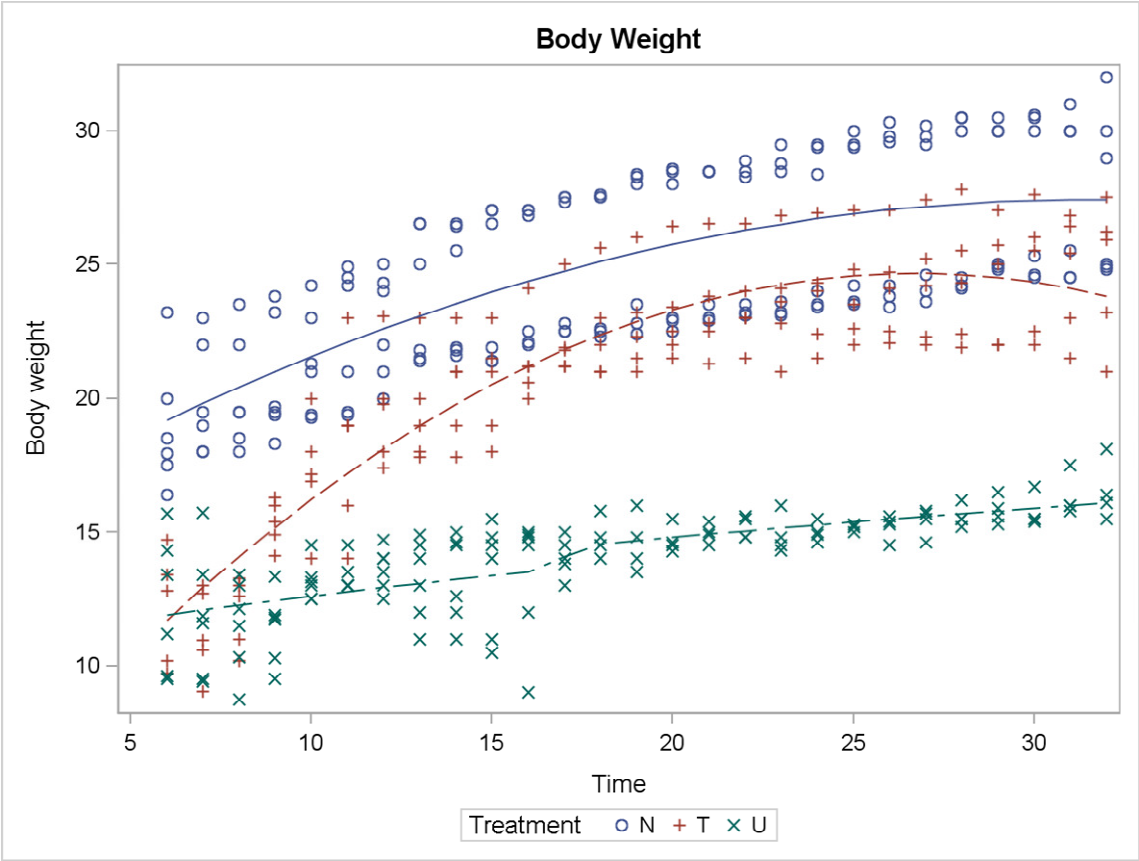

Figure 4.3-2. Body weight of individual mice from normal, untreated and HIV-1SDmEF1αmurSigHutMCM treated group. The curved line represents the fit of curves (R^2) for each group, the blue solid line indicates the wild type group, the red and green dash lines indicate the HIV-1SDmEF1αmurSigHutMCM treated and untreated groups, respectively. The statistical analysis on the fit of curves shows that the mice in the normal group weigh significantly (p<0.001) more on average than the HIV-1SDmEF1αmurSigHutMCM treated and untreated groups. The HIV-1SDmEF1αmurSigHutMCM treated group, weighed significantly (p<0.001) more on average than the untreated group. In addition, the untreated group weighed significantly less (p<0.001) over time compared to the other two groups.

Figure 4.3-3 Physical Appearance

Normal (Top), Untreated (Middle) and HIV-1SDmEF1αmurSigHutMCM treated mice (Bottom) are shown at 6 months after treatment. Compared to an untreated control mouse (middle), the LV treated mouse shows an increase in body size and is indistinguishable from normal. In contrast, an age-matched untreated mut -/- muth2 mouse is obviously smaller than normal. Other than the difference in size, there are no other overt differences in appearance in this model.

Two of the untreated control mut -/- muth2 mice, designated as QUE 8.422 and QUE 8.423, were found dead at the age of 4 months. Neither physical or behavioural abnormalities nor a significant change in body weight was observed in these mice prior to death (Figure 4.3-4). Unfortunately, due to the timing of death, their tissues were also in an advanced stage of autolysis at autopsy. These deaths are consistent with the observed mortality for these mice, approximately 40% at 3 to 4 months [152] even though these mice were a 2-human MCM gene rescue model (Appendix IV) and have significant residual MCM activity.

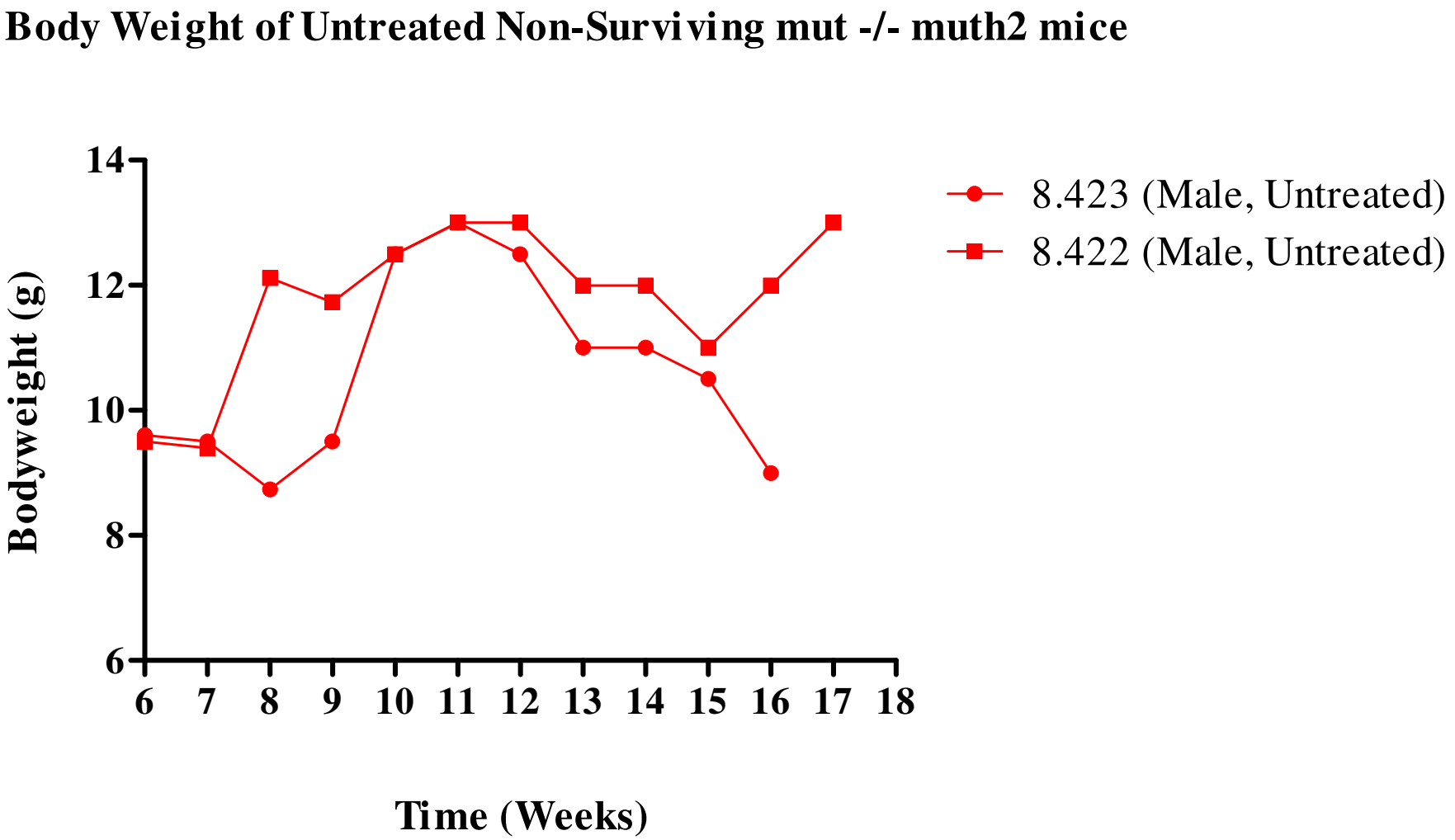

Figure 4.3-4 The body weights of the two untreated mut -/- muth2 controls, QUE 8.422 and 8.423, that died prior to the end of the study period, are shown.

4.3.2.2 Vector Copy Number Measurement by Quantitative PCR

The biodistribution of the vector in the mouse was determined by the detection of the lentiviral *gag* gene sequence vector using quantitative real-time PCR. Overall, high levels of vector were detected in the liver (3.2 ± 1.8 copies per cell), followed by spleen (0.9 ± 0.5 copies per cell). Vector copy number was extremely low in kidney, at 0.01 ± 0.01 copy per cell. As expected, no copies of the vector were detected in either normal control or HIV-1SDmEF1αmurSigHutMCM untreated mut -/- muth2 mice in all the tissues tested (Table 4.3-2 and Table 4.3-3).

Vector Copy Number

Treatment Groups	Liver	Spleen	Kidneys
Normal (n=6)	N.D	N.D	N.D
Untreated (n=6)	N.D	N.D	N.D
HIV-1SDmEF1αmurSigHutMCM treated (n=5)	3.2 ± 1.8	0.9 ± 0.5	0.01 ± 0.01

Table 4.3-2 The vector copy number per cell in selected tissues is shown. Results are presented as the mean ± SE. N.D. indicates not detected.

Vector Copy Number in Individual Treated Mice

Mouse ID	Liver	Spleen	Kidneys
8.403	10.4	2.8	0.02
8.418	1.6	0.9	N.D
10.16	1.6	0.7	N.D
10.27	0.8	0.5	N.D
10.37	1.4	0.2	N.D

Table 4.3-3 Vector copy number per cell in liver, spleen and kidneys are shown for individual treated mice are shown. N.D. indicates not detected.

4.3.2.3 Western Blot Analysis

Western blot analysis of protein extracts prepared from liver was performed to evaluate the expression of human MCM protein 6 months post-treatment. Proteins extracts derived from HEK293T cells were used as a positive control for human MCM. The analyses show a single band at ~83 kDa, indicating the expression of MCM protein in normal mice that is only just detectable in the untreated "rescue" mice (Figure 4.3-5A and B). MCM protein in all members of the HIV-1 SDmEF1αmurSigHutMCM treated group was clearly detectable although of a slightly lower intensity than in the wild type controls (Figure 4.3-5C). A faint band (approximately 76kDa), highlighted in red, was observed in all the untreated mut -/- muth2 mice. These bands are most likely an indication of cross-reacting material as the same bands were also observed in the normal mice at an equal intensity. The observation of a small amount of MCM in the rescue mice agrees with the results of Peters *et al*., (2012) [152], that demonstrate a low level of enzyme activity in these mice [151].

Gel analysis software, ImageJ ver.1.43d, was used to quantify the MCM protein expression level by calculating the area under the curve of each peak that corresponded to the selected band (Figure 4.3-6). The outcome of this calculation was a mean ± SE of 2 ± 0.4 and 0.3 ± 0.1 for normal control and untreated mut -/- muth2 mice, respectively after normalization to loading control. This analysis demonstrated an increase in MCM protein expression in each HIV-1SDmEF1αmurSigHutMCM treated mouse, with a value of 2.8, 2.6, 2.7, 2.1, 1.5 for QUE 8.403, QUE 8.418, QUE 10.16, QUE 10.27 and QUE 10.37, respectively, after normalized to loading control and showed a mean ± SE of 2.3 ± 0.2, not significantly different to the normal controls, consistent with almost complete, if not complete, restoration of MCM protein levels in the liver of the treated mice.

Figure 4.3-5 Western Blot Analysis of MCM Expression in Liver

Western analysis of liver protein extracts (25 μg/lane) probed with antibodies against MCM (83 kDa) and β-actin (42 kDa). (A) Lane 1: marker; Lane 2: HEK293T cell lysates; Lane 3-8 liver protein extracts from normal mice. (B) Lane 1: marker; Lane 2: HEK293T cell lysates; Lane 3-8 liver protein extracts from untreated mut -/- muth2 mice. (C) Lane 1: marker; Lane 2: HEK293T cell lysates; Lane 3-7 liver protein extracts from QUE8.403, QUE8.418, QUE10.16, QUE10.27, QUE10.37 HIV-1SDmEF1αmurSigHutMCM treated mice, respectively.

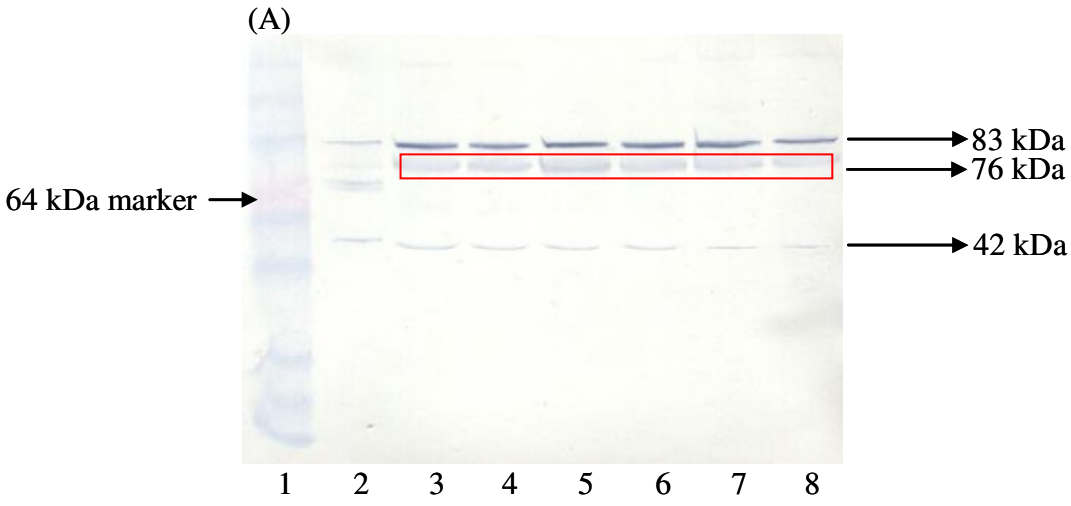
(A)
64 kDa marker
83 kDa
76 kDa
42 kDa
1 2 3 4 5 6 7 8

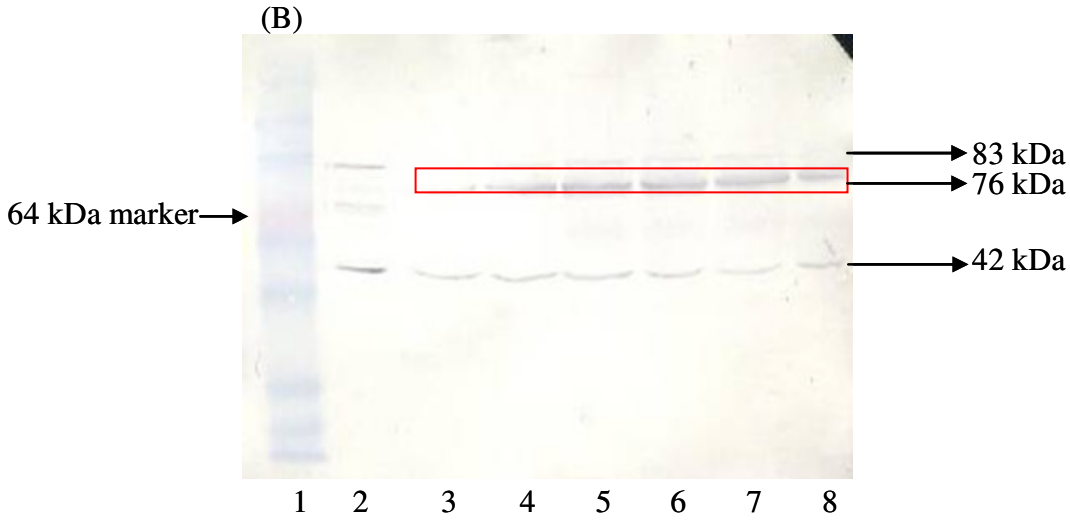
(B)
64 kDa marker
83 kDa
76 kDa
42 kDa
1 2 3 4 5 6 7 8

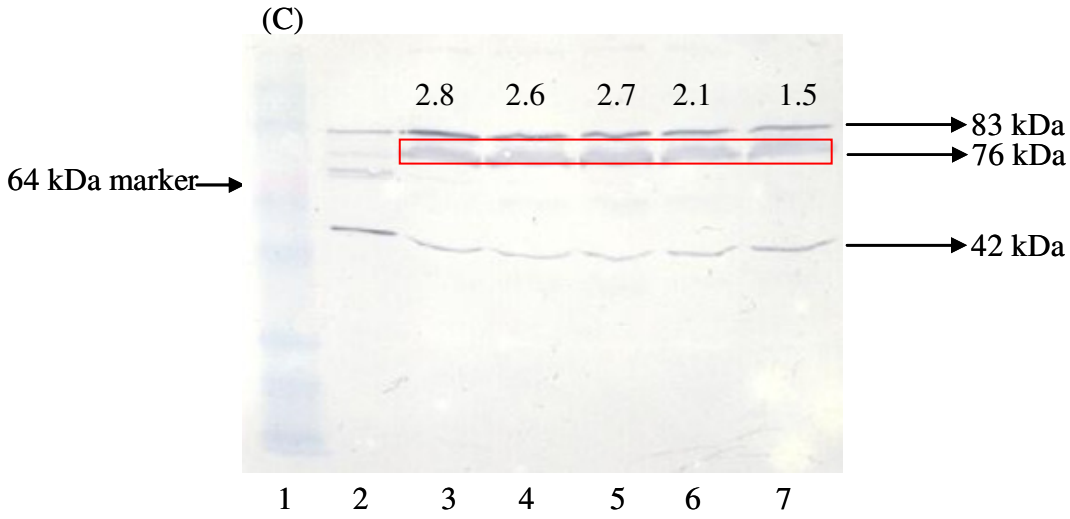
(C)
2.8 2.6 2.7 2.1 1.5
64 kDa marker
83 kDa
76 kDa
42 kDa
1 2 3 4 5 6 7

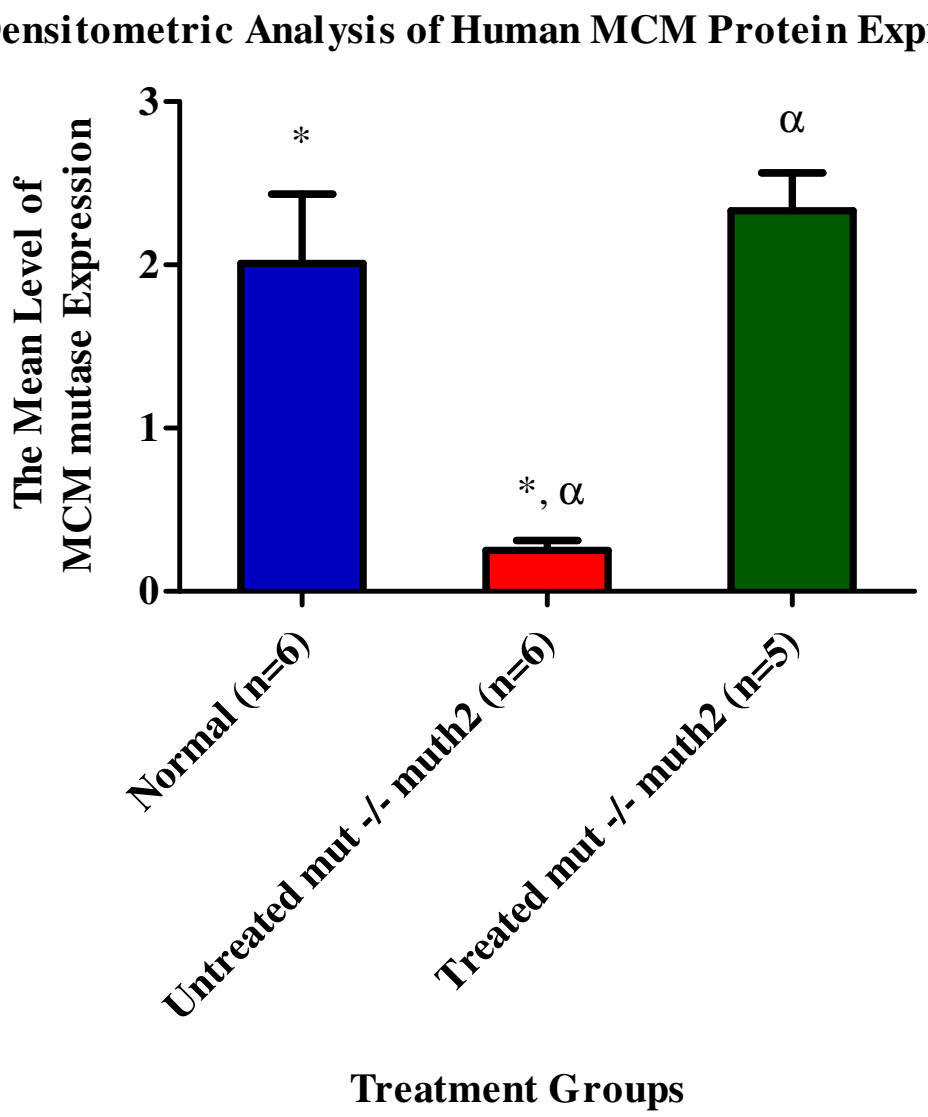

Figure 4.3-6 ImageJ quantification of band intensity for human MCM, after normalization to β-actin, from western analysis (Figure 4.3-5). The figure demonstrates MCM expression in normal mice (n=6), mut -/- muth2 untreated mice (n=6) and HIV-1SDmEF1αmurSigHutMCM treated mice (n=5). The standard bars represent ± one standard error. The * and α indicate significant difference compared to the untreated mut -/- muth2 control (p<0.05). No significant difference was observed between the normal and the HIV-1SDmEF1αmurSigHutMCM treated group. The p value between groups was calculated by using one-way ANOVA with Tukey's post-hoc test.

4.3.2.4 Determination of Hepatic MCM Enzyme Activity

As vector copy number studies confirm that the virus was successfully localized to the liver, liver homogenates were then prepared and assayed for enzyme activity using HPLC as described in section 2.2.3.9.

No enzyme activity was observed in the untreated mut -/- muth2 mice. The mean level of hepatic MCM enzyme activity from the treated group demonstrated an increase of succinyl-coenzyme A production to 66 ± 21 nM / min / μg of total cell protein, equivalent to the enzyme activity level of the wild type control, which was 64 ± 14 nM / min / μg of total cell protein (Figure 4.3-7).

Nevertheless, our data showed no correlation between the vector copy number and the MCM activity. Although a high vector copy number was observed in one of the HIV-1SDmEF1αmurSigHutMCM treated mice, QUE 8.403, with a vector copy number of 10.4, the MCM enzyme activity (111 nM / min / μg of total cell protein) indicated no difference in the enzyme activity than the other treated mice, which ranged from 1.2 to 98 nM / min / μg of total cell protein, which had a 10-fold lower vector copy number.

In addition, it is worthy of note that some variation of MCM enzyme activity, although not great, was observed in the normal liver samples, raising concerns that impurities in the liver had caused false readings. It was observed that the HPLC traces indicated more background peaks when liver extract samples were assayed. Therefore, to investigate the possibility of peak interference, a control assay was run, with normal liver extracts under the conditions described in section 2.2.3.9 but without the addition of the substrate, methylmalonyl coenzyme A. The control assay showed that this variation is unlikely to be due to the background as no evidence of background peaks, resulting from the impurities of the liver extracts that would affect the readings was detected. This analysis appears to still provide a

reliable tool to measure the level of restoration of enzyme activity, especially when the enzyme activity is high, despite the fact that this analysis method is limited by its sensitivity as described in section 2.3.

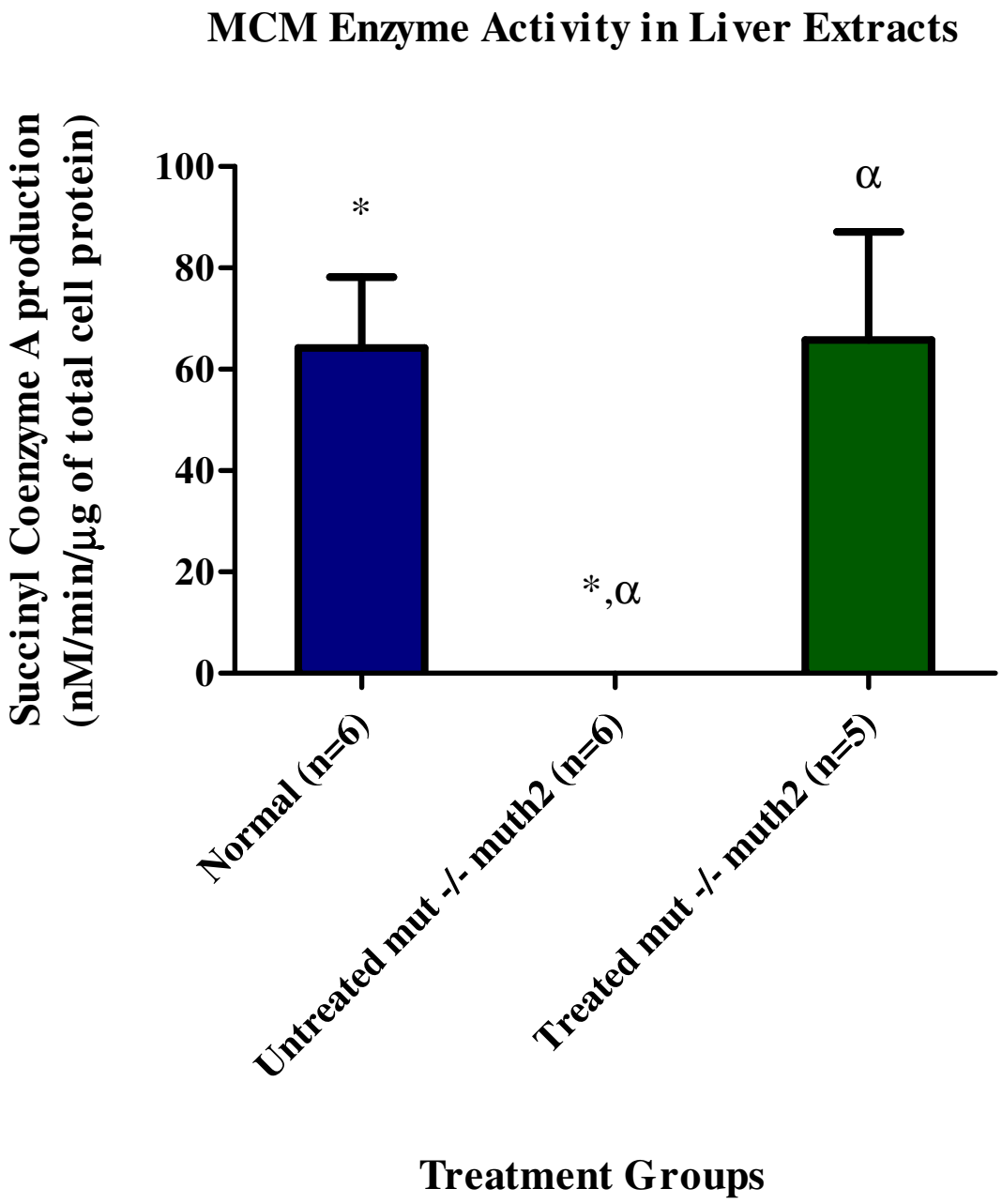

Figure 4.3-7 Hepatic enzyme activity from normal mice (n=6), mut -/- muth2 untreated mice (n=6) and HIV-1SDmEF1αmurSigHutMCM treated mice (n=5). The HIV-1SDmEF1αmurSigHutMCM treated mice had a mean ± SE of 66 ± 21 nM / mins/ µg of total hepatocyte protein and is significantly different (p<0.05) compared to the mut -/- muth2 untreated group (undetectable). The standard bars represent ± one standard error. * and α indicate significant differences between the treatment groups. The p value between groups was calculated using one-way ANOVA with Tukey's post-hoc test.

4.3.2.5 Plasma MMA Measurement

Blood samples were collected from each mouse at 1 week before, and 1 week, and 1, 3, 5 and 6 months post-treatment. Plasma MMA concentrations were measured as described in Section 2.2.2.6 to evaluate the effect of restoration of hepatic MCM enzyme activity. The plasma MMA concentration of each individual mouse over time is shown in Figure 4.3-8. All treated mice demonstrated an acute decrease in plasma MMA level 1 week post-treatment. Thereafter, the plasma MMA concentrations decreased gradually throughout the course of therapy although mouse QUE 8.418 had a slight elevation at 20 weeks. As opposed to the HIV- 1SDmEF1αmurSigHutMCM treated MMA mice, the untreated mut -/- muth2 mice show continued MMA accumulation in plasma throughout this time period.

It should be noted that the untreated affected controls QUE 8.422 and QUE 8.423 deceased earlier during the course of the experiment (at 17 and 16 weeks of age, respectively). Both of these mice presented an abnormally high MMA concentration in plasma prior to death, with values of 993 μM and 954 μM for QUE 8.422 and 8.423, respectively, at 12 weeks of age. Unfortunately we were unable to collect a plasma sample at the time of death, for QUE 8.422. Plasma MMA for QUE 8.423 at time of death was 1024 μM. The data points of each individual mouse from the HIV-1SDmEF1αmurSigHutMCM treated group were integrated by calculating the area under the curve starting from 1 week after treatment until 6 months post-treatment or until death for deceased mice using the trapezoidal rule. On the other hand, the pre-treatment values were included in the integration for both the normal and untreated groups (Figure 4.3-9).

The averaged total AUC result shows that the untreated control had a mean ± SE of 17 ± 3, which was significantly higher (p<0.05, Tukey's post-hoc test) than the normal control (with a mean ± SE of 0.004 ± 0.003). The HIV- 1SDmEF1αmurSigHutMCM treated group displayed a mean ± SE of 9 ± 1, which was significantly lower (p<0.05, Tukey's post-hoc

test) than the untreated mut -/- muth2 mice; but still significantly higher than the normal control group.

Figure 4.3-8 All untreated mut -/- muth2 mice are shown in red and HIV-1SDmEF1αmurSigHutMCM treated mice in green. The averaged plasma concentration of wild-type mice (normal control) is shown in blue.

Plasma MMA Concentration of Individual Mice Over Time

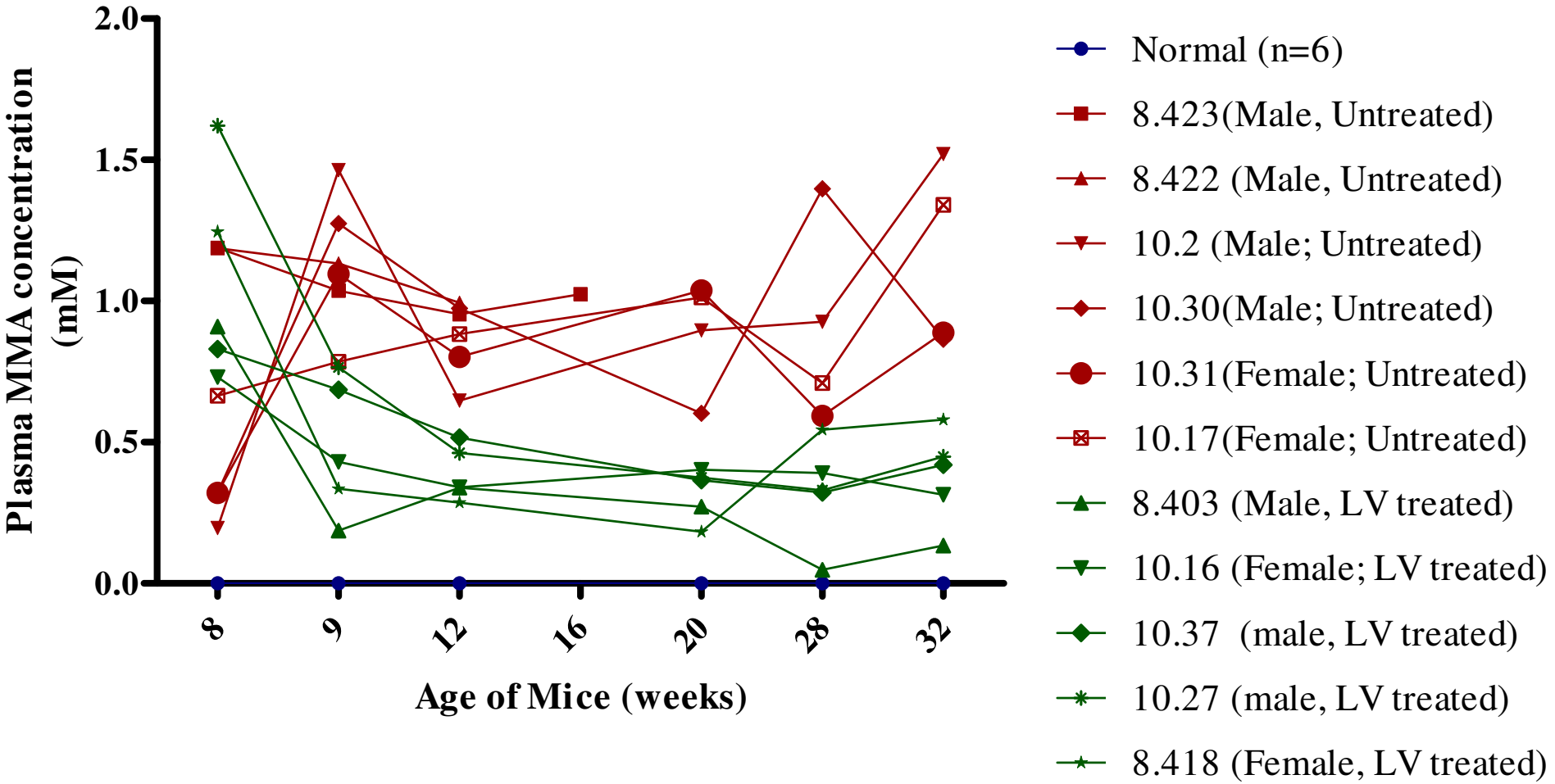

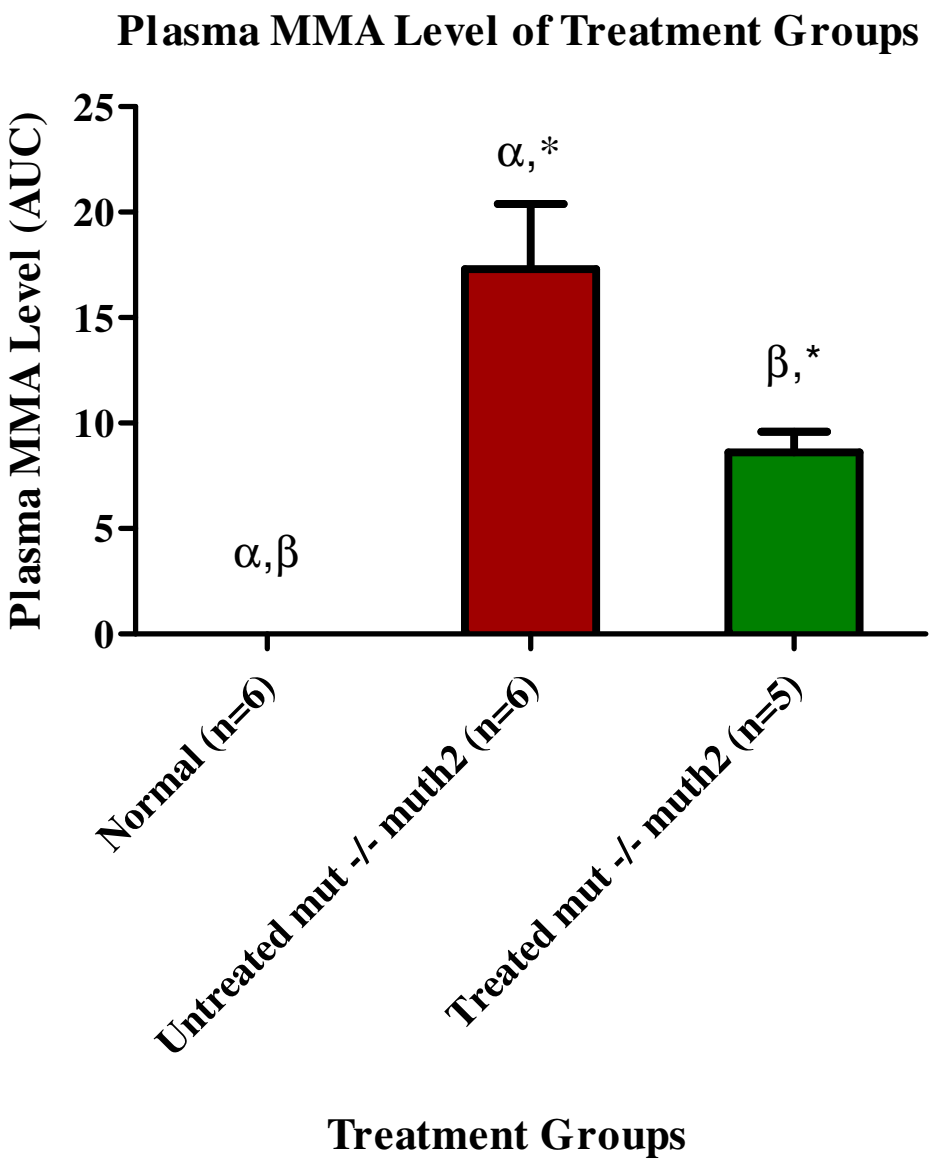

Figure 4.3-9 The data points of each individual mouse were integrated by calculating the area under the curve using the trapezoidal rule as stated and the averaged of total AUC for treatment groups were calculated. Data for normal mice (n=6), mut -/- muth2 untreated mice (n=6) and treated mut -/- muth2 mice (n=5) are shown. The mut -/- muth2 untreated mice had a mean ± SE of 17 ± 3 which is significantly different to normal mice (p<0.05). The LV treated mice had a mean ± SE of 9 ± 1, which is significantly different to normal and untreated groups. The standard bars represent ± one standard error. α, β and * indicate significant difference between treatment groups. The p values were calculated using one-way ANOVA with Tukey's post-hoc test.

4.3.2.6 Urine MMA Analysis

Urine samples from each mouse were collected and assayed on a weekly basis as described in Section 2.2.2.5. The urinary MMA concentration of each mouse was plotted against time as shown in Figure 4.3-10. A similar pattern to the results of the plasma analysis was seen, with the MMA concentration rapidly decreasing 1 week after treatment and then being maintained at a lower level compared to the untreated mut -/- muth2 mice, with the exception of 10.37. It should also be noted that data points for QUE 8.422 at 14 to 16 weeks of age and for QUE 8.423 from 14 to 17 weeks of age are missing due to insufficient urine for analysis being collected.

The data points of each individual mouse from the HIV-1SDmEF1αmurSigHutMCM treated group were integrated by calculating the area under the curve starting from 1 week after treatment until 6 months post-treatment or until death for deceased mice using the trapezoidal rule. On the other hand, the pre-treatment values were included in the integration method for both normal and untreated groups. The result that demonstrates the averaged total AUC of each treatment group is shown in Figure 4.3-11. The untreated mut -/- muth2 mice show a mean ± SE of 6 ± 1 which is significantly higher (p<0.05, Tukey's post-hoc test) than normal mice, which had an averaged value that was below the limit of detection. A mild reduction, approximately 38%, was observed in the treated group, with a mean ± SE of 4 ± 1, compared to the untreated mut -/- muth2 mice, however, this did not reach statistical significance.

Figure 4.3-10 The MMA concentration in the urine of each individual mouse is shown versus time. All untreated mut -/- muth2 mice are shown in red and the HIV-1SDmEF1αmurSigHutMCM treated mice in green. The urine MMA concentration of normal mice was too low to be detected by the GC/MS methodology used. Mice were treated at 8 weeks of age on graph.

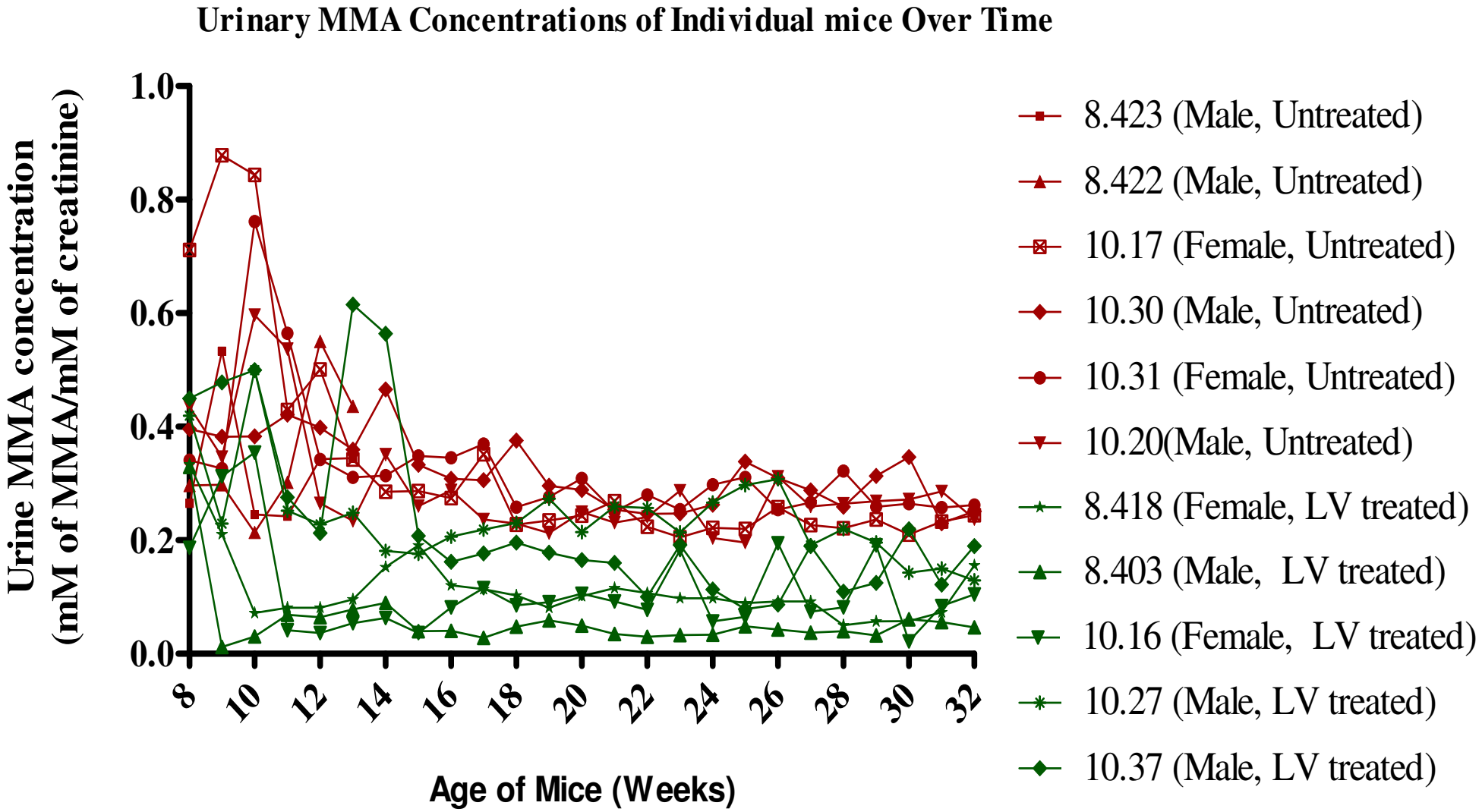
Urinary MMA Concentrations of Individual mice Over Time
Urine MMA concentration
(mM of MMA/mM of creatinine)
1.0
0.8
0.6
0.4
0.2
0.0
8
10
12
14
16
18
20
22
24
26
28
30
32
Age of Mice (Weeks)
8.423 (Male, Untreated)
8.422 (Male, Untreated)
10.17 (Female, Untreated)
10.30 (Male, Untreated)
10.31 (Female, Untreated)
10.20(Male, Untreated)
8.418 (Female, LV treated)
8.403 (Male, LV treated)
10.16 (Female, LV treated)
10.27 (Male, LV treated)
10.37 (Male, LV treated)

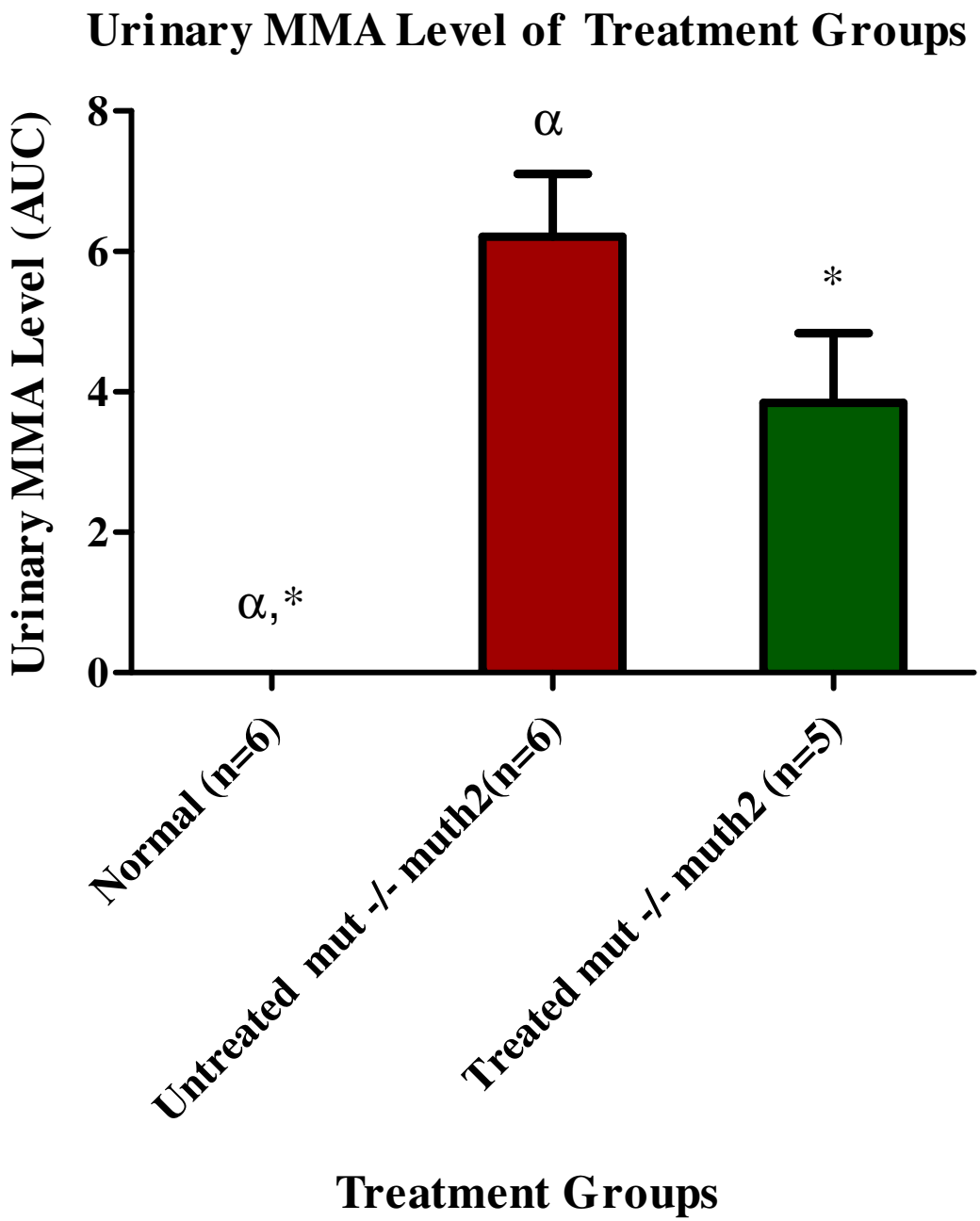

Figure 4.3-11 The data for each individual mouse from Figure 4.3-10 was quantified by integrating the area under the curve as described and the averaged total AUC values were calculated. The averaged total AUC for each group is shown. The mut -/- muth2 untreated mice had a mean ± SE of 6 ± 1 which is significantly different to normal mice (p<0.05). However, there is no significant difference between the untreated and treated group. The standard bars represent ± one standard error. α and * indicate a significance difference between the treatment groups. The p values were calculated using one-way ANOVA with Tukey's post-hoc test.

4.3.2.7 Assessment of MMA Concentration in Liver

The MMA concentration in the liver of each animal was evaluated using homogenised liver samples and the bloodspot method as described in section 2.2.2.7.

The mean concentration of hepatic MMA is shown in Figure 4.3-12. The untreated group demonstrated a mean ± SE of 1003 ± 124 (μM/g tissue) which was significantly different to the mean concentration of hepatic MMA in normal mice, which was 7 ± 1 μM/g tissue (p<0.05, Tukey's post-hoc test). The mean concentration of hepatic MMA was significantly reduced to 133 ± 20 (μM/g tissue) in the HIV-1SDmEF1αmurSigHutMCM treated group (p<0.05, Tukey's post-hoc test), compared to untreated mut -/- muth 2 control, and this was not significantly different to the normal group. In addition, the individual hepatic MMA measurements indicated that the treated mouse QUE 8.403 had the lowest hepatic MMA concentration, at 68 μM/g tissue, compared to the other treated mice, which showed the hepatic MMA concentrations ranging from 125 to 194 μM/g tissue.

The MMA concentration in brain, spleen and kidneys was undetectable in all mice, including untreated MMA mice, with lack of sensitivity of the analytical method used preventing evaluation of the effect of treatment on these tissues.

Figure 4.3-12 Average hepatic MMA concentrations of normal mice (n=6), mut -/- muth2 untreated mice (n=6) and HIV-1SDmEF1αmurSigHutMCM treated mice (n=5) are shown. The mean concentration of hepatic MMA for normal mice, mut -/- muth2 untreated group and HIV-1SDmEF1αmurSigHutMCM treated mice are 7 ± 1 μM/g tissue, 1003 ± 124 μM/g tissue, and 133 ± 20 μM/ g tissue, respectively. Statistical analysis demonstrated a significant difference between the untreated and normal group. Also, the analysis demonstrated a significant reduction (p<0.05) of hepatic MMA level in HIV-1SDmEF1αmurSigHutMCM treated mice compared to the untreated group. However, the analysis showed no significant difference between the HIV-1SDmEF1αmurSigHutMCM treated group and the normal group. The standard bars represent ± one standard error. * and α indicate the significant difference between treatment groups. The p value were calculated using one-way ANOVA with Tukey's post-hoc test.

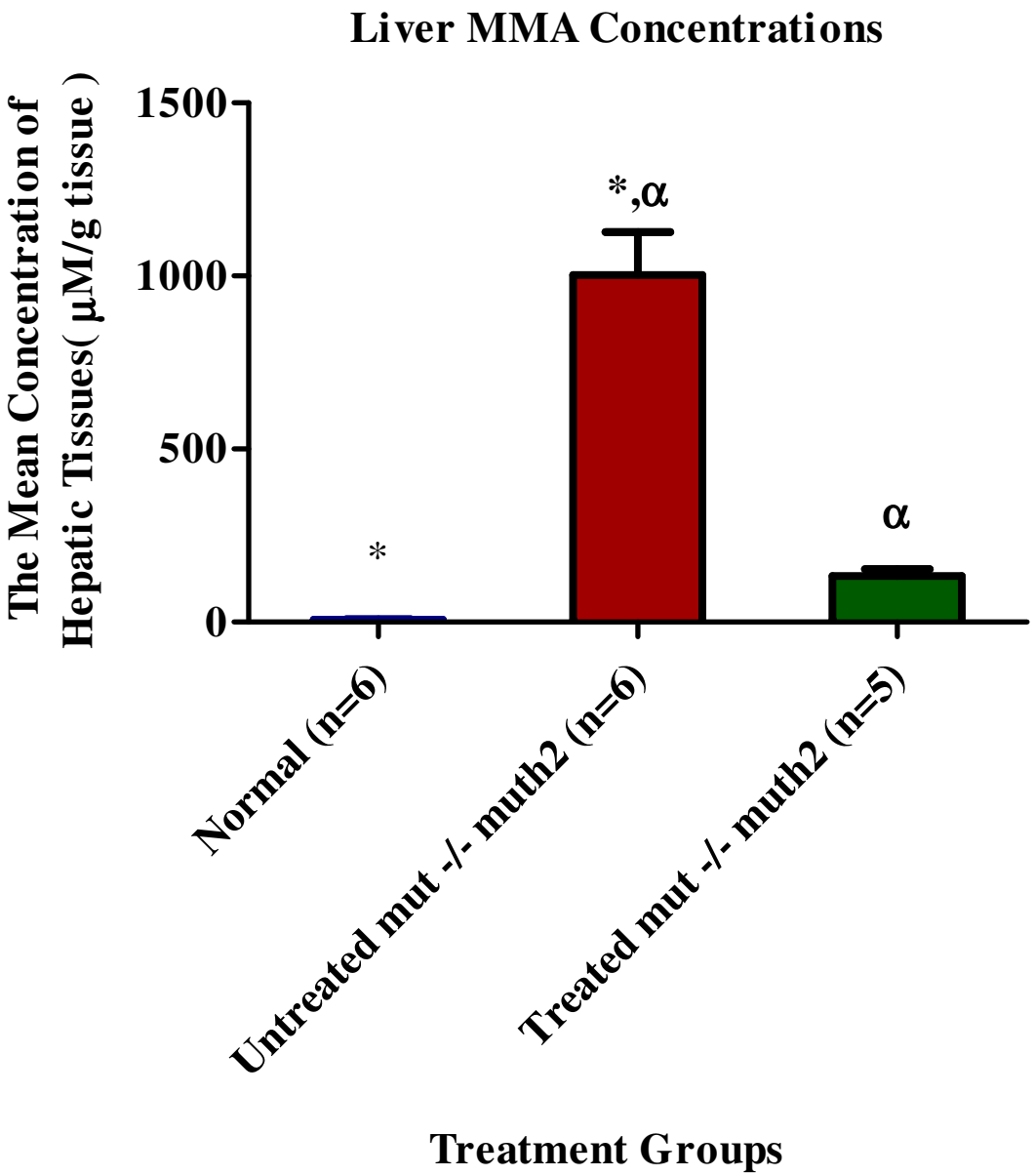
Liver MMA Concentrations
The Mean Concentration of Hepatic Tissues(µM/g tissue)
1500
1000
500
0
*
*,α
α
Normal (n=6)
Untreated mut -/- muth2 (n=6)
Treated mut -/- muth2 (n=5)
Treatment Groups

4.3.3 Discussion

As discussed in the previous section, several strategies were adopted to enhance the expression of the vector encoded human MCM and hence improve vector mediated restoration of MCM metabolism *in vitro* and *in vivo*. These strategies include optimizing the human MCM gene sequence and the use of a murine mitochondrial targeting sequence. The use of the latter modification is supported by the study conducted by Ye *et al*., (2001) [181], in which it was demonstrated that the use of murine mitochondrial targeting sequence improved expression of the human OTC cDNA in mouse hepatocytes. *In vitro* results demonstrated the changes adopted considerably improved the ability of the vector to restore MCM expression in MCM knockout fibroblasts. However, it was not possible to assess which change (codon optimisation or use of a murine signal) was more important in improving expression of MCM or whether both contributed to the result. In practice, the only issue of importance is that expression was significantly improved, hence it was considered appropriate to assess the new vector in the mut -/- muth2 mouse model.

Since the mice injected with HIV- 1SDmEF1αhMCM in the previous chapter at doses of 50 μg p24 equivalent showed no significant improvement in reducing the MMA level in treated animals, we also increased the dose to an average of 130 μg p24 equivalent in a total volume of 300 μL. The use of an improved virus purification protocol facilitated the delivery of the increased dose by greatly reducing the amount of contaminating material contained in the virus preparation. In addition, the mice were pre-treated with 10% dextrose and intralipid prior to the virus delivery to stabilize their metabolic condition and to limit the likelihood of acute metabolic decompensation that would aggravate the condition of the mut -/- muth2 mice during the treatment. The use of intralipid also provides an additional potential advantage. A study by Follenzi *et al*., (2002) [143], has demonstrated that the efficiency of gene transduction into hepatocytes was limited as a result of the vectors uptake by Kupffer cells and liver sinusoidal endothelial cells. Studies using adenovirus have shown the depletion of

these cell types could enhance the gene transfer into parenchymal liver cells, resulting in increased gene expression [144-147]. A recent study suggests the potential use of intralipid to increase the transgene expression by blocking vector uptake into the Kupffer cells [147]. On the basis of these data, it was hypothesized that intralipid may also improve the transduction of hepatocytes by the LV.

Vector copy number was measured to assess the level and biodistribution of gene transduction in the animals. Similar to results obtained in the previous chapter, the liver is the main target for gene delivery by intravenous injection, with an average of 3.2 copies per cell, followed by spleen. The detection of vector 6- months post-treatment indicates the integration of vector into stem cells or long-lived cells. This outcome suggests that the changes made in vector preparation and dosing were successful in improving *in vivo* transduction by an average of 10-fold. In particular, a high level of vector copy was detected in one of the HIV-1SDmEF1αmurSigHutMCM treated mice (QUE 8.403), with 10 copies per cell, indicating that very high levels of transduction are possible. However, it is unclear why this mouse responded so well. Nevertheless, in the other treated mice there was an average of only approximately 1.4 vector copies per cell and transduction was relatively equal, ranging from 0.8 to 1.6 copies/cell. , However, this is still significantly higher than our previous experiments with the mut -/- muth2 mice treated with the original HIV-1SDmEF1αhMCM vector in which transduction ranged from 0.1 to 0.3 copies/cell and with a mean ± SE of 0.2 ± 0.04 copies/cell. The comparison between these two studies, again, indicates the positive correlation of transduction efficiency with the dose of transducing units. This is also supported by the study published by McIntyre *et al*., (2010) [193].

The expression of MCM following gene transduction by western blot analysis reveals that a high level expression was observed in the HIV- 1SDmEF1αmurSigHutMCM treated group.

Software ImageJ enables the quantification of the level of protein expression, with a near 100% of normal protein level expressed in the treated group.

The hepatic enzyme activity measured by HPLC shows a statistically significant increase between the treated and untreated animals with the activity level in treated animals reaching the level seen in wild-type animals. Unexpectedly, despite the detection of low level protein expression in the mut -/- muth2 untreated mice, no hepatic enzyme activity could be detected. This is in contrast to the findings reported by Peters *et al*., (2012) [152] that the mut -/- muth2 mouse model possess approximately 20% of the normal control MCM enzyme activity. One possible explanation for this could be that the enzyme activity was too low to be detected by our HPLC based enzyme assay. This possibility was investigated in a series of mixing experiments, involving the use of different amounts of normal and untreated mut -/- muth2 liver sample mixtures, ranging from 0:100, 2:97.5, 5:95, 7.5:92.5, 10:90, 25:75, 50:50, 75:25, 90:10 and 100:0 as described in section 2.3. This revealed that the lower limit of detection of our HPLC enzyme assay method is about 25 percent of normal. The level of enzyme activity reported for the rescue mice is therefore, of a similar magnitude to the limit of detection of the direct enzyme assay. It is also possible that as an indirect assay for MCM activity, the propionate incorporation assay overstates the level of MCM activity, especially when low levels of activity are present.

As described earlier, our results demonstrated that the improvement of specific infectivity and increasing the dose resulted in the enhancement of the level of gene transduction in the treated animals, leading to a better outcome compared to the first study. One of the HIV-1SDmEF1αmurSigHutMCM treated mice, QUE 8.403, has set a good example. The high level of gene transduction in this mouse, with 10 copies per cell, resulted in a small but noticeable improvement in outcome across the whole range of results, including western blot analysis, plasma, urinary and liver MMA measurement, compared to the other treated mice.

However, the study, which was to investigate the correlation between the integrated vector copy number and the MCM enzyme activity demonstrated that the restoration of MCM enzyme activity in the treated mice was not well-correlated to vector copy number. This suggested that the MCM enzyme activity may possibly be limited by other factors. Support for this idea comes from the study published by Wilkemeyer *et al*., (1993) [179], which proposed the involvement of epigenetic and genetic mechanisms in regulating MCM enzyme activity. This study discussed the fact that, like other nuclear-encoded mitochondrial proteins (NEMPs), the MCM gene contains several mitochondrial coordinating elements such as NRF-2 and Mt-2. NRF-2 has been shown to be responsible for coordinating nuclear and mitochondrial gene expression [179, 222] in which Mt-2 plays a role in regulating promoter activity [223]. It is believed that these elements may function in the same manner in the MCM gene as in other NEMPs, although this remains unclear at this stage.

In addition, numerous regulatory promoter elements have been identified in housekeeping genes that do not have a TATA box. Since MCM is characterized as a TATA-less housekeeping gene, it is speculated that the presence of these regulatory elements in the MCM gene play a part in regulating MCM enzyme activity. Nevertheless, such genetic regulatory systems are absent from the vector suggesting other factors such as the level of protein stability may be involved. Another *in vitro* study conducted by Wilkemeyer *et al*., (1992) [224], which investigated the restoration of propionate metabolism in cultured cells after transfection with retroviral-based vector that expressed murine MCM, demonstrated that MCM is not a rate-limiting enzyme in propionate metabolism. They showed that over-expression of MCM did not increase propionate metabolism above the normal level in cultured fibroblasts and hepatoma cells. It was also proposed that there may be a co-operative phenomenon between individual cells as it was found that the restoration of propionate metabolism in MCM knockout fibroblasts was disproportionally greater than the efficiency of transfection.

Nevertheless, by manipulating the specific infectivity of the virus, increasing the dose of transducing units, the use of a codon-optimized human MCM gene sequence with a murine mitochondrial targeting sequence has significantly restored the MCM enzyme activity in the LV-treated mice compared to the previous study, allowing consistent levels of gene transduction that are sufficiently large to effectively restore enzyme activity to the liver.

Plasma MMA levels are considered by physicians who manage patients with MMAuria the best guide to validate the effect of treatment (Fletcher JM personal communication 2011). We measured plasma MMA levels to show the effects of the restoration of MCM enzyme activity and demonstrated that the plasma MMA concentration of the HIV-1SDmEF1αmurSigHutMCM treated mice was significantly reduced to half the concentration of the untreated group. The decrease in plasma MMA can only be due to the substantial restoration of MCM enzyme activity. Moreover, the MMA level in the liver was significantly decreased, indicating the rapid metabolism and clearance of these MMA metabolites from the animal.

Unlike the plasma MMA analysis, only a modest decrease in MMA levels was found in the urine. This is consistent with the outcomes reported in patients who received liver transplantation and normalized plasma MMA concentrations but not urinary MMA concentration [225]. This is because in metabolic conditions, including MMAuria, in which the pathway is active in the kidney, the urinary metabolite concentrations are markedly influenced by the metabolic processes within the kidneys rather than accurately reflecting whole body metabolism. However, the role of kidney in the whole body mutase enzyme activity is not known although kidney only contains about 18% of the enzyme activity found in the liver [225, 226]. Liver has been the main target for gene therapy in ameliorating the MMAuria disease based on the success in liver transplantation [182]. However, a clinical report published by Chakraprani *et al*., (2002) [105] demonstrated that the occurrence of

progressive renal failure after successful liver transplantation, indicating that the renal metabolic defect is not corrected. This is also suggested by Kaplan *et al*., (2006) [103] and Kasahara *et al*., (2006) [104], who both challenge the rationale of liver transplantation. In fact, a few reports have also suggested that the benefit of either renal or combined transplantation [103-105, 183, 184, 227-230] is greater than that of liver transplantation alone [231-233]. Therefore, it would be of interest to investigate the potential to improve the MMAuria disease with gene therapy targeted to the kidney.

Overall, the reduction of MMA level in plasma and urine due to the restoration of MCM enzyme activity in HIV- 1SDmEF1αmurSigHutMCM treated mice led to an increase in body weight. In addition, the treated mice seemed to cope better with the treatment than the first group of mice treated with the HIV- 1SDmEF1αhMCM vector. This might be attributed to the pre-treatment with both 10% dextrose and intralipid rather than dextrose alone. The use of a more rigorous virus purification procedure is also likely to reduce the immediate response to the administration of the virus. Despite these improvements in the procedure, one of the treated mice, QUE10.25, failed to gain body weight after treatment and eventually died. The autopsy examination showed liver steatosis (macrovesicular and microvesicular). One of the possible explanations is the failure of fatty acid oxidation secondary to the deficiency of MCM [234]. The excess fatty acids would then be mobilised from body fat to the liver causing the fatty liver. Similar finding was observed in the study published by Chandler *et al*., (2009) [101], in which microvesicular and macrovesicular steatosis was observed in the histology of the MMAuria liver. Unfortunately, the tissues had started to decompose and it was impossible to collect a blood sample for testing. The remainders of the HIV-1SDmEF1αmurSigHutMCM treated mice showed no significant adverse effects from the treatment and after 10 weeks were physically indistinguishable from age-matched littermates.

4.4 Conclusion

In conclusion, the data presented in this thesis demonstrates that a significantly improved outcome in our second study following a number of changes, including the use of a codon-optimised HIV-1SDmEF1αmurSigHutMCM along with the addition of murine mitochondrial targeting sequence, the use of intralipid combined with 10% dextrose in order to minimize the adverse metabolic effects of the treated mice associated with administration of the vector. Improvements in vector purification and specific infectivity are also likely to have played a significant role in improving the outcome.

Moreover, the utilization of intralipid may have assisted the achievement of a higher gene transduction in our case. Unpublished data (Appendix V), provided by Chantelle McIntyre, demonstrated an increase in gene transduction after pretreatment with intralipid. However, it is important to note that the difference in virus dosage used in the two different experiments. A lower dose of LV vector (50 μg p24 equivalent) was used in her study compared to our study, in which 130 μg p24 equivalent of LV vector was used. The high amount of virus used in this MMA study itself probably acts to saturate the Kuppfer cell receptors to some extent. In addition, the apparently non-linear relationship between transduction efficiency and enzyme expression, as evidenced by QUE 8.403, warrants further study.

Further improvements in gene delivery could probably be achieved by using a more direct route for vector delivery to the liver such as intrahepatic delivery method. Although, the applicability of these techniques in the mut -/- muth2 model is likely to be problematical due to its physiological fragility, they may be applicable in a clinical setting.

Chapter 5 : General Discussion, Conclusions and Future Work

5.1 General Discussion

The choice of target tissue and the best method of efficient gene delivery to that tissue are critical factors in developing a successful gene therapy strategy. We used IV injection in our study to achieve liver transduction. Numerous studies on the biodistribution of adenovirus after IV injection demonstrate that liver and lung are the main organs targeted. Moreover, a study conducted by Pan *et al*., (2002) [194], which investigated the biodistribution and toxicity of a VSV-G pseudotyped LV in mice after IV injection, indicated a high vector copy number in liver, spleen and bone marrow as measured by real-time quantitative PCR assay. The vector was still detectable after 40 days although its level had reduced. A high level of green fluorescent protein (GFP) transgene was initially observed in bone marrow, liver and spleen, with 5-37%, 12-59% and 20-54% transgene frequency, respectively, 4 days post-injection. However, the level of GFP transgene cells reduced to 4.7-22.7%, 0.3-1.3% and 0.045-0.38% transgene frequency for bone marrow, liver and spleen, respectively, by 40 days due to the existence of abundant abnormal vector particles that contain partial reverse transcripts, and the loss of extrachromosomal proviral DNA. No signal of inflammation indicative of liver toxicity was observed. The results from our study agree with this finding, with a higher vector copy number in the liver than in the other tissues analysed. That the liver appears to be the major target for gene transduction is most likely a result of the hepatic first-pass metabolism effect [235]. In addition, given that only a very small volume of LV, 300 μL, was used for injection, IV injection provides a simple and rapid delivery method to minimize the physiological impact on the mice, an especially important issue due to the metabolic fragility of the mut -/- muth2 mice.

We found a higher vector copy number was associated with a higher level of MCM enzyme activity in the HIV-1 SDmEF1αmurSigHutMCM treated mice than HIV-1SDmEF1αhMCM treated mice. Nevertheless, there was no correlation between the vector copy number and the level of MCM enzyme activity for individual mice treated with HIV-1SDmEF1αmurSigHutMCM. Although further studies are required to confirm this observation (a very high copy number was achieved in only one animal) this suggests that attempts to further improve gene transfer to the liver and hence achieve supranormal MCM expression would not be effective in improving outcomes. One explanation for this phenomenon may be that the enzymes involved in the pathway form a stoichiometric complex.

The apparent lack of correlation between gene transfer and MCM expression may be due to the instability of "surplus" MCM protein. It has already been noted that MCM is not the rate limiting enzyme in the pathway, although the stability of MCM under conditions of supranormal expression has not been studied. This would be worthwhile in order to understand the best way forward in developing MMAuria gene therapy. If supranormal MCM expression cannot be achieved, then targeting other tissues, most obviously the kidney, in addition to the liver, may be the most productive approach disease in the animals.

Numerous studies indicates that the stimulation of immune response by IV injection may hamper the transduction efficiency [236, 237]. A study, in which an Adv vector was administered IV in rats, was shown to induce shock due to the activation of innate immune response molecules [238]. Experiments have been conducted to investigate an alternative delivery method to overcome this issue. A study by Sobrevals *et al*., (2012) [239] demonstrated that delivering AAV vectors through the hepatic artery achieved high transduction efficiency in hepatocytes. However, surgical procedures such as laparotomy and partial hepatectomy are needed in order to inoculate the viral vector directly into the

hepatic artery. Again, this is likely to be a significant challenge in our murine model as well as in MMAuria patients due to the risk of inducing acute metabolic decompensation from the stress of the surgery.

Another possible virus delivery method to improve the efficiency of LV mediated gene transduction to the liver is intrahepatic (IH) injection, in which virus is directly injected into the liver, as described in the study by Chandler *et al*., (2008) [240]. In their study, AAV-serotype 8 that expressed murine MCM was directly injected into the liver of neonatal mut -/- mice several hours after birth resulting in most of the virus being localised, and high levels of mutase being expressed, in the liver. Following this, another study conducted by Carrillo-Carrasco *et al*., (2010) [207], further confirmed these observations. The feasibility of using any of these enhanced virus delivery methods for delivery of the HIV-1SDmEF1αmurSigHutMCM vector in the mut -/- muth2 mouse model needs to be explored.

The ability to transduce both dividing and non-dividing cell types makes LV an attractive tool for gene therapy of genetic liver disorders [241-244]. However, it has been shown that the transduction efficiency into hepatocytes is limited because most of the cells transduced by LV vectors are Kupffer cells [143, 245, 246]. Kuppfer cells are hepatic macrophages which play a major role in phagocytosis and antigen processing. Numerous studies have also demonstrated their activity in clearing several kinds of virus including Adv [247], SIV [248], and vesicular stomatitis virus (VSV) [249].

The use of intralipid in our study might have improved hepatocyte transduction by blocking the Kupffer cell function. The study published by Snoeys *et al.,* (2006) [147] evaluated the effectiveness of L-α-phosphatidylcholine liposomes and intralipid in enhancing the expression of human apolipoprotein (apo) A-I in Balb/c and C57BL/6 mice using Adv. Their study found out that the mice pre-treated with the L-α-phosphatidylcholine liposome and

intralipid 1 hour before the injection of AdvA-I had significantly improved expression of human apo A-I in the liver of both strains. In addition, as discussed in Chapter 4, unpublished data provided by Chantelle McIntyre, which investigated the effect of intralipid pretreatment on transduction efficiency, demonstrated that the transduction efficiency was significantly improved in the liver, spleen and lung of the mice pre-treated with intralipid 1 hour before the injection of 50 μg p24 equivalent of our LV vector. However, as several modifications had been made in attempts to overcome the poor gene transduction and expression observed in our first study, whether the use of intralipid leads to the observation of high vector copy number, is not known. Nonetheless, it is likely that intralipid plays a part in improving the transduction efficiency to some extent.

To date, numerous studies have been performed in order to develop a vector that specifically enhances transgene expression in hepatocytes. One of these strategies is the use of a liver-specific promoter. The EF1-α promoter was used in our study to drive the human MCM transgene expression. Although EF1-α is a strong promoter, it is a non-cell specific promoter. Several studies have been performed to identify and characterize suitable liver specific promoters. Examples of such promoters are mouse albumin, human α1-antitrypsin, hemepexin and thyroid hormone-binding globulin (TBG) promoters. Extensive studies have been done to characterize these promoters. The mouse albumin promoter shows high homology across species [250, 251]. Liver is a major site of synthesis of α1-antitrypsin and hemopexin is produced exclusively in the liver. Analyses by Kramer *et al*., (2003) [252] showed that all these promoters produce a remarkable luciferase reporter gene expression in the liver, particularly the human α1-antitrypsin promoter. These findings agree with the earlier study by Hafenrichter *et al*., (1994) [253], which showed that the human α1-antitrypsin promoter can not only produce a high level of gene expression but also the gene expression persists for at least 6 months. A rAAV-2/8 vector, with the human α1-antitrypsin promoter driving the expression of mouse OTC gene, not only specifically targeted hepatocytes but also

fully corrected the metabolic disorder following a single IP injection. In addition, a clinical study in which a rAAV-2 vector that expressed human factor IX (F.IX) with the use of human α1-antitrypsin promoter was administered to haemophilia B patients provided evidence for the successful correction of the disorder [254]. Nevertheless, the strength of the transgene expression driven by these liver-specific promoters in hepatocytes could be an issue. To date, there is no study that shows the comparison of these liver-specific promoters to EF1-α promoter in terms of the strength of their gene expression ability. However, the Kramer study [252] showed that the strength of these promoters, although specifically expressed in the liver, is less than the CMV promoter, which is known as a non cell-specific promoter. Several comparative studies between EF1-α and CMV promoters demonstrated that the EF1-α promoter possesses an equivalent, if not better, gene expression ability than CMV promoter [255-259]. Therefore, based on these data, it is speculated that the strength of gene expression driven by these liver-specific promoters may not be as strong as the EF1-α promoter. Nonetheless, further studies are required to evaluate their efficiency.

Another advantage of using a liver cell-specific promoter is to help avoid the induction of an immune response. Evidence from a study conducted by Pastore *et al*., (1993) [260], in which gene expression driven by mPEGK, an ubiquitous promoter, and the mouse albumin promoter, a liver specific promoter, was compared demonstrated a reduction in the host humoral immune response when the mouse albumin promoter was used. An alternative liver-specific promoter is the TBG promoter which has previously been characterized as a liver-specific promoter [261]. A number of studies have demonstrated the successful use of the TBG promoter in gene therapy vectors for several diseases including OTC deficiency [262], and apoliprotein deficiency [263]. A study published by Wang *et al*., (2010) [264], in which the efficiency of AAV-8, hu.37 and rh.8 vectors that express GFP driven by the TBG promoter was evaluated in rhesus macaques, showed that a high-level and stable expression of GFP was observed in the hepatocytes of the treated animals with AAV-8 vector. Most

importantly, the results suggested that the use of the TBG promoter resulted in the avoidance of a cytotoxic T-cells lymphocyte (CTL) response. Another study demonstrated the correction of MMAuria in MCM knockout mice with a rAAV vector that used the TBG promoter to drive the expression of the murine MCM gene in liver [207]. The outcomes of this study also suggested that the liver-specific expression of the *mut* gene resulting from the use of the TBG promoter helped to minimize transgene directed immune responses. In conclusion, these studies suggest it would be of interest to investigate the performance of our vector expressing the codon-optimised murSigHutMCM vector using the TBG promoter in place of the EF1-α promoter.

In our study, a high dose of LV vector, 130 µg p24 equivalent, was used in order to achieve a reasonable level of transduction in the liver. However, high doses of vector can also lead to unwanted immune responses. Brunett-Pierri *et al*., (2004) [265] showed the activation of the innate inflammatory response by Adv vectors can lead to acute hepatotoxicity in nonhuman primates. Moreover, they demonstrated the severity of the response is dose-dependent. It is expected that similar consequences would be observed in human patients. Although LV vectors generally seem to be less immunogenic, and the specific infectivity of the LV vector used in this study had been increased to enhance the transduction efficiency per unit of p24, reducing the amount of virus needed to obtain sufficient gene delivery and so minimizing the possibility of triggering the immune response, it would be important to investigate the immune reaction and inflammation that occurs after vector delivery. Several possible strategies to improve the quality of LV vectors that have been discussed in Chapter 1, such as the use of COS-1 cell line for virus production, should be evaluated in terms of their immunogenicety and gene delivery efficiency. Given the apparent limitation of MCM expression after gene transfer to approximately normal levels it may be that sufficient gene transfer to attain this could be achieved with lower doses of vector. Again, a more complete

analysis of the correlation between vector dose, gene transfer and MCM expression is warranted.

AAV has been used extensively for gene therapy. This vector system has delivered many promising results, for example in treating genetic disorders such as OTC deficiency [262], FH syndrome [266], Haemophilia B [267] and others. It has also been used in clinical trials for these diseases. Of all the AAV serotypes, AAV-2 has historically been the most commonly studied. It has been shown to transduce non-proliferating and proliferating cells efficiently and can produce high level, long-term transgene expression. However, as described in the introduction, its small packaging size limits its use in some of the diseases that require a larger size of cDNA. It has also been shown that the humoral immune response induced by AAV-2 may limit its transduction efficiency as it is reported that 40% to 80% of the human population is seropositive for AAV-2 [268]. In addition, the cell-mediated response to the virus, although poorly understood, may play a role in destruction of the transduced cell. One clinical trial reported that AAV-2 failed to treat Haemophilia B in one of the human subjects. It is hypothesized that the failure may be due to the AAV capsid-derived peptides being presented on the hepatocyte cell surface after transduction, leading to recognition by $CD8^+$ T cells and subsequent cell destruction [254].

Therefore, numerous studies have been done to try and overcome these difficulties. Recently, studies have been reported enhanced transduction efficiency with the use of the non-human primate AAV serotype 8 (AAV-8) over AAV-2. One of the advantages of using AAV-8 in gene therapy is that it is distinguished from AAV-2 based on sequence homology analysis. This makes AAV-8 a more appropriate tool for gene therapy as it minimize the chances of inducing the humoral immune response in the transduced host, leading to enhanced transduction efficiency. In one study conducted by Vandendriessche *et al*., (2007) [269], the performance of AAV-8 and AAV-9 in expressing the human F.IX cDNA in mouse liver,

driven by the CMV promoter, was evaluated. The data demonstrated that the use of these serotypes greatly enhanced transgene expression and achieved supra-physiological F.IX levels. These findings are also supported by the study conducted by Carrillo-Carrasco *et al*., (2010) [207] that demonstrated that rescue of a lethal MMAuria-affected mouse model (mut -/-) with an recombinant AAV-8 vector provided long-term phenotypic correction. Nevertheless, using a whole animal [1-^{13}C]-propionate oxidation method, they were only able to demonstrate a mild increase in propionate oxidation in the treated mice, with a value of 32.5 ± 8.1% and 39.8 ± 9.4% for the rAAV-8-TBGmMUT and the rAAV-8-CBAmMUT treated groups, respectively. This compares with 12.6 ± 2.2% oxidation for the untreated group and 69.4 ± 4.3% oxidation for the positive control group (mut +/-). This supports the idea that while restoration of MCM enzyme activity in the liver can lead to a significant decrease of MMA level in plasma it does not completely normalize MMA metabolism. Given that high levels of expression that can be achieved with AAV vectors is also providing some support to the theory that supranormal levels of MCM enzyme activity in the liver may not be achievable, perhaps because, as previously discussed, MCM is not a rate-limiting enzyme in the pathway of propionate metabolism.

In addition, like the other AAV serotypes, the use of AAV-8 in the clinic might be influenced by pre-existing antibodies against AAV-8, leading to poor transduction in patients. In fact, the analysis of serological data published by Gao *et al*., (2004) [270], demonstrated that AAV infections are prevalent in humans. In their study, they showed the detection of endogenous AAV sequences in 18% of all human tissues screened. Of all the AAV serotypes screened, AAV-2 was found the most abundant in human followed by AAV-8. In addition, Vandendriessche *et al*., (2007) [269] had reported that pre-existing antibodies to AAV-8 are detected in 20% of the human population. Thereby, pre-screening for AAV-8 antibodies is supported when this serotype is used on clinical trials and ultimately, other serotypes may be preferred.

LV vectors have also attracted great attention as another potentially useful tool for gene therapy for genetic and other disorders due to their ability to efficiently and stably transduce both non-proliferating and proliferating cells. In our study, a LV vector that expressed the human MCM transgene, driven by EF1-α promoter, was employed in order to treat the MMAuria disease in a mut -/- muth2 mouse model. Western blot analyses indicated the full expression of human MCM transgene in the liver of the treated mice. This resulted in the restoration of MCM enzyme activity, and led to the reduction, but not normalization, of the MMA levels in plasma and urine. In addition, the vector copy number observed in the treated mice sacrificed 6-months post-treatment suggested that long-term correction was achieved. However, the stability of expression over time could not be properly assessed due to the limited nature of the study.

Also, our results are consistent with the reported clinical findings published by Mc Guire *et al*., (2008) [102]. This report demonstrated that the patients who received liver transplant presented a significant clinical improvement even though high levels of MMA excretion still persisted. This could also mean that there are other factors that might contribute to the MMA level observed in these human subjects. One of the reasons may be the MCM enzyme activity found in kidneys. Numerous studies have reported that high level of MCM enzyme activity was observed in liver and kidneys [271-273]. Another study published by Wilkemeyer *et al*., (1993) [179], which investigated the genomic structure of the Mut locus and the role of genetic regulation of enzyme levels in different murine tissues, demonstrated that large amounts of MCM mRNA was found in liver and kidney. Interestingly, their study revealed that the kidneys had levels of MCM mRNA 2-5 times higher than liver and the highest level of total MCM enzyme activity compared to the other murine tissues, even though kidneys are believed to contain only a minor percentage of the MCM activity found in the liver [226].

This is also further supported by the clinical study published by Lubrano *et al*., (2007) [225]. Liver has long been regarded as the major site of MCM enzyme activity and, therefore, liver transplantation for MMAuria patients was performed on this basis. As a result, the conditions of the recipients significantly improved. However, complications after transplant, or elevated MMA levels in plasma and urine, indicative of the failure to fully restore MMA metabolism, was reported in several individuals [105, 184, 227, 228]. In fact, liver transplantation as the curative approach for MMAuria has been challenged [103, 104]. These patients demonstrated neurologic or renal failure-related complications after transplant. In contrast, a better outcome was observed amongst these patients who received either kidney transplantation alone or in combination with liver transplantation. Clinical observation showed the restoration of renal function and the improvement of metabolic disorder with the greatest reduction in urine MMA level in these patients. This is further supported by the clinical study reported by Lubrano *et al*., (2007) [225]. In this report, they provided evidence from a patient who appeared to have normal renal function and who was clinically stable 10 years after kidney transplantation. Nevertheless, the real benefit of kidney transplantation in MMAuria disease is not known. Also, for gene therapy, the consideration of choosing an effective route of administration that targets the kidney needs to be taken into account. Several routes have been studied [274]. Depending on the site of transduction, these delivery methods include intra-renal arterial injection and parenchymal injection. Nevertheless, the involvement of surgical procedures in these delivery methods may cause metabolic decompensation in the mut -/-muth2 mouse model as well as patients. Further studies are required to investigate its feasibility.

Insertional mutagenesis is a potential threat that is shared by all viral vector systems used for gene therapy [275]. The clinical use of gene therapy suffered a major setback with the report of the development of a T-cell leukemia in three X-SCID patients who received gene therapy, using an MMLV vector [112], and by the death of Jesse Gelsinger [276] who received

treatment using an Adv vector, although his death was mainly due to the activation of an immune response to the virus, leading to multiple organ failure and brain death . Although the development of the T-cell leukemia in the X-SCID patients appears complex, and involves specific risk factors that may not be present in other systems the occurrence of insertional mutagenesis in other tissues such as liver cannot be ignored, despite the lack of evidence of this event [277]. The *in vitro* study by Bokhoven *et al*., (2009) demonstrated that LV vectors can be as oncogenic as retroviral vectors [278]. A better understanding of LV's sites of integration preference may allow this risk to be better evaluated. The ability to manipulate the site of integration is likely to be the ultimate approach to increasing the biosafety of LV and retroviral vectors [279].

Despite these issues the first clinical trial using an LV vector has been reported [280]. To date, although no serious adverse events have been noted, the magnitude of these risks remains unknown as is the time it may take before any adverse effects become apparent.

Finally, the mouse model used in our study is a 2-human MCM transgene rescued mouse model. The success in restoring the mutase enzyme activity with the use of human MCM transgene has encouraged our study towards human clinical trials for MMAuria. Also, despite the disadvantages discussed as above, LV is still a good candidate for MMAuria gene therapy although more extensive studies in animal models are needed.

5.2 Conclusion

This study demonstrates the ability of our LV vector to provide a high level of human MCM gene expression *in vitro* and *in vivo*. The human MCM gene was initially cloned into a LV vector and transduced into MCM deficient fibroblasts. Real-time PCR and [^{14}C]-radiolabelled propionate incorporation studies indicated that not only could the human MCM

gene be transduced into fibroblasts but also that it was able to express a functional human MCM *in vitro*.

Following this study, the LV vector was delivered to the mut -/- muth2 murine model in order to investigate its ability to rescue the animal by stably expressing the vector encoded human MCM transgene in the treated mice. However, the preliminary outcomes were not very satisfactory. Physically, only a minor increase in bodyweight over one year was observed compared to the untreated control. In addition, the biochemical analyses showed only a minor reduction in MMA levels in plasma and urine. Liver tissues extracted in the end of the experiment for enzyme activity measurement failed to demonstrate measurable enzyme activity, suggesting that the human MCM enzyme activity was below the sensitivity of the assay, i.e less than about 25% of normal.

Subsequently, the vector was modified in an attempt to enhance transgene expression. These modifications were codon-optimization, a widely used method for enhancing gene expression, and the addition of the murine MCM mitochondrial import signal into the vector to ensure efficient import and localisation of the human enzyme into the murine mitochondria.

Prior to examination of its effect *in vivo*, the modified LV vector was transduced into MCM deficient fibroblasts. Analyses including vector copy number analysis and measurement of MCM enzyme activity were carried out. In comparison to the initial LV vector, HIV-1SDmEF1αhMCM, the codon-optimized LV vector demonstrated the same transduction efficiency as the previous LV vector, with the detection of equivalent vector copy number. However, the direct enzyme activity assay demonstrated that a supranormal enzyme activity was measured in the fibroblast transduced with codon-optimized LV vector, with 5-fold higher level than the wild type control and 2-fold higher than that achieved with the previous

LV vector. Therefore, its efficiency and efficacy were further examined in the mut -/- muth2 mice.

A 6-month preliminary study into the efficiency of a codon-optimized LV vector that expressed murine signalled human MCM mutase showed a significant improvement in parameters compared to the initial study.

The bodyweights indicated a significant increase in the treated mice. The growth of the mut -/- muth2 murine model has been shown to halt 3 months after birth. This may be due to incomplete digestion of essential proteins, resulting from the low residual MCM enzyme activity. In addition, visual observation showed that the untreated mut -/- muth2 mice were less active compared to the normal littermates. In contrast, the bodyweight of the mut -/- muth2 mice treated at 8 weeks old continued to increase, and subsequently reached the lower percentile of normal mouse bodyweight. In addition, the treated mice became more active and started to consume normal food pellets compared to the untreated mice that relied on sunflower seeds most of the time instead of food pellets.

The copy number analysis demonstrated a higher transduction efficiency than seen in the initial study. In both studies the vector primarily localised to the liver and spleen after IV injection. On average the copy number in the liver was 3.2 copies per cell compared to 0.2 copies per cell in the initial study. However, this result was skewed by one mouse having a much higher copy number than the others. An average copy number of 1.4 copies per cell is obtained if this mouse is omitted. This is most likely due to the improvements in gene delivery, including the use of a 2.5-fold higher dose of a higher specific infectivity LV and the use of intralipid as a pre-treatment. The use of a higher dose was made possible by improvements in the virus purification method, including the use of Mustang Q ion-exchange that resulted in a much cleaner virus preparation.

The success of gene transduction greatly improved the biochemical parameters in the treated mut -/- muth2 mice. The biochemical analyses showed a significant reduction in MMA in the plasma and a modest decrease in urine over the 6- month study. In addition, the low level of MMA observed 6 months post-treatment was consistent with a stable and long-term expression of a functional human MCM transgene. The MCM enzyme activity measurement demonstrated the success in restoring the enzyme activity in the mice liver treated with the codon-optimization LV system. However, comparison of the mouse with ten copies of the vector to the other mice suggest a restraint on MCM enzyme activity, perhaps reflecting the fact that it is not a rate limiting enzyme, suggesting that future work should concentrate on restoration of MCM enzyme activity in other tissues, most obviously in the kidney. Nevertheless, the data presented shows that liver gene therapy on its own can very significantly improve the pathology and biochemical abnormalities associated with MMAuria.

5.3 Future Work

The comparison of the data from the initial study and the second study clearly demonstrated that the increase of MCM enzyme activity is dependent on the success of gene transduction. As previously discussed, the use of a liver specific promoter, in particular the TBG promoter, may result in further improvements in gene expression while limiting expression to hepatocytes. This would lead to improve efficacy and less chance of immune reaction to the transgene.

The feasibility of using direct hepatic injection to deliver the virus specifically to the liver could also be considered. Chandler *et al*., (2008) [240] demonstrated that this delivery method could be easily achieved on non-anaesthetized neonatal pups with a 32-gauge needle and a transdermal approach. The biggest advantage of this rapid delivery method is the whole procedure takes only minutes to achieve and, therefore, reduces stress to the mice. The same

delivery method was used in Carrillo-Carrasco's study and they showed the transduction in clusters of hepatocytes with recombinant AAV, leading to the correction of MMAuria in the treated animals [207]. Nevertheless, the disadvantages of this gene delivery method have also been discussed [281]. These disadvantages include less widespread gene delivery and it being limited to only one liver lobe at any given time, with the random nature of the injection sites resulting in inconsistent results, and the potential of complete penetration of needles through liver causing leakage, leading to the failure of vector delivery. In addition, Chandler's and Carrillo-Carrasco's studies, using direct IH injection method, may not be a model relevant to clinical practice. Although direct intrahepatic injection to the liver may be easy to achieve in newborn pups, this may not be the case in human subjects as surgical procedures such as laparotomy may be required in order to target the liver. As mentioned earlier, this event can cause catabolic stress, leading to an acute metabolic decompensation in a MMAuria patient.

Biosafety issues of using LV vectors have always been a concern for gene therapy. The use of a murine model that expresses human MCM means that this animal model will be immune tolerant to human MCM. However, the high dosage of LV vector, 130 µg p24 equivalent, used in our study may cause hepatotoxicity. Therefore, it is important to evaluate the relationship between the vector dose and MCM enzyme activity as well as any toxicity to the liver. Inflammation and hepatotoxicity can be estimated by the determination of the level of glutamic pyruvic transaminase (GPT) in the serum. With the exception of one mouse, no adverse effect was observed after treatment and the conditions of LV treated mut -/- muth2 were, generally, stabilized 24 hours after treatment. This improvement would enable us to collect the blood from the LV treated animals and perform the evaluation of GPT level at 1 and 3 days after treatment to examine the level of hepatotoxicy over the time period immediately after vector delivery [282]. In addition, although unlikely, the VSV-G pseudotyped LV vector might trigger the innate immune system in the treated animal, influencing the transduction efficiency in our study. Thereby, it is of interest to investigate

the feasibility of a more targeted gene delivery strategy such as IH injection in order to minimize the induction of immune response.

As discussed previously, the current rationale for choosing liver as the main therapeutic target is based on the results from liver transplantation and the liver's susceptibility to gene delivery. However, kidneys have been shown to be a second major tissue involved in the propionate catabolic pathway. Studies have shown that the MMA level remains high amongst patients who received only liver transplantation. In addition, complications such as chronic kidney disease and neuropathy persist in patients receiving only liver transplants. A few studies have even questioned the value of liver transplantation and several clinical cases have shown patients who received kidney transplantation alone, or combined liver and kidney transplantation, performed better than those receiving only liver transplants. Thereby, a future study may involve evaluating the efficacy of gene transduction into the kidneys, for example through parenchymal or ureteral administration [283], either alone or in combination with gene delivery to the liver.

In summary, our study demonstrates that the potential of a liver-targeted gene therapy for MMAuria using LV although improvements are required in vector delivery and design in order to improve its efficacy . Furthermore, the possibility of gene delivery to kidney would be likely to offer considerable additional benefit in correcting the disease.

APPENDICES

Appendix I

Homo Sapiens Methylmalonyl coenzyme A mutase (MCM) mutase gene sequence

```
   1 cctggctgtg tggatgtctg acaggtgagg cgggggacgc agaagtgcag ccgccctctc
  61 ccacagcgga gtccaaaaca ggcctaccag tcagttctta tttctattgg gtgtttccat
 121 gctccaccat gttaagagct aagaatcagc ttttttttact ttcacctcat tacctgaggc
 181 aggtaaaaga atcatcaggc tccaggctca tacagcaacg acttctacac cagcaacagc
 241 cccttcaccc agaatgggct gccctggcta aaaagcagct gaaaggcaaa aacccagaag
 301 acctaatatg gcacaccccg gaagggatct ctataaaacc cttgtattcc aagagagata
 361 ctatggactt acctgaagaa cttccaggag tgaagccatt cacacgtgga ccatatccta
 421 ccatgtatac ctttaggccc tggaccatcc gccagtatgc tggttttagt actgtggaag
 481 aaagcaataa gttctataag gacaacatta aggctggtca gcagggatta tcagttgcct
 541 ttgatctggc gacacatcgt ggctatgatt cagacaaccc tcgagttcgt ggtgatgttg
 601 gaatggctgg agttgctatt gacactgtgg aagataccaa aattcttttt gatggaattc
 661 ctttagaaaa aatgtcagtt tccatgacta tgaatggagc agttattcca gttcttgcaa
 721 attttatagt aactggagaa gaacaaggtg tacctaaaga gaaacttact ggtaccatcc
 781 aaaatgatat actaaaggaa tttatggttc gaaatacata cattttcct ccagaaccat
 841 ccatgaaaat tattgctgac atatttgaat atacagcaaa gcacatgcca aaatttaatt
 901 caatttcaat tagtggatac catatgcagg aagcaggggc tgatgccatt ctggagctgg
 961 cctatacttt agcagatgga ttggagtact ctagaactgg actccaggct ggcctgacaa
1021 ttgatgaatt tgcaccaagg ttgtctttct tctggggaat tggaatgaat ttctatatgg
1081 aaatagcaaa gatgagagct ggtagaagac tctgggctca cttaatagag aaaatgtttc
1141 agcctaaaaa ctcaaaatct cttcttctaa gagcacactg tcagacatct ggatggtcac
1201 ttactgagca ggatccctac aataatattg tccgtactgc aatagaagca atggcagcag
1261 tatttggagg gactcagtct ttgcacacaa attcttttga tgaagctttg ggtttgccaa
1321 ctgtgaaaag tgctcgaatt gccaggaaca cacaaatcat cattcaagaa gaatctggga
1381 ttcccaaagt ggctgatcct tggggaggtt cttacatgat ggaatgtctc acaaatgatg
1441 tttatgatgc tgctttaaag ctcattaatg aaattgaaga aatgggtgga atggccaaag
1501 ctgtagctga gggaatacct aaacttcgaa ttgaagaatg tgctgcccga agacaagcta
1561 gaatagattc tggttctgaa gtaattgttg gagtaaataa gtaccagttg gaaaaagaag
1621 acactgtaga agttctggca attgataata cttcagtgcg aaacaggcag attgaaaaac
1681 ttaagaagat caaatccagc agggatcaag ctttggctga acgttgtctt gctgcactaa
1741 ccgaatgtgc tgctagcgga gatggaaata tcctggctct tgcagtggat gcatctcggg
1801 caagatgtac agtgggagaa atcacagatg ccctgaaaaa ggtatttggt gaacataaag
1861 cgaatgatcg aatggtgagt ggagcatatc gccaggaatt tggagaaagt aaagagataa
1921 catctgctat caagagggtt cataaattca tggaacgtga aggtcgcaga cctcgtcttc
1981 ttgtagcaaa aatgggacaa gatggccatg acagaggagc aaaagttatt gctacaggat
2041 ttgctgatct tggttttgat gtggacatag gccctctttt ccagactcct cgtgaagtgg
2101 cccagcaggc tgtggatgcg gatgtgcatg ctgtgggcgt aagcaccctc gctgctggtc
2161 ataaaaccct agttcctgaa ctcatcaaag aacttaactc ccttggacgg ccagatattc
2221 ttgtcatgtg tggaggggtg ataccacctc aggattatga atttctgttt gaagttggtg
2281 tttccaatgt atttggtcct gggactcgaa ttccaaaggc tgccgttcag gtgcttgatg
2341 atattgagaa gtgtttggaa aagaagcagc aatctgtata atatcctctt tttgttttag
2401 cttttgtcta aaatattatt ttagttatga tcaaagaaga gagtaaagct atgtcttcaa
2461 tttaatttca atacctgatt tgtactttcc ttgaaagctt tactttaaaa taccttactt
2521 ataggcctgg tgtcatgcta taagtatgta catacagttt cacttcaaaa aaaaaaaaaa
2581 a
```

Appendix II

Example of the analysis report on the pre-optimization human MCM gene sequence generated by https://www.genscript.com/cgi-bin/tools/rare_codon_analysis

Basic Information	
Organism	Mouse
CDS length	2568

Appendix II-1 Codon Adaptation Index (CAI)

Mouse

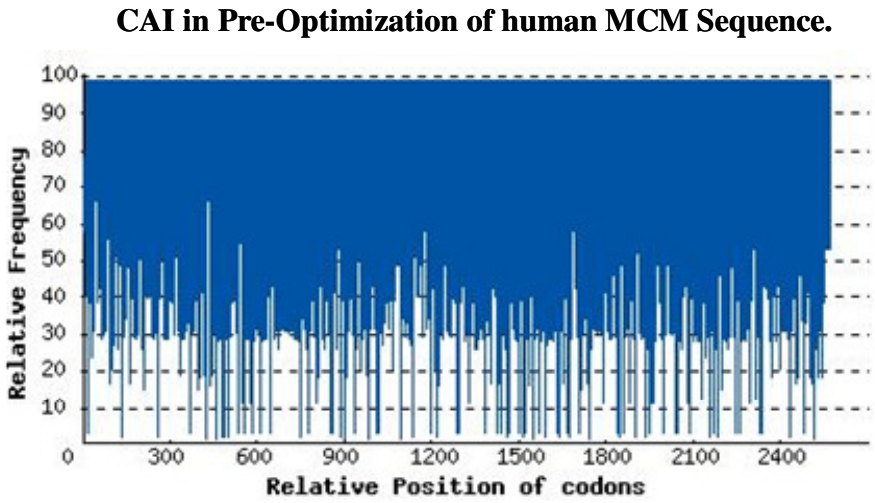

CAI : 0.74

Appendix Figure II-1.1 The distribution of codon usage frequency along the length of the pre-optimization human MCM to be expressed in mouse. The possibility of high protein expression level is correlated to the value of CAI - a CAI of 1.0 is considered to be ideal while a CAI of >0.8 is rated as good for expression in the mouse.

Appendix II-2 Content Adjustment

GC Curve

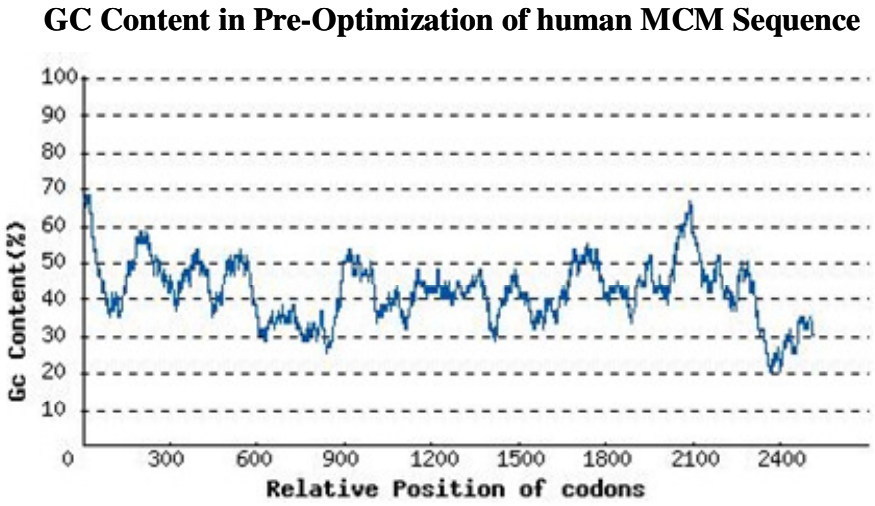

Average GC Content: 42.03

Appendix Figure II-2.1 The ideal percentage range of GC content is between 30% to 70%. Any peaks outside of this range will adversely affect transcriptional and translational efficiency.

Appendix II-3 Codon Frequency Distribution (CFD)

Mouse

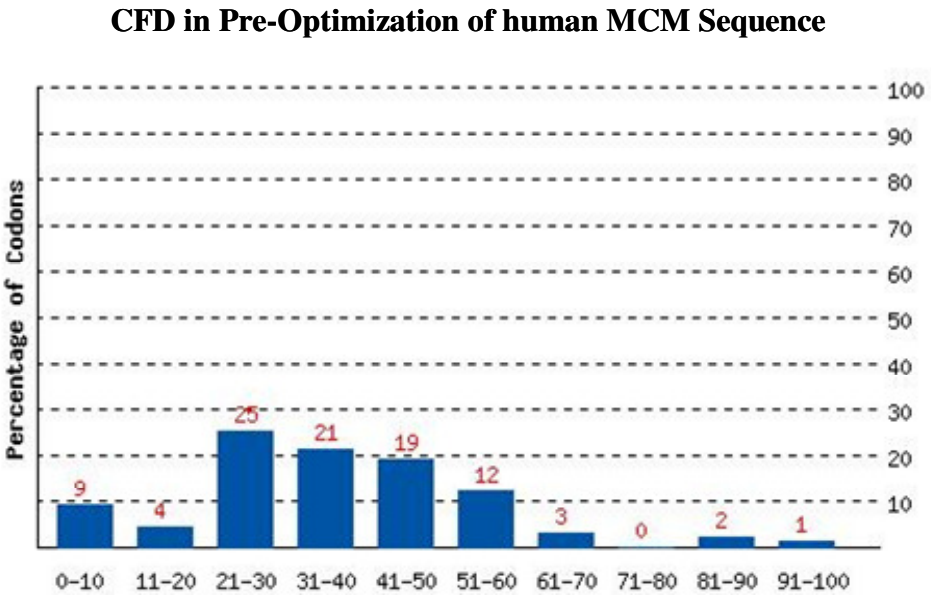

Appendix Figure II-3.1 The percentage distribution of codons in computed codon quality groups. The value of 100 is set for the codon with the highest usage frequency for a given amino acid in the mouse. Codons with values lower than 30 are likely to hamper the expression efficiency.

Appendix II-4 Analysis of Negative CIS Elements and Repeat Sequences

Negative CIS Elements	Negative Repeat Elements
8	23

Summary:

- Codon Adaptation Index (CAI) of the pre-optimization human MCM gene sequence is 0.74
- The GC content of the sequence is 42.03%.
- The percentage of low frequency (<30%) codons based on your target host organism is 38%. This un-optimized gene employs tandem rare codons that can reduce the efficiency of translation or even disengage the translational machinery.

Appendix III

Example of the analysis report on the post-optimization human MCM gene sequence

Codon Optimization Result 120 Centennial Ave Piscataway, NJ 08854, USA

(confidential) Tel: 1-877-436-7274

(1-877-GenScript) Tel: 1-732-885-9188, 1-732-357-3839

Fax: 1-7322-210-0262, 1-732-885-5878

Organism: Mouse;

Gene Name: Mutase

Sequence Type: aa

Optimization Region: 13 – 2256

GC Range: 30 – 70

Addition 5' Sequence: ATCGATACCACC

Addition 3' Sequence: TGAGCATATG

Genetic Code: 1

RE Sites and CIS Pattern:

ClaI(ATCGAT), NdeI(CATATG), EcoRI(GAATTC), BamHI(GGATCC),XbaI(TCTAGA), splice(GGTAAG),splice(GGTGAT),polya(AATAAA),polya(ATTAAA),destabilizing(ATTTA), polyt(TTTTTT),polya(AAAAAAA)

Basic Information	
Organism	Mouse
CDS length	2266

Appendix III-1 Codon Adaptation Index (CAI)

Mouse

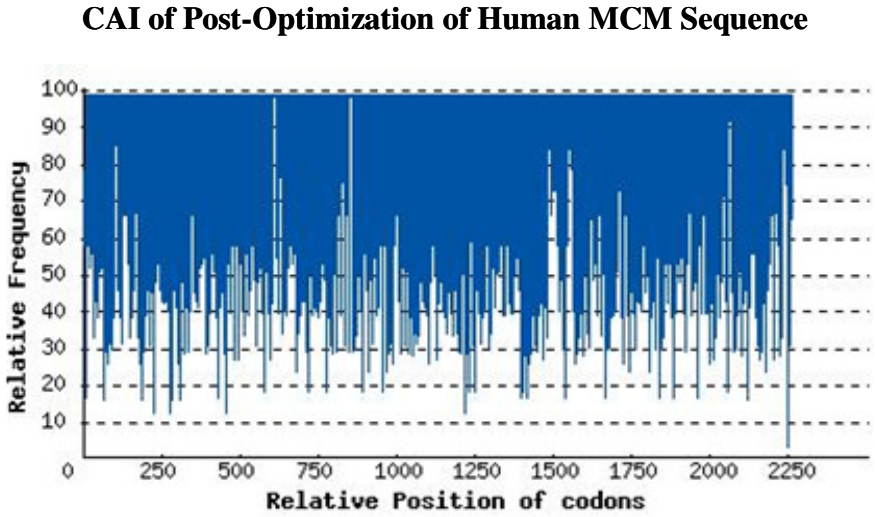

CAI : 0.81

Appendix Figure III-1.1 The distribution of codon usage frequency along the length of the post-optimization human MCM gene sequence to be expressed in mouse. Possibility of high protein expression level is correlated to the value of CAI - a CAI of 1.0 is considered to be ideal while a CAI of >0.8 is rated as good for expression in mouse.

Appendix III-2 GC Content Adjustment

GC Curve

GC Content in Post-Optimization Human MCM Gene Sequence

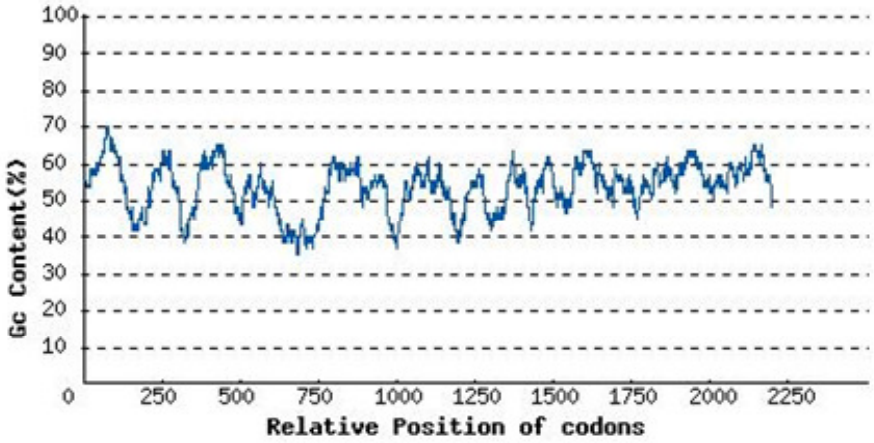

Average GC content : 53.27

Appendix Figure III-2.1 The ideal percentage range of GC content is between 30% to 70%. Any peaks outside of this range will adversely affect transcriptional and translational efficiency.

Appendix III-3 Codon Frequency Distribution (CFD)

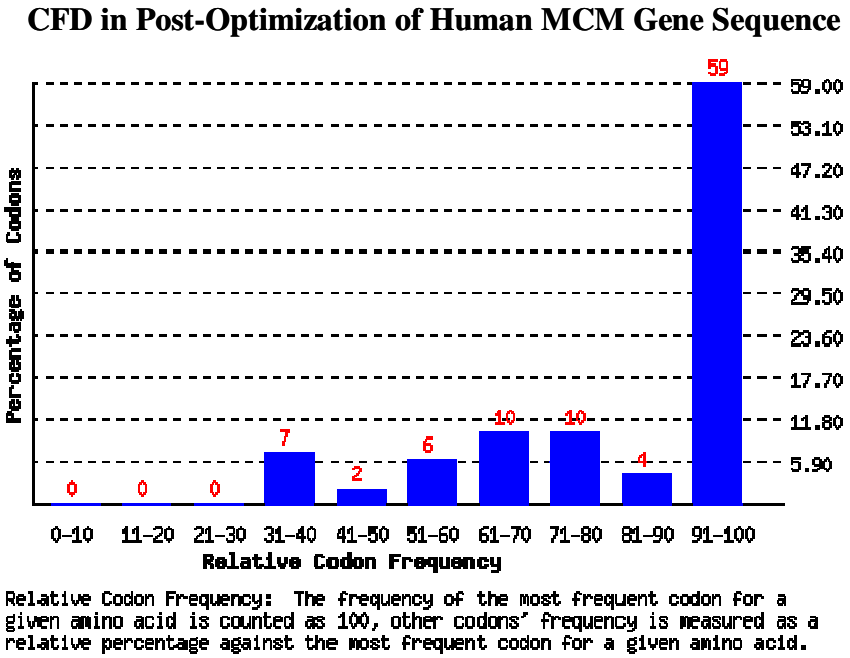

Appendix III-4 Analysis of Negative CIS Elements and Repeat Sequences

Negative CIS Elements	Negative Repeat Elements
0	12

Summary:

- Codon Adaptation Index (CAI) of the post-optimization human MCM gene sequence is 0.81
- The GC content of the sequence is 53.27%.
- The negative CIS elements and negative repeat elements had been reduced to 0 and 12 respectively.

Appendix IV

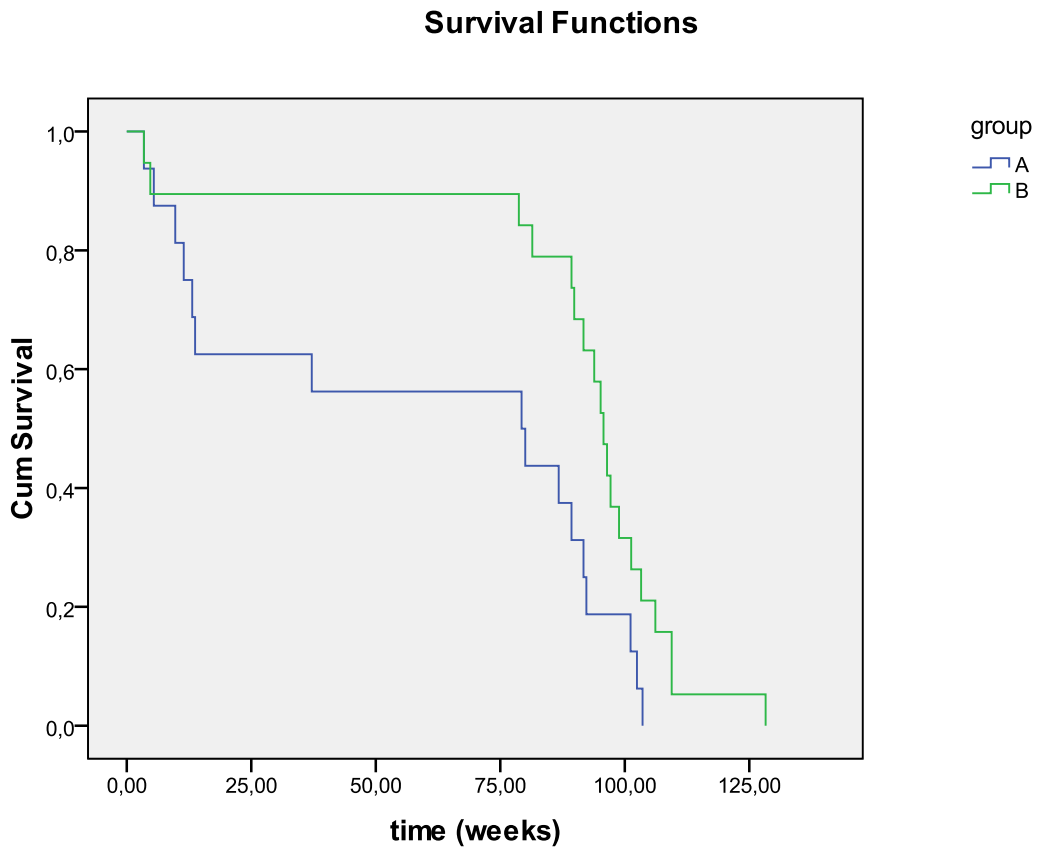

Appendix Figure IV-1 Survival Graph of mut -/- muth2 Mouse Model

This survival graph is provided by Dr. Heidi Peters (2012) [152]. This graph demonstrates the survival rate of the mut -/- muth2 animal model. Group A, which is indicated by the blue solid line, represents the mut -/- muth2 animal model. Group B, which is indicated by the green solid line, represents normal mice.

Appendix V

Appendix Figure V-1 This graph is cited from unpublished data produced by Chantelle McIntyre, in which the efficacy of intralipid in improving the transduction efficiency of LV was assessed. Mice were treated with intralipid, 40 μL/g, prior to the injection of 50 μg of p24 equivalent LV. A significant improvement ($p<0.05$, paired t-test) in gene transduction was observed in liver, spleen and lung of the animals pre-treated with intralipid.

BIBLIOGRAPHY

1. Horster, F. and G.F. Hoffmann, *Pathophysiology, diagnosis, and treatment of methylmalonic aciduria-recent advances and new challenges.* Pediatr Nephrol, 2004. **19**(10): p. 1071-4.

2. Cox, E.V. and A.M. White, *Methylmalonic acid excretion: an index of vitamin-B12 deficiency.* Lancet, 1962. **280**(7261): p. 853-6.

3. White, A.M. and E.V. Cox, *Methylmalonic Acid Excretion and Vitamin B12 Deficiency in the Human.* Ann N Y Acad Sci, 1964. **112**: p. 915-21.

4. Oberholzer, V.G., B. Levin, E.A. Burgess, and W.F. Young, *Methylmalonic aciduria. An inborn error of metabolism leading to chronic metabolic acidosis.* Arch Dis Child, 1967. **42**(225): p. 492-504.

5. Stokke, O., L. Eldjarn, K.R. Norum, J. Steen-johnsen, and S. Halvorsen, *Methylmalonic Acidemia a new inborn error of metabolism which may cause fatal acidosis in the neonatal period.* Scandinavian Journal of Clinical & Laboratory Investigation, 1967. **20**(4): p. 313-328.

6. Rosenberg, L.E., A. Lilljeqvist, and Y.E. Hsia, *Methylmalonic aciduria: metabolic block localization and vitamin B 12 dependency.* Science, 1968. **162**(3855): p. 805-7.

7. Mudd, S.H., H.L. Levy, R.H. Abeles, and J.P. Jennedy, Jr., *A derangement in B 12 metabolism leading to homocystinemia, cystathioninemia and methylmalonic aciduria.* Biochem Biophys Res Commun, 1969. **35**(1): p. 121-6.

8. Wilkemeyer, M.F., A.M. Crane, and F.D. Ledley, *Differential diagnosis of mut and cbl methylmalonic aciduria by DNA-mediated gene transfer in primary fibroblasts.* J Clin Invest, 1991. **87**(3): p. 915-8.

9. Fenton, W.A., A.M. Hack, D. Helfgott, and L.E. Rosenberg, *Biogenesis of the mitochondrial enzyme methylmalonyl-CoA mutase. Synthesis and processing of a precursor in a cell-free system and in cultured cells.* J Biol Chem, 1984. **259**(10): p. 6616-21.

10. Jansen, R., F. Kalousek, W.A. Fenton, L.E. Rosenberg, and F.D. Ledley, *Cloning of full-length methylmalonyl-CoA mutase from a cDNA library using the polymerase chain reaction.* Genomics, 1989. **4**(2): p. 198-205.

11. Isaya, G., F. Kalousek, W.A. Fenton, and L.E. Rosenberg, *Cleavage of precursors by the mitochondrial processing peptidase requires a compatible mature protein or an intermediate octapeptide.* J Cell Biol, 1991. **113**(1): p. 65-76.

12. Matouschek, A., N. Pfanner, and W. Voos, *Protein unfolding by mitochondria. The Hsp70 import motor.* EMBO Rep, 2000. **1**(5): p. 404-10.

13. Thoma, N.H. and P.F. Leadlay, *Homology modeling of human methylmalonyl-CoA mutase: a structural basis for point mutations causing methylmalonic aciduria.* Protein Sci, 1996. **5**(9): p. 1922-7.

14. Ledley, F.D., R. Jansen, S.U. Nham, W.A. Fenton, and L.E. Rosenberg, *Mutation eliminating mitochondrial leader sequence of methylmalonyl-CoA mutase causes muto methylmalonic acidemia.* Proc Natl Acad Sci U S A, 1990. **87**(8): p. 3147-50.

15. Raff, M.L., A.M. Crane, R. Jansen, F.D. Ledley, and D.S. Rosenblatt, *Genetic characterization of a MUT locus mutation discriminating heterogeneity in mut0 and mut- methylmalonic aciduria by interallelic complementation.* J Clin Invest, 1991. **87**(1): p. 203-7.

16. Jansen, R. and F.D. Ledley, *Heterozygous mutations at the mut locus in fibroblasts with mut0 methylmalonic acidemia identified by polymerase-chain-reaction cDNA cloning.* Am J Hum Genet, 1990. **47**(5): p. 808-14.

17. Qureshi, A.A., A.M. Crane, N.V. Matiaszuk, I. Rezvani, F.D. Ledley, and D.S. Rosenblatt, *Cloning and expression of mutations demonstrating intragenic complementation in mut0 methylmalonic aciduria.* J Clin Invest, 1994. **93**(4): p. 1812-9.

18. Crane, A.M., R. Jansen, E.R. Andrews, and F.D. Ledley, *Cloning and expression of a mutant methylmalonyl coenzyme A mutase with altered cobalamin affinity that causes mut- methylmalonic aciduria.* J Clin Invest, 1992. **89**(2): p. 385-91.

19. Crane, A.M. and F.D. Ledley, *Clustering of mutations in methylmalonyl CoA mutase associated with mut- methylmalonic acidemia.* Am J Hum Genet, 1994. **55**(1): p. 42-50.

20. Coulombe, J.T., V.E. Shih, and H.L. Levy, *Massachusetts Metabolic Disorders Screening Program. II. Methylmalonic aciduria.* Pediatrics, 1981. **67**(1): p. 26-31.

21. Sniderman, L.C., M. Lambert, R. Giguere, C. Auray-Blais, B. Lemieux, R. Laframboise, D.S. Rosenblatt, and E.P. Treacy, *Outcome of individuals with low-moderate methylmalonic aciduria detected through a neonatal screening program.* J Pediatr, 1999. **134**(6): p. 675-80.

22. Chace, D.H., J.C. DiPerna, T.A. Kalas, R.W. Johnson, and E.W. Naylor, *Rapid diagnosis of methylmalonic and propionic acidemias: quantitative tandem mass spectrometric analysis of propionylcarnitine in filter-paper blood specimens obtained from newborns.* Clin Chem, 2001. **47**(11): p. 2040-4.

23. Shigematsu, Y., S. Hirano, I. Hata, Y. Tanaka, M. Sudo, N. Sakura, T. Tajima, and S. Yamaguchi, *Newborn mass screening and selective screening using electrospray tandem mass spectrometry in Japan.* J Chromatogr B Analyt Technol Biomed Life Sci, 2002. **776**(1): p. 39-48.

24. Deodato, F., S. Boenzi, F.M. Santorelli, and C. Dionisi-Vici, *Methylmalonic and propionic aciduria.* Am J Med Genet C Semin Med Genet, 2006. **142C**(2): p. 104-12.

25. Matsui, S.M., M.J. Mahoney, and L.E. Rosenberg, *The natural history of the inherited methylmalonic acidemias.* N Engl J Med, 1983. **308**(15): p. 857-61.

26. Zschocke, J. and G.F. Hoffman, *Vademecum Metabolicum : Diagnosis and Treatment of Inborn Errors of Metabolism*. 2011, Schattauer GmbH.

27. Nicolaides, P., J. Leonard, and R. Surtees, *Neurological outcome of methylmalonic acidaemia.* Arch Dis Child, 1998. **78**(6): p. 508-12.

28. Baumgarter, E.R. and C. Viardot, *Long-term follow-up of 77 patients with isolated methylmalonic acidaemia.* J Inherit Metab Dis, 1995. **18**(2): p. 138-42.

29. Massoud, A.F. and J.V. Leonard, *Cardiomyopathy in propionic acidaemia.* Eur J Pediatr, 1993. **152**(5): p. 441-5.

30. Kahler, S.G., W.G. Sherwood, D. Woolf, S.T. Lawless, A. Zaritsky, J. Bonham, C.J. Taylor, J.T. Clarke, P. Durie, and J.V. Leonard, *Pancreatitis in patients with organic acidemias.* J Pediatr, 1994. **124**(2): p. 239-43.

31. Wajner, M., A. Latini, A.T. Wyse, and C.S. Dutra-Filho, *The role of oxidative damage in the neuropathology of organic acidurias: insights from animal studies.* J Inherit Metab Dis, 2004. **27**(4): p. 427-48.

32. Kolker, S., M. Schwab, F. Horster, S. Sauer, A. Hinz, N.I. Wolf, E. Mayatepek, G.F. Hoffmann, J.A. Smeitink, and J.G. Okun, *Methylmalonic acid, a biochemical hallmark of methylmalonic acidurias but no inhibitor of mitochondrial respiratory chain.* J Biol Chem, 2003. **278**(48): p. 47388-93.

33. Wajner, M. and J.C. Coelho, *Neurological dysfunction in methylmalonic acidaemia is probably related to the inhibitory effect of methylmalonate on brain energy production.* J Inherit Metab Dis, 1997. **20**(6): p. 761-8.

34. Brusque, A.M., R. Borba Rosa, P.F. Schuck, K.B. Dalcin, C.A. Ribeiro, C.G. Silva, C.M. Wannmacher, C.S. Dutra-Filho, A.T. Wyse, P. Briones, and M. Wajner, *Inhibition of the mitochondrial respiratory chain complex activities in rat cerebral cortex by methylmalonic acid.* Neurochem Int, 2002. **40**(7): p. 593-601.

35. Maciel, E.N., A.J. Kowaltowski, F.D. Schwalm, J.M. Rodrigues, D.O. Souza, A.E. Vercesi, M. Wajner, and R.F. Castilho, *Mitochondrial permeability transition in neuronal damage promoted by Ca2+ and respiratory chain complex II inhibition.* J Neurochem, 2004. **90**(5): p. 1025-35.

36. Schuck, P.F., R.B. Rosa, L.F. Pettenuzzo, A. Sitta, C.M. Wannmacher, A.T. Wyse, and M. Wajner, *Inhibition of mitochondrial creatine kinase activity from rat cerebral cortex by methylmalonic acid.* Neurochem Int, 2004. **45**(5): p. 661-7.

37. Pettenuzzo, L.F., C. Ferreira Gda, A.L. Schmidt, C.S. Dutra-Filho, A.T. Wyse, and M. Wajner, *Differential inhibitory effects of methylmalonic acid on respiratory chain complex activities in rat tissues.* Int J Dev Neurosci, 2006. **24**(1): p. 45-52.

38. Mirandola, S.R., D.R. Melo, P.F. Schuck, G.C. Ferreira, M. Wajner, and R.F. Castilho, *Methylmalonate inhibits succinate-supported oxygen consumption by interfering with mitochondrial succinate uptake.* J Inherit Metab Dis, 2008. **31**(1): p. 44-54.

39. Morath, M.A., J.G. Okun, I.B. Muller, S.W. Sauer, F. Horster, G.F. Hoffmann, and S. Kolker, *Neurodegeneration and chronic renal failure in methylmalonic aciduria--a pathophysiological approach.* J Inherit Metab Dis, 2008. **31**(1): p. 35-43.

40. Melo, D.R., A.J. Kowaltowski, M. Wajner, and R.F. Castilho, *Mitochondrial energy metabolism in neurodegeneration associated with methylmalonic acidemia.* J Bioenerg Biomembr, 2011. **43**(1): p. 39-46.

41. Okun, J.G., S. Kolker, A. Schulze, D. Kohlmuller, K. Olgemoller, M. Lindner, G.F. Hoffmann, R.J. Wanders, and E. Mayatepek, *A method for quantitative acylcarnitine profiling in human skin fibroblasts using unlabelled palmitic acid: diagnosis of fatty acid oxidation disorders and differentiation between biochemical phenotypes of MCAD deficiency.* Biochim Biophys Acta, 2002. **1584**(2-3): p. 91-8.

42. Kolker, S., S.W. Sauer, R.A. Surtees, and J.V. Leonard, *The aetiology of neurological complications of organic acidaemias--a role for the blood-brain barrier.* J Inherit Metab Dis, 2006. **29**(6): p. 701-4; discussion 705-6.

43. Lash, L.H., *Mitochondrial glutathione transport: physiological, pathological and toxicological implications.* Chem Biol Interact, 2006. **163**(1-2): p. 54-67.

44. McLaughlin, B.A., D. Nelson, I.A. Silver, M. Erecinska, and M.F. Chesselet, *Methylmalonate toxicity in primary neuronal cultures.* Neuroscience, 1998. **86**(1): p. 279-90.

45. Kowaltowski, A.J., R.F. Castilho, and A.E. Vercesi, *Mitochondrial permeability transition and oxidative stress.* FEBS Lett, 2001. **495**(1-2): p. 12-5.

46. Rutledge, S.L., M. Geraghty, E. Mroczek, D. Rosenblatt, and E. Kohout, *Tubulointerstitial nephritis in methylmalonic acidemia.* Pediatr Nephrol, 1993. **7**(1): p. 81-2.

47. Kashtan, C.E., M. Abousedira, S. Rozen, J.C. Manivel, M. McCann, and M. Tuchman, *Chronic Administration of Methylmalonic Acid (MMA) to Rats Causes Proteinuria and Renal Tubular Injury [bull] 1815.* Pediatr Res, 1998. **43**(S4): p. 309-309.

48. Shikano, N., S. Nakajima, T. Kotani, Y. Itoh, R. Nishii, M. Yoshimoto, L.G. Flores, 2nd, H. Saji, N. Ishikawa, and K. Kawai, *Detection of maleate-induced Fanconi syndrome by decreasing accumulation of 125I-3-iodo-alpha-methyl-L-tyrosine in the proximal tubule segment-1 region of renal cortex in mice: a trial of separate evaluation of reabsorption.* Ann Nucl Med, 2006. **20**(3): p. 175-81.

49. Arend, L.J., C.I. Thompson, M.A. Brandt, and W.S. Spielman, *Elevation of intrarenal adenosine by maleic acid decreases GFR and renin release.* Kidney Int, 1986. **30**(5): p. 656-61.

50. D'Angio, C.T., M.J. Dillon, and J.V. Leonard, *Renal tubular dysfunction in methylmalonic acidaemia.* Eur J Pediatr, 1991. **150**(4): p. 259-63.

51. Walter, J.H., A. Michalski, W.M. Wilson, J.V. Leonard, T.M. Barratt, and M.J. Dillon, *Chronic renal failure in methylmalonic acidaemia.* Eur J Pediatr, 1989. **148**(4): p. 344-8.

52. Pajor, A.M., *Molecular properties of sodium/dicarboxylate cotransporters.* J Membr Biol, 2000. **175**(1): p. 1-8.

53. Chen, Z. and L.H. Lash, *Evidence for mitochondrial uptake of glutathione by dicarboxylate and 2-oxoglutarate carriers.* J Pharmacol Exp Ther, 1998. **285**(2): p. 608-18.

54. de Keyzer, Y., V. Valayannopoulos, J.F. Benoist, F. Batteux, F. Lacaille, L. Hubert, D. Chretien, B. Chadefeaux-Vekemans, P. Niaudet, G. Touati, A. Munnich, and P. de Lonlay, *Multiple OXPHOS deficiency in the liver, kidney, heart, and skeletal muscle of patients with methylmalonic aciduria and propionic aciduria.* Pediatr Res, 2009. **66**(1): p. 91-5.

55. Burckhardt, B.C. and G. Burckhardt, *Transport of organic anions across the basolateral membrane of proximal tubule cells.* Rev Physiol Biochem Pharmacol, 2003. **146**: p. 95-158.

56. Sauer, S.W., S. Opp, A. Haarmann, J.G. Okun, S. Kolker, and M.A. Morath, *Long-term exposure of human proximal tubule cells to hydroxycobalamin[c-lactam] as a possible model to study renal disease in methylmalonic acidurias.* J Inherit Metab Dis, 2009. **32**(6): p. 720-7.

57. Prada, C.E., F. Al Jasmi, E.P. Kirk, M. Hopp, O. Jones, N.D. Leslie, and T.A. Burrow, *Cardiac disease in methylmalonic acidemia.* J Pediatr, 2011. **159**(5): p. 862-4.

58. Akar, F.G., D.D. Spragg, R.S. Tunin, D.A. Kass, and G.F. Tomaselli, *Mechanisms underlying conduction slowing and arrhythmogenesis in nonischemic dilated cardiomyopathy.* Circ Res, 2004. **95**(7): p. 717-25.

59. Akar, F.G., R.D. Nass, S. Hahn, E. Cingolani, M. Shah, G.G. Hesketh, D. DiSilvestre, R.S. Tunin, D.A. Kass, and G.F. Tomaselli, *Dynamic changes in conduction velocity and gap junction properties during development of pacing-induced heart failure.* Am J Physiol Heart Circ Physiol, 2007. **293**(2): p. H1223-30.

60. Furchgott, R.F. and K.S. Lee, *High energy phosphates and the force of contraction of cardiac muscle.* Circulation, 1961. **24**: p. 416-32.

61. Lindenmayer, G.E., L.A. Sordahl, and A. Schwartz, *Reevaluation of oxidative phosphorylation in cardiac mitochondria from normal animals and animals in heart failure.* Circ Res, 1968. **23**(3): p. 439-50.

62. Schlattner, U., M. Tokarska-Schlattner, and T. Wallimann, *Mitochondrial creatine kinase in human health and disease.* Biochim Biophys Acta, 2006. **1762**(2): p. 164-80.

63. Bolli, R., B.S. Patel, M.O. Jeroudi, E.K. Lai, and P.B. McCay, *Demonstration of free radical generation in "stunned" myocardium of intact dogs with the use of the spin trap alpha-phenyl N-tert-butyl nitrone.* J Clin Invest, 1988. **82**(2): p. 476-85.

64. Bolli, R. and E. Marban, *Molecular and cellular mechanisms of myocardial stunning.* Physiol Rev, 1999. **79**(2): p. 609-34.

65. Cortassa, S., M.A. Aon, R.L. Winslow, and B. O'Rourke, *A mitochondrial oscillator dependent on reactive oxygen species.* Biophys J, 2004. **87**(3): p. 2060-73.

66. Werns, S.W., J.C. Fantone, A. Ventura, and B.R. Lucchesi, *Myocardial glutathione depletion impairs recovery of isolated blood-perfused hearts after global ischaemia.* J Mol Cell Cardiol, 1992. **24**(11): p. 1215-20.

67. Ceconi, C., S. Curello, A. Cargnoni, R. Ferrari, A. Albertini, and O. Visioli, *The role of glutathione status in the protection against ischaemic and reperfusion damage: effects of N-acetyl cysteine.* J Mol Cell Cardiol, 1988. **20**(1): p. 5-13.

68. Damy, T., M. Kirsch, L. Khouzami, P. Caramelle, P. Le Corvoisier, F. Roudot-Thoraval, J.L. Dubois-Rande, L. Hittinger, C. Pavoine, and F. Pecker, *Glutathione deficiency in cardiac patients is related to the functional status and structural cardiac abnormalities.* PLoS One, 2009. **4**(3): p. e4871.

69. Kasumov, T., A.V. Cendrowski, F. David, K.A. Jobbins, V.E. Anderson, and H. Brunengraber, *Mass isotopomer study of anaplerosis from propionate in the perfused rat heart.* Arch Biochem Biophys, 2007. **463**(1): p. 110-7.

70. Russell, R.R., 3rd, J.I. Mommessin, and H. Taegtmeyer, *Propionyl-L-carnitine-mediated improvement in contractile function of rat hearts oxidizing acetoacetate.* Am J Physiol, 1995. **268**(1 Pt 2): p. H441-7.

71. Laurita, K.R. and D.S. Rosenbaum, *Mechanisms and potential therapeutic targets for ventricular arrhythmias associated with impaired cardiac calcium cycling.* J Mol Cell Cardiol, 2008. **44**(1): p. 31-43.

72. Marquard, J., T. El Scheich, D. Klee, M. Schmitt, T. Meissner, E. Mayatepek, and J. Oh, *Chronic pancreatitis in branched-chain organic acidurias--a case of methylmalonic aciduria and an overview of the literature.* Eur J Pediatr, 2011. **170**(2): p. 241-5.

73. Burlina, A.B., C. Dionisi-Vici, S. Piovan, I. Saponara, A. Bartuli, G. Sabetta, and F. Zacchello, *Acute pancreatitis in propionic acidaemia.* J Inherit Metab Dis, 1995. **18**(2): p. 169-172.

74. Wilson, W.G., S.M. Audenaert, and E.J. Squillaro, *Hyperammonaemia in a preterm infant with isovaleric acidaemia.* J Inherit Metab Dis, 1984. **7**(2): p. 71.

75. Bhoomagoud, M., T. Jung, J. Atladottir, T.R. Kolodecik, C. Shugrue, A. Chaudhuri, E.C. Thrower, and F.S. Gorelick, *Reducing extracellular pH sensitizes the acinar cell to secretagogue-induced pancreatitis responses in rats.* Gastroenterology, 2009. **137**(3): p. 1083-92.

76. Kao, C.H., M.Y. Liu, T.T. Liu, K.J. Hsiao, K.H. Cheng, C.H. Huang, H.Y. Lin, and D.M. Niu, *Growth hormone therapy in neonatal patients with methylmalonic acidemia.* J Chin Med Assoc, 2009. **72**(9): p. 462-7.

77. Wasserstein, M.P., S. Gaddipati, S.E. Snyderman, K. Eddleman, R.J. Desnick, and C. Sansaricq, *Successful pregnancy in severe methylmalonic acidaemia.* J Inherit Metab Dis, 1999. **22**(7): p. 788-94.

78. la Marca, G., S. Malvagia, E. Pasquini, M. Innocenti, M.A. Donati, and E. Zammarchi, *Rapid 2nd-tier test for measurement of 3-OH-propionic and methylmalonic acids on dried blood spots: reducing the false-positive rate for*

propionylcarnitine during expanded newborn screening by liquid chromatography-tandem mass spectrometry. Clin Chem, 2007. **53**(7): p. 1364-9.

79. Morrow, G., 3rd, B. Revsin, C. Mathews, and H. Giles, *A simple, rapid method for prenatal detection of defects in propionate metabolism.* Clin Genet, 1976. **10**(4): p. 218-21.

80. Fowler, B., J.V. Leonard, and M.R. Baumgartner, *Causes of and diagnostic approach to methylmalonic acidurias.* J Inherit Metab Dis, 2008. **31**(3): p. 350-60.

81. Manoli, I. and C.P. Venditti, *Methylmalonic Acidemia*, B.T. In: Pagon RA, Dolan CR, Stephens K, Adam MP. , Editor. 1993, GeneReviews™ [Internet]. Seattle (WA): University of Washington, Seattle; 1993-.

82. Lempp, T.J., T. Suormala, R. Siegenthaler, E.R. Baumgartner, B. Fowler, B. Steinmann, and M.R. Baumgartner, *Mutation and biochemical analysis of 19 probands with mut0 and 13 with mut- methylmalonic aciduria: identification of seven novel mutations.* Mol Genet Metab, 2007. **90**(3): p. 284-90.

83. Ampola, M.G., M.J. Mahoney, E. Nakamura, and K. Tanaka, *Prenatal therapy of a patient with vitamin-B12-responsive methylmalonic acidemia.* N Engl J Med, 1975. **293**(7): p. 313-7.

84. Fenton, W.A., R.A. Gravel, and D.S. Rosenblatt, *Disorders of Propionate and Methylmalonate Metabolism*, in *The metabolic and Molecular Basis of Inherited Disease*, In: Scriver C, Beaudet A, Sly W, and Valle D, Editors. 2001, McGraw Hill, New York. p. 2165-2193.

85. Worthen, H.G., A. al Ashwal, P.T. Ozand, S. Garawi, Z. Rahbeeni, A. al Odaib, S.B. Subramanyam, and M. Rashed, *Comparative frequency and severity of hypoglycemia in selected organic acidemias, branched chain amino acidemia, and disorders of fructose metabolism.* Brain Dev, 1994. **16 Suppl**: p. 81-5.

86. Zechner, R., J.G. Strauss, G. Haemmerle, A. Lass, and R. Zimmermann, *Lipolysis: pathway under construction.* Curr Opin Lipidol, 2005. **16**(3): p. 333-40.

87. Levrat, V., I. Forest, A. Fouilhoux, C. Acquaviva, C. Vianey-Saban, and N. Guffon, *Carglumic acid: an additional therapy in the treatment of organic acidurias with hyperammonemia?* Orphanet J Rare Dis, 2008. **3**: p. 2.

88. Shevell, M.I., N. Matiaszuk, F.D. Ledley, and D.S. Rosenblatt, *Varying neurological phenotypes among muto and mut- patients with methylmalonylCoA mutase deficiency.* Am J Med Genet, 1993. **45**(5): p. 619-24.

89. Diss, E., J. Iams, N. Reed, D.S. Roe, and C. Roe, *Methylmalonic aciduria in pregnancy: a case report.* Am J Obstet Gynecol, 1995. **172**(3): p. 1057-9.

90. Deodato, F., C. Rizzo, S. Boenzi, F. Baiocco, G. Sabetta, and C. Dionisi-Vici, *Successful pregnancy in a woman with mut- methylmalonic acidaemia.* J Inherit Metab Dis, 2002. **25**(2): p. 133-4.

91. Roe, C.R., C.L. Hoppel, T.E. Stacey, R.A. Chalmers, B.M. Tracey, and D.S. Millington, *Metabolic response to carnitine in methylmalonic aciduria. An effective strategy for elimination of propionyl groups.* Arch Dis Child, 1983. **58**(11): p. 916-20.

92. Winter, S., L. Birek, T. Walker, J. Phalin-Roque, M.J. Chandler, C. Field, and E. Zorn, *Therapy of metabolic disorders with intravenous (IV) access ports and long term intravenous L-carnitine therapy.* Southeast Asian J Trop Med Public Health, 1999. **30 Suppl 2**: p. 152-3.

93. Sears, C.L., *A dynamic partnership: celebrating our gut flora.* Anaerobe, 2005. **11**(5): p. 247-51.

94. Mellon, A.F., S.A. Deshpande, J.C. Mathers, and K. Bartlett, *Effect of oral antibiotics on intestinal production of propionic acid.* Arch Dis Child, 2000. **82**(2): p. 169-72.

95. Gibson, G.R., *Fibre and effects on probiotics (the prebiotic concept).* Clinical Nutrition Supplements, 2004. **1**(2): p. 25-31.

96. Beaugerie, L. and J.C. Petit, *Microbial-gut interactions in health and disease. Antibiotic-associated diarrhoea.* Best Pract Res Clin Gastroenterol, 2004. **18**(2): p. 337-52.

97. Snyderman, S.E., C. Sansaricq, P. Norton, and S.V. Phansalkar, *The use of neomycin in the treatment of methylmalonic aciduria.* Pediatrics, 1972. **50**(6): p. 925-7.

98. Treacy, E., L. Arbour, P. Chessex, G. Graham, L. Kasprzak, K. Casey, L. Bell, O. Mamer, and C.R. Scriver, *Glutathione deficiency as a complication of methylmalonic acidemia: response to high doses of ascorbate.* J Pediatr, 1996. **129**(3): p. 445-8.

99. Pinar-Sueiro, S., R. Martinez-Fernandez, S. Lage-Medina, L. Aldamiz-Echevarria, and E. Vecino, *Optic neuropathy in methylmalonic acidemia: the role of neuroprotection.* J Inherit Metab Dis, 2010.

100. Coude, F.X., L. Sweetman, and W.L. Nyhan, *Inhibition by propionyl-coenzyme A of N-acetylglutamate synthetase in rat liver mitochondria. A possible explanation for hyperammonemia in propionic and methylmalonic acidemia.* J Clin Invest, 1979. **64**(6): p. 1544-51.

101. Chandler, R.J., P.M. Zerfas, S. Shanske, J. Sloan, V. Hoffmann, S. DiMauro, and C.P. Venditti, *Mitochondrial dysfunction in mut methylmalonic acidemia.* Faseb J, 2009. **23**(4): p. 1252-61.

102. Mc Guire, P.J., E. Lim-Melia, G.A. Diaz, K. Raymond, A. Larkin, M.P. Wasserstein, and C. Sansaricq, *Combined liver-kidney transplant for the management of methylmalonic aciduria: a case report and review of the literature.* Mol Genet Metab, 2008. **93**(1): p. 22-9.

103. Kaplan, P., C. Ficicioglu, A.T. Mazur, M.J. Palmieri, and G.T. Berry, *Liver transplantation is not curative for methylmalonic acidopathy caused by methylmalonyl-CoA mutase deficiency.* Mol Genet Metab, 2006. **88**(4): p. 322-6.

104. Kasahara, M., R. Horikawa, M. Tagawa, S. Uemoto, S. Yokoyama, Y. Shibata, T. Kawano, T. Kuroda, T. Honna, K. Tanaka, and M. Saeki, *Current role of liver*

transplantation for methylmalonic acidemia: a review of the literature. Pediatr Transplant, 2006. **10**(8): p. 943-7.

105. Chakrapani, A., P. Sivakumar, P.J. McKiernan, and J.V. Leonard, *Metabolic stroke in methylmalonic acidemia five years after liver transplantation.* J Pediatr, 2002. **140**(2): p. 261-3.

106. Nagarajan, S., G.M. Enns, M.T. Millan, S. Winter, and M.M. Sarwal, *Management of methylmalonic acidaemia by combined liver-kidney transplantation.* J Inherit Metab Dis, 2005. **28**(4): p. 517-24.

107. Robbins, P.D. and S.C. Ghivizzani, *Viral vectors for gene therapy.* Pharmacol Ther, 1998. **80**(1): p. 35-47.

108. Ledley, F.D., *Gene therapy in pediatric medicine.* Adv Pediatr, 1996. **43**: p. 1-25.

109. Mulligan, R.C., *The basic science of gene therapy.* Science, 1993. **260**(5110): p. 926-32.

110. Anson, D.S. and J.M. Fletcher, *Gene therapy for disorders affecting children, progress and potential.* J Paediatr Child Health, 2007. **43**(5): p. 323-30.

111. Cavazzana-Calvo, M. and A. Fischer, *Efficacy of gene therapy for SCID is being confirmed.* Lancet, 2004. **364**(9452): p. 2155-6.

112. Hacein-Bey-Abina, S., A. Garrigue, G.P. Wang, J. Soulier, A. Lim, E. Morillon, E. Clappier, L. Caccavelli, E. Delabesse, K. Beldjord, V. Asnafi, E. MacIntyre, L. Dal Cortivo, I. Radford, N. Brousse, F. Sigaux, D. Moshous, J. Hauer, A. Borkhardt, B.H. Belohradsky, U. Wintergerst, M.C. Velez, L. Leiva, R. Sorensen, N. Wulffraat, S. Blanche, F.D. Bushman, A. Fischer, and M. Cavazzana-Calvo, *Insertional oncogenesis in 4 patients after retrovirus-mediated gene therapy of SCID-X1.* J Clin Invest, 2008. **118**(9): p. 3132-42.

113. Engelhardt, J.F., Y. Yang, L.D. Stratford-Perricaudet, E.D. Allen, K. Kozarsky, M. Perricaudet, J.R. Yankaskas, and J.M. Wilson, *Direct gene transfer of human CFTR into human bronchial epithelia of xenografts with E1-deleted adenoviruses.* Nat Genet, 1993. **4**(1): p. 27-34.

114. Wilson, J.M., J.F. Engelhardt, M. Grossman, R.H. Simon, and Y. Yang, *Gene therapy of cystic fibrosis lung disease using E1 deleted adenoviruses: a phase I trial.* Hum Gene Ther, 1994. **5**(4): p. 501-19.

115. Carter, B.J. and T.R. Flotte, *Development of adeno-associated virus vectors for gene therapy of cystic fibrosis.* Curr Top Microbiol Immunol, 1996. **218**: p. 119-44.

116. Koehler, D.R., H. Frndova, K. Leung, E. Louca, D. Palmer, P. Ng, C. McKerlie, P. Cox, A.L. Coates, and J. Hu, *Aerosol delivery of an enhanced helper-dependent adenovirus formulation to rabbit lung using an intratracheal catheter.* J Gene Med, 2005. **7**(11): p. 1409-20.

117. Koehler, D.R., B. Martin, M. Corey, D. Palmer, P. Ng, A.K. Tanswell, and J. Hu, *Readministration of helper-dependent adenovirus to mouse lung.* Gene Ther, 2006. **13**(9): p. 773-80.

118. Cmielewski, P., D.S. Anson, and D.W. Parsons, *Lysophosphatidylcholine as an adjuvant for lentiviral vector mediated gene transfer to airway epithelium: effect of acyl chain length.* Respir Res, 2010. **11**: p. 84.

119. Limberis, M., D.S. Anson, M. Fuller, and D.W. Parsons, *Recovery of airway cystic fibrosis transmembrane conductance regulator function in mice with cystic fibrosis after single-dose lentivirus-mediated gene transfer.* Hum Gene Ther, 2002. **13**(16): p. 1961-70.

120. Kremer, K.L., K.R. Dunning, D.W. Parsons, and D.S. Anson, *Gene delivery to airway epithelial cells in vivo: a direct comparison of apical and basolateral transduction strategies using pseudotyped lentivirus vectors.* J Gene Med, 2007. **9**(5): p. 362-8.

121. Chandler, R.J. and C.P. Venditti, *Long-term rescue of a lethal murine model of methylmalonic acidemia using adeno-associated viral gene therapy.* Mol Ther, 2010. **18**(1): p. 11-6.

122. Yei, S., N. Mittereder, S. Wert, J.A. Whitsett, R.W. Wilmott, and B.C. Trapnell, *In vivo evaluation of the safety of adenovirus-mediated transfer of the human cystic fibrosis transmembrane conductance regulator cDNA to the lung.* Hum Gene Ther, 1994. **5**(6): p. 731-44.

123. Eissa, N.T., C.S. Chu, C. Danel, and R.G. Crystal, *Evaluation of the respiratory epithelium of normals and individuals with cystic fibrosis for the presence of adenovirus E1a sequences relevant to the use of E1a- adenovirus vectors for gene therapy for the respiratory manifestations of cystic fibrosis.* Hum Gene Ther, 1994. **5**(9): p. 1105-14.

124. Zhao, M., S.W. Xiao, J.X. Yang, S.W. Zhang, and Y.Y. Lu, *Detection of p53 gene change and serum antibody level in phase II clinical trial of ad p53 gene therapy.* Zhonghua Yi Xue Za Zhi, 2005. **85**(49): p. 3495-8.

125. Shi, J. and D. Zheng, *An update on gene therapy in China.* Curr Opin Mol Ther, 2009. **11**(5): p. 547-53.

126. Aguilar, L.K., B.W. Guzik, and E. Aguilar-Cordova, *Cytotoxic immunotherapy strategies for cancer: mechanisms and clinical development.* J Cell Biochem, 2011. **112**(8): p. 1969-77.

127. Fukazawa, T., J. Matsuoka, T. Yamatsuji, Y. Maeda, M.L. Durbin, and Y. Naomoto, *Adenovirus-mediated cancer gene therapy and virotherapy (Review).* Int J Mol Med, 2010. **25**(1): p. 3-10.

128. Anson, D.S., *The use of retroviral vectors for gene therapy-what are the risks? A review of retroviral pathogenesis and its relevance to retroviral vector-mediated gene delivery.* Genet Vaccines Ther, 2004. **2**(1): p. 9.

129. Follenzi, A. and S. Gupta, *The promise of lentiviral gene therapy for liver cancer.* J Hepatol, 2004. **40**(2): p. 337-40.

130. Beagles, K.E., L. Peterson, X. Zhang, J. Morris, and H.P. Kiem, *Cyclosporine inhibits the development of green fluorescent protein (GFP)-specific immune responses after*

transplantation of GFP-expressing hematopoietic repopulating cells in dogs. Hum Gene Ther, 2005. **16**(6): p. 725-33.

131. Baekelandt, V., K. Eggermont, M. Michiels, B. Nuttin, and Z. Debyser, *Optimized lentiviral vector production and purification procedure prevents immune response after transduction of mouse brain.* Gene Ther, 2003. **10**(23): p. 1933-40.

132. Edidin, M., *The state of lipid rafts: from model membranes to cells.* Annu Rev Biophys Biomol Struct, 2003. **32**: p. 257-83.

133. Horejsi, V., *The roles of membrane microdomains (rafts) in T cell activation.* Immunol Rev, 2003. **191**: p. 148-64.

134. Le Doux, J.M., J.R. Morgan, R.G. Snow, and M.L. Yarmush, *Proteoglycans secreted by packaging cell lines inhibit retrovirus infection.* J Virol, 1996. **70**(9): p. 6468-73.

135. Le Doux, J.M., J.R. Morgan, and M.L. Yarmush, *Removal of proteoglycans increases efficiency of retroviral gene transfer.* Biotechnol Bioeng, 1998. **58**(1): p. 23-34.

136. Slingsby, J.H., D. Baban, J. Sutton, M. Esapa, T. Price, S.M. Kingsman, A.J. Kingsman, and A. Slade, *Analysis of 4070A envelope levels in retroviral preparations and effect on target cell transduction efficiency.* Hum Gene Ther, 2000. **11**(10): p. 1439-51.

137. Segura, M.M., A. Garnier, Y. Durocher, H. Coelho, and A. Kamen, *Production of lentiviral vectors by large-scale transient transfection of suspension cultures and affinity chromatography purification.* Biotechnol Bioeng, 2007. **98**(4): p. 789-99.

138. Smith, S.L. and T. Shioda, *Advantages of COS-1 monkey kidney epithelial cells as packaging host for small-volume production of high-quality recombinant lentiviruses.* J Virol Methods, 2009. **157**(1): p. 47-54.

139. Sinn, P.L., E.R. Burnight, M.A. Hickey, G.W. Blissard, and P.B. McCray, Jr., *Persistent gene expression in mouse nasal epithelia following feline immunodeficiency virus-based vector gene transfer.* J Virol, 2005. **79**(20): p. 12818-27.

140. Sinn, P.L., J.D. Goreham-Voss, A.C. Arias, M.A. Hickey, W. Maury, C.P. Chikkanna-Gowda, and P.B. McCray, Jr., *Enhanced gene expression conferred by stepwise modification of a nonprimate lentiviral vector.* Hum Gene Ther, 2007. **18**(12): p. 1244-52.

141. Sinn, P.L., A.C. Arias, K.A. Brogden, and P.B. McCray, Jr., *Lentivirus vector can be readministered to nasal epithelia without blocking immune responses.* J Virol, 2008. **82**(21): p. 10684-92.

142. Pichlmair, A., S.S. Diebold, S. Gschmeissner, Y. Takeuchi, Y. Ikeda, M.K. Collins, and C. Reis e Sousa, *Tubulovesicular structures within vesicular stomatitis virus G protein-pseudotyped lentiviral vector preparations carry DNA and stimulate antiviral responses via Toll-like receptor 9.* J Virol, 2007. **81**(2): p. 539-47.

143. Follenzi, A., G. Sabatino, A. Lombardo, C. Boccaccio, and L. Naldini, *Efficient gene delivery and targeted expression to hepatocytes in vivo by improved lentiviral vectors.* Hum Gene Ther, 2002. **13**(2): p. 243-60.

144. Wolff, G., S. Worgall, N. van Rooijen, W.R. Song, B.G. Harvey, and R.G. Crystal, *Enhancement of in vivo adenovirus-mediated gene transfer and expression by prior depletion of tissue macrophages in the target organ.* J Virol, 1997. **71**(1): p. 624-9.

145. Kuzmin, A.I., M.J. Finegold, and R.C. Eisensmith, *Macrophage depletion increases the safety, efficacy and persistence of adenovirus-mediated gene transfer in vivo.* Gene Ther, 1997. **4**(4): p. 309-16.

146. Schiedner, G., S. Hertel, M. Johnston, V. Dries, N. van Rooijen, and S. Kochanek, *Selective depletion or blockade of Kupffer cells leads to enhanced and prolonged hepatic transgene expression using high-capacity adenoviral vectors.* Mol Ther, 2003. **7**(1): p. 35-43.

147. Snoeys, J., G. Mertens, J. Lievens, T. van Berkel, D. Collen, E.A. Biessen, and B. De Geest, *Lipid emulsions potently increase transgene expression in hepatocytes after adenoviral transfer.* Mol Ther, 2006. **13**(1): p. 98-107.

148. Fuller, M. and D.S. Anson, *Helper plasmids for production of HIV-1-derived vectors.* Hum Gene Ther, 2001. **12**(17): p. 2081-93.

149. Anson, D.S. and M. Fuller, *Rational development of a HIV-1 gene therapy vector.* J Gene Med, 2003. **5**(10): p. 829-38.

150. Koldej, R., P. Cmielewski, A. Stocker, D.W. Parsons, and D.S. Anson, *Optimisation of a multipartite human immunodeficiency virus based vector system; control of virus infectivity and large-scale production.* J Gene Med, 2005. **7**(11): p. 1390-9.

151. Peters, H., M. Nefedov, J. Sarsero, J. Pitt, K.J. Fowler, S. Gazeas, S.G. Kahler, and P.A. Ioannou, *A knock-out mouse model for methylmalonic aciduria resulting in neonatal lethality.* J Biol Chem, 2003. **278**(52): p. 52909-13.

152. Peters, H.L., J.J. Pitt, L.R. Wood, N.J. Hamilton, J.P. Sarsero, and N.E. Buck, *Mouse models for methylmalonic aciduria.* PLoS One, 2012. **7**(7): p. e40609.

153. Tanaka, K., D.G. Hine, A. West-Dull, and T.B. Lynn, *Gas-chromatographic method of analysis for urinary organic acids. I. Retention indices of 155 metabolically important compounds.* Clin Chem, 1980. **26**(13): p. 1839-46.

154. Marcell, P.D., S.P. Stabler, E.R. Podell, and R.H. Allen, *Quantitation of methylmalonic acid and other dicarboxylic acids in normal serum and urine using capillary gas chromatography-mass spectrometry.* Anal Biochem, 1985. **150**(1): p. 58-66.

155. Kikuchi, M., H. Hanamizu, K. Narisawa, and K. Tada, *Assay of methylmalonyl CoA mutase with high-performance liquid chromatography.* Clin Chim Acta, 1989. **184**(3): p. 307-13.

156. Reed, E.B. and H. Tarver, *Urinary methylmalonate and hepatic methylmalonyl coenzyme A mutase activity in the vitamin B12-deficient rat.* J Nutr, 1970. **100**(8): p. 935-47.

157. Whitaker, T.R. and A.J. Giorgio, *A direct radioassay of methylmalonyl-coenzyme A mutase using enzymatically synthesized DL-(3- 14 C)methylmalonyl-CoA.* Anal Biochem, 1973. **52**(2): p. 522-32.

158. Willard, H.F. and L.E. Rosenberg, *Inherited deficiencies of human methylmalonyl CaA mutase activity: reduced affinity of mutant apoenzyme for adenosylcobalamin.* Biochem Biophys Res Commun, 1977. **78**(3): p. 927-34.

159. Scott, J.S., A.M. Treston, E.P. Bowman, J.A. Owens, and W.G. Cooksley, *The regulatory roles of liver and kidney in cobalamin (vitamin B12) metabolism in the rat: the uptake and intracellular binding of cobalamin and the activity of the cobalamin-dependent enzymes in response to varying cobalamin supply.* Clin Sci (Lond), 1984. **67**(3): p. 299-306.

160. Morrow, G., 3rd, L.A. Barness, G.J. Cardinale, R.H. Abeles, and J.G. Flaks, *Congenital methylmalonic acidemia: enzymatic evidence for two forms of the disease.* Proc Natl Acad Sci U S A, 1969. **63**(1): p. 191-7.

161. Kolhouse, J.F., S.P. Stabler, and R.H. Allen, *L-methylmalonyl-CoA mutase from human placenta.* Methods Enzymol, 1988. **166**: p. 407-14.

162. Goodey, P.A. and D. Gompertz, *Methylmalonyl CoA mutase--a radiochromatographic assay.* Clin Chim Acta, 1972. **42**(1): p. 119-23.

163. Corkey, B.E., M. Brandt, R.J. Williams, and J.R. Williamson, *Assay of short-chain acyl coenzyme A intermediates in tissue extracts by high-pressure liquid chromatography.* Anal Biochem, 1981. **118**(1): p. 30-41.

164. Snyder, L.R., J.W. Dolan, and P.W. Carr, *The hydrophobic-subtraction model of reversed-phase column selectivity.* J Chromatogr A, 2004. **1060**(1-2): p. 77-116.

165. Schellinger, A.P. and P.W. Carr, *Isocratic and gradient elution chromatography: a comparison in terms of speed, retention reproducibility and quantitation.* J Chromatogr A, 2006. **1109**(2): p. 253-66.

166. Gaire, D., I. Sponne, S. Droesch, A. Charlier, J.P. Nicolas, and D. Lambert, *Comparison of two methods for the measurement of rat liver methylmalonyl-coenzyme A mutase activity: HPLC and radioisotopic assays.* J Nutr Biochem, 1999. **10**(1): p. 56-62.

167. Smith, R.M., W.S. Osborne-White, and G.R. Russell, *Metabolism of propionate by sheep liver. Pathway of propionate metabolism in aged homogenate and mitochondria.* Biochem J, 1967. **104**(2): p. 441-9.

168. Hill, H.Z. and S.I. Goodman, *Detection of inborn errors of metabolism. II. Defects in propionic acid metabolism.* Clin Genet, 1974. **6**(2): p. 73-8.

169. Boquist, L. and I. Ericsson, *Inhibition by streptozotocin of the activity of succinyl-CoA synthetase in vitro and in vivo.* FEBS Lett, 1986. **196**(2): p. 341-3.

170. Strausberg, R.L., E.A. Feingold, L.H. Grouse, J.G. Derge, R.D. Klausner, F.S. Collins, L. Wagner, C.M. Shenmen, G.D. Schuler, S.F. Altschul, B. Zeeberg, K.H. Buetow, C.F. Schaefer, N.K. Bhat, R.F. Hopkins, H. Jordan, T. Moore, S.I. Max, J. Wang, F.

Hsieh, L. Diatchenko, K. Marusina, A.A. Farmer, G.M. Rubin, L. Hong, M. Stapleton, M.B. Soares, M.F. Bonaldo, T.L. Casavant, T.E. Scheetz, M.J. Brownstein, T.B. Usdin, S. Toshiyuki, P. Carninci, C. Prange, S.S. Raha, N.A. Loquellano, G.J. Peters, R.D. Abramson, S.J. Mullahy, S.A. Bosak, P.J. McEwan, K.J. McKernan, J.A. Malek, P.H. Gunaratne, S. Richards, K.C. Worley, S. Hale, A.M. Garcia, L.J. Gay, S.W. Hulyk, D.K. Villalon, D.M. Muzny, E.J. Sodergren, X. Lu, R.A. Gibbs, J. Fahey, E. Helton, M. Ketteman, A. Madan, S. Rodrigues, A. Sanchez, M. Whiting, A. Madan, A.C. Young, Y. Shevchenko, G.G. Bouffard, R.W. Blakesley, J.W. Touchman, E.D. Green, M.C. Dickson, A.C. Rodriguez, J. Grimwood, J. Schmutz, R.M. Myers, Y.S. Butterfield, M.I. Krzywinski, U. Skalska, D.E. Smailus, A. Schnerch, J.E. Schein, S.J. Jones, and M.A. Marra, *Generation and initial analysis of more than 15,000 full-length human and mouse cDNA sequences.* Proc Natl Acad Sci U S A, 2002. **99**(26): p. 16899-903.

171. Willard, H.F., L.M. Ambani, A.C. Hart, M.J. Mahoney, and L.E. Rosenberg, *Rapid prenatal and postnatal detection of inborn errors of propionate, methylmalonate, and cobalamin metabolism: a sensitive assay using cultured cells.* Hum Genet, 1976. **34**(3): p. 277-83.

172. Dorer, D.R. and S. Henikoff, *Expansions of transgene repeats cause heterochromatin formation and gene silencing in Drosophila.* Cell, 1994. **77**(7): p. 993-1002.

173. Allshire, R.C., J.P. Javerzat, N.J. Redhead, and G. Cranston, *Position effect variegation at fission yeast centromeres.* Cell, 1994. **76**(1): p. 157-69.

174. Sutter, N.B., D. Scalzo, S. Fiering, M. Groudine, and D.I. Martin, *Chromatin insulation by a transcriptional activator.* Proc Natl Acad Sci U S A, 2003. **100**(3): p. 1105-10.

175. Ellis, J., *Silencing and variegation of gammaretrovirus and lentivirus vectors.* Hum Gene Ther, 2005. **16**(11): p. 1241-6.

176. Robertson, G., D. Garrick, W. Wu, M. Kearns, D. Martin, and E. Whitelaw, *Position-dependent variegation of globin transgene expression in mice.* Proc Natl Acad Sci U S A, 1995. **92**(12): p. 5371-5.

177. Sharpe, J.A., P.S. Chan-Thomas, J. Lida, H. Ayyub, W.G. Wood, and D.R. Higgs, *Analysis of the human alpha globin upstream regulatory element (HS-40) in transgenic mice.* Embo J, 1992. **11**(12): p. 4565-72.

178. Jarman, A.P., W.G. Wood, J.A. Sharpe, G. Gourdon, H. Ayyub, and D.R. Higgs, *Characterization of the major regulatory element upstream of the human alpha-globin gene cluster.* Mol Cell Biol, 1991. **11**(9): p. 4679-89.

179. Wilkemeyer, M.F., E.R. Andrews, and F.D. Ledley, *Genomic structure of murine methylmalonyl-CoA mutase: evidence for genetic and epigenetic mechanisms determining enzyme activity.* Biochem J, 1993. **296 (Pt 3)**: p. 663-70.

180. Wilkemeyer, M.F., A.M. Crane, and F.D. Ledley, *Primary structure and activity of mouse methylmalonyl-CoA mutase.* Biochem J, 1990. **271**(2): p. 449-55.

181. Ye, X., K.P. Zimmer, R. Brown, C. Pabin, M.L. Batshaw, J.M. Wilson, and M.B. Robinson, *Differences in the human and mouse amino-terminal leader peptides of*

ornithine transcarbamylase affect mitochondrial import and efficacy of adenoviral vectors. Hum Gene Ther, 2001. **12**(9): p. 1035-46.

182. Meyburg, J. and G.F. Hoffmann, *Liver transplantation for inborn errors of metabolism.* Transplantation, 2005. **80**(1 Suppl): p. S135-7.

183. van't Hoff, W., P.J. McKiernan, R.A. Surtees, and J.V. Leonard, *Liver transplantation for methylmalonic acidaemia.* Eur J Pediatr, 1999. **158 Suppl 2**: p. S70-4.

184. Hsui, J.Y., Y.H. Chien, S.Y. Chu, F.L. Lu, H.L. Chen, M.J. Ho, P.H. Lee, and W.L. Hwu, *Living-related liver transplantation for methylmalonic acidemia: report of one case.* Acta Paediatr Taiwan, 2003. **44**(3): p. 171-3.

185. Palmowski, M.J., L. Lopes, Y. Ikeda, M. Salio, V. Cerundolo, and M.K. Collins, *Intravenous injection of a lentiviral vector encoding NY-ESO-1 induces an effective CTL response.* J Immunol, 2004. **172**(3): p. 1582-7.

186. Dominguez, E., T. Marais, N. Chatauret, S. Benkhelifa-Ziyyat, S. Duque, P. Ravassard, R. Carcenac, S. Astord, A. Pereira de Moura, T. Voit, and M. Barkats, *Intravenous scAAV9 delivery of a codon-optimized SMN1 sequence rescues SMA mice.* Hum Mol Genet, 2011. **20**(4): p. 681-93.

187. Kim, D.W., T. Uetsuki, Y. Kaziro, N. Yamaguchi, and S. Sugano, *Use of the human elongation factor 1 alpha promoter as a versatile and efficient expression system.* Gene, 1990. **91**(2): p. 217-23.

188. Uetsuki, T., A. Naito, S. Nagata, and Y. Kaziro, *Isolation and characterization of the human chromosomal gene for polypeptide chain elongation factor-1 alpha.* J Biol Chem, 1989. **264**(10): p. 5791-8.

189. Thiele, D., P. Cottrelle, F. Iborra, J.M. Buhler, A. Sentenac, and P. Fromageot, *Elongation factor 1 alpha from Saccharomyces cerevisiae. Rapid large-scale purification and molecular characterization.* J Biol Chem, 1985. **260**(5): p. 3084-9.

190. Mizushima, S. and S. Nagata, *pEF-BOS, a powerful mammalian expression vector.* Nucleic Acids Res, 1990. **18**(17): p. 5322.

191. Wakabayashi-Ito, N. and S. Nagata, *Characterization of the regulatory elements in the promoter of the human elongation factor-1 alpha gene.* J Biol Chem, 1994. **269**(47): p. 29831-7.

192. Gill, D.R., S.E. Smyth, C.A. Goddard, I.A. Pringle, C.F. Higgins, W.H. Colledge, and S.C. Hyde, *Increased persistence of lung gene expression using plasmids containing the ubiquitin C or elongation factor 1alpha promoter.* Gene Ther, 2001. **8**(20): p. 1539-46.

193. McIntyre, C., S. Byers, and D.S. Anson, *Correction of mucopolysaccharidosis type IIIA somatic and central nervous system pathology by lentiviral-mediated gene transfer.* J Gene Med, 2010. **12**(9): p. 717-28.

194. Pan, D., R. Gunther, W. Duan, S. Wendell, W. Kaemmerer, T. Kafri, I.M. Verma, and C.B. Whitley, *Biodistribution and toxicity studies of VSVG-pseudotyped lentiviral*

vector after intravenous administration in mice with the observation of in vivo transduction of bone marrow. Mol Ther, 2002. **6**(1): p. 19-29.

195. van der Wegen, P., R. Louwen, A.M. Imam, R.M. Buijs-Offerman, M. Sinaasappel, F. Grosveld, and B.J. Scholte, *Successful treatment of UGT1A1 deficiency in a rat model of Crigler-Najjar disease by intravenous administration of a liver-specific lentiviral vector.* Mol Ther, 2006. **13**(2): p. 374-81.

196. Kaleko, M., J.V. Garcia, and A.D. Miller, *Persistent gene expression after retroviral gene transfer into liver cells in vivo.* Hum Gene Ther, 1991. **2**(1): p. 27-32.

197. Park, F., K. Ohashi, and M.A. Kay, *Therapeutic levels of human factor VIII and IX using HIV-1-based lentiviral vectors in mouse liver.* Blood, 2000. **96**(3): p. 1173-6.

198. Charrier, S., M. Ferrand, M. Zerbato, G. Precigout, A. Viornery, S. Bucher-Laurent, S. Benkhelifa-Ziyyat, O.W. Merten, J. Perea, and A. Galy, *Quantification of lentiviral vector copy numbers in individual hematopoietic colony-forming cells shows vector dose-dependent effects on the frequency and level of transduction.* Gene Ther, 2011. **18**(5): p. 479-87.

199. Abordo-Adesida, E., A. Follenzi, C. Barcia, S. Sciascia, M.G. Castro, L. Naldini, and P.R. Lowenstein, *Stability of lentiviral vector-mediated transgene expression in the brain in the presence of systemic antivector immune responses.* Hum Gene Ther, 2005. **16**(6): p. 741-51.

200. Kobayashi, H., D. Carbonaro, K. Pepper, D. Petersen, S. Ge, H. Jackson, H. Shimada, R. Moats, and D.B. Kohn, *Neonatal gene therapy of MPS I mice by intravenous injection of a lentiviral vector.* Mol Ther, 2005. **11**(5): p. 776-89.

201. Wang, L., H. Morizono, J. Lin, P. Bell, D. Jones, D. McMenamin, H. Yu, M.L. Batshaw, and J.M. Wilson, *Preclinical evaluation of a clinical candidate AAV8 vector for ornithine transcarbamylase (OTC) deficiency reveals functional enzyme from each persisting vector genome.* Mol Genet Metab, 2012. **105**(2): p. 203-11.

202. Ward, N.J., S.M. Buckley, S.N. Waddington, T. Vandendriessche, M.K. Chuah, A.C. Nathwani, J. McIntosh, E.G. Tuddenham, C. Kinnon, A.J. Thrasher, and J.H. McVey, *Codon optimization of human factor VIII cDNAs leads to high-level expression.* Blood, 2011. **117**(3): p. 798-807.

203. Moreno-Carranza, B., M. Gentsch, S. Stein, A. Schambach, G. Santilli, E. Rudolf, M.F. Ryser, S. Haria, A.J. Thrasher, C. Baum, S. Brenner, and M. Grez, *Transgene optimization significantly improves SIN vector titers, gp91phox expression and reconstitution of superoxide production in X-CGD cells.* Gene Ther, 2009. **16**(1): p. 111-8.

204. Gonin, P. and C. Gaillard, *Gene transfer vector biodistribution: pivotal safety studies in clinical gene therapy development.* Gene Ther, 2004. **11 Suppl 1**: p. S98-S108.

205. Berraondo, P., J. Crettaz, L. Ochoa, A. Paneda, J. Prieto, I.F. Troconiz, and G. Gonzalez-Aseguinolaza, *Intrahepatic injection of recombinant adeno-associated virus serotype 2 overcomes gender-related differences in liver transduction.* Hum Gene Ther, 2006. **17**(6): p. 601-10.

206. Mitchell, M., M. Jerebtsova, M.L. Batshaw, K. Newman, and X. Ye, *Long-term gene transfer to mouse fetuses with recombinant adenovirus and adeno-associated virus (AAV) vectors.* Gene Ther, 2000. **7**(23): p. 1986-92.

207. Carrillo-Carrasco, N., R.J. Chandler, S. Chandrasekaran, and C.P. Venditti, *Liver-directed recombinant adeno-associated viral gene delivery rescues a lethal mouse model of methylmalonic acidemia and provides long-term phenotypic correction.* Hum Gene Ther, 2010. **21**(9): p. 1147-54.

208. Massaer, M., P. Mazzu, M. Haumont, M. Magi, V. Daminet, A. Bollen, and A. Jacquet, *High-level expression in mammalian cells of recombinant house dust mite allergen ProDer p 1 with optimized codon usage.* Int Arch Allergy Immunol, 2001. **125**(1): p. 32-43.

209. Holm, L., *Codon usage and gene expression.* Nucleic Acids Res, 1986. **14**(7): p. 3075-87.

210. Bernardi, G. and G. Bernardi, *Codon usage and genome composition.* J Mol Evol, 1985. **22**(4): p. 363-5.

211. Uno, M., K. Ito, and Y. Nakamura, *Functional specificity of amino acid at position 246 in the tRNA mimicry domain of bacterial release factor 2.* Biochimie, 1996. **78**(11-12): p. 935-43.

212. Kanaya, S., Y. Yamada, M. Kinouchi, Y. Kudo, and T. Ikemura, *Codon usage and tRNA genes in eukaryotes: correlation of codon usage diversity with translation efficiency and with CG-dinucleotide usage as assessed by multivariate analysis.* J Mol Evol, 2001. **53**(4-5): p. 290-8.

213. Comeron, J.M., *Selective and mutational patterns associated with gene expression in humans: influences on synonymous composition and intron presence.* Genetics, 2004. **167**(3): p. 1293-304.

214. Urrutia, A.O. and L.D. Hurst, *Codon usage bias covaries with expression breadth and the rate of synonymous evolution in humans, but this is not evidence for selection.* Genetics, 2001. **159**(3): p. 1191-9.

215. Urrutia, A.O. and L.D. Hurst, *The signature of selection mediated by expression on human genes.* Genome Res, 2003. **13**(10): p. 2260-4.

216. Lavner, Y. and D. Kotlar, *Codon bias as a factor in regulating expression via translation rate in the human genome.* Gene, 2005. **345**(1): p. 127-38.

217. Kotlar, D. and Y. Lavner, *The action of selection on codon bias in the human genome is related to frequency, complexity, and chronology of amino acids.* BMC Genomics, 2006. **7**: p. 67.

218. Ren, L., G. Gao, D. Zhao, M. Ding, J. Luo, and H. Deng, *Developmental stage related patterns of codon usage and genomic GC content: searching for evolutionary fingerprints with models of stem cell differentiation.* Genome Biol, 2007. **8**(3): p. R35.

219. Kim, C.H., Y. Oh, and T.H. Lee, *Codon optimization for high-level expression of human erythropoietin (EPO) in mammalian cells.* Gene, 1997. **199**(1-2): p. 293-301.

220. Konu, O. and M.D. Li, *Correlations between mRNA expression levels and GC contents of coding and untranslated regions of genes in rodents.* J Mol Evol, 2002. **54**(1): p. 35-41.

221. Rowley, C.R., P.L. Sinn, L. Bullinga, P.B. McCray, and B.L. Davidson, *A Rapid and Effective Lentivirus Purification Procedure.* Mol Ther, 2004. **9**(S1): p. S32-S32.

222. Virbasius, J.V. and R.C. Scarpulla, *Transcriptional activation through ETS domain binding sites in the cytochrome c oxidase subunit IV gene.* Mol Cell Biol, 1991. **11**(11): p. 5631-8.

223. Suzuki, H., Y. Hosokawa, H. Toda, M. Nishikimi, and T. Ozawa, *Common protein-binding sites in the 5'-flanking regions of human genes for cytochrome c1 and ubiquinone-binding protein.* J Biol Chem, 1990. **265**(14): p. 8159-63.

224. Wilkemeyer, M., J. Stankovics, T. Foy, and F.D. Ledley, *Propionate metabolism in cultured human cells after overexpression of recombinant methylmalonyl CoA mutase: implications for somatic gene therapy.* Somat Cell Mol Genet, 1992. **18**(6): p. 493-505.

225. Lubrano, R., M. Elli, M. Rossi, E. Travasso, C. Raggi, P. Barsotti, C. Carducci, and P. Berloco, *Renal transplant in methylmalonic acidemia: could it be the best option? Report on a case at 10 years and review of the literature.* Pediatr Nephrol, 2007. **22**(8): p. 1209-14.

226. Andrews, E., R. Jansen, A.M. Crane, S. Cholin, D. McDonnell, and F.D. Ledley, *Expression of recombinant human methylmalonyl-CoA mutase: in primary mut fibroblasts and Saccharomyces cerevisiae.* Biochem Med Metab Biol, 1993. **50**(2): p. 135-44.

227. Nyhan, W.L., J.J. Gargus, K. Boyle, R. Selby, and R. Koch, *Progressive neurologic disability in methylmalonic acidemia despite transplantation of the liver.* Eur J Pediatr, 2002. **161**(7): p. 377-9.

228. Kayler, L.K., R.M. Merion, S. Lee, R.S. Sung, J.D. Punch, S.M. Rudich, J.G. Turcotte, D.A. Campbell, Jr., R. Holmes, and J.C. Magee, *Long-term survival after liver transplantation in children with metabolic disorders.* Pediatr Transplant, 2002. **6**(4): p. 295-300.

229. Huang, H.P., Y.H. Chien, L.M. Huang, Y.H. Ni, M.H. Chang, M.C. Ho, P.H. Lee, and W.L. Hwu, *Viral infections and prolonged fever after liver transplantation in young children with inborn errors of metabolism.* J Formos Med Assoc, 2005. **104**(9): p. 623-9.

230. Morioka, D., M. Kasahara, Y. Takada, J.P. Corrales, A. Yoshizawa, S. Sakamoto, K. Taira, E.Y. Yoshitoshi, H. Egawa, H. Shimada, and K. Tanaka, *Living donor liver transplantation for pediatric patients with inheritable metabolic disorders.* Am J Transplant, 2005. **5**(11): p. 2754-63.

231. Lubrano, R., P. Scoppi, P. Barsotti, E. Travasso, S. Scateni, S. Cristaldi, and M.A. Castello, *Kidney transplantation in a girl with methylmalonic acidemia and end stage renal failure.* Pediatr Nephrol, 2001. **16**(11): p. 848-51.

232. Coman, D., J. Huang, S. McTaggart, O. Sakamoto, T. Ohura, J. McGill, and J. Burke, *Renal transplantation in a 14-year-old girl with vitamin B12-responsive cblA-type methylmalonic acidaemia.* Pediatr Nephrol, 2006. **21**(2): p. 270-3.

233. Van Calcar, S.C., C.O. Harding, P. Lyne, K. Hogan, R. Banerjee, H. Sollinger, R.E. Rieselbach, and J.A. Wolff, *Renal transplantation in a patient with methylmalonic acidaemia.* J Inherit Metab Dis, 1998. **21**(7): p. 729-37.

234. Glasgow, A.M. and H.P. Chase, *Effect of propionic acid on fatty acid oxidation and ureagenesis.* Pediatr Res, 1976. **10**(7): p. 683-6.

235. Lalka, D., R.K. Griffith, and C.L. Cronenberger, *The hepatic first-pass metabolism of problematic drugs.* J Clin Pharmacol, 1993. **33**(7): p. 657-69.

236. Zhou, H.S., D.P. Liu, and C.C. Liang, *Challenges and strategies: the immune responses in gene therapy.* Med Res Rev, 2004. **24**(6): p. 748-61.

237. Bessis, N., F.J. GarciaCozar, and M.C. Boissier, *Immune responses to gene therapy vectors: influence on vector function and effector mechanisms.* Gene Ther, 2004. **11 Suppl 1**: p. S10-7.

238. Xu, Z., J.S. Smith, J. Tian, and A.P. Byrnes, *Induction of shock after intravenous injection of adenovirus vectors: a critical role for platelet-activating factor.* Mol Ther, 2010. **18**(3): p. 609-16.

239. Sobrevals, L., M. Enguita, C. Rodriguez, J. Gonzalez-Rojas, P. Alzaguren, N. Razquin, J. Prieto, and P. Fortes, *AAV vectors transduce hepatocytes in vivo as efficiently in cirrhotic as in healthy rat livers.* Gene Ther, 2012. **19**(4): p. 411-7.

240. Chandler, R.J. and C.P. Venditti, *Adenovirus-mediated gene delivery rescues a neonatal lethal murine model of mut(0) methylmalonic acidemia.* Hum Gene Ther, 2008. **19**(1): p. 53-60.

241. Zufferey, R., D. Nagy, R.J. Mandel, L. Naldini, and D. Trono, *Multiply attenuated lentiviral vector achieves efficient gene delivery in vivo.* Nat Biotechnol, 1997. **15**(9): p. 871-5.

242. Zufferey, R., T. Dull, R.J. Mandel, A. Bukovsky, D. Quiroz, L. Naldini, and D. Trono, *Self-inactivating lentivirus vector for safe and efficient in vivo gene delivery.* J Virol, 1998. **72**(12): p. 9873-80.

243. Kafri, T., U. Blomer, D.A. Peterson, F.H. Gage, and I.M. Verma, *Sustained expression of genes delivered directly into liver and muscle by lentiviral vectors.* Nat Genet, 1997. **17**(3): p. 314-7.

244. Naldini, L., U. Blomer, P. Gallay, D. Ory, R. Mulligan, F.H. Gage, I.M. Verma, and D. Trono, *In vivo gene delivery and stable transduction of nondividing cells by a lentiviral vector.* Science, 1996. **272**(5259): p. 263-7.

245. Pfeifer, A., T. Kessler, M. Yang, E. Baranov, N. Kootstra, D.A. Cheresh, R.M. Hoffman, and I.M. Verma, *Transduction of liver cells by lentiviral vectors: analysis in living animals by fluorescence imaging.* Mol Ther, 2001. **3**(3): p. 319-22.

246. Kang, Y., C.S. Stein, J.A. Heth, P.L. Sinn, A.K. Penisten, P.D. Staber, K.L. Ratliff, H. Shen, C.K. Barker, I. Martins, C.M. Sharkey, D.A. Sanders, P.B. McCray, Jr., and B.L. Davidson, *In vivo gene transfer using a nonprimate lentiviral vector pseudotyped with Ross River Virus glycoproteins.* J Virol, 2002. **76**(18): p. 9378-88.

247. Alemany, R., K. Suzuki, and D.T. Curiel, *Blood clearance rates of adenovirus type 5 in mice.* J Gen Virol, 2000. **81**(Pt 11): p. 2605-9.

248. Zhang, L., P.J. Dailey, A. Gettie, J. Blanchard, and D.D. Ho, *The liver is a major organ for clearing simian immunodeficiency virus in rhesus monkeys.* J Virol, 2002. **76**(10): p. 5271-3.

249. Brunner, K.T., D. Hurez, C.R. Mc, and B. Benacerraf, *Blood clearance of P32-labeled vesicular stomatitis and Newcastle disease viruses by the reticuloendothelial system in mice.* J Immunol, 1960. **85**: p. 99-105.

250. Cereghini, S., M. Raymondjean, A.G. Carranca, P. Herbomel, and M. Yaniv, *Factors involved in control of tissue-specific expression of albumin gene.* Cell, 1987. **50**(4): p. 627-38.

251. Schorpp, M., W. Kugler, U. Wagner, and G.U. Ryffel, *Hepatocyte-specific promoter element HP1 of the Xenopus albumin gene interacts with transcriptional factors of mammalian hepatocytes.* J Mol Biol, 1988. **202**(2): p. 307-20.

252. Kramer, M.G., M. Barajas, N. Razquin, P. Berraondo, M. Rodrigo, C. Wu, C. Qian, P. Fortes, and J. Prieto, *In vitro and in vivo comparative study of chimeric liver-specific promoters.* Mol Ther, 2003. **7**(3): p. 375-85.

253. Hafenrichter, D.G., K.P. Ponder, S.D. Rettinger, S.C. Kennedy, X. Wu, R.S. Saylors, and M.W. Flye, *Liver-directed gene therapy: evaluation of liver specific promoter elements.* J Surg Res, 1994. **56**(6): p. 510-7.

254. Manno, C.S., G.F. Pierce, V.R. Arruda, B. Glader, M. Ragni, J.J. Rasko, M.C. Ozelo, K. Hoots, P. Blatt, B. Konkle, M. Dake, R. Kaye, M. Razavi, A. Zajko, J. Zehnder, P.K. Rustagi, H. Nakai, A. Chew, D. Leonard, J.F. Wright, R.R. Lessard, J.M. Sommer, M. Tigges, D. Sabatino, A. Luk, H. Jiang, F. Mingozzi, L. Couto, H.C. Ertl, K.A. High, and M.A. Kay, *Successful transduction of liver in hemophilia by AAV-Factor IX and limitations imposed by the host immune response.* Nat Med, 2006. **12**(3): p. 342-7.

255. Zheng, C. and B.J. Baum, *Evaluation of viral and mammalian promoters for use in gene delivery to salivary glands.* Mol Ther, 2005. **12**(3): p. 528-36.

256. Magnusson, T., R. Haase, M. Schleef, E. Wagner, and M. Ogris, *Sustained, high transgene expression in liver with plasmid vectors using optimized promoter-enhancer combinations.* J Gene Med, 2011. **13**(7-8): p. 382-91.

257. Mao, G., F. Marotta, J. Yu, L. Zhou, Y. Yu, L. Wang, and D. Chui, *DNA context and promoter activity affect gene expression in lentiviral vectors.* Acta Biomed, 2008. **79**(3): p. 192-6.

258. Qin, J.Y., L. Zhang, K.L. Clift, I. Hulur, A.P. Xiang, B.Z. Ren, and B.T. Lahn, *Systematic comparison of constitutive promoters and the doxycycline-inducible promoter.* PLoS One, 2010. **5**(5): p. e10611.

259. Nakai, H., R.W. Herzog, J.N. Hagstrom, J. Walter, S.H. Kung, E.Y. Yang, S.J. Tai, Y. Iwaki, G.J. Kurtzman, K.J. Fisher, P. Colosi, L.B. Couto, and K.A. High, *Adeno-associated viral vector-mediated gene transfer of human blood coagulation factor IX into mouse liver.* Blood, 1998. **91**(12): p. 4600-7.

260. Pastore, L., N. Morral, H. Zhou, R. Garcia, R.J. Parks, S. Kochanek, F.L. Graham, B. Lee, and A.L. Beaudet, *Use of a liver-specific promoter reduces immune response to the transgene in adenoviral vectors.* Hum Gene Ther, 1999. **10**(11): p. 1773-81.

261. Hayashi, Y., Y. Mori, O.E. Janssen, T. Sunthornthepvarakul, R.E. Weiss, K. Takeda, M. Weinberg, H. Seo, G.I. Bell, and S. Refetoff, *Human thyroxine-binding globulin gene: complete sequence and transcriptional regulation.* Mol Endocrinol, 1993. **7**(8): p. 1049-60.

262. Moscioni, D., H. Morizono, R.J. McCarter, A. Stern, J. Cabrera-Luque, A. Hoang, J. Sanmiguel, D. Wu, P. Bell, G.P. Gao, S.E. Raper, J.M. Wilson, and M.L. Batshaw, *Long-term correction of ammonia metabolism and prolonged survival in ornithine transcarbamylase-deficient mice following liver-directed treatment with adeno-associated viral vectors.* Mol Ther, 2006. **14**(1): p. 25-33.

263. Lebherz, C., J. Sanmiguel, J.M. Wilson, and D.J. Rader, *Gene transfer of wild-type apoA-I and apoA-I Milano reduce atherosclerosis to a similar extent.* Cardiovasc Diabetol, 2007. **6**: p. 15.

264. Wang, L., R. Calcedo, H. Wang, P. Bell, R. Grant, L.H. Vandenberghe, J. Sanmiguel, H. Morizono, M.L. Batshaw, and J.M. Wilson, *The pleiotropic effects of natural AAV infections on liver-directed gene transfer in macaques.* Mol Ther, 2010. **18**(1): p. 126-34.

265. Brunetti-Pierri, N., D.J. Palmer, A.L. Beaudet, K.D. Carey, M. Finegold, and P. Ng, *Acute toxicity after high-dose systemic injection of helper-dependent adenoviral vectors into nonhuman primates.* Hum Gene Ther, 2004. **15**(1): p. 35-46.

266. Lebherz, C., G. Gao, J.P. Louboutin, J. Millar, D. Rader, and J.M. Wilson, *Gene therapy with novel adeno-associated virus vectors substantially diminishes atherosclerosis in a murine model of familial hypercholesterolemia.* J Gene Med, 2004. **6**(6): p. 663-72.

267. Mount, J.D., R.W. Herzog, D.M. Tillson, S.A. Goodman, N. Robinson, M.L. McCleland, D. Bellinger, T.C. Nichols, V.R. Arruda, C.D. Lothrop, Jr., and K.A. High, *Sustained phenotypic correction of hemophilia B dogs with a factor IX null mutation by liver-directed gene therapy.* Blood, 2002. **99**(8): p. 2670-6.

268. Grossman, Z., E. Mendelson, F. Brok-Simoni, F. Mileguir, Y. Leitner, G. Rechavi, and B. Ramot, *Detection of adeno-associated virus type 2 in human peripheral blood cells.* J Gen Virol, 1992. **73 (Pt 4)**: p. 961-6.

269. Vandendriessche, T., L. Thorrez, A. Acosta-Sanchez, I. Petrus, L. Wang, L. Ma, D.E.W. L, Y. Iwasaki, V. Gillijns, J.M. Wilson, D. Collen, and M.K. Chuah, *Efficacy*

and safety of adeno-associated viral vectors based on serotype 8 and 9 vs. lentiviral vectors for hemophilia B gene therapy. J Thromb Haemost, 2007. **5**(1): p. 16-24.

270. Gao, G., L.H. Vandenberghe, M.R. Alvira, Y. Lu, R. Calcedo, X. Zhou, and J.M. Wilson, *Clades of Adeno-associated viruses are widely disseminated in human tissues.* J Virol, 2004. **78**(12): p. 6381-8.

271. Beck, W.S., M. Flavin, and S. Ochoa, *Metabolism of propionic acid in animal tissues. III. Formation of succinate.* J Biol Chem, 1957. **229**(2): p. 997-1010.

272. Peters, J.P. and J.M. Elliot, *Effects of cobalt or hydroxycobalamin supplementation on vitamin B-12 content and (S)-methylmalonyl-CoA mutase activity of tissue from cobalt-depleted sheep.* J Nutr, 1984. **114**(4): p. 660-70.

273. Kennedy, D.G., A. Cannavan, A. Molloy, F. O'Harte, S.M. Taylor, S. Kennedy, and W.J. Blanchflower, *Methylmalonyl-CoA mutase (EC 5.4.99.2) and methionine synthetase (EC 2.1.1.13) in the tissues of cobalt-vitamin B12 deficient sheep.* Br J Nutr, 1990. **64**(3): p. 721-32.

274. Isaka, Y., *Gene therapy targeting kidney diseases: routes and vehicles.* Clin Exp Nephrol, 2006. **10**(4): p. 229-35.

275. Brunetti-Pierri, N., *Gene therapy for inborn errors of liver metabolism: progress towards clinical applications.* Ital J Pediatr, 2008. **34**(1): p. 2.

276. Teichler Zallen, D., *US gene therapy in crisis.* Trends Genet, 2000. **16**(6): p. 272-5.

277. High, K.A., *Update on progress and hurdles in novel genetic therapies for hemophilia.* Hematology Am Soc Hematol Educ Program, 2007: p. 466-72.

278. Bokhoven, M., S.L. Stephen, S. Knight, E.F. Gevers, I.C. Robinson, Y. Takeuchi, and M.K. Collins, *Insertional gene activation by lentiviral and gammaretroviral vectors.* J Virol, 2009. **83**(1): p. 283-94.

279. Frederickson, R.M., *Integrating ideas on insertional mutagenesis by gene transfer vectors.* Mol Ther, 2007. **15**(7): p. 1228-32.

280. Manilla, P., T. Rebello, C. Afable, X. Lu, V. Slepushkin, L.M. Humeau, K. Schonely, Y. Ni, G.K. Binder, B.L. Levine, R.R. MacGregor, C.H. June, and B. Dropulic, *Regulatory considerations for novel gene therapy products: a review of the process leading to the first clinical lentiviral vector.* Hum Gene Ther, 2005. **16**(1): p. 17-25.

281. Shen, Z.P., A.A. Brayman, L. Chen, and C.H. Miao, *Ultrasound with microbubbles enhances gene expression of plasmid DNA in the liver via intraportal delivery.* Gene Ther, 2008. **15**(16): p. 1147-55.

282. Christ, M., B. Louis, F. Stoeckel, A. Dieterle, L. Grave, D. Dreyer, J. Kintz, D. Ali Hadji, M. Lusky, and M. Mehtali, *Modulation of the inflammatory properties and hepatotoxicity of recombinant adenovirus vectors by the viral E4 gene products.* Hum Gene Ther, 2000. **11**(3): p. 415-27.

283. Gusella, G.L., E. Fedorova, B. Hanss, D. Marras, M.E. Klotman, and P.E. Klotman, *Lentiviral gene transduction of kidney.* Hum Gene Ther, 2002. **13**(3): p. 407-14.